# FOREWORD

This publication was prepared under contract for the Joint Publications Research Service as a translation or foreign-language research service to the various federal government departments.

The contents of this material in no way represent the policies, views or attitudes of the U. S. Government or of the parties to any distribution arrangement.

## PROCUREMENT OF JPRS REPORTS

All JPRS reports may be ordered from the Office of Technical Services. Reports published prior to 1 February 1963 can be provided, for the most part, only in photocopy (xerox). Those published after 1 February 1963 will be provided in printed form.

Details on special subscription arrangements for JPRS social science reports will be provided upon request.

No cumulative subject index or catalog of all JPRS reports has been compiled.

All JPRS reports are listed in the Monthly Catalog of U. S. Government Publications, available on subscription at $4.50 per year ($6.00 foreign), including an annual index, from the Superintendent of Documents, U. S. Government Printing Office, Washington 25, D. C.

All JPRS scientific and technical reports are cataloged and subject-indexed in Technical Translations, published semimonthly by the Office of Technical Services, and also available on subscription ($12.00 per year domestic, $16.00 foreign) from the Superintendent of Documents. Semiannual indexes to Technical Translations are available at additional cost.

JPRS: 18,819

# RECENT DEVELOPMENTS IN GEOPHYSICS

- USSR -

[Following are translations of articles from Voprosy Geofiziki, Uchenyye Zapiski Leningradskogo Ordena Lenina Gosudarstvennogo Universiteta imeni A.A. Zhdanova, Seriya Fizicheskikh i Geologicheskikh Nauk (Problems of Geophysics, Scientific Notes of the Leningrad State University imeni A.A. Zhdanov, Laureate of the Order of Lenin, Physics and Geology Series), Vol 303, No 13, Leningrad, 1962.]

## Table of Contents

Page

# MEASURING THE COMPONENTS OF THE EARTH'S GEOMAGNETIC FIELD BY THE PROTON RESONANCE METHOD

V. D. Lomanyy, A. G. Prokof'yev, and B. M. Yanovskiy

pp. 3-15

## Introduction

All magnetic observatories in the USSR at present use classical methods to measure H (the horizontal component) and Z (the vertical component). The error in H as so measured is 2-3 $\gamma$, while that in Z for latitudes between 50 and 60° is 5-10 $\gamma$. One of the proton-resonance methods (free nuclear induction) can measure the field to 1 part in $10^{-5}$, which corresponds to not more than 0.5 $\gamma$ at the above latitudes; this represents a great improvement. The method gives the strength of the total field, so either component can be measured alone only if the other is first balanced out by a field of comparable homogeneity. Helmholtz coils can provide this if the homogeneous-field region is larger than the detector (a vessel containing water). Here we describe an apparatus for measuring Z and give some values.

## 1. Theoretical Principles of the Free Nuclear Induction Method

Any atomic nucleus has a mechanical moment p and a magnetic moment $\mu$; $\mu/p = \pm\gamma$ is called the gyromagnetic ratio, the sign indicating the direction of $\mu$ relative to p. The protons in (say) water have no preferred orientation in the absence of an external field, but a field H (steady) gives them an additional energy $\Delta E \simeq \mu H$, which causes $\mu$ to take the direction of H. Quantum theory indicates that the projection of p on the direction of H can take 2m + 1 values, in which m is the magnetic quantum number; m = ½ for the proton, so it has two orientations (along and opposed to the field). Boltzmann's theory indicates that the proportion parallel to the field is greater than that antiparallel, so there is an excess moment $\mu_i$ in the

direction of H (the substance is paramagnetic). The magnetic moment per unit volume is $J_o = xH$, in which x is the nuclear paramagnetic susceptibility:

$$x = \frac{Ng_i^2\mu_i^2 m(m+1)}{3kT},$$

in which N is the number of nuclei in unit volume, k is Boltzmann's constant, and T is absolute temperature.

The interaction between H and $\mu$ is accompanied by interactions between the nuclei individually and collectively. The latter (interaction with the lattice) causes the temperature t' of the nuclear-spin system to be the temperature t" of the lattice in the usual state; but t' becomes larger than t" when a magnetic field is applied, and a certain time $T_1$ (the longitudinal relaxation time) is needed for the system to return to thermodynamic equilibrium. This means that the vector does not rise to $J_o = xH$ instantly but instead rises in accordance with $J = J_o[1 - \exp(-t/T)]$, in which t is time.

The interaction between the spins is caused by the local magnetic field H' produced by adjacent nuclei, so spins initially moving in phase in response to H after a time $T_2$ differ by $\Delta\omega \sim \gamma H'$; $T_2 \propto 1/\Delta\omega$ and is called the transverse relaxation time. The commonest method of exciting free nuclear induction is to switch of an accessory strong magnetic field H very rapidly, this polarizing field is first applied perpendicular to $H_t$, the field to be measured. Then, after a time of about $T_1$, when $\vec{J}$ is approaching its equilibrium value, this H is removed rapidly (so rapidly that $\vec{J}$ does not alter in orientation). The oriented protons are then subject to $H_t$, the couple on the moment $\vec{\mu}_i$ from $\vec{H}_t$ being $\vec{C} = [\vec{\mu}_i\vec{H}_t]$.

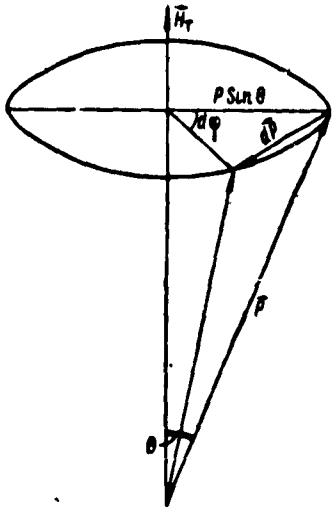


Fig. 1.

The equation of motion, in the absence of relaxation, is

$$\frac{d\vec{P}_i}{dt} = \vec{C} = [\vec{\mu}_i\vec{H}_T] = \gamma[\vec{P}_i\vec{H}_T], \qquad (1)$$

for $\vec{\mu}_i = \gamma\vec{P}_i$. We multiply both sides scalarly by $\vec{P}_i$ and get

$\vec{P}_i(d\vec{P}_i/dt) = 0$, so $\vec{P}$ lies at 90° to $d\vec{P}$, the modulus of $\vec{P}$ being constant, so the motion of $\vec{P}$ is that of precession about the direction of $H_t$.

Let $\theta$ be the angle between $\vec{P}$ and $\vec{H}_t$ (Fig. 1); then $d\vec{P}_i$ can be put as $\vec{P}_i \sin\theta d\varphi$, so

$$\frac{d\vec{P}_i}{dt} = \vec{P}_i \sin\theta \frac{d\varphi}{dt} = \omega \vec{P}_i \sin\theta,$$

in which $\omega$ is the angular velocity of $\vec{P}$. We replace $d\vec{P}_i/dt$ here to get

$$\omega = \frac{\mu_i H_T \sin\theta}{\vec{P}_i \sin\theta} = \frac{\mu_i}{\vec{P}_i} H_T = \gamma H_T,$$

in which $\omega$ is the Larmor precession frequency.

Equation (1) should be put as follows if relaxation effects are present, for these resemble damping; replacing $\mu_i$ by J, we have

$$\frac{dJ_x}{dt} = -\gamma [\vec{J}\vec{H}_T]_x - \frac{J_x}{T_2},$$
$$\frac{dJ_y}{dt} = \gamma [\vec{J}\vec{H}_T]_y - \frac{J_y}{T_2},$$
$$\frac{dJ_z}{dt} = -\frac{J_0 - J_z}{T_1}.$$

The conditions for t = 0 are

$$J_0^2 = J_{x0}^2 + J_{y0}^2 = (\varkappa H)^2, \quad J_z = 0, \quad \& \frac{dJ_x}{dt} = \frac{dJ_y}{dt} = 0,$$

and the solution to the equations is

$$J_x = J_0 e^{-\frac{t}{T_1}} \cos(\omega t + \varphi_0),$$
$$J_y = J_0 e^{-\frac{t}{T_1}} \sin(\omega t + \varphi_0),$$
$$J_z = J_0 \left(1 - e^{-\frac{t}{T_1}}\right),$$

in which $\omega = \gamma H_t$ and $\varphi_0$ is the initial phase. Then $\vec{J}$ precesses around $\vec{H}_t$ with a frequency $\omega$ and has a decreasing amplitude; a

cylindrical coil having its axis in the plane of rotation then has a current induced in it. The amplitude of this signal does not depend on the orientation of the coil in the xOy plane but it does depend on the inclination in the zOy plane, for this affects the effective area intersecting the flux. The signal decays gradually, but its amplitude remains adequate for several seconds provided that the relaxation time is long.

The magnetic induction $B_x$ corresponding to $J_x$ is $4\pi J_x$, so the flux linkage $\Phi$ is $B_x SN\beta\sin(\alpha)$, in which S is the effective area of one turn, $\alpha$ is the angle between $J_x$ and $H_t$, $\beta$ is the filling factor, and N is the number of turns. We assume that $\sin\alpha = 1$ and $\beta = 1$, so the induced emf is

$$E = -\frac{1}{c}\frac{d\Phi}{dt} = \frac{4\pi}{c} NJ_0\omega\sin\omega t.$$

The power corresponding to this signal is

$$P = \frac{1}{r}\left(E_{max}\frac{1}{\sqrt{2}}\right)^2 = \frac{1}{r}\frac{16\pi^2}{2c^2}\omega^2 S^2 N^2 x^2 H^2, \qquad (2)$$

in which r is the circuit resistance. In our case the parameters were $r = 185\,\Omega$, $N = 2550$, $S = 6.2$ cm$^2$, and $H = 1100$ oe. These give with (2) that $P = 2.1 \times 10^{-13}$ w and that $E = (2rP)^{1/2} = 9$ μv, so the signal is rather weak; even an H of 1100 oe gives a signal comparable with the noise, but narrow-band filters eliminate most of this. The signal-to-noise ratio is about 7 or 8 in the present system.

## 2. The Apparatus

The apparatus for detecting and measuring the frequency given by Z has two main parts, namely the Helmholtz coils with the sample and the electronic equipment for measuring the frequency. Figure 2 shows the block diagram; the Helmholtz coils 1 balance out the horizontal component. The sample (distilled water) 4 lies at the center of the coils and is enclosed in the pickup coil 3; this last is itself enclosed in the polarizing coil 2. The emf in coil 3 has the frequency $\omega$; it is amplified by the preamplifier 5 and then is doubled in frequency by the multiplier 6, after which it is again amplified and is fed to the mixer 7, where it is mixed with a signal of frequency $\omega_0$ from the calibrated generator 8. The two frequencies are similar, and the beat frequency $\omega_b = \omega_0 - \omega$ is detected by the detector 9; this is passed through the matching stage 10 to the oscillographs 11 and 12. The MPO-2 oscillograph records the beat frequency on film, together with time marks provided by

the generator.

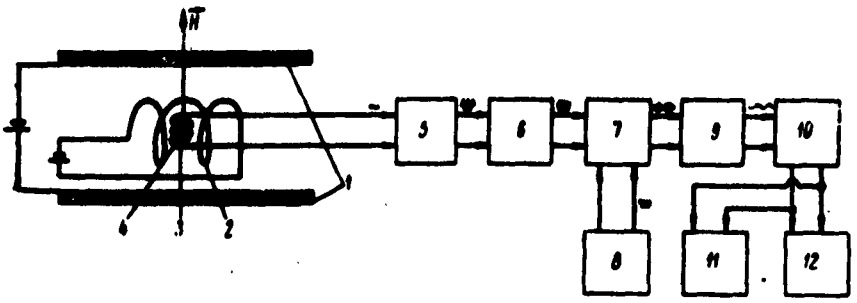


Fig. 2.

The Helmholtz coils (Fig. 3) consist of two flat discs 1 of plexiglass 360 mm in diameter each bearing 112 turns. These discs are fixed to the plexiglass cube 2 (edge 180 mm), the cube being supported on the cylinder 3 mounted on the goniometer stage 4. The leveling screws 5 are used to set the axis of the coils horizontal, the stage providing a means of setting in the correct direction. The cube contains the polarizing coil, within which there is the pickup coil, which is wound on the tube containing the distilled water. The polarizing coil has its axis normal to the axis of the Helmholtz coils and to the axis of the pickup coil. The above dimensions give the Helmholtz coils a field constant of 2.8 oe/a, so the horizontal component at Leningrad (0.15 oe) is balanced by a current of about 55 ma.

The polarizing coil is a straight solenoid lying in a horizontal plane; it has 2200 turns of copper wire (diameter 1 mm) and its constant is 125 oe/a.

The pickup coil consists of 2550 turns (diameter 0.26 mm) and forms part of a tuned circuit in the amplifier; it is tuned to 2075 c/s and its Q is 15-17.

The specimen (distilled water) is contained in a sealed plastic cube of side 2.5 cm (volume 16 cc). This size corresponds to the region of homogeneity. Four of the sides act as former for the pickup coil, so $\beta \approx 1$.

The signal produced by J is amplified by system giving a good signal-to-noise ratio that is stable and not sensitive to external interference. The four-tube system has an over-all gain of $5 \times 10^5$; the first tube (6Zh1P) is triode-connected, to minimize noise in this stage. The main source of noise is the

fluctuations in the coil, though; Nyquist's formula gives this noise voltage as $u^2 = 4kTR\Delta f$, in which k is Boltzmann's constant. T is temperature (°K), $\Delta f$ is bandwidth, and R is resistance.

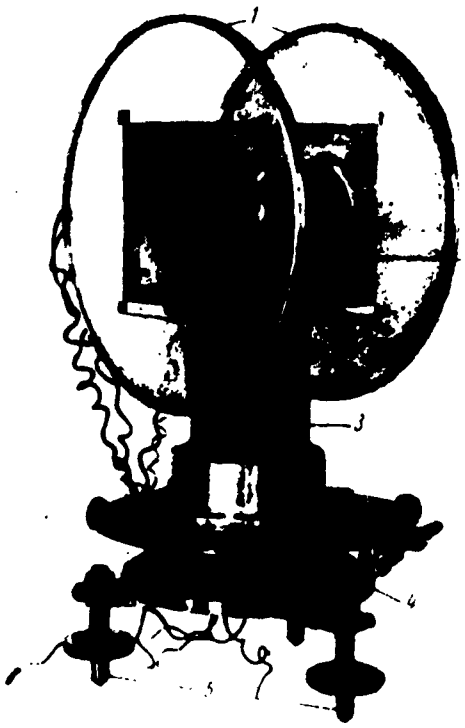


Fig. 3.

Clearly, one way of minimizing the noise is to make the amplifier of small $\Delta f$, but too small a value is undesirable, for the permissible range of variation in L is then small. The $\Delta f$ chosen was $\pm$ 60 c/s for the above central frequency of 2075 c/s; then $\sqrt{u}$ is about 1 μv. The contribution from the 6Zh1P makes the total only 1.5 μv at most, which means a signal-to-noise ratio of 7-8.

The high gain* makes a severe demand on the screening, for any interference entering in the early stages may distort or even mask the signal. All the input circuits were carefully screened, each stage being contained in a separate screened box, the tubes and variable capacitors being enclosed in special screens. Screened cables and couplers were used

*amplification coefficient of $5 \cdot 10^5$

throughout, all screens being grounded. The polarizing coil was short-circuited and grounded when not carrying current; it then acted as a screen for the pickup coil.

The frequency-converting unit includes the doubler, the amplifying filter, the mixer, and a cathode follower. The doubler reduces $\Delta f_c/f_c$ for a given $\Delta f_c$ (error of frequency measurement); it consists of a 6Zh1P whose plate circuit contains the primary of a transformer, whose second is connected to a full-wave rectifier (DGTs-23 diodes). The signal at the output of the doubler is reduced in amplitude and somewhat distorted, so $2f_c$ is isolated and amplified by a stage containing a 6N9S. The mixer compares $2f_c$ with the standard frequency (from a quartz crystal) of 4166 c/s; at the plate of the mixer there appears the beat (difference) frequency $f_b$. A detector containing a DGTs-27 diode is used to isolate $f_b$. The cathode follower feeds the loop oscillograph with the beat frequency, the bias for the tube being produced by a resistance of 200 $\Omega$, only the alternating component reaching the MPO-2 oscillograph (via a 20 $\mu$F capacitor). The quartz oscillator is designed to maintain a fixed frequency within 0.0001%, the fundamental standard being a 100 kc crystal, whose frequency remains constant to this order after it has been running for two hours. The frequency of 4166.6 c/s is generated by successive division by 4 and 6 from 100 kc, the filtered and amplified product being fed to the mixer.

The 100 kc quartz crystal is enclosed in a thermostatic vessel; it forms the first stage in a self-excited oscillator, where it replaces the usual tuned circuit in the grid circuit. This stage uses half a 6N1P. The plate circuit is tuned to 120 kc to improve the stability and is also decoupled. The positive half-cycles are passed to the 4:1 division stage via a circuit consisting of a DGTs-25 diode, a capacitor, and a resistor.

## 3. Results

The horizontal component H is balanced out by setting the axis of the Helmholtz coils in the plane of the magnetic meridian and in the horizontal plane. Any such setting is made with a certain error, so we must consider the effect on the measured Z of any error in balancing H.

Let the coil make an angle $\alpha$ with the horizontal plane (Fig. 4) and an angle $180 - \beta$ with the plane of the magnetic meridian; let the actual field of the coil be $H_1$, which differs from H by $\Delta H = H - H_1$. Then the residual field at the center is given by

$$Z'^2 = (Z + H_1 \sin\alpha)^2 + (H - H_1 \cos\alpha \cdot \cos\beta)^2 + H_1^2 \sin^2\beta,$$

which, if we neglect quantities of the fourth order in $\Delta H$, $\alpha$, and $\beta$ (which are all small), we have

$$Z' - Z = H_1 \sin\alpha + \frac{1}{2}\frac{(\Delta H)^2}{Z} + \frac{1}{2}\frac{H^2}{Z}(\alpha^2 + \beta^2).$$

The largest term is the first, but this is readily eliminated by turning the coil through 180° and taking a second reading Z"; $\alpha$ and $\beta$ then change sign, so $H_1 \sin\alpha$ does so as well. Then Z' - Z and Z" - Z give us the relative error $\Delta Z/Z$ as

$$\frac{\Delta Z}{Z} = \frac{1}{2}\frac{(\Delta H)^2}{Z^2} + \frac{1}{2}\frac{H^2}{Z^2}(\alpha^2 + \beta^2).$$

For example, if the error in balancing H is $\Delta H/H = 0.01$

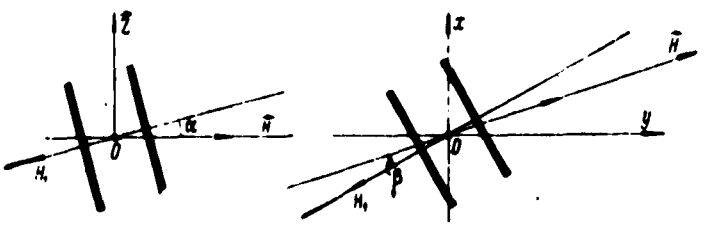


Fig. 4.

and if $\alpha = \beta = 1°$, we have $\Delta Z/Z = 0.00005$, of which 1/7 arises from $\Delta H$ and 6/7 from $\alpha$ and $\beta$.

The H/Z found in the USSR range from 0.001 (in the polar regions) to 0.75, so the $\Delta Z/Z$ for the above conditions range from 0 to 0.00018. The error from all causes can be kept below 0.01% if H is balanced out to within a few % and the angles are correct within 1°.

The current required by the coils at their present site is about 55 ma; the exact value may be determined by experiment.

Let the current be I for exact compensation, which gives a beat frequency $f_b$. Then currents $I_1 = I - \Delta I$ and $I_2 = I + \Delta I$ give $Z' = Z + \Delta Z$ and $f = f_0 + \Delta f$, and so on; this enables one to find $I_1$ and $I_2$ such that $f_b = 0$, which is easily observed. Then the correct current is

$$I = (I_1 + I_2)/2.$$

Our measurements gave I as 53.5 ma, which agrees well with the value calculated above; the precession signal was recorded at intervals of 1 ma from 40 to 70 ma, and also at intervals of 0.5 ma near the point of compensation.

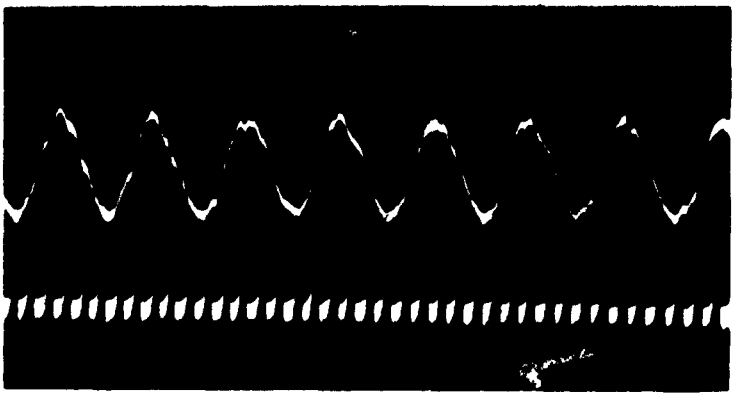

Fig. 5.

Measurements of Z were made at the Kavgolovo laboratory of the All-Union Metrology Research Institute, which is outside the city, on 15 May 1960; recordings were made of the beat frequency and also of time marks separated by 0.01 sec (Fig. 5 is typical). The 19 pairs of measurements are listed in the table. Readings were taken simultaneously from an M-14 magnetometer; recordings were made of the variations in H with a variation instrument. The Z-variometer provided corrections and so enabled us to establish the error of the method; the H variations provided a check on the deviations from exact compensation. One scale division on the M-14 is equivalent to 10 γ, and the readings can be made to within 0.1 division, so the correction for variation can be made to 1 γ. The H-variometer recording showed no major changes during the experiment, and the compensation remained within the permitted limits.

The table shows that the standard deviation is

$$\sigma_{f_b} = \sqrt{\frac{\Sigma(\Delta f)^2}{n(n-1)}} = 0.016 \text{ c/s},$$

in which n is the number of observations; then $f_b = 14.151 \pm 0.016$ c/s. The compensation-current tests showed that $f_o > 2f_c$, for zero beat was obtained for $I_1$ and $I_2$ that were respectively larger and smaller than $I_1$ so $f_o = 2f(Z + \Delta Z)$, in which $f(Z + \Delta Z)$ is the precession frequency for currents $I_1$ and $I_2$.

$\vec{P}_i(d\vec{P}_i/dt) = 0$, so $\vec{P}$ lies at 90° to $d\vec{P}$, the modulus of $\vec{P}$ being constant, so the motion of $\vec{P}$ is that of precession about the direction of $H_t$.

Let $\theta$ be the angle between $\vec{P}$ and $\vec{H}_t$ (Fig. 1); then $d\vec{P}_i$ can be put as $\vec{P}_i \sin\theta d\varphi$, so

$$\frac{d\vec{P}_i}{dt} = \vec{P}_i \sin\theta \frac{d\varphi}{dt} = \omega \vec{P}_i \sin\theta,$$

in which $\omega$ is the angular velocity of $\vec{P}$. We replace $d\vec{P}_i/dt$ here to get

$$\omega = \frac{\mu_i H_T \sin\theta}{\vec{P}_i \sin\theta} = \frac{\mu_i}{\vec{P}_i} H_T = \gamma H_T,$$

in which $\omega$ is the Larmor precession frequency.

Equation (1) should be put as follows if relaxation effects are present, for these resemble damping; replacing $\mu_i$ by J, we have

$$\frac{dJ_x}{dt} = -\gamma [\vec{J}\vec{H}_T]_x - \frac{J_x}{T_2},$$

$$\frac{dJ_y}{dt} = \gamma [\vec{J}\vec{H}_T]_y - \frac{J_y}{T_2},$$

$$\frac{dJ_z}{dt} = -\frac{J_0 - J_z}{T_1}.$$

The conditions for t = 0 are

$$J_0 = J_{x0} + J_{y0} = (\mu H)^2, \quad J_z = 0, \text{ и } \frac{dJ_x}{dt} = \frac{dJ_y}{dt} = 0,$$

and the solution to the equations is

$$J_x = J_0 e^{-\frac{t}{T_1}} \cos(\omega t + \varphi_0),$$

$$J_y = J_0 e^{-\frac{t}{T_1}} \sin(\omega t + \varphi_0),$$

$$J_z = J_0 \left(1 - e^{-\frac{t}{T_1}}\right),$$

in which $\omega = \gamma H_t$ and $\varphi_0$ is the initial phase. Then $\vec{J}$ precesses around $\vec{H}_t$ with a frequency $\omega$ and has a decreasing amplitude; a

cylindrical coil having its axis in the plane of rotation then has a current induced in it. The amplitude of this signal does not depend on the orientation of the coil in the xOy plane but it does depend on the inclination in the zOy plane, for this affects the effective area intersecting the flux. The signal decays gradually, but its amplitude remains adequate for several seconds provided that the relaxation time is long.

The magnetic induction $B_x$ corresponding to $J_x$ is $4\pi J_x$, so the flux linkage $\Phi$ is $B_x SN\beta \sin(\alpha)$, in which S is the effective area of one turn, $\alpha$ is the angle between $J_x$ and $H_t$, $\beta$ is the filling factor, and N is the number of turns. We assume that $\sin \alpha = 1$ and $\beta = 1$, so the induced emf is

$$E = -\frac{1}{c}\frac{d\Phi}{dt} = \frac{4\pi}{c} NJ_0 \omega \sin \omega t.$$

The power corresponding to this signal is

$$P = \frac{1}{r}\left(E_{max}\frac{1}{\sqrt{2}}\right)^2 = \frac{1}{r}\frac{16\pi^2}{2c^2}\omega^2 S^2 N^2 \varkappa^2 H^2, \qquad (2)$$

in which r is the circuit resistance. In our case the parameters were $r = 185\Omega$, N = 2550, S = 6.2 $cm^2$, and H = 1100 oe. These give with (2) that $P = 2.1 \times 10^{-13}$ w and that $E = (2rP)^{1/2} = 9$ μv, so the signal is rather weak; even an H of 1100 oe gives a signal comparable with the noise, but narrow-band filters eliminate most of this. The signal-to-noise ratio is about 7 or 8 in the present system.

## 2. The Apparatus

The apparatus for detecting and measuring the frequency given by Z has two main parts, namely the Helmholtz coils with the sample and the electronic equipment for measuring the frequency. Figure 2 shows the block diagram; the Helmholtz coils 1 balance out the horizontal component. The sample (distilled water) 4 lies at the center of the coils and is enclosed in the pickup coil 3; this last is itself enclosed in the polarizing coil 2. The emf in coil 3 has the frequency $\omega$; it is amplified by the preamplifier 5 and then is doubled in frequency by the multiplier 6, after which it is again amplified and is fed to the mixer 7, where it is mixed with a signal of frequency $\omega_0$ from the calibrated generator 8. The two frequencies are similar, and the beat frequency $\omega_b = \omega_0 - \omega$ is detected by the detector 9; this is passed through the matching stage 10 to the oscillographs 11 and 12. The MPO-2 oscillograph records the beat frequency on film, together with time marks provided by

the generator.

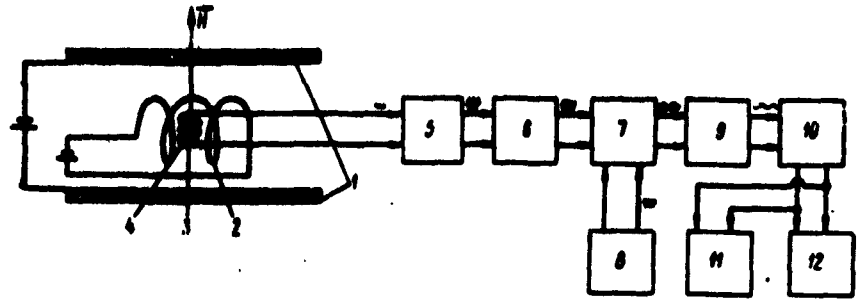


Fig. 2.

The Helmholtz coils (Fig. 3) consist of two flat discs 1 of plexiglass 360 mm in diameter each bearing 112 turns. These discs are fixed to the plexiglass cube 2 (edge 180 mm), the cube being supported on the cylinder 3 mounted on the goniometer stage 4. The leveling screws 5 are used to set the axis of the coils horizontal, the stage providing a means of setting in the correct direction. The cube contains the polarizing coil, within which there is the pickup coil, which is wound on the tube containing the distilled water. The polarizing coil has its axis normal to the axis of the Helmholtz coils and to the axis of the pickup coil. The above dimensions give the Helmholtz coils a field constant of 2.8 oe/a, so the horizontal component at Leningrad (0.15 oe) is balanced by a current of about 55 ma.

The polarizing coil is a straight solenoid lying in a horizontal plane; it has 2200 turns of copper wire (diameter 1 mm) and its constant is 125 oe/a.

The pickup coil consists of 2550 turns (diameter 0.26 mm) and forms part of a tuned circuit in the amplifier; it is tuned to 2075 c/s and its Q is 15-17.

The specimen (distilled water) is contained in a sealed plastic cube of side 2.5 cm (volume 16 cc). This size corresponds to the region of homogeneity. Four of the sides act as former for the pickup coil, so $\beta \approx 1$.

The signal produced by J is amplified by system giving a good signal-to-noise ratio that is stable and not sensitive to external interference. The four-tube system has an over-all gain of $5 \times 10^5$; the first tube (6Zh1P) is triode-connected, to minimize noise in this stage. The main source of noise is the

fluctuations in the coil, though; Nyquist's formula gives this noise voltage as $u^2 = 4kTR\Delta f$, in which k is Boltzmann's constant. T is temperature (°K), $\Delta f$ is bandwidth, and R is resistance.

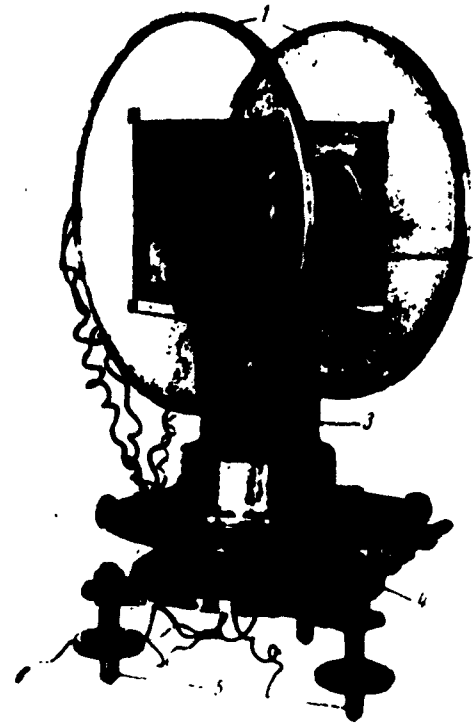


Fig. 3.

Clearly, one way of minimizing the noise is to make the amplifier of small $\Delta f$, but too small a value is undesirable, for the permissable range of variation in Z is then small. The $\Delta f$ chosen was $\pm 60$ c/s for the above central frequency of 2075 c/s; then $\sqrt{u}$ is about 1 μv. The contribution from the 6Zh1P makes the total only 1.5 μv at most, which means a signal-to-noise ratio of 7-8.

The high gain* makes a severe demand on the screening, for any interference entering in the early stages may distort or even mask the signal. All the input circuits were carefully screened, each stage being contained in a separate screened box, the tubes and variable capacitors being enclosed in special screens. Screened cables and couplers were used

*amplification coefficient of $5 \cdot 10^5$

throughout, all screens being grounded. The polarizing coil was short-circuited and grounded when not carrying current; it then acted as a screen for the pickup coil.

The frequency-converting unit includes the doubler, the amplifying filter, the mixer, and a cathode follower. The doubler reduces $\Delta f_c/f_c$ for a given $\Delta f_c$ (error of frequency measurement); it consists of a 6Zh1P whose plate circuit contains the primary of a transformer, whose second is connected to a full-wave rectifier (DGTs-23 diodes). The signal at the output of the doubler is reduced in amplitude and somewhat distorted, so $2f_c$ is isolated and amplified by a stage containing a 6N9S. The mixer compares $2f_c$ with the standard frequency (from a quartz crystal) of 4166 c/s; at the plate of the mixer there appears the beat (difference) frequency $f_b$. A detector containing a DGTs-27 diode is used to isolate $f_b$. The cathode follower feeds the loop oscillograph with the beat frequency, the bias for the tube being produced by a resistance of 200 Ω, only the alternating component reaching the MPO-2 oscillograph (via a 20 μF capacitor). The quartz oscillator is designed to maintain a fixed frequency within 0.0001%, the fundamental standard being a 100 kc crystal, whose frequency remains constant to this order after it has been running for two hours. The frequency of 4166.6 c/s is generated by successive division by 4 and 6 from 100 kc, the filtered and amplified product being fed to the mixer.

The 100 kc quartz crystal is enclosed in a thermostatic vessel; it forms the first stage in a self-excited oscillator, where it replaces the usual tuned circuit in the grid circuit. This stage uses half a 6N1P. The plate circuit is tuned to 120 kc to improve the stability and is also decoupled. The positive half-cycles are passed to the 4:1 division stage via a circuit consisting of a DGTs-25 diode, a capacitor, and a resistor.

## 3. Results

The horizontal component H is balanced out by setting the axis of the Helmholtz coils in the plane of the magnetic meridian and in the horizontal plane. Any such setting is made with a certain error, so we must consider the effect on the measured Z of any error in balancing H.

Let the coil make an angle α with the horizontal plane (Fig. 4) and an angle 180 - β with the plane of the magnetic meridian; let the actual field of the coil be $H_1$, which differs from H by $\Delta H = H - H_1$. Then the residual field at the center is given by

$$Z'^2 = (Z + H_1 \sin\alpha)^2 + (H - H_1 \cos\alpha \cdot \cos\beta)^2 + H_1^2 \sin^2\beta,$$

which, if we neglect quantities of the fourth order in $\Delta H$, $\alpha$, and $\beta$ (which are all small), we have

$$Z' - Z = H_1 \sin\alpha + \frac{1}{2}\frac{(\Delta H)^2}{Z} + \frac{1}{2}\frac{H^2}{Z}(\alpha^2 + \beta^2).$$

The largest term is the first, but this is readily eliminated by turning the coil through 180° and taking a second reading Z"; $\alpha$ and $\beta$ then change sign, so $H_1 \sin\alpha$ does so as well. Then Z' - Z and Z" - Z give us the relative error $\Delta Z/Z$ as

$$\frac{\Delta Z}{Z} = \frac{1}{2}\frac{(\Delta H)^2}{Z^2} + \frac{1}{2}\frac{H^2}{Z^2}(\alpha^2 + \beta^2).$$

For example, if the error in balancing H is $\Delta H/H = 0.01$

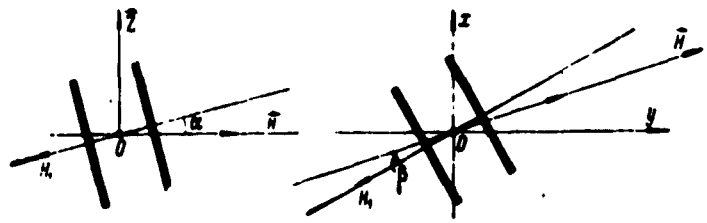


Fig. 4.

and if $\alpha = \beta = 1°$, we have $\Delta Z/Z = 0.00055$, of which 1/7 arises from $\Delta H$ and 6/7 from $\alpha$ and $\beta$.

The H/Z found in the USSR range from 0.001 (in the polar regions) to 0.75, so the $\Delta Z/Z$ for the above conditions range from 0 to 0.00018. The error from all causes can be kept below 0.01% if H is balanced out to within a few % and the angles are correct within 1°.

The current required by the coils at their present site is about 55 ma; the exact value may be determined by experiment.

Let the current be I for exact compensation, which gives a beat frequency $f_b$. Then currents $I_1 = I - \Delta I$ and $I_2 = I + \Delta I$ give $Z' = Z + \Delta Z$ and $f = f_0 + \Delta f$, and so on; this enables one to find $I_1$ and $I_2$ such that $f_b = 0$, which is easily observed. Then the correct current is

$$I = (I_1 + I_2)/2.$$

Our measurements gave I as 53.5 ma, which agrees well with the value calculated above; the precession signal was recorded at intervals of 1 ma from 40 to 70 ma, and also at intervals of 0.5 ma near the point of compensation.

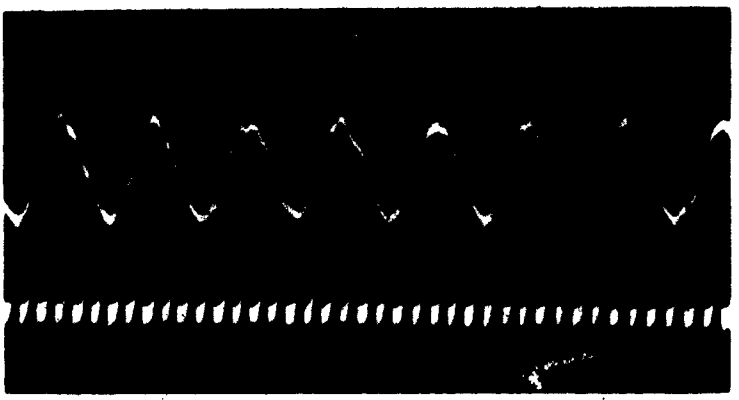

Fig. 5.

Measurements of Z were made at the Kavgolovo laboratory of the All-Union Metrology Research Institute, which is outside the city, on 15 May 1960; recordings were made of the beat frequency and also of time marks separated by 0.01 sec (Fig. 5 is typical). The 19 pairs of measurements are listed in the table. Readings were taken simultaneously from an M-14 magnetometer; recordings were made of the variations in H with a variation instrument. The Z-variometer provided corrections and so enabled us to establish the error of the method; the H variations provided a check on the deviations from exact compensation. One scale division on the M-14 is equivalent to 10 γ, and the readings can be made to within 0.1 division, so the correction for variation can be made to 1 γ. The H-variometer recording showed no major changes during the experiment, and the compensation remained within the permitted limits.

The table shows that the standard deviation is

$$\sigma_{f_0} = \sqrt{\frac{\Sigma(\Delta f)^2}{n(n-1)}} = 0.016 \text{ c/s},$$

in which n is the number of observations; then $f_0 = 14.151 \pm 0.016$ c/s. The compensation-current tests showed that $f_0 > 2f_c$, for zero beat was obtained for $I_1$ and $I_2$ that were respectively larger and smaller than $I_1$ so $f_0 = 2f(Z + \Delta Z)$, in which $f(Z + \Delta Z)$ is the precession frequency for currents $I_1$ and $I_2$.

| № | Observations | | | Reading S e n | $\Delta S$ | $\Delta' f_b = \Sigma \Delta S$ | $f_b$ | $\Delta f_b$ | $(\Delta f_b)^2$ |
|---|---|---|---|---|---|---|---|---|---|
| | $f_b$ 0° | $f_b$ 180° | $f_{b.av}$ | | | | | | |
| 1 | 16,09 | 12,69 | 14,39 | 7,70 | −0,20 | −0,16 | 14,23 | 0,08 | 0,0064 |
| 2 | 16,01 | 12,63 | 14,32 | 7,70 | −0,20 | −0,16 | 14,16 | 0,01 | 0,0001 |
| 3 | 16,12 | 12,71 | 14,41 | 7,70 | −0,20 | −0,16 | 14,25 | 0,10 | 0,0100 |
| 4 | 16,09 | 12,66 | 14,37 | 7,70 | −0,20 | −0,16 | 14,21 | 0,06 | 0,0036 |
| 5 | 15,70 | 12,62 | 14,16 | 7,50 | 0,00 | 0,00 | 14,16 | 0,01 | 0,0001 |
| 6 | 15,74 | 12,62 | 14,18 | 7,50 | 0,00 | 0,00 | 14,18 | 0,03 | 0,0009 |
| 7 | 15,62 | 12,48 | 14,05 | 7,40 | 0,10 | 0,08 | 14,13 | 0,02 | 0,0004 |
| 8 | 15,76 | 12,62 | 14,19 | 7,50 | 0,00 | 0,00 | 14,19 | 0,04 | 0,0006 |
| 9 | 15,58 | 12,27 | 13,93 | 7,40 | 0,10 | 0,08 | 14,01 | 0,14 | 0,0196 |
| 10 | 15,59 | 12,28 | 13,93 | 7,40 | 0,10 | 0,08 | 14,01 | 0,14 | 0,0196 |
| 11 | 15,60 | 12,45 | 14,02 | 7,40 | 0,10 | 0,08 | 14,10 | 0,05 | 0,0025 |
| 12 | 15,71 | 12,62 | 14,16 | 7,50 | 0,00 | 0,00 | 14,16 | 0,01 | 0,0001 |
| 13 | 15,71 | 12,62 | 14,16 | 7,50 | 0,00 | 0,00 | 14,16 | 0,01 | 0,0001 |
| 14 | 15,62 | 12,49 | 14,05 | 7,50 | 0,00 | 0,00 | 14,05 | 0,10 | 0,0100 |
| 15 | 15,65 | 12,58 | 14,12 | 7,50 | 0,00 | 0,00 | 14,12 | 0,03 | 0,0009 |
| 16 | 15,67 | 12,61 | 14,14 | 7,50 | 0,00 | 0,00 | 14,14 | 0,01 | 0,0001 |
| 17 | 15,65 | 12,54 | 14,10 | 7,50 | 0,00 | 0,00 | 14,10 | 0,05 | 0,0025 |
| 18 | 15,80 | 12,66 | 14,23 | 7,50 | 0,00 | 0,00 | 14,23 | 0,08 | 0,0064 |
| 19 | 15,77 | 12,63 | 14,20 | 7,50 | 0,00 | 0,00 | 14,20 | 0,05 | 0,0025 |
| Mean | | | | 7,50 | | | 14,151 | | Σ 0,0874 |

But $f(Z + \Delta Z)$ was larger than $f(Z)$ (= $f_c$), so $f_b > 2f_c$, which means that $f_b$ must be subtracted from $f_b$ to give $2f_c$, so

$$f_c = 1/2\,(4166.667 - 14,151) = (2676.258 \pm 0,008)\ c/s;$$

but $\gamma = 2.67513 \times 10^4$ (in $\text{muss}^{-1}\text{sec}^{-1}$) so

$$Z = \frac{6.28318 \cdot 2076.26}{2.67513 \cdot 10^4} = (48765.8 \pm 0.2) \cdot 10^{-5}\ \text{oe}.$$

## Bibliography


1. Arkadyev, V. K. Zh. Russ. Fiz.-Khim. Obshch., ser. fiz.,* 45, 312 (1913).
2. Bonch-Bruyevich, A. M. Primeneniye elektronnyye lamp v eksperimental'noy fizike (Use of Electron Tubes in Experimental Physics). Moscow, Gostekhizdat, 1954.
3. Dorfman, A. G. Magnitnyye svoystva atomnogo yadra (Magnetic Properties of the Atomic Nucleus). Moscow-Leningrad, Gostekhizdat, 1948.
4. Landau, L. D. and E. M. Lifshits. Mekhanika (Mechanics). Moscow, Fizmatgiz, 1958.
5. Logachev, A. A. Metody magnitorazvedki (Magnetic Survey Methods). Moscow, Gostekhizdat, 1951.
6. Semat, H. Introduction to Atomic Physics. Moscow, Izd. Inost. Lit., 1948.
7. Siforov, M. A. Radiopriyemniki sverkhysokikh chastot (VHF Radio Receivers). Moscow, Oborongiz, 1957.
8. Frish, S. E. and A. Ye. Timoreva. Kurs obshchey fiziki (A Course of General Physics). Moscow-Leningrad, Gostekhizdat, 1952.
9. Frolkin, I. A. Impul'snaya tekhnika (Pulse Techniques). Moscow, Izd. Sov. Radio, 1960.
10. Andrew, E. R. Nuclear Magnetic Resonance. Moscow, Izd. Inost. Lit., 1957.
11. Yanovskiy, B. M. Zemnoy magnetizm (Terrestrial Magnetism). Moscow, Gostekhizdat, 1953.
12. Bloch, F. Phys. Rev., 70, 460 (1946).
13. Packard and Varian. Phys. Rev., 93, 941 (1954).
14. Parcell, E. M., H. C. Torrey, and R. V. Pound. Phys. Rev., 69, 37, 1946.
15. A. Herrinck. Bull. Séances Acad. Bay. Sci. Coll., 4, 3, 743-754 (1958).


*Journal of the Russian Physicochemical Society

# USING NATURAL ELECTROMAGNETIC VARIATIONS FOR INVESTIGATION OF THE EARTH'S UPPER LAYERS

M. N. Berdichevskiy, B. Ye. Bryunelli, A. Ye. Lantsov, and O. M. Raspopov

pp. 49-55

## Introduction

The theory developed by Tikhonov [6], Cagniard [7], and others has been used at Leningrad University and at the All-Union Geophysics Research Institute in new magnetotelluric survey methods, namely magnetotelluric profiling (MTP) and magnetovariation surveying (MVS) [1,4]. MTP consists in recording variations of period 10-60 sec (short-period variations) in the geoelectric field and in the horizontal components of the geomagnetic field at one point only. The mean ratio of these variations indicates the total conductance of the section, which gives an indication of the relief in the reference (high-resistance) horizon. MVS is analogous to the widely used telluric-current methods [3], except that here the geomagnetic variations are recorded instead of the geoelectric ones. The maximal variations in the horizontal components are associated with increased values of the total conductance, which are commonly related to troughs in the crystalline basement.

These methods have become of practical value in studies on the upper layers of the crust as a result of the design of a sensitive short-period magnetometer [5] by Bryunelli at the Department of the Physics of the Earth's Crust at Leningrad University. The first field trials of magnetotelluric methods were made in 1957 in the Tyumen region*[1], and the work was extended in 1958 by the present authors to the Druskininkai-Prenay-Sovetsk profile (about 250 km long) in the Polish-Lithuanian depression, which represents a major trough in the crystalline basement filled with sediments of Paleozoic age. The central part contains Permian gypsum beds within the Paleozoic sediments; these beds are of very high resistance

*Tyumenskaya Oblast'

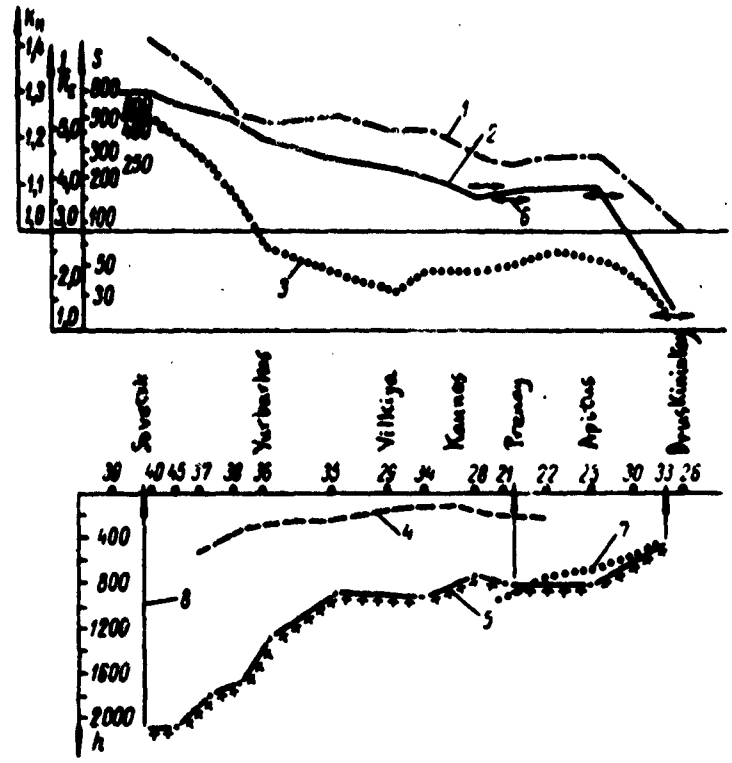


Fig. 1. Magnetotelluric results for the Druskininkay-Sovetsk profile: 1) mean geomagnetic field $K_H$ from MVS; 2) total conductance S of sediments from MTP; 3) reciprocal of the mean telluric field, from telluric-current methods; 4) surface of Permian gypsum from resistance surveys; 5) surface of crystalline rocks from MTP; 6) total conductance of sediments from vertical and frequency sounding techniques; 7) surface of crystalline basement from seismic surveys; 8) deep of the crystalline basement from drilling.

and represent an obstacle to the use of vertical electrical sounding for examining the crystalline basement. Figure 1 shows a section along the above profile, which shows that the thickness of the sediment cover rises from 400 m near

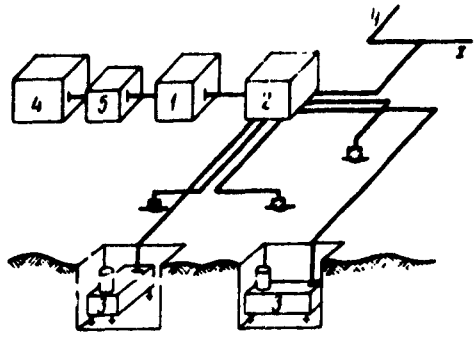


Fig. 2. Apparatus for magnetotelluric studies: 1) oscillograph; 2) switching box; 3) magnetometers; 4) radio station; 5) remote-controlled switch.

Druskininkay to 2100 m near Sovetsk (from drillings).

The apparatus for the magnetotelluric surveys consisted of a four-channel oscillograph coupled to a switching box, two grounded electrical measuring lines, two H-magnetometers, and a radio station with remote-controlled switch. The lines were at right angles and had an arbitrary azimuth, while the magnetometers were set parallel to the lines in shallow pits. The observations were made simultaneously at two points, as in telluric-current methods, the operations being synchronized with remote-controlled switches (Fig. 2).

1. Processing and Results from MTP Recordings.

The processing consists of measuring the apparent amplitudes and periods of 15-30 quasisinusoidal pulses in $E_x$, $E_y$, $H_x$, and $H_y$, from which are deduced the principal axes of the polarization ellipses for the telluric and magnetic fields. The mean period of the associated variations is given by

$$T = \frac{T_x E_x + T_y E_y}{E_x + E_y}, \qquad (1)$$

in which $T_x$ is the mean period for $E_x$ (in sec) and $T_y$ is the same for $E_y$.

The resulting E, H, and T are inserted in the general MTP formula for horizontally homogeneous stratification [4]:

$$S = 796\left[\frac{H}{E} + \sqrt{\frac{T}{10\rho_n}}\right], \qquad (2)$$

in which S is the total longitudinal conductance (mho) and $\rho_n$ is the specific resistance of the reference horizon ($\Omega$-m). A statistical treatment of the individual results eliminates the dependence on azimuth and so improves the accuracy of S. The $\rho_n$ of (2) was taken as 700 $\Omega$-m in the calculations; this was the value given by our magnetotelluric soundings on a nearby area. Figure 3 shows a magnetotelluric sounding curve,

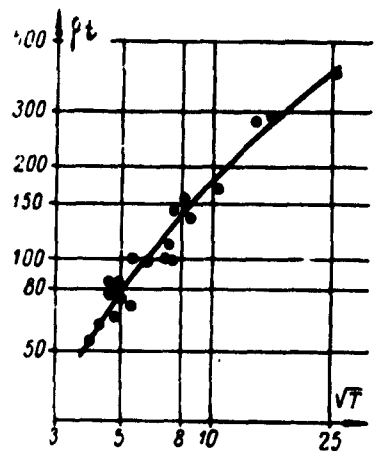


Fig. 3. Magnetotelluric sounding curve.

the ordinate being the apparent resistance $\rho_t$ in Ω-m as given by the formula [6]

$$\rho_t = 0{,}2T\left[\frac{E_x}{H_y}\right]^2,$$

in which $E_x$ is the amplitude of the telluric variations (μv/km), $H_y$ is the amplitude of the geomagnetic variations (γ), and T is the period (sec).

The values of $E_x$, $H_y$, and T were deduced by harmonic analysis of the pulses, the latitudinal component of H and the longitudinal component of E being used. The resulting curve approaches closely the right-hand branch of the theoretical curve for a two-layer section lying above a high-resistance base. A method analogous to that already described [2] was used to interpret this curve and to determine the reference horizon.

Figure 1 shows the curve for the S of the sediments, which rises from 27 mho near Druskininkay to 800 mho near Sovetsk. Repeat measurements indicate that the error in S ranges from 1 to 7%, with a mean of 3%, with values of 15-30% at a few points where the high-resistance gypsum deposits tail off and the wave pattern becomes very complicated. The MTP results agree well with those from logs in deep boreholes and from previous electrical surveys, which shows that the crystalline basement acts as the reference horizon in this region in spite of the high-resistance gypsum beds.

The MTP results were given a quantitative interpretation on the basis of drillings at Sovetsk, Prenay, and Druskininkay, which extended down to the crystalline rocks. The mean $\rho_e$ (longitudinal resistance) of the sediments between boreholes was deduced by linear interpolation; the thickness of the sediments was deduced from

$$h = \rho_e \cdot S.$$

Figure 1 shows the results in the form of the relief of the basement. The results agree with those from seismic

surveys.

## 2. Processing and Results from MVS Recordings

The ellipses method used for telluric currents is employed here; the points derived from transforming the magnetic variation vectors lie closely around arcs of ellipses, which shows that the fluctuating horizontal components of the geomagnetic field at points p and q are related by

$$H_{xq} = aH_{xp} + bH_{yp},$$
$$H_{yq} = cH_{xp} + dH_{yp},$$

in which a, b, c, and d are constants. Theory shows that these are dependent on the directions of the x and y axes as well as on the electrical parameters of the rocks around p and q. The principal parameter used in MVS is $K_H$, which we call the mean magnetic strength; it is the square root of the ratio of the synchronous closed hodographs for the magnetic field and is given by

$$K_H = \frac{\sqrt{AB}}{R},$$

in which A and B are the semiaxes of the ellipse and R is the radius of the circle whose transform is that ellipse. The error in the determination of this parameter is found to be 2-4% in our numerous repeat measurements.

Figure 1 shows $K_H$ for the Druskininkay-Sovetsk profile; it also shows $K_E$, the mean telluric field. Both are taken as unity for the region around Druskininkay. $K_H$ increases as the basement becomes deeper (as the theory of MVS would indicate), becoming 1.42 at Sovetsk, the total anomaly thus being 42%, which is at least 10 times the possible experimental error. Some details of the structure can be seen on the curve for $K_H$, in particular the margins and the central (deepest) part of the depression. The relative anomaly in the alternating geomagnetic field is much less than that in the telluric-current field (the 42% change in $K_H$ corresponds to a sixfold change in $K_E$), so MVS is likely to be of value in regional studies for areas in which telluric-current methods cannot be used. These results confirm that the main theoretical deductions concerning these methods are correct.

In conclusion, we consider the future prospects for the above two methods. The MTP method is of the greater practical interest; it seems likely to replace telluric-current methods in many regions and may well greatly reduce

the cost of electrical surveys, for it eliminates the need for reference grids and base measurements. Moreover, MTP gives a more precise indication of the structure, for the total conductance is determined directly. In particular, it substantially simplifies the stratigraphic assignment of the reference horizon, and it may improve the quantitative calculations so necessary in geology.

The MVS method may prove of great value in regional studies on the permafrost regions of Siberia, for insulating horizons have very little effect on the alternating geomagnetic field. Moreover, MVS may be more productive than telluric-current methods, for it can be operated with simple automatic equipment.

Bibliography


1. Alekseyev, A. M., M. N. Berdichevskiy, B. Ye. Bryunelli, and O. A. Burdo. Nablyudeniya korotkoperiodicheskikh variatsiy elektromagnitnogo polya Zemli [Observation of the short-period variations in the elctromagnetic field of the Earth]. Izv. Akad. Nauk SSSR, ser. geofiz., [News of the Academy of Sciences of the USSR, geophysics series], no. 8 (1959).
2. Berdichevskiy, M. N. K voprosu ob opredeleniya summarnoy prodol'noy provodimosti hadopornykh otlozheniy [Determination of the total longitudinal conductance of strata above reference horizons]. Razvedochnaya i Promyshlovaya Geofizika [Prospecting and Industrial Geophysics], no. 19 (1957).
3. Idem. Elektrorazvedka metodom telluricheskikh tokov [Electrical Prospecting by the Telluric-Current Method]. Moscow, Gostoptekhizdat, 1959.
4. Berdichevskiy, M. N. and B. Ye. Bryunelli. Teoreticheskiye predposylki magnitnotellurichеskogo profilirovaniya [Theoretical principles of magnetotelluric profiling]. Izv. Akad. Nauk SSSR, ser. geofiz., no.7. 1959.
5. Bryunelli, B. Ye., O. M. Raspopov, and B. M. Yanovskiy. Vysokochustvitel'naya mikrovariatsionnaya ustanovka LGU i rezul'taty yeye raboty [The Leningrad University high-sensitivity microvariation apparatus and some results from its use]. Ibid., no. 8 (1959).
6. Tikhonov, A. N. and A. N. Shakhsuvarov. O vozmozhnosti ispol'zovaniya impedansa yestestvennogo elektromagnitnogo polya Zemli dlya issledovaniya yeye verkhnikh sloyev [Possible use of the impedance of the natural electromagnetic field of the Earth for studying the upper layers]. Ibid., No. 4 (1956).
7. Cagniard, L. Basic theory of the magnetotelluric method of geophysical prospecting. Geophysics, 18, no. 3 (1953).

# PLOTTING MAGNETOTELLURIC SOUNDING CURVES ACCORDING TO RECORDINGS OF SHORT-PERIOD VARIATIONS IN THE NATURAL GEOMAGNETIC FIELD

pp. 56-66 A. V. Kovtun

1. The following assumptions form the basis of the theory of magnetotelluric sounding (MTS). Fluctuations in the electric currents in the upper atmosphere produce plane electromagnetic waves whose time dependence is exp(iωt). The Earth is assumed to be flat and to consist of homogeneous layers, so Maxwell's equations can be solved (apart from a constant factor representing the amplitude of the incident wave), the impedance at the surface of the Earth being then

$$Z=\frac{E_x(\omega)}{H_y(\omega)}, \qquad (1)$$

in which $E_x$ and $H_y$ are the mutually perpendicular horizontal field components at the surface [1,6,9], these being dependent solely on frequency and on the structure of the Earth. The individual waves $E_x(\omega)$ and $H_y(\omega)$ are isolated from simultaneous recordings of $E_x$ and $H_y$ to find the relation of Z to $\omega$, which is compared with theoretical curves to determine the nature and parameters of the structure.

These natural variations of periods from 5 sec upwards have been used to examine the electrical structure at great depths since Bryunelli's high-sensitivity short-period magnetometer was developed at the Department of the Physics of the Earth's crust at Leningrad University, this being suitable for use in the field [1,2,8]. The following deductions are based on results from two expeditions made jointly with the All-Union Geophysics Research Institute in conjunction with the Borok

geophysics station*.

Leaving aside any discussion of the theoretical assumptions and of the technical methods of recording the variations (for which see [1,2,8]), I now discuss the practical aspects of the isolation of particular frequencies from the recordings, the object being to construct MTS curves.

2. The short-period variations may be divided into persistent (Pc) and transient (Pt) types; the first type may persist for hours with only slight changes in period and amplitude, the usual ranges being respectively 10-120 sec and 1-2 γ. The Pc are most common in the morning hours; they are not always strong, and as a rule they have only one main period on any given day. The Pt take the form of short bursts of oscillations of decreasing amplitude; they are best seen during the night hours. Even the Pc are not steady-state oscillations, though, which makes it difficult to isolate particular frequencies.

Harmonic analysis of the recordings is essential if the recordings do not indicate a steady state. Let the incident fields $E_x^0$ and $H_y^0$ represent a plane pulse of arbitrary but finite duration; the fields recorded at the surface are $E_x(t)$ and $H_y(t)$, which can be represented as Fourier integrals:

$$E_x(t)=\frac{1}{2\pi}\int_{-\infty}^{\infty} e^{i\omega t}\tilde{E}_x(\omega)\,d\omega,$$

$$H_y(t)=\frac{1}{2\pi}\int_{-\infty}^{\infty} e^{i\omega t}\tilde{H}_y(\omega)\,d\omega,$$

in which ~ denotes quantities representing spectral densities at the Earth's surface:

$$\tilde{E}_x(\omega)=\int_{-\infty}^{\infty} e^{-i\omega t}E_x(t)\,dt, \qquad (2)$$

$$\tilde{H}_y(\omega)=\int_{-\infty}^{\infty} e^{-i\omega t}H_y(t)\,dt.$$

---

*About 10 years have passed since Tikhonov's and Cagniard's papers appeared, but MTS curves have not yet come into use, though the simpler and more rapid magnetotelluric profiling (MTP) [1,2] has been used.

The ratio of these spectral densities is the impedance of the plane wave at the surface:

$$Z=\frac{\tilde{E}_x(\omega)}{\tilde{H}_y(\omega)}. \qquad (3)$$

That is, any varying oscillation should, strictly speaking, be handled by reference to the Fourier integrals for $E_x(t)$ and $H_y(t)$ if Z is to be found. Numerical calculations [5]x show that the build-up time for the electric field is virtually

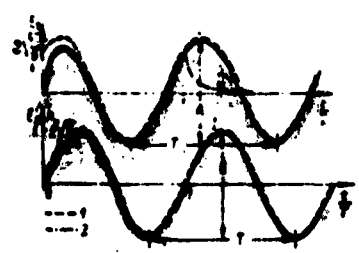

Fig. 1. Build-up of an electromagnetic field over a homogeneous half-space: 1) steady-state field; 2) shape of field pulse II if the incident wave terminates at point 1; $\beta = \sigma/\varepsilon$ (ratio of conductivity to dielectric constant for a homogeneous Earth.

independent of the conductivity; this time is proportional to $T = 2\pi/\omega$ if the Earth may be treated as a uniform half-space, and the steady value is reached within 10% after a time $T/3$ from the start of the plane wave. Transient effects for the magnetic field over a conducting medium are negligible, for the correction for the transient component is small relative to the steady-state component. Figure 1 illustrates the build-up of an electromagnetic field above a homogeneous body.

3. A correct conception of the buildup enables one to avoid tedious calculations on Fourier integrals in many cases; the 'visible amplitudes' may be used to isolate frequencies. This method is as follows. The recordings are examined for a train of pulses whose shape is close to sinusoidal, the distance between adjacent maxima being taken as the period; the visible amplitude of the train is then twice the amplitude for that period (Fig. 1). It is necessary to be very careful in the use of this method, as calculations on transient effects show, for the following reasons.

1) The method is not applicable to single isolated field deviations.

2) The method is applicable only to the middle part of a train of two or three waves differing only slightly in amplitude and period; the first and last waves must be excluded.

3) Transient effects usually alter the shape of the electric-field wave; any lack of correspondance between the wave shapes for the two fields (provided that the two lines have identical characteristics), and especially any difference in the distances between maxima, is a direct indication of transient effects, so such waves must be excluded. The Pc type is the best for this purpose, for the waves can usually be treated as sinusoidal, in spite of some variation in amplitude and period. It is seldom possible to use the Pt type for this purpose.

4. The above method was used with simultaneous recordings made around the Baltic coast in the summer of 1958 at points along the line from Prenay to Sovetsk. The recordings were of inadequate duration and related mainly to one time of day, so the spectrum of the oscillations was rather restricted; only short sections of the frequency curves could be constructed. More interesting results were obtained from continuous recordings at Borok from January to October 1959 [8]. Figure 2 shows curves constructed a) for the north electric component and east magnetic component, and b) for the east and north components as above. Here $\sqrt{T}$ and $\rho$ in $\Omega$-m, being given by

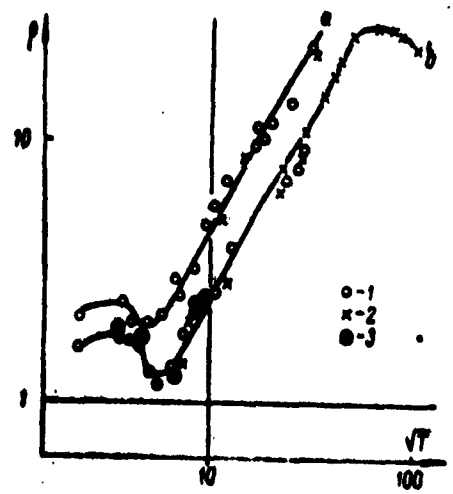


Fig. 2. MTS curves: a) NS, b) EW as constructed 1) from visible amplitudes, 2) by harmonic analysis, 3) from films with $\tau$ = 11 sec after correction for sensitivity.

$$\rho = 0{,}2T\left(\frac{E_x}{H_y}\right)^2, \qquad (4)$$

in which T is in sec, $E_x$ and $H_y$ being measured respectively in mv/km and $\gamma$. The recordings were continuous and were made with a strip speed of 6 mm/min, which provided a means of examining T between 10 and 700 sec. The lack of agreement between curves a and b is a result of inexact setting of the magnetometers relative to the directions used for the electric

components. Recalculation (correction) was possible for $T > 200$ sec, and this gave the same $\rho$ for the two directions. This type of error merely causes a parallel displacement of the curve, which does not interfere with a study of the structure. Physical meanings can be given to the average parameters determined independently from the two curves.

5. As a rule, the $\rho$ given by different recordings for a given period, and even sometimes by one recording, are not the same; the spread in the $\rho$ derived by means of visible amplitudes may be as much as 40-60%, and it is not a consequence of inadequacy in the theory. The spread is largely random and results particularly from errors in the electric-field measurements.

Calculations show that the maximum error in the $\rho$ of (4) may be as much as 80% in some cases, the sources of this being errors in the measurements of $E_x$ and $H_y$ (these may be 10-20% for a mean amplitude of 10 mm), errors in the calibration (not less than 5%), and errors resulting from the frequency response of the instruments (at least 5%). This means that no physical significance can be assigned to individual values; only the general trend (from statistical treatment) is significant. For example, the EW curve of Fig. 2 represents the result of recordings of total duration over 100 hr. The mean-square error of $\rho$ in some cases exceeded 15%, in part because few readings were used. A major improvement here can come only from the use of more sensitive equipment.

There are also systematic errors in the results; for example, the frequency characteristics of the lines were known only for $T \leq 400$ sec. Adjustments were made for $T > 400$ sec by means of theoretical formulas for the magnetometers, which may have given some systematic errors in the $\rho$. Another source of systematic error occurs in the calibration, for which square waves are used. The differing frequency characteristics of the recording instruments for E and H cause an appreciable distortion of the calibration pulses (especially for the magnetic measurements). The amplitude of the pulse at the start may differ from that at the end by 1-2 mm. It is usual to take mean values and to assign the resulting sensitivity to the frequency for which the response of the instrument is maximal; but this is correct only if the maximum in the spectral density for the pulse corresponds to the frequency of maximum response, which is not always so. Some of the recordings at Borok were made with the frequency response of Fig. 3a ($\tau = 11$ sec) for the magnetic channel, for example. Here pulses of duration 1 min were used in the calibration; Fig. 3b shows the spectral density of the pulse, whose maximum lies at 180-200 sec for a duration of 60 sec; the frequency of maximum response corresponds to 30 sec, though. This feature was neglected in the initial processing, so all $\rho$ from this recording deviated greatly from the mean, $\bar{\rho}$.

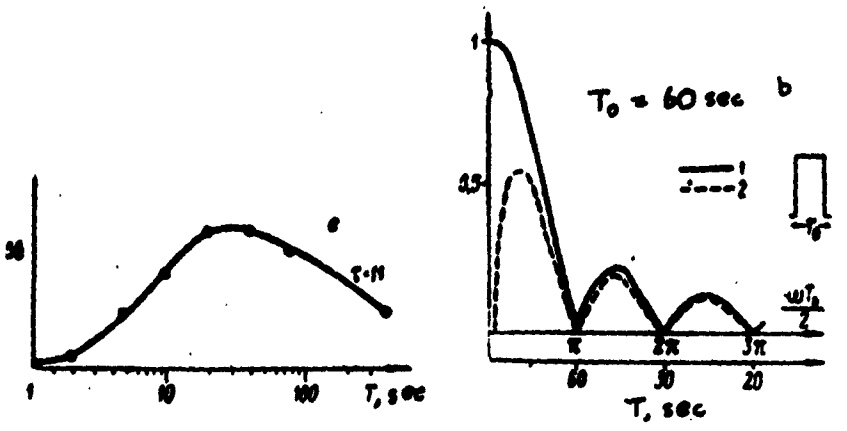


Fig. 3. Change in pulse spectrum after passage through a magnetic measuring line: a) frequency response of the line ($\tau$ = 11 sec), b) spectral density of a square pulse; 1) before, 2) after passage through the line.

Correction for $\tau$ = 11 sec brought all the $\rho$ very close to $\tilde{\rho}$ (Fig. 2). This example shows that care is needed in order to eliminate errors of this type.

6. The Pc type rather rarely has T > 100 sec, so it is necessary to consider bursts of oscillations in order to examine the larger T. The main difficulty here is to select a section for harmonic analysis, for isolated oscillations of fair amplitude are not very common. Incorrect termination of a burst can give rise to large errors in the spectral density.

The cause of the errors is as follows. Let us suppose that the incident wave is an arbitrary function of time; the spectral density of the incident field has a particular meaning for each instant, and so the signal recorded at the Earth's surface from a fraction of the incident wave has a different but related spectral density. However, the main difficulty is that the corresponding electric and magnetic signals are not readily isolated.

The following example illustrates this. Let the incident wave be sinusoidal (Fig. 1) and stop at the time corresponding to point 1. The $E_x$ recorded at the surface will persist past this point (on account of the transient response), but the corresponding magnetic field will vanish almost instantly, for the transient response for this is negligible. It is clear that, if (3) applies precisely to the $H_y$ and $E_x$ of pulse II, the spectral densities of pulses (0-1) in $E_x$ and $H_y$ do not satisfy this

relation; the ratio of the spectral densities of the two has no physical significance. The longer the pulse, the smaller the error introduced by transient effects and the closer the spectral densities to the true values; but it is difficult to estimate the error without calculations on the build-up times for electromagnetic processes in the particular medium. This means that a pulse should not be terminated artificially unless there is some especially compelling reason.

Gol'tsman's method [3,4] is convenient for the analysis of single pulses, for it enables to replace the integration of (2) by a summation without incurring major errors. The corresponding theorem is as follows [2]:

The spectral density $S(\omega)$ of any function f(t) having a spectrum restricted to the region $|\omega| < \omega_0$ may be put as

$$S(\omega) = \Delta t \sum_{k=-\infty}^{\infty} f(k\Delta t) e^{-i\omega k \frac{\pi}{\omega_0}}, \qquad (5)$$

in which $f(k\Delta t)$ are values of f(t) taken at intervals $\Delta t = \pi/\omega_0$.

The limiting frequency $\omega_0$ is readily determined from the shape of the pulse in the following way: $\Delta t$ is made such that the narrowest peak has 4-6 points on it. The summation of (5) presents no difficulty if the number of points is small; vector addition of the terms is sufficient if there are only 20-30 terms. Moreover, for numbers of points less than 73 one can find the spectral density at equally spaced points by means of nomograms [3] or a harmonic analyzer [4].

Several pulse trains differing in length and spectral composition were chosen; the spectral densities were such as to provide values of $\rho$ for T from 36 to 4000 sec. Figure 4 shows one of these. The error in $\rho$ may be 40-80%, on account of large errors in the amplitudes, so the maximum error was considered for each case; only those frequencies for which $\rho$ was likely to be in error by less than 15% were used. The resulting points (Fig. 2) lie close to the curve given by the visible-amplitude method.

7. The EW curve (Fig. 2) was constructed for the range of T from 10 to 4000 sec in these two ways, the range for the NS curve being 10 to 1000 sec. These curves do not provide a reliable interpretation of the structure around Borok without reference to additional information on the upper layers (ones extending down to depths of about 3 km). The conductance of the upper layers near Borok is found reliably as 1600 mho; the general structure at depth can be deduced. The slope of the low-frequency asymptote indicates that the ratio of the resistivity

of the crystalline basement to the resistivity of the conducting layers is over 300.

The behavior of $\rho$ for T small indicates that the conducting layers have a complicated structure. The fall in $\rho$ for T large (which needs to be checked) would correspond to a sharp increase in conductivity at a depth of 300-500 km.

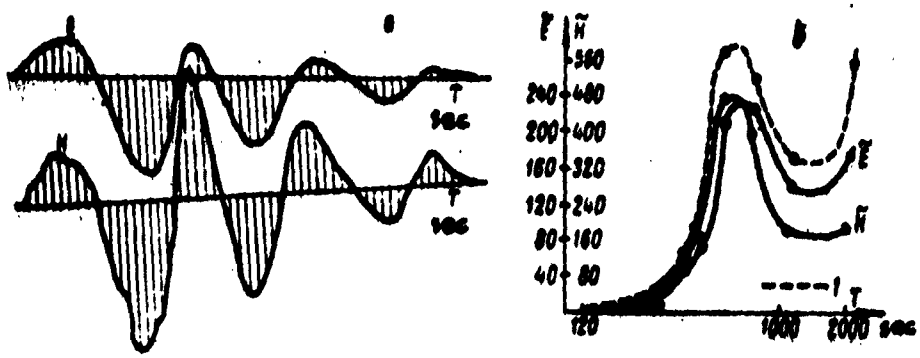


Fig. 4. Spectra of field pulses: a) train of duration 37 min, amplitudes read at intervals of 1 min; b) spectral densities of $\tilde{E}$ and $\tilde{H}$ (the broken line is the curve for $\tilde{H}$ corrected for the frequency response of the instrument).

8. The above results indicate that the following conditions must be satisfied in order to obtain reliable information:

1) The amplitude- and phase-response curves of the instruments recording E and H must be carefully examined;

2) Calibrations should be made with pulse trains; if square waves are used, the conversion factors for instruments differing in frequency response must be examined carefully;

3) The visible-amplitude method may be used, provided allowance is made for all distortions that may be introduced by transient effects; the results must be given a statistical treatment in order to minimize random errors;

4) Waves of T 100 sec are best examined by analysis of short pulse trains of high amplitude, Fourier integrals being used in conjunction with the above theorem in order to simplify the calculations.

I am indebted to students R. Latypova, G. Pokrovskiy, and N. Rudneva for assistance with the calculations.

## Bibliography


1. Berdichevskiy, M. N. and B. Ye. Bryunelli. Teoreticheskiye predposylki magnitotelluricheskogo profilirovaniya [Theoretical assumptions of magnetotelluric profiling]. Izv. Akad. Nauk SSSR, ser. geofiz. [News of the Academy of Sciences of the USSR, geophysics series], no. 7, 1959.
2. Bryunelli, B. Ye., M. N. Berdichevskiy, A. M. Alekseyev, and O. A. Burdo. Nablyudeniya korotkoperiodicheskikh variatsiy elektromagnitnogo polya Zemli [Observations on the short-period variations in the electromagnetic field of the Earth]. Ibid., No. 8, 1959.
3. Goltsman, F. M and Yu. I. Limbakh. Prikladnaya Geofizika [Applied Geophysics], No. 21, 1958.
4. Goltsman, F. M. and T. D. Kalinina. Ibid., No. 21, 1958.
5. K-vtun, A. A. and S. M. Novoselova. Ustanovleniye poley nad sloistoy strukturoy [Build-up of fields over a layered structure]. Nch. Zap. LGU [archives of Leningrad University], No. 286, 1960.
6. Tikhonov, A. N. Ob opredeleniya elektricheskikh kharakteristik glubokikh sloyev zemnoy kory [Determination of the electrical chatacteristics of the deep layers of the Earth's crust]. Dokl. Akad. Nauk SSSR [Proceedings of the Academy of Sciences of the USSR], No. 2, 1950.
7. Kharkevich, A. A. Spektry i analiz [Spectra and Analysis]. Moscow, Gostekhizdat, 1957, pp. 87-90.
8. Yanovskiy, B. M., B. Ye. Bryunelli, and O. M. Raspopov. Mikrovariatsionnaya stantsiya [A microvariation station]. Izv. Akad. Nauk SSSR, ser. geofiz., No. 5, 1960.
9. Cagniard, L. Basic theory of the magnetotelluric method. Geophysics, 18, No. 3, 1953.

CALCULATION OF THE LOW-FREQUENCY DIPOLE FIELD IN THE FAR ZONE

L. B. Gasanenko and G. P. Sholpo

pp. 67-77

## Introduction

We have previously shown [1] that functions $\bar{F}$ and $\bar{F}'$ enable one to express the field components in the far zone for a dipole at the surface of a horizontally layered Earth:

$$\bar{F}(q)=\frac{1}{a}\int_0^\infty J_0(mr)\,\frac{m\,dm}{m+l\alpha}, \tag{0,1}$$

$$\bar{F}'(q)=-\frac{1}{a^2}\int_0^\infty J_1(mr)\,\frac{m^2\,dm}{m+l\alpha}, \tag{0,2}$$

in which r is the distance from the source to the point of observation, a is a complex parameter dependent on frequency and on the electrical structure of the section $q = ar$, and $J_0$ and $J_1$ are Bessel functions of the first kind. We have also shown that the earlier expressions [2] for $\bar{F}$ and $\bar{F}'$ for real arguments may be extended to complex arguments.

Here we deduce the main properties of $\bar{F}$ and $\bar{F}'$, as well as those of the related functions $G_0$ and $G_{-1}$, we give some calculations on frequency sounding curves for the far zone above a three-layer section. It is convenient in what follows to use these expressions:

$$\bar{F}(q)=\frac{1}{q}-lG_0(lq); \tag{0,3}$$

$$\bar{F}'(q)=-\frac{1}{q^2}+G_{-1}(lq). \tag{0,4}$$

Also, $G_0$ and $G_{-1}$ are defined by

$$G_0(rb) = \int_0^\infty J_0(mr)\,\frac{dm}{m+b}; \tag{0,5}$$

$$G_{-1}(rb) = 1 - G_1(rb) = \frac{\partial}{\partial(rb)} G_0(rb). \tag{0,6}$$

For simplicity, we use the notation $b = ia$, so $b = |b|\exp(i\psi)$, in which $|\psi| < \pi$. Standard integrals [3,4] give us that

$$G_0(rb) = \frac{\pi}{2}\,|H_0(rb) - Y_0(rb)|; \tag{0,7}$$

$$G_{-1}(rb) = \frac{\pi}{2}\,|H_{-1}(rb) - Y_{-1}(rb)|. \tag{0,8}$$

Some properties of $G_0$ and $G_{-1}$ are considered below.

## 1. Integral Representations

Expressions (0,7) and (0,8) in principle enable one to calculate the G functions from Struve's function and Bessel functions of the second kind; such calculations are convenient if $|rb| < 7$, while asymptotic expressions are of practically useful accuracy for $|rb| > 14$. This makes it convenient to use quadratures of the integral representations for the range $7 < |rb| < 14$. The integral representation of Struve's function [3]

$$H_\nu(z) = Y_\nu(z) + \frac{\left(\frac{z}{2}\right)^{\nu-1}}{\Gamma\left(\nu+\frac{1}{2}\right)\Gamma\left(\frac{1}{2}\right)} \int_0^{\infty\exp(i\beta)} e^{-u}\left(1+\frac{u^2}{z^2}\right)^{\nu-\frac{1}{2}} du,$$

$$\left(-\frac{\pi}{2} < \beta < \frac{\pi}{2};\ -\frac{\pi}{2}+\beta < \arg z < \frac{\pi}{2}+\beta;\ \text{all } \nu\right)$$

give us that

$$G_0(z) = \int_0^{\infty\exp(i\beta)} e^{-u}\,\frac{du}{\sqrt{u^2+z^2}}; \tag{1,1}$$

$$G_{-1}(z) = z - z \int_0^{\infty \exp(i\beta)} e^{-u} \frac{du}{(u^2 + z^2)^{3/2}} \qquad (1,2)$$

the conditions for $\beta$ and arg z being as before. It is clearly more convenient to perform integration with respect to the real axis; if arg q < 0, the integral representations take the form

$$G_0(iq) = \int_0^\infty e^{-x} \frac{dx}{\sqrt{x^2 - y^2}}; \quad (\arg q < 0); \qquad (1,3)$$

$$G_{-1}(iq) = -iq \int_0^\infty e^{-x} \frac{dx}{(x^2 - q^2)^{3/2}}; \quad (\arg q < 0). \qquad (1,4a)$$

If arg q > 0, integration along the real axis gives an additional integral along a section from u = q to $\infty \exp(i\beta)$, $\beta > \arg q$. This latter integral is included to give

$$G_0(iq) = \int_0^\infty \frac{e^{-x}dx}{\sqrt{x^2 - q^2}} + 2K_0(q); \quad (\arg q > 0) \qquad (1,3b)$$

and analagously

$$G_{-1}(iq) = -iq \int_0^\infty \frac{e^{-x}dx}{(x^2 - q^2)^{3/2}} + i2K_1(q); \quad (\arg q > 0). \qquad (1,4b)$$

Practical applications sometimes make it convenient to use integral representations of the G in terms of Bessel functions of the third kind; these are obtained by replacing the Bessel functions of the first kind in (0,5) and (0,6) by combinations of those of the third kind:

$$J_\nu(x) = \frac{1}{2}\left[H_\nu^{(1)}(x) + H_\nu^{(2)}(x)\right].$$

Then the integral with respect to the real axis splits into two:

$$G_0(rb) = \frac{1}{2}\int_0^\infty H_0^{(1)}(rx) \frac{dx}{x+b} + \frac{1}{2}\int_0^\infty H_0^{(2)}(rx) \frac{dx}{x+b}; \qquad (1,5)$$

$$G_{-1}(rb) = -\frac{1}{2b}\int_0^\infty H_1^{(1)}(rx) \frac{xdx}{x+b} - \frac{1}{2b}\int_0^\infty H_1^{(2)}(rx) \frac{xdx}{x+b}. \qquad (1,6)$$

Now we transfer to integration in the plane of the complex

variable $z = x + iy$; $H_0^{(1)}(z)$ and $H_1^{(1)}(z)$ tend to zero as $z \to \infty$ in the upper half-plane, as do $H_0^{(2)}(z)$ and $H_1^{(2)}(z)$ in the lower half-plane, so the integrals containing $H_0^{(1)}(x)$ and $H_1^{(1)}(x)$ may be replaced by ones with respect to the positive imaginary axis (0 to $i\infty$) and those containing $H_0^{(2)}(x)$ and $H_1^{(2)}(x)$ by ones with respect to the negative imaginary axis (0 to $-i\infty$).

If $|\arg b| < \pi/2$ ($\arg q < 0$), the poles of the integrands in (1,5) and (1,6) lie in the left half-plane, so by alteration of the integration paths we have

$$O_0(iq) = iq\frac{2}{\pi}\int_0^\infty K_0(y)\frac{dy}{y^2-q^2} \quad (\arg q < 0), \tag{1,7a}$$

$$O_{-1}(iq) = -\frac{2}{\pi}\int_0^\infty K_1(y)\frac{y\,dy}{y^2-q^2} \quad (\arg q < 0). \tag{1,8a}$$

If now $\arg b > \pi/2$ ($\arg q > 0$), we have to alter the paths for the integrals containing $H_0^{(2)}$ and $H_1^{(2)}$ to avoid a pole in the fourth quadrant. The integrals of the K functions are thereby altered, the integral representations becoming

$$O_0(iq) = iq\frac{2}{\pi}\int_0^\infty K_0(y)\frac{dy}{y^2-q^2} + 2K_0(q) \quad (\arg q > 0), \tag{1,7b}$$

$$O_{-1}(iq) = -\frac{2}{\pi}\int_0^\infty K_1(y)\frac{y\,dy}{y^2-q^2} + i2K_1(q) \quad (\arg q > 0). \tag{1,8b}$$

It is readily seen that (1,3) and (1,4) are equivalent to (1,7) and (1,8); in fact, if in

$$J(s) = \frac{2s}{\pi}\int_0^\infty K_0(y)\frac{dy}{y^2+s^2}\,; \quad s = iq$$

we replace K by its integral representation ([3], p. 206)

$$K_0(y) = \int_0^\infty \frac{\cos yt}{\sqrt{1+t^2}}\,dt,$$

and alter the order of integration, we have

$$J(s) = \frac{2}{\pi}\int_0^\infty \frac{dt}{\sqrt{1+t^2}}\int_0^\infty \frac{s\cos yt}{y^2+s^2}\,dy.$$

But

$$\int_0^\infty \frac{s\cos yt}{y^2+s^2}\,dy = \begin{cases} \frac{\pi}{2}e^{-st}, & \text{if } \operatorname{Re} s > 0; \\ -\frac{\pi}{2}e^{st}, & \text{if } \operatorname{Re} s < 0; \end{cases}$$

and

$$J(lq) = \begin{cases} \int_0^\infty e^{-lqt}\frac{dt}{\sqrt{1+t^2}}; & \text{if } \operatorname{Re} lq > 0; \\ -\int_0^\infty e^{lqt}\frac{dt}{\sqrt{1+t^2}}; & \text{if } \operatorname{Re} lq < 0. \end{cases}$$

The substitutions

$$lqt = x \text{ where } \operatorname{Re} lq > 0,$$
$$lqt = -x \text{ where } \operatorname{Re} lq < 0$$

give us that

$$J(lq) = \int_0^\infty e^{-x}\frac{dx}{\sqrt{x^2-q^2}},$$

which makes it obvious that (1,3a) is equivalent to (1,7). The equivalence of (1,4a) to (1,3a) follows from (0,6) and the equivalence of (1,3) and (1,7)*.

## 2. Asymptotic Expansions

Asymptotic expressions for the G follow from the asymptotic expansion for Struve functions ([3], p. 163):

$$\mathbf{H}_\nu(z) = Y_\nu(z) + \frac{1}{\pi}\sum_{m=0}^{p-1}\frac{\Gamma\left(m+\frac{1}{2}\right)}{\Gamma\left(\nu+\frac{1}{2}-m\right)}\left(\frac{z}{2}\right)^{\nu-2m-1} + O(z^{\nu-2p-1}),$$

---

*(1,7) and (1,8) imply for $0 \le \varphi \le \pi/2$ that

$$G_0(lpe^{l\varphi}) = -\overline{G_0(lpe^{-l\varphi})} + 2K_0(pe^{l\varphi}),$$
$$G_1(lpe^{l\varphi}) = \overline{G_1(lpe^{-l\varphi})} - l2K_1(pe^{l\varphi}),$$

in which the bars denote complex conjugates.

in which $|\arg z| < \pi$. Putting $z = iq$ and $\nu = 0$ and $-1$, we have

$$O_0(iq) = \frac{1}{I}\sum_{m=0}^{p-1}\frac{[(2m-1)!!]^2}{q^{2m+1}} + O(q^{-2p-1}); \qquad (2,1)$$

$$O_{-1}(iq) = \sum_{m=0}^{p-1}\frac{(2m-1)!!(2m-1)!!}{q^{2m+2}} + O(q^{-2p-2}). \qquad (2,2)$$

The asymptotic expressions are readily derived from the integral representations if we observe that the main contribution for large $\mathrm{Re}(q^2)$ comes from parts of the integration path for which the variable of integration is much less than q. We expand the $(x^2 - q^2)^{-\frac{1}{2}}$ of (1,3) and the $1/(y^2 - q^2)$ of (1,7) as power series in the variable and integrate the series term by term to get

$$O_0(iq) = \frac{1}{I}\sum_{m=0}^{p-1}\frac{[(2m-1)!!]^2}{q^{2m+1}} + 2\nu K_0(q) + O(q^{-2p-1});$$

$$O_{-1}(iq) = \sum_{m=0}^{p-1}\frac{(2m-1)!!(2m-1)!!}{q^{2m+2}} + i2\nu K_1(q) + O(q^{-2p-2});$$

$$\bar{F}(q) = -\sum_{m=1}^{p-1}\frac{[(2m-1)!!]^2}{q^{2m+1}} - i2\nu K_0(q) + O(q^{-2p-1});$$

$$\bar{F}'(q) = \sum_{m=1}^{p-1}\frac{(2m+1)!!(2m-1)!!}{q^{2m+2}} + i2\nu K_1(q) + O(q^{-2p-2}),$$

in which $\nu$ takes the following values: (MacDonald function):

$$\nu = 0 \text{ where } \arg q < 0,$$
$$\nu = 1\,2 \text{ " } \arg q = 0,$$
$$\nu = 1 \text{ " } \arg q > 0.$$

More convenient approximate expressions that converge for all values of q may be derived as follows. The representations

(2,1) and (2,2) were deduced via integrals of the type

$$F(a)=\int_0^\infty p(x)\cdot f(x^\mu+a)\,dx,$$

in which p(x) is a weighting function that decreases rapidly as $x$ increases; it is exp(-x) for (1,3) and (1,4), $K_0(x)$ for (1,7), and $xK_1(x)$ for (1,8). Approximate values for such integrals may be obtained by replacing $f(x^\mu + a)$ by a few of its early terms in a series around the zero point; but this is not the best approximation, for more accurate expressions are obtained if instead of n terms of a simple power series for f we use a polynomial of the same degree that provides quadratures of the highest degree of accuracy [5]. Then the approximate value of the integral is determined by the quadrature sum

$$F(a)\approx\sum_{k=1}^{n}A_k f(x_k+a),$$

in which

$$A_k=\frac{a_n}{a_{n-1}}\cdot\frac{1}{P_n'(x_k)\,P_{n-1}(x_k)},$$

$a_n$ being the coefficient to the term of highest degree in the orthonormalized polynomial of degree n, $P_n(x) = a_n x^n + b_n x^{n-1} + \ldots\ldots$; and the $x_k$ being the roots of $P_n(x)$.

The larger a, the more precise the value given by this sum, and so the expression may be considered as asymptotic.

If f is $f(x + a)$ and $p(x) = x^m\exp(-x)$ $(m = 1, 2, 3, \ldots)$, the polynomials we require are the Tschebyscheff-Laguerre polynomials, so the coefficients in the sum and the roots are known. If $\mu \neq 1$ or if m is not an integer, we require a new system of orthogonal polynomials containing powers of $x^\mu$.

If

$$p(x)=K_0(x)x^m,$$
$$p(x)=K_1(x)x^m,$$

we again need to construct a suitable system of orthogonal polynomials, whose roots must be found; the coefficients in the sum must also be calculated. The methods to be used here are standard.

The components of the electromagnetic field in the far zone involve integrals whose weighting functions are $(2/\pi)K_0(y)$, $(2y/\pi)K_1(y)$, and $(2y^3/\pi)K_3(y)$; there is also the function $f(y^2) = 1/(y^2 - q^2)$ to consider.

The roots of polynomials in $y^2$ that are orthogonal on the half-axis $(0,\infty)$ and the coefficients of the quadrature sums for integrals of the form

$$\frac{2}{\pi}\int_0^\infty K_n(y)\,y^m f(y^2)\,dy$$

are given in the table.

| | $y_1^2$ | $A_1$ | $y_s^2$ | $A_s$ |
|---|---|---|---|---|
| $\frac{2}{\pi}K_0(y)$ | 1 | 1 | ${}_1y_2^2$ 0,683994<br>${}_2y_2^2 = 26,316006$ | $A_2$ 0,987671<br>${}_2A_2 = 0,0123286$ |
| $\frac{2}{\pi}K_1(y)\,y$ | 3 | 1 | ${}_1y_2^2 = 1,972244$<br>${}_2y_2^2 = 38,027756$ | ${}_1A_2 = 0,9714952$<br>${}_2A_2 = 0,0285048$ |
| $\frac{2}{3\pi}K_1(y)\,y^3$ | 15 | 1 | ${}_1y_2^2 = 9,921970$<br>${}_2y_2^2 = 74,078030$ | ${}_1A_2 = 0,9208488$<br>${}_2A_2 = 0,0791512$ |

## 3. Power Series

The usual definitions of cylindrical functions [3] readily show that $G_0(z)$ and $G_1(z)$ are defined by power series:

$$G_0(z)=\sum_{m=0}^{\infty}(-1)^m\left\{\frac{z^{2m+1}}{[(2m+1)!!]^2}-\frac{z^{2m}}{2^{2m}(m!)^2}\left(\ln z+C'-\sum_{k=1}^{m}\frac{1}{k}\right)\right\};$$

$$G_1(z)=\frac{1}{z}-\sum_{m=1}^{\infty}(-1)^m\left\{\frac{z^{2m}}{(2m+1)!!(2m-1)!!}-\frac{z^{2m-1}}{2^{2m-1}(m-1)!\,m!}\times\left(\ln z+C'-\frac{1}{2m}-\sum_{k=1}^{m-1}\frac{1}{k}\right)\right\},$$

$$C'=-0,11593152.$$

For z = iq we have

$$Q_0(iq)=\sum_{m=0}^{\infty}\left\{\frac{iq^{2m+1}}{[(2m+1)!!]^2}-\frac{q^{2m}}{2^{2m}(m!)^2}\left(\ln q+i\frac{\pi}{2}+C'-\sum_{k=1}^{m}\frac{1}{k}\right)\right\};$$

$$Q_1(iq)=-\frac{i}{q}-\sum_{m=1}^{\infty}\left\{\frac{q^{2m}}{(2m+1)!!(2m-1)!!}+\frac{iq^{2m-1}}{2^{2m-1}(m-1)!\,m!}\right.$$
$$\left.\times\left(\ln q+i\frac{\pi}{2}+C'-\frac{1}{2m}-\sum_{k=1}^{m-1}\frac{1}{k}\right)\right\}.$$

and for $\bar{F}(q)$ and $\bar{F}'(q)$

$$\bar{F}(q)=\frac{1}{q}+\sum_{m=0}^{\infty}\left\{\frac{q^{2m+1}}{[(2m+1)!!]^2}+\frac{iq^{2m}}{2^{2m}(m!)^2}\left(\ln q+i\frac{\pi}{2}+C'-\sum_{k=1}^{m}\frac{1}{k}\right)\right\};$$

$$\bar{F}'(q)=1+\frac{i}{q}-\frac{1}{q^2}+\sum_{m=1}^{\infty}\left\{\frac{q^{2m}}{(2m+1)!!(2m-1)!!}+\frac{iq^{2m-1}}{2^{2m-1}(m-1)!\,m!}\right.$$
$$\left.\times\left(\ln q+i\frac{\pi}{2}+C'-\frac{1}{2m}-\sum_{k=1}^{m-1}\frac{1}{k}\right)\right\}.$$

The functions have many values (on account of the presence of the logarithm of the independent variable), which difficulty can be removed by assuming that the z plane is cut off along the negative real axis.

## 4. Field Components

The dipole is magnetic and vertical; it lies at the exposed surface of an N-layer horizontal structure in which only the base is nonconducting ($\sigma_l \neq 0$ for $l = 1, 2, \ldots, N-1$; $\sigma_N = 0$). The field components are expressed in terms of $\bar{F}(q)$ and $\bar{F}'(q)$ as follows [V]:

$$e_\varphi=-2\Phi_1 q^2\bar{F}'(q);$$
$$h_z=2\Phi_1[1+q^2F(q)];$$
$$h_r=-i2\Phi_1 q^2\bar{F}'(q),$$

in which

$$\Phi_1=\kappa_N z_1^2:\tilde{\rho}_m;\quad q=\frac{r}{d_1}\Phi_0;\quad \Phi_0=-i\frac{\kappa_1 d_1 N^2_1}{\tilde{\rho}_m};$$

$$\tilde{\rho}_\omega = {}_N z_1^2 + ({}_N z_1^2 - 1) \prod_{l=2}^{N-1} \frac{{}_N z_l^2 - 1}{{}_N z_l^2 - \frac{\sigma_l}{\sigma_{l-1}}};$$

the effective impedance at the top edge of the first layer in the N-layer structure is

$${}_N z_1 = \operatorname{cth}\left[\varkappa_1 d_1 + \operatorname{arcth} \sqrt{\frac{\sigma_1}{\sigma_2}}\, {}_N z_2\right],$$

and the corresponding impedances for the other layers are given by analogous expressions. The apparent resistivities are given by

$$\frac{\tilde{\rho}^{\varphi}_{\omega}}{\rho_1} = \frac{e_{\varphi}}{e_{\varphi\,\text{n.s}}} = i\,\frac{8\pi^2}{6}\left(\frac{\lambda_1}{d_1}\right)^{-2}\left(\frac{r}{d_1}\right)^2 e_{\varphi};$$

$$\frac{\tilde{\rho}^{z}_{\omega}}{\rho_1} = \frac{h_z}{h_{z\,\text{n.s}}} = i\,\frac{8\pi^2}{18}\left(\frac{\lambda_1}{d_1}\right)^{-2}\left(\frac{r}{d_1}\right)^2 h_z;$$

$$\sqrt{\frac{\tilde{\rho}^{r}_{\omega}}{\rho_1}} = \frac{h_r}{h_{r\,\text{n.s}}} = \sqrt{i}\,\frac{2\pi\sqrt{2}}{6}\left(\frac{\lambda_1}{d_1}\right)^{-1}\left(\frac{r}{d_1}\right) h_r,$$

in which

$$e_{\varphi\,\text{n.s}} = \frac{6}{\varkappa_1^2 r^3}; \quad \varkappa_1 = 2{,}81\sqrt{f\sigma_1}\ \text{км}^{-1};$$

$$h_{z\,\text{n.s}} = \frac{18}{\varkappa_1^3 r^3}; \qquad f \text{ in c/s.}$$

$h_{rH.B} = 6/\varkappa_1 r$, and $\sigma_1$ is in $\text{ohm}^{-1}.\text{m}^{-1}$.

Tables of $\Phi_0$ and $\Phi_1$ as functions of $\lambda_1/d_1$ and of $\bar{F}$ and $\bar{F}^1$ as functions of q enable one to construct frequency-sounding curves for the far zone by means of elementary calculations.

The figure shows the apparent resistivity as deduced from the electric field of a vertical magnetic dipole at the surface of a three-layer structure whose parameters are

$$\frac{\rho_2}{\rho_1} = \frac{1}{4}; \quad \frac{d_2}{d_1} = 3; \quad \rho_3 = \infty.$$

The full lines represent curves derived from asymptotic expressions for the far zone; the broken lines, curves for

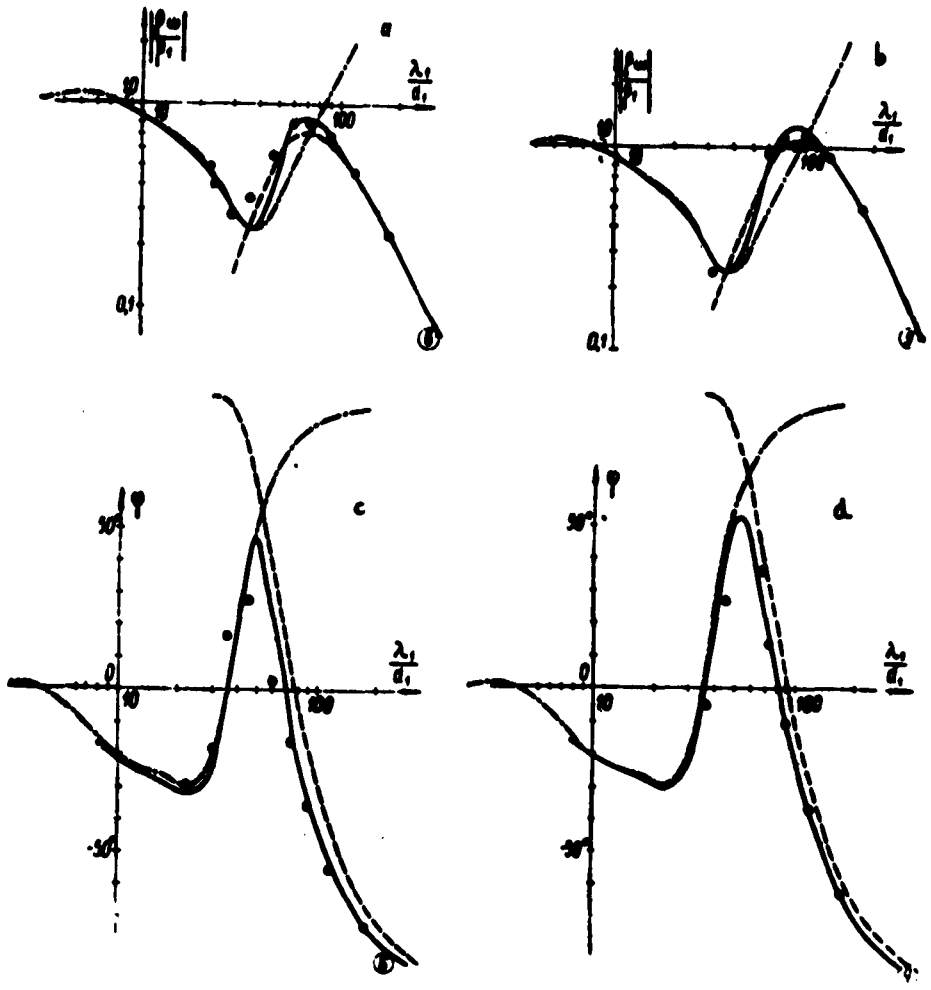


the S zone; and the dot-and-dash lines, wave curves. The points represent values derived from quadratures of the integral solutions, and the encircled figures give the ratio of the distance to the depth of the base.

Numerical integration has been used to test the amplitude and phase curves, and also the wave curves and the curves

for the S zone; it appears that the asymptote for the far zone gives much better approximation than that for the wave zone at high frequencies and than that for the S zone for low frequencies, the range being that used in frequency sounding. The frequency-sounding curves for r = 6D and r = 9D show that the amplitude and phase curves for the magnetic-source electric-detector method may be calculated from the formulas for the far zone provided that the distance from source to detector is more than six times the distance down to the insulating base. If a magnetic detector is used, the distances must be much larger before the asymptote for the far zone gives acceptable accuracy.

Bibliography


1. Vanyan, L. L., L. B. Gasanenko, and G. P. Sholpo. Asimptoticheskoye predstavleniye elektromagnitnogo polya nizkochastotnogo dipolya [Asymptotic representation of the electromagnetic field of a low-frequency dipole]. Uch. Zap. Leningrad. Gos. Univ. [Archives of Leningrad University], No. 286 (1960).
2. Gasanenko, L. B. and G. P. Sholpo. K teoriii elektromagnitnogo zondirovaniya [Theory of electromagnetic sounding]. Ibid., No. 286, 1960.
3. Watson, G. N. Theory of Bessel Functions, vol. 1. Izd. Inost. Lit., 1948.
4. Bursian, V. R. Teoriya elektromagnitnykh poley, primenyayemykh v elektrorazvedke (Theory of the Electromagnetic Fields used in Electrical Prospecting), part 2, Izd. Leningrad. Gos. Univ., 1936.
5. Krylov, V. I. Priblizhennoye vychisleniye integralov (Approximate Calculation of Integrals). Moscow, Fizmatgiz, 1959.

# SOME FUNCTIONS OF THE COMPLEX ARGUMENT WHICH APPEAR IN THE LOW-FREQUENCY FIELD THEORY

L. B. Gasanenko, G. P. Sholpo, and E. I. Terekhin

pp. 78-109

Problems of the fields produced by a low-frequency source often have integral solutions that can be expressed via functions $G_0$ and $G_1$ of complex argument (e.g., a vertical magnetic dipole in air [6], an infinitely long cable [1], remote dipole sources at the surface of a horizontally bedded structure [4]). Bursian remarked on the value of tables of these long ago [1], but they appear not yet to have been published.

Recent rapid developments in the geophysical uses of low-frequency fields have made such tables vital in geophysics; but specialists dealing with the publication of tabulated functions have been forced to concentrate on tables of greater use in mathematics. For this reason, workers in the Geoelectricity Laboratory of the Physics Research Institute at Leningrad University in 1959 decided to tabulate these functions and related ones.

The functions $G_n(z)$ are [1] defined by

$$G_n(z) = \frac{\pi}{2} |H_n(z) - Y_n(z)|.$$

The properties of Struve and Weber functions give rise to the following properties of $G_n(z)$:

$$G_{n-1}(z) + G_{n+1}(z) = \frac{2n}{z} G_n(z) + \frac{z^n}{(2n+1)!!},$$

$$\frac{d}{dz} G_n(z) = G_{n-1}(z) - \frac{n}{z} G_n(z),$$

$$\frac{d}{dz} |z^n G_n(z)| = z^n G_{n-1}(z),$$

$$\frac{d}{dz}\left[\frac{1}{z^n}G_n(z)\right]=\frac{1}{z^n}\left[G_{n-1}(z)-\frac{2n}{z}G_n(z)\right]=\frac{1}{z^n}\left[G_{n+1}(z)-\frac{z^n}{(2n+1)!!}\right].$$

$$G_n(\rho,-\varphi)=\overline{G_n(\rho,\varphi)},$$

in which $G_n(\rho,\varphi)$ denotes a function of $z=\rho\exp(i\varphi)$ and $G_n(\rho,-\varphi)$ denotes a function of $\bar{z}=\rho\exp(-i\varphi)$:

$$G_n(\rho,\varphi)=\mathrm{Re}\,G_n(\rho,\varphi)+i\,\mathrm{Im}\,G_n(\rho,\varphi);$$
$$\overline{G_n(\rho,\varphi)}=\mathrm{Re}\,G_n(\rho,\varphi)-i\,\mathrm{Im}\,G_n(\rho,\varphi).$$

The relation between $H_n(z)$ and $L_n(z)$ is [2]

$$H_n(iz)=i^{n+1}L_n(z),$$

so

$$G_0(iz)=\frac{\pi}{2}[iL_0(z)-Y_0(iz)];$$

$$G_1(iz)=-\frac{\pi}{2}[L_1(z)+Y_1(iz)].$$

The functions $\bar{F}(z)$ and $\bar{F}'(z)$ that are used to express the field components in the far zone of a low-frequency dipole [4] are given by

$$\bar{F}(z)=\frac{1}{z}-iG_0(iz);$$

$$\bar{F}'(z)=1-\frac{1}{z^2}-G_1(iz).$$

The following tables* are for $G_0(iz)$ and $G_1(iz)$ (Table 1), and also for $z^2\bar{F}'(z)$ (Table 2) as functions of $z=\rho\exp(i\varphi)$ for the following values of the modulus and phase of the independent variable:

$$\rho=0(0{,}1)6;\quad \varphi=\pm 0(5^0)45^0;$$

$$G_{0,1}(iz)=\mathrm{Re}\,G_{0,1}(iz)+i\,\mathrm{Im}\,G_{0,1}(iz);$$

in which

$$z^2\bar{F}'(z)=|z^2\bar{F}'(z)|\,e^{i\alpha}.$$

---

*We were assisted in the work of tabulation by L. N. D'yachenko, N. A. Skorman, O. A. Cherdyntsova, and L. N. Molotkova. The calculations were performed at Leningrad Mechanized Accounting Works with desk calculating machines.

Table 1.

$\varphi = 0$

| $\rho$ | $\mathrm{Re}G_0$ | $-\mathrm{Im}G_0$ | $\mathrm{Re}G_1$ | $-\mathrm{Im}G_1$ | $\rho$ | $\mathrm{Re}G_0$ | $-\mathrm{Im}G_0$ | $\mathrm{Re}G_1$ | $-\mathrm{Im}G_1$ |
|---|---|---|---|---|---|---|---|---|---|
| 0 | $\infty$ | 1,5708 | 0 | $\infty$ | 3,0 | 0,0347 | 0,3646 | 0,8746 | 0,0402 |
| 0,1 | 2,4271 | 1,4746 | 0,0753 | 9,9638 | 3,1 | 0,0310 | 0,3524 | 0,8816 | 0,0356 |
| 0,2 | 1,7527 | 1,3856 | 0,1445 | 4,7760 | 3,2 | 0,0276 | 0,3409 | 0,8882 | 0,0316 |
| 0,3 | 1,3725 | 1,3033 | 0,2081 | 3,0560 | 3,3 | 0,0246 | 0,3300 | 0,8943 | 0,0281 |
| 0,4 | 1,1145 | 1,2271 | 0,2666 | 2,1844 | 3,4 | 0,0220 | 0,3197 | 0,9000 | 0,0250 |
| 0,5 | 0,9244 | 1,1565 | 0,3204 | 1,6564 | 3,5 | 0,0196 | 0,3100 | 0,9053 | 0,0222 |
| 0,6 | 0,7775 | 1,0910 | 0,3699 | 1,3028 | 3,6 | 0,0175 | 0,3008 | 0,9103 | 0,0198 |
| 0,7 | 0,6605 | 1,0303 | 0,4154 | 1,0503 | 3,7 | 0,0156 | 0,2920 | 0,9149 | 0,0176 |
| 0,8 | 0,5653 | 0,9740 | 0,4573 | 0,8618 | 3,8 | 0,0140 | 0,2838 | 0,9192 | 0,0157 |
| 0,9 | 0,4867 | 0,9217 | 0,4960 | 0,7165 | 3,9 | 0,0125 | 0,2759 | 0,9233 | 0,0140 |
| 1,0 | 0,4210 | 0,8731 | 0,5316 | 0,6019 | 4,0 | 0,0112 | 0,2684 | 0,9271 | 0,0125 |
| 1,1 | 0,3656 | 0,8279 | 0,5644 | 0,5098 | 4,1 | 0,0100 | 0,2613 | 0,9306 | 0,0111 |
| 1,2 | 0,3185 | 0,7859 | 0,5946 | 0,4346 | 4,2 | 0,0089 | 0,2545 | 0,9339 | 0,0099 |
| 1,3 | 0,2782 | 0,7467 | 0,6225 | 0,3725 | 4,3 | 0,0080 | 0,2481 | 0,9370 | 0,0089 |
| 1,4 | 0,2437 | 0,7103 | 0,6482 | 0,3208 | 4,4 | 0,0071 | 0,2419 | 0,9400 | 0,0079 |
| 1,5 | 0,2138 | 0,6763 | 0,6720 | 0,2774 | 4,5 | 0,0064 | 0,2361 | 0,9427 | 0,0071 |
| 1,6 | 0,1880 | 0,6446 | 0,6939 | 0,2406 | 4,6 | 0,0057 | 0,2305 | 0,9453 | 0,0063 |
| 1,7 | 0,1655 | 0,6151 | 0,7142 | 0,2094 | 4,7 | 0,0051 | 0,2251 | 0,9477 | 0,0057 |
| 1,8 | 0,1459 | 0,5874 | 0,7330 | 0,1828 | 4,8 | 0,0046 | 0,2200 | 0,9500 | 0,0051 |
| 1,9 | 0,1288 | 0,5616 | 0,7504 | 0,1597 | 4,9 | 0,0041 | 0,2151 | 0,9521 | 0,0045 |
| 2,0 | 0,1139 | 0,5374 | 0,7664 | 0,1399 | 5,0 | 0,0037 | 0,2104 | 0,9541 | 0,0040 |
| 2,1 | 0,1008 | 0,5148 | 0,7812 | 0,1227 | 5,1 | 0,0033 | 0,2059 | 0,9560 | 0,0036 |
| 2,2 | 0,0893 | 0,4936 | 0,7949 | 0,1079 | 5,2 | 0,0030 | 0,2016 | 0,9578 | 0,0032 |
| 2,3 | 0,0791 | 0,4738 | 0,8077 | 0,0950 | 5,3 | 0,0027 | 0,1975 | 0,9595 | 0,0029 |
| 2,4 | 0,0702 | 0,4552 | 0,8196 | 0,0837 | 5,4 | 0,0024 | 0,1935 | 0,9611 | 0,0026 |
| 2,5 | 0,0623 | 0,4377 | 0,8305 | 0,0739 | 5,5 | 0,0021 | 0,1897 | 0,9626 | 0,0023 |
| 2,6 | 0,0554 | 0,4212 | 0,8406 | 0,0653 | 5,6 | 0,0019 | 0,1860 | 0,9641 | 0,0021 |
| 2,7 | 0,0492 | 0,4058 | 0,8501 | 0,0577 | 5,7 | 0,0017 | 0,1825 | 0,9654 | 0,0019 |
| 2,8 | 0,0438 | 0,3912 | 0,8588 | 0,0511 | 5,8 | 0,0015 | 0,1791 | 0,9667 | 0,0017 |
| 2,9 | 0,0390 | 0,3775 | 0,8670 | 0,0453 | 5,9 | 0,0014 | 0,1759 | 0,9679 | 0,0015 |
| | | | | | 6,0 | 0,0012 | 0,1727 | 0,9691 | 0,0013 |

$\varphi = 5°$

Cont'd

| $\rho$ | $\mathrm{Re}G_0$ | $-\mathrm{Im}G_0$ | $\mathrm{Re}G_1$ | $\mathrm{Im}G_1$ | $\rho$ | $\mathrm{Re}G_0$ | $-\mathrm{Im}G_0$ | $\mathrm{Re}G_1$ | $-\mathrm{Im}G_1$ |
|---|---|---|---|---|---|---|---|---|---|
| 0 | $\infty$ | 1,6581 | $-\infty$ | $\infty$ | 3,0 | 0,0097 | 0,3740 | 0,8630 | 0,0195 |
| 0,1 | 2,4189 | 1,5609 | —0,2049 | 9,8097 | 3,1 | —0,0022 | 0,3609 | 0,8712 | 0,0158 |
| 0,2 | 1,7375 | 1,4696 | —0,3027 | 4,7455 | 3,2 | —0,0047 | 0,3486 | 0,8788 | 0,0126 |
| 0,3 | 1,3513 | 1,3840 | —0,0947 | 3,0274 | 3,3 | —0,0069 | 0,3369 | 0,8858 | 0,0098 |
| 0,4 | 1,0883 | 1,3042 | 0,0367 | 2,1551 | 3,4 | —0,0087 | 0,3260 | 0,8923 | 0,0075 |
| 0,5 | 0,8939 | 1,2296 | 0,1351 | 1,6261 | 3,5 | —0,0102 | 0,3156 | 0,8984 | 0,0054 |
| 0,6 | 0,7435 | 1,1601 | 0,2151 | 1,2712 | 3,6 | —0,0116 | 0,3058 | 0,9041 | 0,0037 |
| 0,7 | 0,6236 | 1,0953 | 0,2830 | 1,0176 | 3,7 | —0,0127 | 0,2966 | 0,9093 | 0,0022 |
| 0,8 | 0,5261 | 1,0349 | 0,3424 | 0,8283 | 3,8 | —0,0136 | 0,2878 | 0,9142 | 0,0009 |
| 0,9 | 0,4456 | 0,9786 | 0,3950 | 0,6825 | 3,9 | —0,0143 | 0,2795 | 0,9188 | —0,0002 |
| 1,0 | 0,3785 | 0,9261 | 0,4421 | 0,5675 | 4,0 | —0,0150 | 0,2716 | 0,9231 | —0,0011 |
| 1,1 | 0,3221 | 0,8772 | 0,4847 | 0,4751 | 4,1 | —0,0156 | 0,2641 | 0,9270 | —0,0019 |
| 1,2 | 0,2743 | 0,8317 | 0,5234 | 0,4001 | 4,2 | —0,0159 | 0,2570 | 0,9307 | —0,0025 |
| 1,3 | 0,2336 | 0,7899 | 0,5586 | 0,3383 | 4,3 | —0,0162 | 0,2503 | 0,9342 | —0,0031 |
| 1,4 | 0,1988 | 0,7496 | 0,5907 | 0,2870 | 4,4 | —0,0164 | 0,2438 | 0,9374 | —0,0035 |
| 1,5 | 0,1690 | 0,7126 | 0,6201 | 0,2440 | 4,5 | —0,0166 | 0,2377 | 0,9405 | —0,0039 |
| 1,6 | 0,1433 | 0,6780 | 0,6471 | 0,2079 | 4,6 | —0,0167 | 0,2319 | 0,9433 | —0,0042 |
| 1,7 | 0,1212 | 0,6458 | 0,6719 | 0,1773 | 4,7 | —0,0167 | 0,2264 | 0,9459 | —0,0044 |
| 1,8 | 0,1021 | 0,6157 | 0,6947 | 0,1513 | 4,8 | —0,0167 | 0,2210 | 0,9484 | —0,0046 |
| 1,9 | 0,0856 | 0,5876 | 0,7157 | 0,1292 | 4,9 | —0,0167 | 0,2160 | 0,9508 | —0,0048 |
| 2,0 | 0,0713 | 0,5613 | 0,7350 | 0,1102 | 5,0 | —0,0166 | 0,2112 | 0,9530 | —0,0049 |
| 2,1 | 0,0589 | 0,5367 | 0,7528 | 0,0940 | 5,1 | —0,0166 | 0,2065 | 0,9550 | —0,0049 |
| 2,2 | 0,0482 | 0,5136 | 0,7692 | 0,0801 | 5,2 | —0,0164 | 0,2021 | 0,9569 | —0,0050 |
| 2,3 | 0,0389 | 0,4920 | 0,7844 | 0,0681 | 5,3 | —0,0163 | 0,1979 | 0,9588 | —0,0050 |
| 2,4 | 0,0308 | 0,4718 | 0,7984 | 0,0577 | 5,4 | —0,0162 | 0,1938 | 0,9606 | —0,0050 |
| 2,5 | 0,0238 | 0,4528 | 0,8114 | 0,0488 | 5,5 | —0,0160 | 0,1899 | 0,9621 | —0,0050 |
| 2,6 | 0,0178 | 0,4350 | 0,8233 | 0,0411 | 5,6 | —0,0158 | 0,1862 | 0,9636 | —0,0049 |
| 2,7 | 0,0125 | 0,4183 | 0,8344 | 0,0345 | 5,7 | —0,0157 | 0,1826 | 0,9650 | —0,0049 |
| 2,8 | 0,0080 | 0,4026 | 0,8447 | 0,0287 | 5,8 | —0,0155 | 0,1791 | 0,9664 | —0,0048 |
| 2,9 | 0,0041 | 0,3879 | 0,8542 | 0,0238 | 5,9 | —0,0153 | 0,1758 | 0,9677 | —0,0048 |
| | | | | | 6,0 | —0,0151 | 0,1726 | 0,9689 | —0,0047 |

$\varphi = 10°$ Cont'd.

| $\rho$ | $\mathrm{Re}G_0$ | $-\mathrm{Im}G_0$ | $\mathrm{Re}G_1$ | $-\mathrm{Im}G_1$ | $\rho$ | $\mathrm{Re}G_0$ | $-\mathrm{Im}G_0$ | $\mathrm{Re}G_1$ | $-\mathrm{Im}G_1$ |
|---|---|---|---|---|---|---|---|---|---|
| 0 | $\infty$ | 1,7453 | $-\infty$ | $\infty$ | 3,0 | −0,0359 | 0,3809 | 0,9589 | −0,0043 |
| 0,1 | 2,4106 | 1,6479 | −1,6790 | 9,6801 | 3,1 | −0,0378 | 0,3660 | 0,9532 | −0,0060 |
| 0,2 | 1,7219 | 1,5547 | −0,7446 | 4,6774 | 3,2 | −0,0393 | 0,3537 | 0,9718 | −0,0091 |
| 0,3 | 1,3292 | 1,4663 | −0,3964 | 2,9735 | 3,3 | −0,0404 | 0,3413 | 0,9798 | −0,0109 |
| 0,4 | 1,0607 | 1,3829 | −0,1927 | 2,1067 | 3,4 | −0,0413 | 0,3296 | 0,9871 | −0,0124 |
| 0,5 | 0,8616 | 1,3045 | −0,0501 | 1,5780 | 3,5 | −0,0419 | 0,3186 | 0,9939 | −0,0135 |
| 0,6 | 0,7072 | 1,2309 | 0,0602 | 1,2262 | 3,6 | −0,0423 | 0,3082 | 0,9998 | −0,0144 |
| 0,7 | 0,5841 | 1,1619 | 0,1505 | 0,9730 | 3,7 | −0,0426 | 0,2984 | 0,9961 | −0,0151 |
| 0,8 | 0,4839 | 1,0973 | 0,2272 | 0,7840 | 3,8 | −0,0426 | 0,2892 | 0,9116 | −0,0156 |
| 0,9 | 0,4013 | 1,0368 | 0,2939 | 0,6384 | 3,9 | −0,0426 | 0,2805 | 0,9166 | −0,0160 |
| 1,0 | 0,3326 | 0,9803 | 0,3528 | 0,5238 | 4,0 | −0,0424 | 0,2722 | 0,9213 | −0,0162 |
| 1,1 | 0,2749 | 0,9275 | 0,4063 | 0,4319 | 4,1 | −0,0421 | 0,2644 | 0,9256 | −0,0163 |
| 1,2 | 0,2263 | 0,8781 | 0,4525 | 0,3574 | 4,2 | −0,0418 | 0,2570 | 0,9297 | −0,0163 |
| 1,3 | 0,1851 | 0,8320 | 0,4952 | 0,2962 | 4,3 | −0,0414 | 0,2500 | 0,9334 | −0,0162 |
| 1,4 | 0,1500 | 0,7889 | 0,5339 | 0,2456 | 4,4 | −0,0409 | 0,2433 | 0,9369 | −0,0160 |
| 1,5 | 0,1202 | 0,7486 | 0,5692 | 0,2036 | 4,5 | −0,0404 | 0,2370 | 0,9402 | −0,0158 |
| 1,6 | 0,0947 | 0,7110 | 0,6014 | 0,1684 | 4,6 | −0,0399 | 0,2310 | 0,9432 | −0,0156 |
| 1,7 | 0,0730 | 0,6759 | 0,6309 | 0,1388 | 4,7 | −0,0393 | 0,2253 | 0,9461 | −0,0153 |
| 1,8 | 0,0544 | 0,6431 | 0,6579 | 0,1139 | 4,8 | −0,0387 | 0,2198 | 0,9487 | −0,0150 |
| 1,9 | 0,0385 | 0,6125 | 0,6827 | 0,0929 | 4,9 | −0,0381 | 0,2146 | 0,9512 | −0,0147 |
| 2,0 | 0,0250 | 0,5838 | 0,7054 | 0,0751 | 5,0 | −0,0375 | 0,2097 | 0,9535 | −0,0144 |
| 2,1 | 0,0134 | 0,5570 | 0,7263 | 0,0600 | 5,1 | −0,0369 | 0,2050 | 0,9560 | −0,0140 |
| 2,2 | 0,0036 | 0,5319 | 0,7455 | 0,0472 | 5,2 | −0,0363 | 0,2006 | 0,9577 | −0,0137 |
| 2,3 | −0,0047 | 0,5085 | 0,7632 | 0,0364 | 5,3 | −0,0357 | 0,1961 | 0,9596 | −0,0133 |
| 2,4 | −0,0119 | 0,4865 | 0,7795 | 0,0273 | 5,4 | −0,0351 | 0,1920 | 0,9613 | −0,0130 |
| 2,5 | −0,0179 | 0,4660 | 0,7945 | 0,0195 | 5,5 | 0,0345 | 0,1881 | 0,9630 | −0,0126 |
| 2,6 | −0,0229 | 0,4467 | 0,8084 | 0,0130 | 5,6 | 0,0339 | 0,1843 | 0,9646 | −0,0123 |
| 2,7 | −0,0271 | 0,4286 | 0,8212 | 0,0075 | 5,7 | −0,0333 | 0,1807 | 0,9660 | −0,0119 |
| 2,8 | −0,0306 | 0,4117 | 0,8329 | 0,0028 | 5,8 | −0,0327 | 0,1772 | 0,9674 | −0,0116 |
| 2,9 | −0,0335 | 0,3958 | 0,8438 | 0,0010 | 5,9 | −0,0321 | 0,1738 | 0,9687 | −0,0112 |
| | | | | | 6,0 | −0,0316 | 0,1706 | 0,9699 | −0,0109 |

$\varphi = 15°$ Cont'd.

| $\rho$ | $\mathrm{Re}G_0$ | $-\mathrm{Im}G_0$ | $\mathrm{Re}G_1$ | $-\mathrm{Im}G_1$ | $\rho$ | $\mathrm{Re}G_0$ | $-\mathrm{Im}G_0$ | $\mathrm{Re}G_1$ | $-\mathrm{Im}G_1$ |
|---|---|---|---|---|---|---|---|---|---|
| 0 | $\infty$ | 1,8825 | $-\infty$ | $\infty$ | 3,0 | —0,0751 | 0,3849 | 0,8478 | —0,0812 |
| 0,1 | 2,4822 | 1,7356 | — 2,5404 | 9,4980 | 3,1 | —0,0758 | 0,3699 | 0,8582 | —0,0826 |
| 0,2 | 1,7058 | 1,6410 | —1,1866 | 4,5722 | 3,2 | —0,0762 | 0,3568 | 0,8679 | —0,0836 |
| 0,3 | 1,2863 | 1,5601 | —0,6948 | 2,8948 | 3,3 | —0,0762 | 0,3426 | 0,8767 | —0,0842 |
| 0,4 | 1,0818 | 1,4635 | — 0,4201 | 2,0694 | 3,4 | —0,0759 | 0,3302 | 0,8849 | —0,0845 |
| 0,5 | 0,8276 | 1,3814 | — 0,2341 | 1,5183 | 3,5 | —0,0755 | 0,3186 | 0,8924 | —0,0846 |
| 0,6 | 0,6686 | 1,3037 | 0,0939 | 1,1677 | 3,6 | —0,0748 | 0,3076 | 0,8993 | —0,0845 |
| 0,7 | 0,5420 | 1,2374 | 0,0185 | 0,9165 | 3,7 | —0,0740 | 0,2973 | 0,9057 | —0,0842 |
| 0,8 | 0,4388 | 1,1615 | 0,1126 | 0,7288 | 3,8 | 0,0731 | 0,2876 | 0,9117 | —0,0837 |
| 0,9 | 0,3537 | 1,0967 | 0,1934 | 0,5843 | 3,9 | —0,0721 | 0,2785 | 0,9171 | —0,0832 |
| 1,0 | 0,2831 | 1,0356 | 0,2640 | 0,4706 | 4,0 | —0,0710 | 0,2699 | 0,9222 | —0,0825 |
| 1,1 | 0,2239 | 0,9788 | 0,3266 | 0,3797 | 4,1 | —0,0699 | 0,2618 | 0,9268 | —0,0818 |
| 1,2 | 0,1742 | 0,9253 | 0,3825 | 0,3062 | 4,2 | — 0,0687 | 0,2541 | 0,9312 | —0,0810 |
| 1,3 | 0,1323 | 0,8753 | 0,4329 | 0,2460 | 4,3 | —0,0674 | 0,2469 | 0,9352 | —0,0802 |
| 1,4 | 0,0970 | 0,8284 | 0,4784 | 0,1966 | 4,4 | —0,0662 | 0,2400 | 0,9389 | —0,0794 |
| 1,5 | 0,0670 | 0,7846 | 0,5197 | 0,1557 | 4,5 | —0,0649 | 0,2335 | 0,9423 | —0,0785 |
| 1,6 | 0,0418 | 0,7437 | 0,5574 | 0,1218 | 4,6 | —0,0637 | 0,2274 | 0,9455 | —0,0777 |
| 1,7 | 0,0204 | 0,7054 | 0,5917 | 0,0936 | 4,7 | —0,0624 | 0,2215 | 0,9484 | —0,0768 |
| 1,8 | 0,0024 | 0,6696 | 0,6231 | 0,0701 | 4,8 | —0,0612 | 0,2160 | 0,9511 | —0,0759 |
| 1,9 | —0,0128 | 0,6361 | 0,6518 | 0,0504 | 4,9 | —0,0599 | 0,2107 | 0,9537 | —0,0751 |
| 2,0 | — 0,0255 | 0,6049 | 0,6781 | 0,0341 | 5,0 | —0,0587 | 0,2057 | 0,9560 | —0,0742 |
| 2,1 | —0,0362 | 0,5757 | 0,7022 | 0,0205 | 5,1 | —0,0575 | 0,2010 | 0,9582 | —0,0734 |
| 2,2 | —0,0450 | 0,5484 | 0,7244 | 0,0092 | 5,2 | —0,0564 | 0,1965 | 0,9603 | —0,0726 |
| 2,3 | —0,0523 | 0,5228 | 0,7447 | 0,0001 | 5,3 | —0,0552 | 0,1921 | 0,9622 | —0,0718 |
| 2,4 | —0,0582 | 0,4990 | 0,7634 | — 0,0078 | 5,4 | —0,0541 | 0,1880 | 0,9639 | —0,0711 |
| 2,5 | — 0,0631 | 0,4767 | 0,7805 | 0,0141 | 5,5 | —0,0530 | 0,1841 | 0,9656 | —0,0703 |
| 2,6 | — 0,0669 | 0,4558 | 0,7963 | — 0,0193 | 5,6 | —0,0519 | 0,1803 | 0,9671 | —0,0696 |
| 2,7 | —0,0699 | 0,4363 | 0,8108 | — 0,0234 | 5,7 | — 0,0509 | 0,1767 | 0,9686 | —0,0689 |
| 2,8 | —0,0722 | 0,4180 | 0,8242 | —0,0267 | 5,8 | — 0,0499 | 0,1733 | 0,9699 | — 0,0683 |
| 2,9 | —0,0739 | 0,4009 | 0,8365 | — 0,0292 | 5,9 | — 0,0489 | 0,1699 | 0,9712 | —0,0676 |
| | | | | | 6,0 | — 0,0480 | 0,1668 | 0,9724 | —0,0670 |

$\varphi = 20°$

Cont'd

| $\rho$ | $\mathrm{Re}G_0$ | $-\mathrm{Im}G_0$ | $\mathrm{Re}G_1$ | $-\mathrm{Im}G_1$ | $\rho$ | $\mathrm{Re}G_0$ | $-\mathrm{Im}G_0$ | $\mathrm{Re}G_1$ | $-\mathrm{Im}G_1$ |
|---|---|---|---|---|---|---|---|---|---|
| 0 | $\infty$ | 1,9199 | $-\infty$ | $\infty$ | 3,0 | −0,1171 | 0,3856 | 0,8454 | −0,0612 |
| 0,1 | 2,3938 | 1,8246 | −3,3826 | 9,2289 | 3,1 | −0,1165 | 0,3695 | 0,8569 | −0,0611 |
| 0,2 | 1,6895 | 1,7286 | −1,6168 | 4,4307 | 3,2 | −0,1155 | 0,3545 | 0,8675 | −0,0606 |
| 0,3 | 1,2827 | 1,6357 | −0,9880 | 2,7918 | 3,3 | −0,1142 | 0,3404 | 0,8773 | −0,0599 |
| 0,4 | 1,0018 | 1,5461 | −0,6441 | 1,9535 | 3,4 | −0,1126 | 0,3273 | 0,8862 | −0,0588 |
| 0,5 | 0,7919 | 1,4604 | −0,4157 | 1,4415 | 3,5 | −0,1109 | 0,3150 | 0,8944 | −0,0576 |
| 0,6 | 0,6282 | 1,3787 | −0,2463 | 1,0961 | 3,6 | −0,1090 | 0,3035 | 0,9019 | −0,0563 |
| 0,7 | 0,4972 | 1,3012 | −0,1121 | 0,8482 | 3,7 | −0,1070 | 0,2927 | 0,9088 | −0,0548 |
| 0,8 | 0,3905 | 1,2277 | 0,0009 | 0,6629 | 3,8 | −0,1050 | 0,2826 | 0,9151 | −0,0532 |
| 0,9 | 0,3026 | 1,1584 | 0,0938 | 0,5202 | 3,9 | −0,1028 | 0,2731 | 0,9209 | −0,0516 |
| 1,0 | 0,2297 | 1,0930 | 0,1763 | 0,4080 | 4,0 | −0,1007 | 0,2642 | 0,9263 | −0,0499 |
| 1,1 | 0,1688 | 1,0314 | 0,2490 | 0,3185 | 4,1 | −0,0985 | 0,2558 | 0,9312 | −0,0483 |
| 1,2 | 0,1178 | 0,9736 | 0,3138 | 0,2463 | 4,2 | −0,0963 | 0,2479 | 0,9357 | −0,0466 |
| 1,3 | 0,0751 | 0,9193 | 0,3720 | 0,1876 | 4,3 | −0,0942 | 0,2405 | 0,9398 | −0,0449 |
| 1,4 | 0,0392 | 0,8683 | 0,4245 | 0,1397 | 4,4 | −0,0920 | 0,2335 | 0,9436 | −0,0432 |
| 1,5 | 0,0091 | 0,8206 | 0,4721 | 0,1003 | 4,5 | −0,0899 | 0,2269 | 0,9471 | −0,0416 |
| 1,6 | −0,0160 | 0,7759 | 0,5153 | 0,0690 | 4,6 | −0,0878 | 0,2207 | 0,9503 | −0,0400 |
| 1,7 | −0,0370 | 0,7341 | 0,5547 | 0,0414 | 4,7 | −0,0858 | 0,2149 | 0,9533 | −0,0385 |
| 1,8 | −0,0544 | 0,6950 | 0,5907 | 0,0195 | 4,8 | −0,0838 | 0,2093 | 0,9560 | −0,0370 |
| 1,9 | −0,0688 | 0,6585 | 0,6236 | 0,0017 | 4,9 | −0,0818 | 0,2041 | 0,9585 | −0,0355 |
| 2,0 | −0,0806 | 0,6243 | 0,6536 | −0,0129 | 5,0 | −0,0800 | 0,1991 | 0,9608 | −0,0341 |
| 2,1 | −0,0902 | 0,5924 | 0,6811 | −0,0248 | 5,1 | −0,0781 | 0,1944 | 0,9630 | −0,0327 |
| 2,2 | −0,0979 | 0,5626 | 0,7063 | −0,0343 | 5,2 | −0,0763 | 0,1899 | 0,9649 | −0,0314 |
| 2,3 | −0,1039 | 0,5348 | 0,7294 | −0,0418 | 5,3 | −0,0746 | 0,1856 | 0,9668 | −0,0302 |
| 2,4 | −0,1086 | 0,5089 | 0,7506 | −0,0478 | 5,4 | −0,0729 | 0,1816 | 0,9685 | −0,0290 |
| 2,5 | −0,1121 | 0,4846 | 0,7700 | −0,0523 | 5,5 | −0,0713 | 0,1777 | 0,9700 | −0,0278 |
| 2,6 | −0,1146 | 0,4620 | 0,7878 | −0,0557 | 5,6 | −0,0698 | 0,1740 | 0,9715 | −0,0267 |
| 2,7 | −0,1162 | 0,4409 | 0,8046 | −0,0582 | 5,7 | −0,0683 | 0,1705 | 0,9728 | −0,0256 |
| 2,8 | −0,1171 | 0,4212 | 0,8191 | −0,0598 | 5,8 | −0,0668 | 0,1672 | 0,9741 | −0,0246 |
| 2,9 | −0,1174 | 0,4028 | 0,8328 | −0,0608 | 5,9 | −0,0654 | 0,1639 | 0,9752 | −0,0237 |
| | | | | | 6,0 | −0,0640 | 0,1609 | 0,9763 | −0,0228 |

$\varphi = 28°$

Cont'd

| $\rho$ | $\mathrm{Re}G_0$ | $-\mathrm{Im}G_0$ | $\mathrm{Re}G_1$ | $-\mathrm{Im}G_1$ | $\rho$ | $\mathrm{Re}G_0$ | $-\mathrm{Im}G_0$ | $\mathrm{Re}G_1$ | $-\mathrm{Im}G_1$ |
|---|---|---|---|---|---|---|---|---|---|
| 0 | $\infty$ | 2,0071 | $-\infty$ | $\infty$ | 3,0 | —0,1622 | 0,3823 | 0,8473 | —0,0943 |
| 0,1 | 2,3855 | 1,9131 | —4,1992 | 8,8908 | 3,1 | —0,1599 | 0,3651 | 0,8600 | —0,0924 |
| 0,2 | 1,6729 | 1,8176 | —2,0350 | 4,2539 | 3,2 | —0,1573 | 0,3491 | 0,8716 | —0,0902 |
| 0,3 | 1,2585 | 1,7231 | —1,2736 | 2,6651 | 3,3 | —0,1544 | 0,3342 | 0,8821 | —0,0878 |
| 0,4 | 0,9706 | 1,6310 | —0,8632 | 1,8497 | 3,4 | —0,1514 | 0,3203 | 0,8918 | —0,0852 |
| 0,5 | 0,7545 | 1,5419 | —0,5938 | 1,3498 | 3,5 | —0,1482 | 0,3073 | 0,9006 | —0,0824 |
| 0,6 | 0,5854 | 1,4563 | —0,3962 | 1,0117 | 3,6 | —0,1448 | 0,2953 | 0,9086 | —0,0796 |
| 0,7 | 0,4497 | 1,3744 | —0,2407 | 0,7684 | 3,7 | —0,1415 | 0,2840 | 0,9159 | —0,0767 |
| 0,8 | 0,3391 | 1,2964 | —0,1128 | 0,5863 | 3,8 | —0,1381 | 0,2735 | 0,9225 | —0,0738 |
| 0,9 | 0,2479 | 1,2222 | —0,0042 | 0,4460 | 3,9 | —0,1346 | 0,2637 | 0,9286 | —0,0709 |
| 1,0 | 0,1722 | 1,1520 | 0,0900 | 0,3358 | 4,0 | —0,1312 | 0,2545 | 0,9341 | —0,0681 |
| 1,1 | 0,1092 | 1,0857 | 0,1729 | 0,2482 | 4,1 | —0,1279 | 0,2460 | 0,9391 | —0,0653 |
| 1,2 | 0,0567 | 1,0231 | 0,2467 | 0,1777 | 4,2 | —0,1246 | 0,2380 | 0,9437 | —0,0625 |
| 1,3 | 0,0129 | 0,9641 | 0,3129 | 0,1204 | 4,3 | —0,1213 | 0,2305 | 0,9478 | —0,0598 |
| 1,4 | —0,0237 | 0,9087 | 0,3726 | 0,0745 | 4,4 | —0,1181 | 0,2234 | 0,9516 | —0,0572 |
| 1,5 | —0,0540 | 0,8566 | 0,4266 | 0,0370 | 4,5 | —0,1150 | 0,2169 | 0,9551 | —0,0547 |
| 1,6 | —0,0791 | 0,8078 | 0,4757 | 0,0065 | 4,6 | —0,1120 | 0,2107 | 0,9582 | —0,0523 |
| 1,7 | —0,0998 | 0,7621 | 0,5204 | —0,0182 | 4,7 | —0,1091 | 0,2049 | 0,9611 | —0,0499 |
| 1,8 | —0,1166 | 0,7193 | 0,5612 | —0,0380 | 4,8 | —0,1062 | 0,1994 | 0,9637 | —0,0477 |
| 1,9 | —0,1301 | 0,6793 | 0,5984 | —0,0538 | 4,9 | —0,1035 | 0,1942 | 0,9661 | —0,0455 |
| 2,0 | —0,1409 | 0,6419 | 0,6324 | —0,0664 | 5,0 | —0,1009 | 0,1894 | 0,9682 | —0,0435 |
| 2,1 | —0,1493 | 0,6070 | 0,6635 | —0,0761 | 5,1 | —0,0983 | 0,1848 | 0,9702 | —0,0415 |
| 2,2 | —0,1556 | 0,5744 | 0,6920 | —0,0835 | 5,2 | —0,0958 | 0,1805 | 0,9720 | —0,0397 |
| 2,3 | —0,1603 | 0,5441 | 0,7180 | —0,0890 | 4,3 | —0,0935 | 0,1763 | 0,9736 | —0,0379 |
| 2,4 | —0,1634 | 0,5158 | 0,7418 | —0,0928 | 5,4 | —0,0912 | 0,1725 | 0,9751 | —0,0362 |
| 2,5 | —0,1654 | 0,4894 | 0,7635 | —0,0953 | 5,5 | —0,0890 | 0,1688 | 0,9765 | —0,0346 |
| 2,6 | —0,1662 | 0,4648 | 0,7834 | —0,0966 | 5,6 | —0,0869 | 0,1653 | 0,9777 | —0,0331 |
| 2,7 | —0,1662 | 0,4419 | 0,8016 | —0,0971 | 5,7 | —0,0849 | 0,1619 | 0,9787 | —0,0316 |
| 2,8 | —0,1654 | 0,4206 | 0,8183 | —0,0967 | 5,8 | —0,0830 | 0,1588 | 0,9799 | —0,0302 |
| 2,9 | —0,1641 | 0,4008 | 0,8334 | —0,0958 | 5,9 | —0,0811 | 0,1557 | 0,9809 | —0,0289 |
| | | | | | 6,0 | —0,0794 | 0,1528 | 0,9818 | —0,0277 |

Cont'd

$\gamma = 30°$

| $\rho$ | $\mathrm{Re}G_0$ | $-\mathrm{Im}G_0$ | $\mathrm{Re}G_1$ | $-\mathrm{Im}G_1$ | $\rho$ | $\mathrm{Re}G_0$ | $-\mathrm{Im}G_0$ | $\mathrm{Re}G_1$ | $-\mathrm{Im}G_1$ |
|---|---|---|---|---|---|---|---|---|---|
| 0 | $-\infty$ | 2,0944 | $-\infty$ | $\infty$ | 3,0 | −0,2105 | 0,3744 | 0,8545 | −0,1396 |
| 0,1 | −2,3772 | 2,0930 | −4,9842 | 8,4843 | 3,1 | −0,2063 | 0,3559 | 0,8683 | −0,1266 |
| 0,2 | −1,8562 | 1,9080 | −2,4380 | 4,9432 | 3,2 | −0,2018 | 0,3389 | 0,8808 | −0,1223 |
| 0,3 | −1,2389 | 1,8125 | −1,5604 | 2,5159 | 3,3 | −0,1971 | 0,3230 | 0,8922 | −0,1179 |
| 0,4 | −0,9886 | 1,7182 | −1,0761 | 1,7296 | 3,4 | −0,1922 | 0,3084 | 0,9024 | −0,1133 |
| 0,5 | −0,7156 | 1,6260 | −0,7675 | 1,2439 | 3,5 | −0,1872 | 0,2948 | 0,9117 | 0,1088 |
| 0,6 | −0,5405 | 1,5366 | −0,5427 | 0,9148 | 3,6 | −0,1822 | 0,2822 | 0,9201 | −0,1042 |
| 0,7 | −0,3995 | 1,4504 | −0,3668 | 0,6774 | 3,7 | −0,1772 | 0,2705 | 0,9277 | −0,0996 |
| 0,8 | −0,2843 | 1,3677 | −0,2225 | 0,4992 | 3,8 | −0,1722 | 0,2597 | 0,9346 | −0,0952 |
| 0,9 | −0,1892 | 1,2887 | −0,1003 | 0,3619 | 3,9 | −0,1672 | 0,2496 | 0,9408 | −0,0906 |
| 1,0 | −0,1104 | 1,2134 | 0,0015 | 0,2542 | 4,0 | 0,1624 | 0,2403 | 0,9463 | 0,0865 |
| 1,1 | −0,0449 | 1,1418 | 0,0987 | 0,1675 | 4,1 | −0,1576 | 0,2317 | 0,9513 | −0,0824 |
| 1,2 | 0,0096 | 1,0730 | 0,1816 | 0,1001 | 4,2 | −0,1530 | 0,2236 | 0,9558 | −0,0784 |
| 1,3 | 0,0548 | 1,0104 | 0,2559 | 0,0451 | 4,3 | −0,1485 | 0,2161 | 0,9598 | −0,0745 |
| 1,4 | 0,0922 | 0,9497 | 0,3230 | 0,0009 | 4,4 | −0,1441 | 0,2092 | 0,9635 | −0,0708 |
| 1,5 | 0,1230 | 0,8929 | 0,3838 | −0,0346 | 4,5 | −0,1399 | 0,2027 | 0,9667 | −0,0672 |
| 1,6 | 0,1482 | 0,8395 | 0,4389 | −0,0629 | 4,6 | −0,1358 | 0,1967 | 0,9696 | −0,0639 |
| 1,7 | 0,1685 | 0,7894 | 0,4893 | 0,0854 | 4,7 | −0,1318 | 0,1911 | 0,9722 | −0,0606 |
| 1,8 | 0,1847 | 0,7424 | 0,5352 | 0,1029 | 4,8 | 0,1281 | 0,1858 | 0,9745 | −0,0576 |
| 1,9 | 0,1973 | 0,6985 | 0,5770 | −0,1164 | 4,9 | −0,1244 | 0,1809 | 0,9766 | −0,0546 |
| 2,0 | 0,2069 | 0,6575 | 0,6152 | −0,1266 | 5,0 | −0,1209 | 0,1763 | 0,9785 | −0,0519 |
| 2,1 | 0,2140 | 0,6192 | 0,6502 | −0,1339 | 5,1 | −0,1176 | 0,1720 | 0,9801 | −0,0492 |
| 2,2 | 0,2189 | 0,5834 | 0,6820 | −0,1388 | 5,2 | −0,1144 | 0,1679 | 0,9816 | −0,0468 |
| 2,3 | 0,2219 | 0,5502 | 0,7112 | −0,1418 | 5,3 | −0,1113 | 0,1641 | 0,9829 | −0,0444 |
| 2,4 | 0,2233 | 0,5192 | 0,7378 | −0,1432 | 5,4 | −0,1084 | 0,1605 | 0,9840 | −0,0422 |
| 2,5 | 0,2234 | 0,4904 | 0,7620 | −0,1432 | 5,5 | −0,1056 | 0,1571 | 0,9851 | −0,0404 |
| 2,6 | 0,2223 | 0,4636 | 0,7841 | −0,1421 | 5,6 | −0,1030 | 0,1539 | 0,9860 | −0,0382 |
| 2,7 | 0,2204 | 0,4387 | 0,8043 | −0,1402 | 5,7 | −0,1004 | 0,1509 | 0,9868 | −0,0363 |
| 2,8 | 0,2176 | 0,4156 | 0,8226 | −0,1375 | 5,8 | −0,0980 | 0,1480 | 0,9875 | −0,0346 |
| 2,9 | 0,2143 | 0,3942 | 0,8393 | −0,1343 | 5,9 | −0,0957 | 0,1452 | 0,9882 | −0,0329 |
| | | | | | 6,0 | 0,0935 | 0,1426 | 0,9888 | −0,0314 |

Cont'd

$\varphi = 36°$

| $\rho$ | $\mathrm{Re}G_0$ | $-\mathrm{Im}G_0$ | $\mathrm{Re}G_1$ | $-\mathrm{Im}G_1$ | $\rho$ | $\mathrm{Re}G_0$ | $-\mathrm{Im}G_0$ | $\mathrm{Re}G_1$ | $-\mathrm{Im}G_1$ |
|---|---|---|---|---|---|---|---|---|---|
| 0 | $\infty$ | 2,1817 | $-\infty$ | $\infty$ | 3,0 | −0,2625 | 0,3089 | 0,8679 | −0,1089 |
| 0,1 | 2,2891 | 2,0966 | −5,7315 | 8,0125 | 3,1 | −0,2559 | 0,3411 | 0,8828 | −0,1636 |
| 0,2 | 1,8986 | 1,9908 | −2,8231 | 3,8092 | 3,2 | −0,2492 | 0,3229 | 0,8968 | −0,1567 |
| 0,3 | 1,2988 | 1,9040 | −1,8157 | 2,3451 | 3,3 | −0,2422 | 0,3861 | 0,9063 | −0,1499 |
| 0,4 | 0,9885 | 1,8080 | −1,2812 | 1,5911 | 3,4 | −0,2351 | 0,2906 | 0,9192 | −0,1431 |
| 0,5 | 0,6753 | 1,7131 | −0,9357 | 1,1245 | 3,5 | −0,2280 | 0,2764 | 0,9289 | −0,1363 |
| 0,6 | 0,4885 | 1,6201 | −0,6851 | 0,8061 | 3,6 | −0,2210 | 0,2633 | 0,9376 | −0,1297 |
| 0,7 | 0,3465 | 1,5297 | −0,4897 | 0,5755 | 3,7 | −0,2140 | 0,2513 | 0,9453 | −0,1231 |
| 0,8 | 0,2261 | 1,4422 | −0,3297 | 0,4020 | 3,8 | −0,2071 | 0,2402 | 0,9522 | −0,1168 |
| 0,9 | 0,1286 | 1,3581 | −0,1942 | 0,2681 | 3,9 | −0,2003 | 0,2300 | 0,9583 | −0,1106 |
| 1,0 | 0,0440 | 1,2774 | −0,0769 | 0,1631 | 4,0 | −0,1936 | 0,2207 | 0,9638 | −0,1047 |
| 1,1 | −0,0245 | 1,2004 | 0,0265 | 0,0798 | 4,1 | −0,1874 | 0,2121 | 0,9686 | −0,0990 |
| 1,2 | −0,0814 | 1,1271 | 0,1185 | 0,0135 | 4,2 | −0,1812 | 0,2041 | 0,9728 | −0,0935 |
| 1,3 | −0,1284 | 1,0575 | 0,2012 | −0,0394 | 4,3 | −0,1752 | 0,1968 | 0,9765 | −0,0882 |
| 1,4 | −0,1670 | 0,9917 | 0,2760 | −0,0815 | 4,4 | −0,1694 | 0,1901 | 0,9797 | −0,0833 |
| 1,5 | −0,1986 | 0,9295 | 0,3438 | −0,1147 | 4,5 | −0,1638 | 0,1840 | 0,9825 | −0,0785 |
| 1,6 | −0,2228 | 0,8710 | 0,4054 | −0,1407 | 4,6 | −0,1585 | 0,1783 | 0,9850 | −0,0740 |
| 1,7 | −0,2429 | 0,8159 | 0,4616 | −0,1607 | 4,7 | −0,1534 | 0,1730 | 0,9871 | −0,0698 |
| 1,8 | −0,2585 | 0,7643 | 0,5129 | −0,1758 | 4,8 | −0,1486 | 0,1681 | 0,9889 | −0,0658 |
| 1,9 | −0,2712 | 0,7159 | 0,5598 | −0,1866 | 4,9 | −0,1439 | 0,1636 | 0,9905 | −0,0620 |
| 2,0 | −0,2796 | 0,6707 | 0,6025 | −0,1940 | 5,0 | −0,1396 | 0,1595 | 0,9918 | −0,0584 |
| 2,1 | −0,2852 | 0,6285 | 0,6416 | −0,1985 | 5,1 | −0,1353 | 0,1556 | 0,9930 | −0,0551 |
| 2,2 | −0,2883 | 0,5892 | 0,6772 | −0,2007 | 5,2 | −0,1313 | 0,1520 | 0,9939 | −0,0519 |
| 2,3 | −0,2894 | 0,5526 | 0,7097 | −0,2008 | 5,3 | −0,1275 | 0,1486 | 0,9947 | −0,0490 |
| 2,4 | −0,2888 | 0,5186 | 0,7393 | −0,1993 | 5,4 | −0,1239 | 0,1455 | 0,9954 | −0,0463 |
| 2,5 | −0,2868 | 0,4870 | 0,7663 | −0,1964 | 5,5 | −0,1204 | 0,1425 | 0,9959 | −0,0437 |
| 2,6 | −0,2835 | 0,4577 | 0,7904 | −0,1925 | 5,6 | −0,1172 | 0,1398 | 0,9963 | −0,0413 |
| 2,7 | −0,2793 | 0,4306 | 0,8130 | −0,1878 | 5,7 | −0,1141 | 0,1372 | 0,9967 | −0,0390 |
| 2,8 | −0,2743 | 0,4055 | 0,8332 | −0,1823 | 5,8 | −0,1112 | 0,1348 | 0,9969 | −0,0370 |
| 2,9 | −0,2686 | 0,3823 | 0,8514 | −0,1764 | 5,9 | −0,1084 | 0,1324 | 0,9971 | −0,0350 |
| | | | | | 6,0 | −0,1058 | 0,1303 | 0,9973 | −0,0332 |

$\varphi = 45°$

Cont'd

| $\rho$ | $\mathrm{Re}G_0$ | $-\mathrm{Im}G_0$ | $\mathrm{Re}G_1$ | $-\mathrm{Im}G_1$ | $\rho$ | $\mathrm{Re}G_0$ | $-\mathrm{Im}G_0$ | $\mathrm{Re}G_1$ | $-\mathrm{Im}G_1$ |
|---|---|---|---|---|---|---|---|---|---|
| 0 | $\infty$ | 2,2669 | $-\infty$ | $\infty$ | 3,0 | −0,3184 | 0,3407 | 0,8886 | −0,2127 |
| 0,1 | 2,3612 | 2,1849 | −6,4356 | 7,4790 | 3,1 | −0,3091 | 0,3194 | 0,9049 | −0,2031 |
| 0,2 | 1,6231 | 2,0932 | −3,1873 | 3,5268 | 3,2 | −0,2995 | 0,3000 | 0,9192 | −0,1934 |
| 0,3 | 1,1836 | 1,9977 | −2,0681 | 2,1541 | 3,3 | −0,2899 | 0,2821 | 0,9319 | −0,1837 |
| 0,4 | 0,8718 | 1,9006 | −1,4775 | 1,4382 | 3,4 | −0,2802 | 0,2659 | 0,9432 | −0,1741 |
| 0,5 | 0,6336 | 1,8034 | −1,0975 | 0,9923 | 3,5 | −0,2705 | 0,2510 | 0,9532 | −0,1647 |
| 0,6 | 0,4444 | 1,7071 | −0,8228 | 0,6861 | 3,6 | −0,2610 | 0,2375 | 0,9620 | −0,1555 |
| 0,7 | 0,2908 | 1,6126 | −0,6090 | 0,4633 | 3,7 | −0,2516 | 0,2252 | 0,9698 | −0,1466 |
| 0,8 | 0,1644 | 1,5204 | −0,4339 | 0,2960 | 3,8 | −0,2424 | 0,2140 | 0,9765 | −0,1380 |
| 0,9 | 0,0597 | 1,4309 | −0,2857 | 0,1648 | 3,9 | −0,2335 | 0,2038 | 0,9823 | −0,1297 |
| 1,0 | −0,0273 | 1,3447 | −0,1528 | 0,0626 | 4,0 | −0,2248 | 0,1946 | 0,9874 | −0,1216 |
| 1,1 | −0,0996 | 1,2618 | −0,0436 | −0,0182 | 4,1 | −0,2165 | 0,1862 | 0,9917 | −0,1142 |
| 1,2 | −0,1593 | 1,1825 | 0,0678 | −0,0824 | 4,2 | −0,2084 | 0,1786 | 0,9954 | −0,1070 |
| 1,3 | −0,2086 | 1,1069 | 0,1490 | −0,1322 | 4,3 | −0,2007 | 0,1717 | 0,9985 | −0,1002 |
| 1,4 | −0,2488 | 1,0350 | 0,2317 | −0,1729 | 4,4 | −0,1932 | 0,1655 | 1,0011 | −0,0937 |
| 1,5 | −0,2812 | 0,9669 | 0,3068 | −0,2039 | 4,5 | −0,1862 | 0,1598 | 1,0032 | −0,0876 |
| 1,6 | −0,3070 | 0,9026 | 0,3753 | −0,2274 | 4,6 | −0,1794 | 0,1547 | 1,0049 | −0,0818 |
| 1,7 | −0,3270 | 0,8420 | 0,4379 | −0,2448 | 4,7 | −0,1730 | 0,1500 | 1,0063 | −0,0764 |
| 1,8 | −0,3420 | 0,7850 | 0,4960 | −0,2571 | 4,8 | −0,1669 | 0,1458 | 1,0073 | −0,0713 |
| 1,9 | −0,3527 | 0,7315 | 0,5472 | −0,2650 | 4,9 | −0,1611 | 0,1420 | 1,0081 | −0,0666 |
| 2,0 | −0,3598 | 0,6815 | 0,5950 | −0,2694 | 5,0 | −0,1557 | 0,1385 | 1,0087 | −0,0622 |
| 2,1 | −0,3637 | 0,6348 | 0,6385 | −0,2708 | 5,1 | −0,1505 | 0,1353 | 1,0090 | −0,0581 |
| 2,2 | −0,3649 | 0,5912 | 0,6783 | −0,2696 | 5,2 | −0,1456 | 0,1324 | 1,0092 | −0,0542 |
| 2,3 | −0,3639 | 0,5508 | 0,7144 | −0,2665 | 5,3 | −0,1410 | 0,1297 | 1,0092 | −0,0507 |
| 2,4 | −0,3609 | 0,5132 | 0,7474 | −0,2616 | 5,4 | −0,1367 | 0,1273 | 1,0091 | −0,0474 |
| 2,5 | −0,3564 | 0,4784 | 0,7773 | −0,2555 | 5,5 | −0,1326 | 0,1250 | 1,0089 | −0,0443 |
| 2,6 | −0,3505 | 0,4462 | 0,8044 | −0,2482 | 5,6 | −0,1287 | 0,1229 | 1,0086 | −0,0415 |
| 2,7 | −0,3436 | 0,4165 | 0,8289 | −0,2401 | 5,7 | −0,1251 | 0,1210 | 1,0083 | −0,0389 |
| 2,8 | −0,3358 | 0,3891 | 0,8510 | −0,2314 | 5,8 | −0,1217 | 0,1192 | 1,0078 | −0,0365 |
| 2,9 | −0,3273 | 0,3641 | 0,8709 | −0,2222 | 5,9 | −0,1185 | 0,1175 | 1,0074 | −0,0343 |
| | | | | | 6,0 | −0,1155 | 0,1159 | 1,0069 | −0,0323 |

$\varphi = 45°$

Cont'd

| $\rho$ | $\mathrm{Re}G_0$ | $-\mathrm{Im}G_0$ | $\mathrm{Re}G_1$ | $-\mathrm{Im}G_1$ | $\rho$ | $\mathrm{Re}G_0$ | $-\mathrm{Im}G_0$ | $\mathrm{Re}G_1$ | $-\mathrm{Im}G_1$ |
|---|---|---|---|---|---|---|---|---|---|
| 0 | $\infty$ | 2,3662 | $-\infty$ | $\infty$ | 3,0 | −0,3789 | 0,3124 | 0,9187 | −0,2588 |
| 0,1 | 2,3636 | 2,2770 | −7,0912 | 6,8880 | 3,1 | −0,3662 | 0,2895 | 0,9359 | −0,2454 |
| 0,2 | 1,6068 | 2,1881 | −3,5281 | 3,2251 | 3,2 | −0,3533 | 0,2686 | 0,9511 | −0,2321 |
| 0,3 | 1,1583 | 2,0937 | −2,3058 | 1,9444 | 3,3 | −0,3403 | 0,2497 | 0,9644 | −0,2190 |
| 0,4 | 0,8376 | 1,9962 | −1,6638 | 1,2711 | 3,4 | −0,3274 | 0,2325 | 0,9761 | −0,2061 |
| 0,5 | 0,5908 | 1,8972 | −1,2521 | 0,8482 | 3,5 | −0,3146 | 0,2171 | 0,9862 | −0,1935 |
| 0,6 | 0,3935 | 1,7980 | −0,9552 | 0,5557 | 3,6 | −0,3020 | 0,2032 | 0,9950 | −0,1812 |
| 0,7 | 0,2323 | 1,6996 | −0,7243 | 0,3414 | 3,7 | −0,2897 | 0,1907 | 1,0024 | −0,1694 |
| 0,8 | 0,0992 | 1,6027 | −0,5351 | 0,1786 | 3,8 | −0,2777 | 0,1795 | 1,0088 | −0,1581 |
| 0,9 | −0,0115 | 1,5079 | −0,3746 | 0,0522 | 3,9 | −0,2661 | 0,1696 | 1,0140 | −0,1473 |
| 1,0 | −0,1037 | 1,4158 | −0,2350 | −0,0471 | 4,0 | −0,2549 | 0,1607 | 1,0184 | −0,1369 |
| 1,1 | −0,1804 | 1,3267 | −0,1114 | −0,1256 | 4,1 | −0,2441 | 0,1528 | 1,0219 | −0,1271 |
| 1,2 | −0,2438 | 1,2409 | −0,0007 | −0,1876 | 4,2 | −0,2338 | 0,1458 | 1,0247 | −0,1178 |
| 1,3 | −0,2960 | 1,1587 | 0,0993 | −0,2363 | 4,3 | −0,2240 | 0,1396 | 1,0268 | −0,1090 |
| 1,4 | −0,3383 | 1,0802 | 0,1901 | −0,2740 | 4,4 | −0,2146 | 0,1341 | 1,0284 | −0,1008 |
| 1,5 | −0,3721 | 1,0055 | 0,2730 | −0,3026 | 4,5 | −0,2057 | 0,1293 | 1,0294 | −0,0931 |
| 1,6 | −0,3986 | 0,9346 | 0,3488 | −0,3236 | 4,6 | −0,1973 | 0,1251 | 1,0300 | −0,0858 |
| 1,7 | −0,4188 | 0,8676 | 0,4182 | −0,3383 | 4,7 | −0,1893 | 0,1214 | 1,0303 | −0,0791 |
| 1,8 | −0,4334 | 0,8044 | 0,4817 | −0,3476 | 4,8 | −0,1818 | 0,1182 | 1,0302 | −0,0729 |
| 1,9 | −0,4431 | 0,7451 | 0,5399 | −0,3524 | 4,9 | −0,1747 | 0,1153 | 1,0298 | −0,0671 |
| 2,0 | −0,4488 | 0,6895 | 0,5931 | −0,3534 | 5,0 | −0,1681 | 0,1129 | 1,0292 | −0,0617 |
| 2,1 | −0,4509 | 0,6375 | 0,6416 | −0,3513 | 5,1 | −0,1619 | 0,1107 | 1,0284 | −0,0568 |
| 2,2 | −0,4499 | 0,5891 | 0,6860 | −0,3466 | 5,2 | −0,1561 | 0,1088 | 1,0274 | −0,0523 |
| 2,3 | −0,4464 | 0,5441 | 0,7263 | −0,3396 | 5,3 | −0,1506 | 0,1072 | 1,0263 | −0,0481 |
| 2,4 | −0,4407 | 0,5023 | 0,7630 | −0,3310 | 5,4 | −0,1455 | 0,1058 | 1,0251 | −0,0443 |
| 2,5 | −0,4333 | 0,4637 | 0,7962 | −0,3209 | 5,5 | −0,1408 | 0,1045 | 1,0239 | −0,0408 |
| 2,6 | −0,4243 | 0,4281 | 0,8262 | −0,3097 | 5,6 | −0,1364 | 0,1033 | 1,0226 | −0,0377 |
| 2,7 | −0,4141 | 0,3963 | 0,8533 | −0,2977 | 5,7 | −0,1323 | 0,1023 | 1,0213 | −0,0348 |
| 2,8 | −0,4030 | 0,3652 | 0,8776 | −0,2850 | 5,8 | −0,1284 | 0,1014 | 1,0199 | −0,0322 |
| 2,9 | −0,3912 | 0,3376 | 0,8993 | −0,2720 | 5,9 | −0,1249 | 0,1006 | 1,0186 | −0,0299 |
| | | | | | 6,0 | 0,1216 | 0,0998 | 1,0173 | 0,0278 |

$\varphi = -5°$

Cont'd

| $\rho$ | $\mathrm{Re}G_0$ | $-\mathrm{Im}G_0$ | $\mathrm{Re}G_1$ | $-\mathrm{Im}G_1$ |
|---|---|---|---|---|
| 0 | $\infty$ | 1,4835 | $\infty$ | $\infty$ |
| 0,1 | 2,4350 | 1,3889 | 0,9550 | 9,6223 |
| 0,2 | 1,7674 | 1,3028 | 0,5909 | 4,7686 |
| 0,3 | 1,3927 | 1,2240 | 0,5098 | 3,0593 |
| 0,4 | 1,1394 | 1,1516 | 0,4958 | 2,1943 |
| 0,5 | 0,9532 | 1,0850 | 0,5045 | 1,6711 |
| 0,6 | 0,8095 | 1,0236 | 0,5236 | 1,3209 |
| 0,7 | 0,6950 | 0,9669 | 0,5468 | 1,0710 |
| 0,8 | 0,6019 | 0,9145 | 0,5715 | 0,8845 |
| 0,9 | 0,5248 | 0,8660 | 0,5963 | 0,7407 |
| 1,0 | 0,4603 | 0,8210 | 0,6205 | 0,6272 |
| 1,1 | 0,4058 | 0,7793 | 0,6437 | 0,5356 |
| 1,2 | 0,3593 | 0,7406 | 0,6658 | 0,4610 |
| 1,3 | 0,3193 | 0,7046 | 0,6865 | 0,3992 |
| 1,4 | 0,2849 | 0,6711 | 0,7061 | 0,3475 |
| 1,5 | 0,2549 | 0,6399 | 0,7244 | 0,3039 |
| 1,6 | 0,2289 | 0,6108 | 0,7415 | 0,2669 |
| 1,7 | 0,2061 | 0,5837 | 0,7574 | 0,2352 |
| 1,8 | 0,1861 | 0,5584 | 0,7723 | 0,2080 |
| 1,9 | 0,1685 | 0,5347 | 0,7861 | 0,1845 |
| 2,0 | 0,1530 | 0,5125 | 0,7990 | 0,1642 |
| 2,1 | 0,1392 | 0,4917 | 0,8110 | 0,1464 |
| 2,2 | 0,1270 | 0,4722 | 0,8222 | 0,1309 |
| 2,3 | 0,1162 | 0,4540 | 0,8326 | 0,1173 |
| 2,4 | 0,1065 | 0,4368 | 0,8423 | 0,1054 |
| 2,5 | 0,0979 | 0,4207 | 0,8513 | 0,0949 |
| 2,6 | 0,0902 | 0,4055 | 0,8597 | 0,0856 |
| 2,7 | 0,0833 | 0,3912 | 0,8675 | 0,0774 |
| 2,8 | 0,0770 | 0,3778 | 0,8749 | 0,0700 |
| 2,9 | 0,0714 | 0,3650 | 0,8817 | 0,0636 |

| $\rho$ | $\mathrm{Re}G_0$ | $-\mathrm{Im}G_0$ | $\mathrm{Re}G_1$ | $-\mathrm{Im}G_1$ |
|---|---|---|---|---|
| 3,0 | 0,0664 | 0,3531 | 0,8880 | 0,0578 |
| 3,1 | 0,0619 | 0,3417 | 0,8940 | 0,0526 |
| 3,2 | 0,0578 | 0,3310 | 0,8995 | 0,0480 |
| 3,3 | 0,0540 | 0,3209 | 0,9047 | 0,0438 |
| 3,4 | 0,0507 | 0,3112 | 0,9096 | 0,0401 |
| 3,5 | 0,0476 | 0,3021 | 0,9141 | 0,0368 |
| 3,6 | 0,0448 | 0,2935 | 0,9184 | 0,0338 |
| 3,7 | 0,0423 | 0,2853 | 0,9224 | 0,0311 |
| 3,8 | 0,0400 | 0,2775 | 0,9261 | 0,0286 |
| 3,9 | 0,0379 | 0,2700 | 0,9296 | 0,0264 |
| 4,0 | 0,0359 | 0,2630 | 0,9329 | 0,0244 |
| 4,1 | 0,0342 | 0,2562 | 0,9360 | 0,9226 |
| 4,2 | 0,0325 | 0,2498 | 0,9389 | 0,0210 |
| 4,3 | 0,0310 | 0,2437 | 0,9416 | 0,0195 |
| 4,4 | 0,0297 | 0,2378 | 0,9442 | 0,0182 |
| 4,5 | 0,0284 | 0,2323 | 0,9466 | 0,0169 |
| 4,6 | 0,0272 | 0,2269 | 0,9489 | 0,0158 |
| 4,7 | 0,0261 | 0,2218 | 0,9511 | 0,0148 |
| 4,8 | 0,0251 | 0,2169 | 0,9531 | 0,0138 |
| 4,9 | 0,0242 | 0,2122 | 0,9550 | 0,0129 |
| 5,0 | 0,0233 | 0,2077 | 0,9568 | 0,0122 |
| 5,1 | 0,0225 | 0,2043 | 0,9585 | 0,0114 |
| 5,2 | 0,0218 | 0,1992 | 0,9601 | 0,0108 |
| 5,3 | 0,0211 | 0,1952 | 0,9616 | 0,0102 |
| 5,4 | 0,0204 | 0,1914 | 0,9631 | 0,0096 |
| 5,5 | 0,0198 | 0,1877 | 0,9645 | 0,00907 |
| 5,6 | 0,0192 | 0,1842 | 0,9658 | 0,00859 |
| 5,7 | 0,0187 | 0,1808 | 0,9670 | 0,00814 |
| 5,8 | 0,0182 | 0,1775 | 0,9682 | 0,00773 |
| 5,9 | 0,0177 | 0,1743 | 0,9693 | 0,00735 |
| 6,0 | 0,0172 | 0,1712 | 0,9704 | 0,00699 |

$\varphi = -10°$ Cont'd

| $\rho$ | $\mathrm{Re}G_0$ | $-\mathrm{Im}G_0$ | $\mathrm{Re}G_1$ | $-\mathrm{Im}G_1$ | $\rho$ | $\mathrm{Re}G_0$ | $-\mathrm{Im}G_0$ | $\mathrm{Re}G_1$ | $-\mathrm{Im}G_1$ |
|---|---|---|---|---|---|---|---|---|---|
| 0 | $\infty$ | 1,3963 | $\infty$ | $\infty$ | 3,0 | 0,0958 | 0,3397 | 0,9030 | 0,0724 |
| 0,1 | 2,4428 | 1,3039 | 1,8276 | 9,7152 | 3,1 | 0,0906 | 0,3291 | 0,9079 | 0,0667 |
| 0,2 | 1,7814 | 1,2210 | 1,0332 | 4,7236 | 3,2 | 0,0858 | 0,3192 | 0,9124 | 0,0616 |
| 0,3 | 1,4120 | 1,1460 | 0,8084 | 3,0373 | 3,3 | 0,0815 | 0,3097 | 0,9167 | 0,0570 |
| 0,4 | 1,1630 | 1,0775 | 0,7213 | 2,1850 | 3,4 | 0,0775 | 0,3008 | 0,9207 | 0,0529 |
| 0,5 | 0,9802 | 1,0149 | 0,6862 | 1,6700 | 3,5 | 0 0738 | 0,2923 | 0,9245 | 0,0491 |
| 0,6 | 0,8393 | 0,9575 | 0,6752 | 1,3257 | 3,6 | 0,0704 | 0,2842 | 0,9280 | 0,0456 |
| 0,7 | 0,7271 | 0,9047 | 0,6764 | 1,0800 | 3,7 | 0,0673 | 0,2765 | 0,9314 | 0,0425 |
| 0,8 | 0,6358 | 0,8561 | 0,6841 | 0,8966 | 3,8 | 0,0644 | 0,2692 | 0,9345 | 0,0397 |
| 0,9 | 0,5601 | 0,8112 | 0,6953 | 0,7552 | 3,9 | 0,0618 | 0,2622 | 0,9374 | 0,0371 |
| 1,0 | 0,4966 | 0,7698 | 0,7084 | 0,6434 | 4,0 | 0,0593 | 0,2556 | 0,9402 | 0,0347 |
| 1,1 | 0,4428 | 0,7314 | 0,7222 | 0,5533 | 4,1 | 0,0570 | 0,2492 | 0,9428 | 0,0325 |
| 1,2 | 0,3967 | 0,6959 | 0,7363 | 0,4796 | 4,2 | 0,0549 | 0,2432 | 0,9453 | 0,0306 |
| 1,3 | 0,3571 | 0,6627 | 0,7502 | 0,4184 | 4,3 | 0,0529 | 0,2374 | 0,9476 | 0,0287 |
| 1,4 | 0,3227 | 0,6320 | 0,7638 | 0,3671 | 4,4 | 0,0510 | 0,2318 | 0,9498 | 0,0270 |
| 1,5 | 0,2927 | 0,6034 | 0,7768 | 0,3238 | 4,5 | 0,0493 | 0,2266 | 0,9519 | 0,0255 |
| 1,6 | 0,2665 | 0,5767 | 0,7892 | 0,2868 | 4,6 | 0,0477 | 0,2215 | 0,9538 | 0,0241 |
| 1,7 | 0,2434 | 0,5518 | 0,8010 | 0,2551 | 4,7 | 0,0462 | 0,2166 | 0,9557 | 0,0227 |
| 1,8 | 0,2230 | 0,5286 | 0,8121 | 0,2278 | 4,8 | 6,0447 | 0,2120 | 0,9574 | 0,0215 |
| 1,9 | 0,2049 | 0,5069 | 0,8226 | 0,2040 | 4,9 | 0,0434 | 0,2075 | 0,9591 | 0,0204 |
| 2,0 | 0,1889 | 0,4865 | 0,8325 | 0,1834 | 5,0 | 0,0421 | 0,2032 | 0,9607 | 0,0193 |
| 2,1 | 0,1745 | 0,4675 | 0,8417 | 0,1652 | 5,1 | 0,0409 | 0,1991 | 0,9618 | 0,0184 |
| 2,2 | 0,1617 | 0,4496 | 0,8504 | 0,1494 | 5,2 | 0,0398 | 0,1951 | 0,9636 | 0,0175 |
| 2,3 | 0,1503 | 0,4324 | 0,8586 | 0,1353 | 5,3 | 0,0388 | 0,1913 | 0,9649 | 0,0166 |
| 2,4 | 0,1399 | 0,4170 | 0,8662 | 0,1229 | 5,4 | 0,0378 | 0,1876 | 0,9662 | 0,0158 |
| 2,5 | 0,1306 | 0,4021 | 0,8734 | 0,1119 | 5,5 | 0,0368 | 0,1841 | 0,9674 | 0,0151 |
| 2,6 | 0,1223 | 0,3882 | 0,8801 | 0,1022 | 5,6 | 0,0359 | 0,1807 | 0,9685 | 0,0144 |
| 2,7 | 0,1147 | 0,3750 | 0,8864 | 0,0934 | 5,7 | 0,0351 | 0,1774 | 0,9696 | 0,0138 |
| 2,8 | 0,1078 | 0,3625 | 0,8923 | 0,0856 | 5,8 | 0,0343 | 0,1742 | 0,9707 | 0,0132 |
| 2,9 | 0,1015 | 0,3508 | 0,8978 | 0,0786 | 5,9 | 0,0335 | 0,1711 | 0,9717 | 0,0126 |
| | | | | | 6,0 | 0,0328 | 0,1682 | 0,9726 | 0,0121 |

$\varphi = -18°$ Cont'd

| $\rho$ | $\mathrm{Re}G_0$ | $-\mathrm{Im}G_0$ | $\mathrm{Re}G_1$ | $-\mathrm{Im}G_1$ | $\rho$ | $\mathrm{Re}G_0$ | $-\mathrm{Im}G_0$ | $\mathrm{Re}G_1$ | $-\mathrm{Im}G_1$ |
|---|---|---|---|---|---|---|---|---|---|
| 0 | $\infty$ | 1,3090 | $\infty$ | $\infty$ | 3,0 | 0,1230 | 0,3246 | 0,9191 | 0,0840 |
| 0,1 | 2,4502 | 1,2194 | 2,6865 | 9,5335 | 3,1 | 0,1172 | 0,3149 | 0,9228 | 0,0781 |
| 0,2 | 1,7948 | 1,1402 | 1,4681 | 4,6413 | 3,2 | 0,1119 | 0,3057 | 0,9264 | 0,0726 |
| 0,3 | 1,4302 | 1,0691 | 1,1016 | 2,9902 | 3,3 | 0,1070 | 0,2969 | 0,9298 | 0,0677 |
| 0,4 | 1,1851 | 1,0047 | 0,9430 | 2,1567 | 3,4 | 0,1025 | 0,2886 | 0,9330 | 0,0632 |
| 0,5 | 1,0055 | 0,9462 | 0,8644 | 1,6535 | 3,5 | 0,0983 | 0,2807 | 0,9360 | 0,0591 |
| 0,6 | 0,8671 | 0,8927 | 0,8237 | 1,3172 | 3,6 | 0,0944 | 0,2732 | 0,9388 | 0,0554 |
| 0,7 | 0,7589 | 0,8438 | 0,8033 | 1,0773 | 3,7 | 0,0907 | 0,2660 | 0,9415 | 0,0519 |
| 0,8 | 0,6671 | 0,7988 | 0,7944 | 0,8983 | 3,8 | 0,0873 | 0,2592 | 0,9440 | 0,0488 |
| 0,9 | 0,5926 | 0,7574 | 0,7924 | 0,7602 | 3,9 | 0,0842 | 0,2526 | 0,9464 | 0,0459 |
| 1,0 | 0,5300 | 0,7198 | 0,7946 | 0,6510 | 4,0 | 0,0812 | 0,2464 | 0,9486 | 0,0432 |
| 1,1 | 0,4768 | 0,6839 | 0,7994 | 0,5628 | 4,1 | 0,0785 | 0,2405 | 0,9506 | 0,0408 |
| 1,2 | 0,4311 | 0,6513 | 0,8058 | 0,4906 | 4,2 | 0,0759 | 0,2348 | 0,9528 | 0,0385 |
| 1,3 | 0,3917 | 0,6209 | 0,8131 | 0,4304 | 4,3 | 0,0735 | 0,2294 | 0,9547 | 0,0364 |
| 1,4 | 0,3573 | 0,5928 | 0,8208 | 0,3800 | 4,4 | 0,0712 | 0,2242 | 0,9565 | 0,0345 |
| 1,5 | 0,3273 | 0,5666 | 0,8288 | 0,3373 | 4,5 | 0,0691 | 0,2192 | 0,9582 | 0,0327 |
| 1,6 | 0,3009 | 0,5422 | 0,8367 | 0,3007 | 4,6 | 0,0670 | 0,2144 | 0,9598 | 0,0310 |
| 1,7 | 0,2775 | 0,5194 | 0,8445 | 0,2693 | 4,7 | 0,0651 | 0,2098 | 0,9614 | 0,0296 |
| 1,8 | 0,2568 | 0,4982 | 0,8520 | 0,2421 | 4,8 | 0,0633 | 0,2054 | 0,9628 | 0,0281 |
| 1,9 | 0,2383 | 0,4783 | 0,8593 | 0,2184 | 4,9 | 0,0616 | 0,2012 | 0,9642 | 0,0267 |
| 2,0 | 0,2218 | 0,4596 | 0,8663 | 0,1976 | 5,0 | 0,0600 | 0,1971 | 0,9655 | 0,0255 |
| 2,1 | 0,2069 | 0,4422 | 0,8729 | 0,1794 | 5,1 | 0,0585 | 0,1932 | 0,9668 | 0,0243 |
| 2,2 | 0,1936 | 0,4258 | 0,8793 | 0,1634 | 5,2 | 0,0570 | 0,1894 | 0,9680 | 0,0232 |
| 2,3 | 0,1816 | 0,4104 | 0,8853 | 0,1491 | 5,3 | 0,0557 | 0,1858 | 0,9691 | 0,0222 |
| 2,4 | 0,1707 | 0,3959 | 0,8910 | 0,1365 | 5,4 | 0,0544 | 0,1823 | 0,9702 | 0,0212 |
| 2,5 | 0,1608 | 0,3822 | 0,8964 | 0,1252 | 5,5 | 0,0531 | 0,1789 | 0,9712 | 0,0203 |
| 2,6 | 0,1518 | 0,3694 | 0,9014 | 0,1151 | 5,6 | 0,0519 | 0,1757 | 0,9722 | 0,0195 |
| 2,7 | 0,1436 | 0,3572 | 0,9062 | 0,1061 | 5,7 | 0,0508 | 0,1725 | 0,9731 | 0,0187 |
| 2,8 | 0,1362 | 0,3458 | 0,9108 | 0,0980 | 5,8 | 0,0497 | 0,1695 | 0,9740 | 0,0180 |
| 2,9 | 0,1293 | 0,3349 | 0,9150 | 0,0906 | 5,9 | 0,0487 | 0,1666 | 0,9748 | 0,0173 |
| | | | | | 6,0 | 0,0477 | 0,1637 | 0,9756 | 0,0166 |

$\varphi = -20°$

Cont'd

| $\rho$ | $\mathrm{Re}G_0$ | $-\mathrm{Im}G_0$ | $\mathrm{Re}G_1$ | $-\mathrm{Im}G_1$ | $\rho$ | $\mathrm{Re}G_0$ | $-\mathrm{Im}G_0$ | $\mathrm{Re}G_1$ | $-\mathrm{Im}G_1$ |
|---|---|---|---|---|---|---|---|---|---|
| 0 | $\infty$ | 1,2217 | $\infty$ | $\infty$ | 3,0 | 0,1482 | 0,3082 | 0,9358 | 0,0928 |
| 0,1 | 2,4574 | 1,1355 | 3,5252 | 9,2785 | 3,1 | 0,1419 | 0,2992 | 0,9386 | 0,0887 |
| 0,2 | 1,8076 | 1,0603 | 1,8924 | 4,5223 | 3,2 | 0,1361 | 0,2907 | 0,9412 | 0,0810 |
| 0,3 | 1,4473 | 0,9933 | 1,3874 | 2,9186 | 3,3 | 0,1306 | 0,2826 | 0,9437 | 0,0789 |
| 0,4 | 1,2068 | 0,9331 | 1,1589 | 2,1097 | 3,4 | 0,1256 | 0,2749 | 0,9460 | 0,0712 |
| 0,5 | 1,0290 | 0,8786 | 1,0378 | 1,6217 | 3,5 | 0,1209 | 0,2676 | 0,9483 | 0,0669 |
| 0,6 | 0,8928 | 0,8290 | 0,9682 | 1,2958 | 3,6 | 0,1166 | 0,2606 | 0,9504 | 0,0629 |
| 0,7 | 0,7844 | 0,7838 | 0,9267 | 1,0634 | 3,7 | 0,1125 | 0,2540 | 0,9524 | 0,0593 |
| 0,8 | 0,6960 | 0,7424 | 0,9017 | 0,8899 | 3,8 | 0,1087 | 0,2476 | 0,9544 | 0,0559 |
| 0,9 | 0,6225 | 0,7043 | 0,8869 | 0,7560 | 3,9 | 0,1051 | 0,2415 | 0,9562 | 0,0529 |
| 1,0 | 0,5607 | 0,6693 | 0,8786 | 0,6500 | 4,0 | 0,1017 | 0,2358 | 0,9579 | 0,0500 |
| 1,1 | 0,5080 | 0,6369 | 0,8758 | 0,5644 | 4,1 | 0,0986 | 0,2302 | 0,9596 | 0,0474 |
| 1,2 | 0,4627 | 0,6070 | 0,8737 | 0,4941 | 4,2 | 0,0956 | 0,2249 | 0,9611 | 0,0449 |
| 1,3 | 0,4234 | 0,5793 | 0,8746 | 0,4357 | 4,3 | 0,0928 | 0,2198 | 0,9626 | 0,0426 |
| 1,4 | 0,3991 | 0,5536 | 0,8768 | 0,3864 | 4,4 | 0,0901 | 0,2150 | 0,9640 | 0,0405 |
| 1,5 | 0,3589 | 0,5297 | 0,8799 | 0,3447 | 4,5 | 0,0876 | 0,2103 | 0,9653 | 0,0385 |
| 1,6 | 0,3323 | 0,5074 | 0,8835 | 0,3089 | 4,6 | 0,0853 | 0,2058 | 0,9666 | 0,0367 |
| 1,7 | 0,3087 | 0,4866 | 0,8875 | 0,2780 | 4,7 | 0,0830 | 0,2015 | 0,9678 | 0,0350 |
| 1,8 | 0,2876 | 0,4672 | 0,8916 | 0,2512 | 4,8 | 0,0809 | 0,1974 | 0,9690 | 0,0334 |
| 1,9 | 0,2688 | 0,4490 | 0,8958 | 0,2278 | 4,9 | 0,0789 | 0,1934 | 0,9701 | 0,0319 |
| 2,0 | 0,2519 | 0,4310 | 0,9001 | 0,2072 | 5,0 | 0,0769 | 0,1896 | 0,9711 | 0,0305 |
| 2,1 | 0,2366 | 0,4160 | 0,9042 | 0,1891 | 5,1 | 0,0751 | 0,1859 | 0,9721 | 0,0292 |
| 2,2 | 0,2228 | 0,4010 | 0,9083 | 0,1731 | 5,2 | 0,0734 | 0,1823 | 0,9731 | 0,0280 |
| 2,3 | 0,2103 | 0,3869 | 0,9123 | 0,1589 | 5,3 | 0,0717 | 0,1789 | 0,9740 | 0,0268 |
| 2,4 | 0,1989 | 0,3736 | 0,9161 | 0,1462 | 5,4 | 0,0701 | 0,1756 | 0,9748 | 0,0257 |
| 2,5 | 0,1885 | 0,3611 | 0,9197 | 0,1348 | 5,5 | 0,0686 | 0,1724 | 0,9757 | 0,0247 |
| 2,6 | 0,1790 | 0,3493 | 0,9233 | 0,1246 | 5,6 | 0,0671 | 0,1693 | 0,9765 | 0,0237 |
| 2,7 | 0,1703 | 0,3382 | 0,9266 | 0,1154 | 5,7 | 0,0657 | 0,1664 | 0,9772 | 0,0228 |
| 2,8 | 0,1623 | 0,3276 | 0,9298 | 0,1071 | 5,8 | 0,0644 | 0,1635 | 0,9779 | 0,0219 |
| 2,9 | 0,1549 | 0,3176 | 0,9329 | 0,0996 | 5,9 | 0,0631 | 0,1607 | 0,9786 | 0,0211 |
| | | | | | 6,0 | 0,0619 | 0,1580 | 0,9793 | 0,0203 |

Cont'd

$\gamma = -25°$

| $\rho$ | $\mathrm{Re}G_0$ | $-\mathrm{Im}G_0$ | $\mathrm{Re}G_1$ | $-\mathrm{Im}G_1$ | $\rho$ | $\mathrm{Re}G_0$ | $-\mathrm{Im}G_0$ | $\mathrm{Re}G_1$ | $-\mathrm{Im}G_1$ |
|---|---|---|---|---|---|---|---|---|---|
| 0 | $\infty$ | 1,1345 | $\infty$ | $\infty$ | 3,0 | 0,1718 | 0,2995 | 0,9539 | 0,0999 |
| 0,1 | 2,4642 | 1,0622 | 4,3374 | 8,9522 | 3,1 | 0,1645 | 0,2858 | 0,9548 | 0,0927 |
| 0,2 | 1,8195 | 0,9812 | 2,3030 | 4,3677 | 3,2 | 0,1583 | 0,2744 | 0,9568 | 0,0869 |
| 0,3 | 1,4634 | 0,9185 | 1,6638 | 2,8231 | 3,3 | 0,1526 | 0,2670 | 0,9580 | 0,0817 |
| 0,4 | 1,2280 | 0,8625 | 1,3675 | 2,0446 | 3,4 | 0,1470 | 0,2589 | 0,9596 | 0,0769 |
| 0,5 | 1,0508 | 0,8120 | 1,2052 | 1,5752 | 3,5 | 0,1419 | 0,2532 | 0,9611 | 0,0725 |
| 0,6 | 0,9166 | 0,7663 | 1,1077 | 1,2619 | 3,6 | 0,1372 | 0,2467 | 0,9625 | 0,0684 |
| 0,7 | 0,8098 | 0,7247 | 1,0459 | 1,0395 | 3,7 | 0,1327 | 0,2406 | 0,9639 | 0,0647 |
| 0,8 | 0,7225 | 0,6867 | 1,0063 | 0,8717 | 3,8 | 0,1285 | 0,2347 | 0,9652 | 0,0612 |
| 0,9 | 0,6500 | 0,6518 | 0,9782 | 0,7430 | 3,9 | 0,1245 | 0,2291 | 0,9665 | 0,0580 |
| 1,0 | 0,5888 | 0,6196 | 0,9600 | 0,6410 | 4,0 | 0,1208 | 0,2237 | 0,9677 | 0,0550 |
| 1,1 | 0,5365 | 0,5903 | 0,9476 | 0,5585 | 4,1 | 0,1175 | 0,2186 | 0,9689 | 0,0522 |
| 1,2 | 0,4914 | 0,5630 | 0,9394 | 0,4907 | 4,2 | 0,1139 | 0,2137 | 0,9700 | 0,0497 |
| 1,3 | 0,4529 | 0,5378 | 0,9343 | 0,4343 | 4,3 | 0,1108 | 0,2090 | 0,9711 | 0,0473 |
| 1,4 | 0,4180 | 0,5144 | 0,9312 | 0,3867 | 4,4 | 0,1078 | 0,2044 | 0,9721 | 0,0450 |
| 1,5 | 0,3878 | 0,4926 | 0,9296 | 0,3462 | 4,5 | 0,1050 | 0,2001 | 0,9730 | 0,0430 |
| 1,6 | 0,3610 | 0,4723 | 0,9292 | 0,3115 | 4,6 | 0,1023 | 0,1959 | 0,9740 | 0,0410 |
| 1,7 | 0,3371 | 0,4534 | 0,9296 | 0,2815 | 4,7 | 0,0997 | 0,1919 | 0,9749 | 0,0392 |
| 1,8 | 0,3158 | 0,4357 | 0,9304 | 0,2554 | 4,8 | 0,0973 | 0,1880 | 0,9757 | 0,0375 |
| 1,9 | 0,2966 | 0,4191 | 0,9318 | 0,2325 | 4,9 | 0,0950 | 0,1843 | 0,9765 | 0,0359 |
| 2,0 | 0,2793 | 0,4036 | 0,9334 | 0,2124 | 5,0 | 0,0928 | 0,1807 | 0,9773 | 0,0344 |
| 2,1 | 0,2637 | 0,3891 | 0,9352 | 0,1946 | 5,1 | 0,0907 | 0,1773 | 0,9780 | 0,0330 |
| 2,2 | 0,2495 | 0,3754 | 0,9371 | 0,1788 | 5,2 | 0,0887 | 0,1740 | 0,9787 | 0,0316 |
| 2,3 | 0,2366 | 0,3625 | 0,9391 | 0,1648 | 5,3 | 0,0867 | 0,1708 | 0,9794 | 0,0304 |
| 2,4 | 0,2247 | 0,3504 | 0,9411 | 0,1522 | 5,4 | 0,0849 | 0,1677 | 0,9801 | 0,0292 |
| 2,5 | 0,2139 | 0,3390 | 0,9432 | 0,1409 | 5,5 | 0,0831 | 0,1647 | 0,9807 | 0,0281 |
| 2,6 | 0,2039 | 0,3282 | 0,9452 | 0,1306 | 5,6 | 0,0814 | 0,1618 | 0,9813 | 0,0270 |
| 2,7 | 0,1948 | 0,3180 | 0,9472 | 0,1216 | 5,7 | 0,0798 | 0,1590 | 0,9818 | 0,0260 |
| 2,8 | 0,1863 | 0,3083 | 0,9491 | 0,1133 | 5,8 | 0,0783 | 0,1563 | 0,9824 | 0,0251 |
| 2,9 | 0,1785 | 0,2992 | 0,9510 | 0,1058 | 5,9 | 0,0768 | 0,1537 | 0,9829 | 0,0242 |
| | | | | | 6,0 | 0,0753 | 0,1512 | 0,9834 | 0,0233 |

$\varphi = -30°$

*Cont'd*

| $\rho$ | $\mathrm{Re}G_0$ | $-\mathrm{Im}G_0$ | $\mathrm{Re}G_1$ | $-\mathrm{Im}G_1$ | $\rho$ | $\mathrm{Re}G_0$ | $-\mathrm{Im}G_0$ | $\mathrm{Re}G_1$ | $-\mathrm{Im}G_1$ |
|---|---|---|---|---|---|---|---|---|---|
| 0 | $\infty$ | 1,0472 | $\infty$ | $\infty$ | 3,0 | 0,1924 | 0,2717 | 0,9889 | 0,1023 |
| 0,1 | 2,4706 | 0,9898 | 5,1169 | 8,5572 | 3,1 | 0,1853 | 0,2642 | 0,9708 | 0,0961 |
| 0,2 | 1,8308 | 0,9029 | 2,6968 | 4,1787 | 3,2 | 0,1787 | 0,2570 | 0,9716 | 0,0904 |
| 0,3 | 1,4783 | 0,8446 | 1,9286 | 2,7045 | 3,3 | 0,1725 | 0,2502 | 0,9724 | 0,0852 |
| 0,4 | 1,2428 | 0,7928 | 1,5674 | 1,9620 | 3,4 | 0,1667 | 0,2437 | 0,9733 | 0,0804 |
| 0,5 | 1,0709 | 0,7464 | 1,3655 | 1,5146 | 3,5 | 0,1612 | 0,2376 | 0,9741 | 0,0760 |
| 0,6 | 0,9385 | 0,7044 | 1,2413 | 1,2159 | 3,6 | 0,1561 | 0,2316 | 0,9749 | 0,0719 |
| 0,7 | 0,8330 | 0,6664 | 1,1600 | 1,0031 | 3,7 | 0,1513 | 0,2260 | 0,9756 | 0,0681 |
| 0,8 | 0,7468 | 0,6317 | 1,1045 | 0,8141 | 3,8 | 0,1467 | 0,2206 | 0,9764 | 0,0646 |
| 0,9 | 0,6750 | 0,6000 | 1,0656 | 0,7216 | 3,9 | 0,1424 | 0,2155 | 0,9771 | 0,0613 |
| 1,0 | 0,6143 | 0,5706 | 1,0278 | 0,6241 | 4,0 | 0,1384 | 0,2106 | 0,9779 | 0,0583 |
| 1,1 | 0,5625 | 0,5440 | 1,0175 | 0,5454 | 4,1 | 0,1346 | 0,2058 | 0,9785 | 0,0555 |
| 1,2 | 0,5176 | 0,5200 | 1,0026 | 0,4807 | 4,2 | 0,1309 | 0,2012 | 0,9792 | 0,0529 |
| 1,3 | 0,4786 | 0,4963 | 0,9917 | 0,4267 | 4,3 | 0,1275 | 0,1969 | 0,9799 | 0,0504 |
| 1,4 | 0,4443 | 0,4751 | 0,9836 | 0,3811 | 4,4 | 0,1242 | 0,1927 | 0,9805 | 0 0481 |
| 1,5 | 0,4140 | 0,4553 | 0,9777 | 0,3423 | 4,5 | 0,1211 | 0,1887 | 0,9811 | 0,0460 |
| 1,6 | 0,3870 | 0,4369 | 0,9733 | 0,3089 | 4,6 | 0,1181 | 0,1848 | 0,9817 | 0,0440 |
| 1,7 | 0,3630 | 0,4198 | 0,9703 | 0,2800 | 4,7 | 0,1153 | 0,1811 | 0,9822 | 0,0421 |
| 1,8 | 0,3414 | 0,4037 | 0,9681 | 0,2549 | 4,8 | 0,1126 | 0,1775 | 0,9828 | 0,0403 |
| 1,9 | 0,3219 | 0,3887 | 0,9667 | 0,2328 | 4,9 | 0,1100 | 0,1741 | 0,9833 | 0,0387 |
| 2,0 | 0,3043 | 0,3747 | 0,9658 | 0,2133 | 5,0 | 0,1076 | 0,1708 | 0,9838 | 0,0371 |
| 2,1 | 0,2883 | 0,3614 | 0,9654 | 0,1961 | 5,1 | 0,1052 | 0,1676 | 0,9843 | 0,0356 |
| 2,2 | 0,2738 | 0,3490 | 0,9653 | 0,1808 | 5,2 | 0,1030 | 0,1645 | 0,9847 | 0,0342 |
| 2,3 | 0,2604 | 0,3373 | 0,9654 | 0,1671 | 5,3 | 0,1008 | 0,1615 | 0,9852 | 0,0329 |
| 2,4 | 0,2482 | 0,3263 | 0,9658 | 0,1548 | 5,4 | 0,0987 | 0,1586 | 0,9856 | 0,0317 |
| 2,5 | 0,2370 | 0,3159 | 0,9663 | 0,1437 | 5,5 | 0,0968 | 0,1559 | 0,9860 | 0,0302 |
| 2,6 | 0,2267 | 0,3061 | 0,9669 | 0,1338 | 5,6 | 0,0948 | 0,1532 | 0,9864 | 0,0294 |
| 2,7 | 0,2171 | 0,2968 | 0,9676 | 0,1248 | 5,7 | 0,0930 | 0,1506 | 0,9868 | 0,0284 |
| 2,8 | 0,2083 | 0,2880 | 0,9683 | 0,1166 | 5,8 | 0,0912 | 0,1480 | 0,9872 | 0,0274 |
| 2,9 | 0,2001 | 0,2796 | 0,9691 | 0,1091 | 5,9 | 0,0896 | 0,1456 | 0,9875 | 0,0264 |
| | | | | | 6,0 | 0,0879 | 0,1433 | 0,9879 | 0,0255 |

$\varphi = -35°$

Cont'd

| $\rho$ | $\mathrm{Re}G_0$ | $-\mathrm{Im}G_0$ | $\mathrm{Re}G_1$ | $-\mathrm{Im}G_1$ | $\rho$ | $\mathrm{Re}G_0$ | $-\mathrm{Im}G_0$ | $\mathrm{Re}G_1$ | $-\mathrm{Im}G_1$ |
|---|---|---|---|---|---|---|---|---|---|
| 0 | $\infty$ | 0,9599 | $\infty$ | $\infty$ | 3,0 | 0,2117 | 0,2520 | 0,9867 | 0,1031 |
| 0,1 | 2,4766 | 0,8869 | 5,8578 | 8,0965 | 3,1 | 0,2043 | 0,2452 | 0,9867 | 0,0972 |
| 0,2 | 1,8412 | 0,8253 | 3,0709 | 3,9568 | 3,2 | 0,1973 | 0,2387 | 0,9867 | 0,0916 |
| 0,3 | 1,4921 | 0,7715 | 2,1801 | 2,5639 | 3,3 | 0,1908 | 0,2325 | 0,9867 | 0,0865 |
| 0,4 | 1,2592 | 0,7240 | 1,7570 | 1,8626 | 3,4 | 0,1846 | 0,2266 | 0,9868 | 0,0818 |
| 0,5 | 1,0892 | 0,6816 | 1,5176 | 1,4403 | 3,5 | 0,1789 | 0,2209 | 0,9870 | 0,0774 |
| 0,6 | 0,9584 | 0,6434 | 1,3679 | 1,1585 | 3,6 | 0,1734 | 0,2155 | 0,9872 | 0,0734 |
| 0,7 | 0,8541 | 0,6088 | 1,2681 | 0,9576 | 3,7 | 0,1683 | 0,2104 | 0,9874 | 0,0697 |
| 0,8 | 0,7688 | 0,5773 | 1,1986 | 0,8076 | 3,8 | 0,1635 | 0,2055 | 0,9876 | 0,0662 |
| 0,9 | 0,6977 | 0,5485 | 1,1486 | 0,6918 | 3,9 | 0,1589 | 0,2008 | 0,9878 | 0,0630 |
| 1,0 | 0,6375 | 0,5222 | 1,1117 | 0,5999 | 4,0 | 0,1545 | 0,1962 | 0,9880 | 0,0599 |
| 1,1 | 0,5860 | 0,4979 | 1,0839 | 0,5255 | 4,1 | 0,1504 | 0,1919 | 0,9883 | 0,0571 |
| 1,2 | 0,5413 | 0,4756 | 1,0627 | 0,4643 | 4,2 | 0,1465 | 0,1878 | 0,9885 | 0,0545 |
| 1,3 | 0,5024 | 0,4549 | 1,0463 | 0,4131 | 4,3 | 0,1428 | 0,1838 | 0,9888 | 0,0521 |
| 1,4 | 0,4681 | 0,4354 | 1,0335 | 0,3700 | 4,4 | 0,1393 | 0,1799 | 0,9890 | 0,0498 |
| 1,5 | 0,4377 | 0,4179 | 1,0235 | 0,3331 | 4,5 | 0,1359 | 0,1763 | 0,9893 | 0,0476 |
| 1,6 | 0,4106 | 0,4013 | 1,0156 | 0,3014 | 4,6 | 0,1327 | 0,1727 | 0,9895 | 0,0456 |
| 1,7 | 0,3864 | 0,3858 | 1,0093 | 0,2739 | 4,7 | 0,1296 | 0,1693 | 0,9898 | 0,0437 |
| 1,8 | 0,3645 | 0,3714 | 1,0043 | 0,2500 | 4,8 | 0,1267 | 0,1660 | 0,9900 | 0,0419 |
| 1,9 | 0,3448 | 0,3578 | 1,0003 | 0,2289 | 4,9 | 0,1239 | 0,1629 | 0,9902 | 0,0403 |
| 2,0 | 0,3269 | 0,3451 | 0,9971 | 0,2103 | 5,0 | 0,1212 | 0,1598 | 0,9905 | 0,0387 |
| 2,1 | 0,3106 | 0,3332 | 0,9946 | 0,1938 | 5,1 | 0,1186 | 0,1569 | 0,9907 | 0,0372 |
| 2,2 | 0,2958 | 0,3220 | 0,9926 | 0,1791 | 5,2 | 0,1162 | 0,1540 | 0,9909 | 0,0358 |
| 2,3 | 0,2821 | 0,3114 | 0,9910 | 0,1659 | 5,3 | 0,1138 | 0,1513 | 0,9912 | 0,0344 |
| 2,4 | 0,2696 | 0,3015 | 0,9897 | 0,1541 | 5,4 | 0,1116 | 0,1486 | 0,9914 | 0,0332 |
| 2,5 | 0,2580 | 0,2921 | 0,9888 | 0,1434 | 5,5 | 0,1094 | 0,1460 | 0,9916 | 0,0320 |
| 2,6 | 0,2473 | 0,2832 | 0,9879 | 0,1338 | 5,6 | 0,1073 | 0,1436 | 0,9918 | 0,0309 |
| 2,7 | 0,2374 | 0,2747 | 0,9875 | 0,1251 | 5,7 | 0,1053 | 0,1412 | 0,9920 | 0,0298 |
| 2,8 | 0,2282 | 0,2668 | 0,9872 | 0,1171 | 5,8 | 0,1033 | 0,1388 | 0,9923 | 0,0288 |
| 2,9 | 0,2197 | 0,2592 | 0,9869 | 0,1099 | 5,9 | 0,1014 | 0,1366 | 0,9924 | 0,0278 |
| | | | | | 6,0 | 0,0966 | 0,1344 | 0,9926 | 0,0269 |

Cont'd

$\gamma = -45°$

| $\rho$ | $\mathrm{Re}G_0$ | $-\mathrm{Im}G_0$ | $\mathrm{Re}G_1$ | $-\mathrm{Im}G_1$ | $\rho$ | $\mathrm{Re}G_0$ | $-\mathrm{Im}G_0$ | $\mathrm{Re}G_1$ | $-\mathrm{Im}G_1$ |
|---|---|---|---|---|---|---|---|---|---|
| 0 | $\infty$ | 0,8727 | $\infty$ | $\infty$ | 3,0 | 0,2291 | 0,2315 | 1,0030 | 0,1018 |
| 0,1 | 2,4822 | 0,8049 | 6,5547 | 7,5736 | 3,1 | 0,2214 | 0,2253 | 1,0021 | 0,0960 |
| 0,2 | 1,8508 | 0,7483 | 3,4226 | 3,7038 | 3,2 | 0,2142 | 0,2194 | 1,0013 | 0,0907 |
| 0,3 | 1,5047 | 0,6992 | 2,4163 | 2,4024 | 3,3 | 0,2073 | 0,2138 | 1,0007 | 0,0857 |
| 0,4 | 1,2741 | 0,6560 | 1,9850 | 1,7475 | 3,4 | 0,2009 | 0,2085 | 1,0001 | 0,0812 |
| 0,5 | 1,1060 | 0,6175 | 1,6603 | 1,3532 | 3,5 | 0,1949 | 0,2034 | 0,9996 | 0,0770 |
| 0,6 | 0,9765 | 0,5829 | 1,4867 | 1,0902 | 3,6 | 0,1892 | 0,1985 | 0,9992 | 0,0731 |
| 0,7 | 0,8732 | 0,5517 | 1,3697 | 0,9027 | 3,7 | 0,1838 | 0,1939 | 0,9988 | 0,0694 |
| 0,8 | 0,7887 | 0,5234 | 1,2870 | 0,7627 | 3,8 | 0,1787 | 0,1894 | 0,9985 | 0,0661 |
| 0,9 | 0,7182 | 0,4975 | 1,2265 | 0,6545 | 3,9 | 0,1738 | 0,1852 | 0,9983 | 0,0629 |
| 1,0 | 0,6585 | 0,4739 | 1,1810 | 0,5687 | 4,0 | 0,1692 | 0,1811 | 0,9980 | 0,0600 |
| 1,1 | 0,6072 | 0,4521 | 1,1464 | 0,4992 | 4,1 | 0,1649 | 0,1771 | 0,9979 | 0,0573 |
| 1,2 | 0,5627 | 0,4320 | 1,1192 | 0,4419 | 4,2 | 0,1607 | 0,1734 | 0,9977 | 0,0547 |
| 1,3 | 0,5238 | 0,4135 | 1,0978 | 0,3941 | 4,3 | 0,1568 | 0,1697 | 0,9976 | 0,0523 |
| 1,4 | 0,4894 | 0,3963 | 1,0806 | 0,3536 | 4,4 | 0,1530 | 0,1663 | 0,9975 | 0,0501 |
| 1,5 | 0,4590 | 0,3803 | 1,0668 | 0,3191 | 4,5 | 0,1494 | 0,1629 | 0,9974 | 0,0480 |
| 1,6 | 0,4318 | 0,3655 | 1,0555 | 0,2894 | 4,6 | 0,1460 | 0,1597 | 0,9973 | 0,0460 |
| 1,7 | 0,4074 | 0,3516 | 1,0462 | 0,2635 | 4,7 | 0,1427 | 0,1566 | 0,9973 | 0,0441 |
| 1,8 | 0,3854 | 0,3386 | 1,0385 | 0,2409 | 4,8 | 0,1396 | 0,1536 | 0,9973 | 0,0424 |
| 1,9 | 0,3654 | 0,3265 | 1,0321 | 0,2211 | 4,9 | 0,1366 | 0,1507 | 0,9972 | 0,0407 |
| 2,0 | 0,3473 | 0,3151 | 1,0268 | 0,2035 | 5,0 | 0,1337 | 0,1479 | 0,9972 | 0,0392 |
| 2,1 | 0,3307 | 0,3044 | 1,0223 | 0,1879 | 5,1 | 0,1310 | 0,1452 | 0,9971 | 0,0377 |
| 2,2 | 0,3156 | 0,2944 | 1,0186 | 0,1740 | 5,2 | 0,1283 | 0,1426 | 0,9971 | 0,0363 |
| 2,3 | 0,3016 | 0,2849 | 1,0154 | 0,1615 | 5,3 | 0,1258 | 0,1401 | 0,9972 | 0,0350 |
| 2,4 | 0,2888 | 0,2759 | 1,0127 | 0,1503 | 5,4 | 0,1233 | 0,1377 | 0,9972 | 0,0337 |
| 2,5 | 0,2769 | 0,2675 | 1,0104 | 0,1402 | 5,5 | 0,1210 | 0,1354 | 0,9972 | 0,0325 |
| 2,6 | 0,2659 | 0,2595 | 1,0084 | 0,1310 | 5,6 | 0,1187 | 0,1331 | 0,9972 | 0,0314 |
| 2,7 | 0,2558 | 0,2519 | 1,0067 | 0,1227 | 5,7 | 0,1165 | 0,1309 | 0,9972 | 0,0303 |
| 2,8 | 0,2469 | 0,2447 | 1,0053 | 0,1151 | 5,8 | 0,1144 | 0,1288 | 0,9972 | 0,0293 |
| 2,9 | 0,2374 | 0,2376 | 1,0041 | 0,1082 | 5,9 | 0,1124 | 0,1267 | 0,9972 | 0,0283 |
| | | | | | 6,0 | 0,1104 | 0,1247 | 0,9972 | 0,0274 |

$\varphi = -45°$ *Cont'd*

| $\rho$ | $\mathrm{Re}G_0$ | $-\mathrm{Im}G_0$ | $\mathrm{Re}G_1$ | $-\mathrm{Im}G_1$ | $\rho$ | $\mathrm{Re}G_0$ | $-\mathrm{Im}G_0$ | $\mathrm{Re}G_1$ | $-\mathrm{Im}G_1$ |
|---|---|---|---|---|---|---|---|---|---|
| 0 | $\infty$ | 0,7854 | $\infty$ | $\infty$ | 3,0 | 0,2448 | 0,2102 | 1,0185 | 0,0882 |
| 0,1 | 2,4873 | 0,7233 | 7,2021 | 6,9925 | 3,1 | 0,2368 | 0,2047 | 1,0168 | 0,0827 |
| 0,2 | 1,8605 | 0,6718 | 3,7492 | 3,4217 | 3,2 | 0,2293 | 0,1994 | 1,0153 | 0,0877 |
| 0,3 | 1,5161 | 0,6275 | 2,6356 | 2,2213 | 3,3 | 0,2222 | 0,1944 | 1,0140 | 0,0830 |
| 0,4 | 1,2876 | 0,5886 | 2,1003 | 1,6175 | 3,4 | 0,2156 | 0,1897 | 1,0128 | 0,0787 |
| 0,5 | 1,1210 | 0,5540 | 1,7927 | 1,2541 | 3,5 | 0,2093 | 0,1851 | 1,0117 | 0,0747 |
| 0,6 | 0,9928 | 0,5231 | 1,5970 | 1,0118 | 3,6 | 0,2033 | 0,1807 | 1,0107 | 0,0710 |
| 0,7 | 0,8904 | 0,4952 | 1,4620 | 0,8390 | 3,7 | 0,1977 | 0,1766 | 1,0098 | 0,0676 |
| 0,8 | 0,8066 | 0,4699 | 1,3689 | 0,7100 | 3,8 | 0,1924 | 0,1726 | 1,0091 | 0,0644 |
| 0,9 | 0,7366 | 0,4469 | 1,2988 | 0,6103 | 3,9 | 0,1873 | 0,1687 | 1,0083 | 0,0614 |
| 1,0 | 0,6772 | 0,4258 | 1,2456 | 0,5311 | 4,0 | 0,1825 | 0,1651 | 1,0077 | 0,0586 |
| 1,1 | 0,6261 | 0,4064 | 1,2044 | 0,4670 | 4,1 | 0,1779 | 0,1615 | 1,0071 | 0,0560 |
| 1,2 | 0,5817 | 0,3886 | 1,1718 | 0,4141 | 4,2 | 0,1736 | 0,1582 | 1,0066 | 0,0535 |
| 1,3 | 0,5429 | 0,3721 | 1,1457 | 0,3699 | 4,3 | 0,1694 | 0,1549 | 1,0061 | 0,0512 |
| 1,4 | 0,5085 | 0,3568 | 1,1245 | 0,3325 | 4,4 | 0,1655 | 0,1518 | 1,0057 | 0,0491 |
| 1,5 | 0,4780 | 0,3427 | 1,1071 | 0,3006 | 4,5 | 0,1617 | 0,1488 | 1,0052 | 0,0471 |
| 1,6 | 0,4507 | 0,3295 | 1,0927 | 0,2730 | 4,6 | 0,1581 | 0,1459 | 1,0049 | 0,0452 |
| 1,7 | 0,4262 | 0,3171 | 1,0807 | 0,2491 | 4,7 | 0,1546 | 0,1431 | 1,0045 | 0,0434 |
| 1,8 | 0,4040 | 0,3056 | 1,0706 | 0,2281 | 4,8 | 0,1513 | 0,1404 | 1,0042 | 0,0417 |
| 1,9 | 0,3838 | 0,2948 | 1,0620 | 0,2097 | 4,9 | 0,1481 | 0,1378 | 1,0039 | 0,0401 |
| 2,0 | 0,3655 | 0,2847 | 1,0547 | 0,1934 | 5,0 | 0,1451 | 0,1353 | 1,0037 | 0,0386 |
| 2,1 | 0,3487 | 0,2752 | 1,0484 | 0,1788 | 5,1 | 0,1421 | 0,1328 | 1,0034 | 0,0371 |
| 2,2 | 0,3333 | 0,2662 | 1,0430 | 0,1659 | 5,2 | 0,1393 | 0,1305 | 1,0032 | 0,0358 |
| 2,3 | 0,3191 | 0,2578 | 1,0383 | 0,1542 | 5,3 | 0,1366 | 0,1282 | 1,0030 | 0,0345 |
| 2,4 | 0,3060 | 0,2498 | 1,0343 | 0,1437 | 5,4 | 0,1340 | 0,1260 | 1,0028 | 0,0333 |
| 2,5 | 0,2939 | 0,2423 | 1,0307 | 0,1342 | 5,5 | 0,1315 | 0,1239 | 1,0027 | 0,0321 |
| 2,6 | 0,2826 | 0,2352 | 1,0276 | 0,1257 | 5,6 | 0,1291 | 0,1219 | 1,0025 | 0,0311 |
| 2,7 | 0,2722 | 0,2284 | 1,0249 | 0,1178 | 5,7 | 0,1268 | 0,1199 | 1,0023 | 0,0300 |
| 2,8 | 0,2624 | 0,2220 | 1,0225 | 0,1107 | 5,8 | 0,1245 | 0,1179 | 1,0022 | 0,0290 |
| 2,9 | 0,2533 | 0,2160 | 1,0204 | 0,1042 | 5,9 | 0,1224 | 0,1161 | 1,0021 | 0,0281 |
| | | | | | 6,0 | 0,1203 | 0,1143 | 1,0019 | 0,0272 |

Table 2.

$\varphi = 4°$

| p | $\lvert\varphi^{2}F'\rvert$ | a | p | $\lvert\varphi^{2}F'\rvert$ | a |
|---|---|---|---|---|---|
| 0 | 1,0000 | 3,1416 | 3,0 | 0,3887 | 1,2279 |
| 0,1 | 0,9956 | 3,0425 | 3,1 | 0,3691 | 1,1882 |
| 0,2 | 0,9845 | 2,9463 | 3,2 | 0,3550 | 1,1496 |
| 0,3 | 0,9686 | 2,8537 | 3,3 | 0,3415 | 1,1120 |
| 0,4 | 0,9493 | 2,7646 | 3,4 | 0,3285 | 1,0753 |
| 0,5 | 0,9277 | 2,6788 | 3,5 | 0,3160 | 1,0396 |
| 0,6 | 0,9043 | 2,5963 | 3,6 | 0,3039 | 1,0048 |
| 0,7 | 0,8798 | 2,5168 | 3,7 | 0,2923 | 0,9710 |
| 0,8 | 0,8545 | 2,4400 | 3,8 | 0,2813 | 0,9380 |
| 0,9 | 0,8289 | 2,3659 | 3,9 | 0,2706 | 0,9057 |
| 1,0 | 0,8030 | 2,2942 | 4,0 | 0,2603 | 0,8744 |
| 1,1 | 0,7772 | 2,2249 | 4,1 | 0,2505 | 0,8440 |
| 1,2 | 0,7516 | 2,1577 | 4,2 | 0,2410 | 0,8143 |
| 1,3 | 0,7263 | 2,0926 | 4,3 | 0,2320 | 0,7855 |
| 1,4 | 0,7013 | 2,0295 | 4,4 | 0,2233 | 0,7573 |
| 1,5 | 0,6769 | 1,9682 | 4,5 | 0,2149 | 0,7301 |
| 1,6 | 0,6530 | 1,9088 | 4,6 | 0,2069 | 0,7036 |
| 1,7 | 0,6296 | 1,8510 | 4,7 | 0,1992 | 0,6777 |
| 1,8 | 0,6069 | 1,7949 | 4,8 | 0,1918 | 0,6526 |
| 1,9 | 0,5848 | 1,7409 | 4,9 | 0,1847 | 0,6281 |
| 2,0 | 0,5633 | 1,6872 | 5,0 | 0,1780 | 0,6043 |
| 2,1 | 0,5426 | 1,6356 | 5,1 | 0,1714 | 0,5814 |
| 2,2 | 0,5223 | 1,5853 | 5,2 | 0,1652 | 0,5588 |
| 2,3 | 0,5028 | 1,5364 | 5,3 | 0,1592 | 0,5373 |
| 2,4 | 0,4839 | 1,4888 | 5,4 | 0,1535 | 0,5161 |
| 2,5 | 0,4656 | 1,4424 | 5,5 | 0,1472 | 0,4957 |
| 2,6 | 0,4481 | 1,3972 | 5,6 | 0,1426 | 0,4758 |
| 2,7 | 0,4311 | 1,3532 | 5,7 | 0,1385 | 0,4566 |
| 2,8 | 0,4147 | 1,3103 | 5,8 | 0,1327 | 0,4381 |
| 2,9 | 0,3989 | 1,2686 | 5,9 | 0,1280 | 0,4199 |
| | | | 6,0 | 0,1235 | 0,4028 |

$\varphi = 5°$

| p | $\lvert\varphi^{2}F'\rvert$ | a | p | $\lvert\varphi^{2}F'\rvert$ | a |
|---|---|---|---|---|---|
| 0 | 1,0000 | 3,1416 | 3,0 | 0,4283 | 1,1273 |
| 0,1 | 1,0042 | 3,0421 | 3,1 | 0,4123 | 1,0840 |
| 0,2 | 1,0010 | 2,9445 | 3,2 | 0,3969 | 1,0419 |
| 0,3 | 0,9922 | 2,8498 | 3,3 | 0,3820 | 1,0009 |
| 0,4 | 0,9792 | 2,7581 | 3,4 | 0,3676 | 0,9607 |
| 0,5 | 0,9639 | 2,6695 | 3,5 | 0,3537 | 0,9215 |
| 0,6 | 0,9443 | 2,5839 | 3,6 | 0,3403 | 0,8832 |
| 0,7 | 0,9237 | 2,5010 | 3,7 | 0,3274 | 0,8459 |
| 0,8 | 0,9018 | 2,4209 | 3,8 | 0,3151 | 0,8096 |
| 0,9 | 0,8789 | 2,3432 | 3,9 | 0,3031 | 0,7741 |
| 1,0 | 0,8553 | 2,2680 | 4,0 | 0,2916 | 0,7396 |
| 1,1 | 0,8312 | 2,1950 | 4,1 | 0,2806 | 0,7058 |
| 1,2 | 0,8070 | 2,1241 | 4,2 | 0,2699 | 0,6731 |
| 1,3 | 0,7827 | 2,0553 | 4,3 | 0,2596 | 0,6410 |
| 1,4 | 0,7584 | 1,9885 | 4,4 | 0,2498 | 0,6098 |
| 1,5 | 0,7343 | 1,9235 | 4,5 | 0,2403 | 0,5794 |
| 1,6 | 0,7105 | 1,8602 | 4,6 | 0,2312 | 0,5497 |
| 1,7 | 0,6870 | 1,7987 | 4,7 | 0,2224 | 0,5207 |
| 1,8 | 0,6640 | 1,7388 | 4,8 | 0,2141 | 0,4930 |
| 1,9 | 0,6413 | 1,6804 | 4,9 | 0,2060 | 0,4659 |
| 2,0 | 0,6192 | 1,6235 | 5,0 | 0,1982 | 0,4393 |
| 2,1 | 0,5976 | 1,5681 | 5,1 | 0,1907 | 0,4131 |
| 2,2 | 0,5765 | 1,5141 | 5,2 | 0,1836 | 0,3884 |
| 2,3 | 0,5560 | 1,4615 | 5,3 | 0,1768 | 0,3640 |
| 2,4 | 0,5360 | 1,4101 | 5,4 | 0,1702 | 0,3408 |
| 2,5 | 0,5166 | 1,3600 | 5,5 | 0,1638 | 0,3172 |
| 2,6 | 0,4978 | 1,3111 | 5,6 | 0,1578 | 0,2947 |
| 2,7 | 0,4796 | 1,2635 | 5,7 | 0,1520 | 0,2736 |
| 2,8 | 0,4619 | 1,2170 | 5,8 | 0,1463 | 0,2521 |
| 2,9 | 0,4448 | 1,1716 | 5,9 | 0,1409 | 0,2321 |
| | | | 6,0 | 0,1359 | 0,2130 |

$\varphi = 10°$

| p | $\lvert q^2F' \rvert$ | α | p | $\lvert q^2F' \rvert$ | α |
|---|---|---|---|---|---|
| 0 | 1,0000 | 3,1416 | 3,0 | 0,4826 | 1,0294 |
| 0,1 | 1,0129 | 3,0425 | 3,1 | 0,4651 | 0,9824 |
| 0,2 | 1,0181 | 2,9441 | 3,2 | 0,4481 | 0,93[illegible] |
| 0,3 | 1,0170 | 2,8478 | 3,3 | 0,4317 | 0,8915 |
| 0,4 | 1,0109 | 2,7541 | 3,4 | 0,4158 | 0,8475 |
| 0,5 | 1,0009 | 2,6630 | 3,5 | 0,4003 | 0,8047 |
| 0,6 | 0,9876 | 2,5745 | 3,6 | 0,3854 | 0,7628 |
| 0,7 | 0,9718 | 2,4887 | 3,7 | 0,3710 | 0,7218 |
| 0,8 | 0,9540 | 2,4053 | 3,8 | 0,3570 | 0,6818 |
| 0,9 | 0,9345 | 2,3243 | 3,9 | 0,3436 | 0,6426 |
| 1,0 | 0,9139 | 2,2456 | 4,0 | 0,3305 | 0,6045 |
| 1,1 | 0,8922 | 2,1691 | 4,1 | 0,3180 | 0,5672 |
| 1,2 | 0,8699 | 2,0947 | 4,2 | 0,3059 | 0,5308 |
| 1,3 | 0,8470 | 2,0222 | 4,3 | 0,2942 | 0,4953 |
| 1,4 | 0,8239 | 1,9517 | 4,4 | 0,2830 | 0,4606 |
| 1,5 | 0,8006 | 1,8830 | 4,5 | 0,2721 | 0,4268 |
| 1,6 | 0,7772 | 1,8160 | 4,6 | 0,2617 | 0,3940 |
| 1,7 | 0,7539 | 1,7506 | 4,7 | 0,2517 | 0,3617 |
| 1,8 | 0,7308 | 1,6869 | 4,8 | 0,2420 | 0,3301 |
| 1,9 | 0,7078 | 1,6247 | 4,9 | 0,2326 | 0,2997 |
| 1,0 | 0,6852 | 1,5640 | 5,0 | 0,2237 | 0,2700 |
| 1,1 | 0,6629 | 1,5048 | 5,1 | 0,2154 | 0,2415 |
| 1,2 | 0,6410 | 1,4469 | 5,2 | 0,2069 | 0,2128 |
| 1,3 | 0,6195 | 1,3904 | 5,3 | 0,1989 | 0,1852 |
| 1,4 | 0,5985 | 1,3352 | 5,4 | 0,1912 | 0,1586 |
| 2,5 | 0,5779 | 1,2813 | 5,5 | 0,1839 | 0,1326 |
| 2,6 | 0,5578 | 1,2286 | 5,6 | 0,1766 | 0,1080 |
| 2,7 | 0,5382 | 1,1770 | 5,7 | 0,1701 | 0,0836 |
| 2,8 | 0,5192 | 1,1267 | 5,8 | 0,1636 | 0,0596 |
| 2,9 | 0,5007 | 1,0775 | 5,9 | 0,1573 | 0,0360 |
| | | | 6,0 | 0,1514 | 0,0144 |

Cont'd

$\varphi = 15°$

| p | $\lvert q^2F' \rvert$ | α | p | $\lvert q^2F' \rvert$ | α |
|---|---|---|---|---|---|
| 0 | 1,0000 | 3,1416 | 3,0 | 0,5494 | 0,9849 |
| 0,1 | 1,0217 | 3,0436 | 3,1 | 0,5303 | 0,8839 |
| 0,2 | 1,0356 | 2,9452 | 3,2 | 0,5116 | 0,8389 |
| 0,3 | 1,0428 | 2,8479 | 3,3 | 0,4934 | 0,7850 |
| 0,4 | 1,0444 | 2,7525 | 3,4 | 0,4757 | 0,7370 |
| 0,5 | 1,0414 | 2,6593 | 3,5 | 0,4585 | 0,6902 |
| 0,6 | 1,0344 | 2,5684 | 3,6 | 0,4417 | 0,6442 |
| 0,7 | 1,0242 | 2,4799 | 3,7 | 0,4255 | 0,5991 |
| 0,8 | 1,0114 | 2,3936 | 3,8 | 0,4097 | 0,5553 |
| 0,9 | 0,9962 | 2,3095 | 3,9 | 0,3944 | 0,5121 |
| 1,0 | 0,9793 | 2,2276 | 4,0 | 0,3796 | 0,4700 |
| 1,1 | 0,9608 | 2,1477 | 4,1 | 0,3653 | 0,4288 |
| 1,2 | 0,9411 | 2,0698 | 4,2 | 0,3514 | 0,3884 |
| 1,3 | 0,9205 | 1,9938 | 4,3 | 0,3380 | 0,3490 |
| 1,4 | 0,8991 | 1,9196 | 4,4 | 0,3251 | 0,3105 |
| 1,5 | 0,8771 | 1,8472 | 4,5 | 0,3126 | 0,2727 |
| 1,6 | 0,8547 | 1,7765 | 4,6 | 0,3005 | 0,2358 |
| 1,7 | 0,8320 | 1,7074 | 4,7 | 0,2888 | 0,2002 |
| 1,8 | 0,8091 | 1,6399 | 4,8 | 0,2776 | 0,1648 |
| 1,9 | 0,7862 | 1,5739 | 4,9 | 0,2668 | 0,1305 |
| 2,0 | 0,7634 | 1,5093 | 5,0 | 0,2563 | 0,09704 |
| 2,1 | 0,7406 | 1,4461 | 5,1 | 0,2462 | 0,06382 |
| 2,2 | 0,7181 | 1,3844 | 5,2 | 0,2365 | 0,03229 |
| 2,3 | 0,6956 | 1,3239 | 5,3 | 0,2272 | 0,00154 |
| 2,4 | 0,6737 | 1,2647 | 5,4 | 0,2182 | −0,02890 |
| 2,5 | 0,6520 | 1,2068 | 5,5 | 0,2096 | −0,05811 |
| 2,6 | 0,6307 | 1,1501 | 5,6 | 0,2013 | −0,08653 |
| 2,7 | 0,6097 | 1,0946 | 5,7 | 0,1933 | −0,11472 |
| 2,8 | 0,5892 | 1,0402 | 5,8 | 0,1857 | −0,14196 |
| 2,9 | 0,5691 | 0,9870 | 5,9 | 0,1782 | −0,16831 |
| | | | 6,0 | 0,1711 | −0,19361 |

$\varphi = 26°$

| $\rho$ | $\lvert\varphi^2 F'\rvert$ | $\alpha$ | $\rho$ | $\lvert\varphi^2 F'\rvert$ | $\alpha$ |
|---|---|---|---|---|---|
| 0 | 1,0000 | 3,1416 | 3,0 | 0,6323 | 0,8448 |
| 0,1 | 1,0385 | 3,0456 | 3,1 | 0,6114 | 0,7896 |
| 0,2 | 1,0635 | 2,9476 | 3,2 | 0,5908 | 0,7353 |
| 0,3 | 1,0696 | 2,8510 | 3,3 | 0,5707 | 0,6822 |
| 0,4 | 1,0797 | 2,7535 | 3,4 | 0,5510 | 0,6300 |
| 0,5 | 1,0845 | 2,6587 | 3,5 | 0,5317 | 0,5788 |
| 0,6 | 1,0848 | 2,5658 | 3,6 | 0,5129 | 0,5286 |
| 0,7 | 1,0813 | 2,4749 | 3,7 | 0,4946 | 0,4793 |
| 0,8 | 1,0744 | 2,3860 | 3,8 | 0,4767 | 0,4310 |
| 0,9 | 1,0646 | 2,2990 | 3,9 | 0,4593 | 0,3837 |
| 1,0 | 1,0524 | 2,2141 | 4,0 | 0,4424 | 0,3372 |
| 1,1 | 1,0380 | 2,1311 | 4,1 | 0,4259 | 0,2915 |
| 1,2 | 1,0219 | 2,0499 | 4,2 | 0,4100 | 0,2468 |
| 1,3 | 1,0043 | 1,9704 | 4,3 | 0,3944 | 0,2030 |
| 1,4 | 0,9854 | 1,8928 | 4,4 | 0,3794 | 0,1602 |
| 1,5 | 0,9655 | 1,8168 | 4,5 | 0,3649 | 0,11823 |
| 1,6 | 0,9447 | 1,7424 | 4,6 | 0,3507 | 0,07699 |
| 1,7 | 0,9233 | 1,6696 | 4,7 | 0,3371 | 0,03673 |
| 1,8 | 0,9013 | 1,5983 | 4,8 | 0,3239 | −0,00257 |
| 1,9 | 0,8789 | 1,5284 | 4,9 | 0,3111 | −0,04103 |
| 2,0 | 0,8563 | 1,4599 | 5,0 | 0,2988 | −0,0789 |
| 2,1 | 0,8335 | 1,3929 | 5,1 | 0,2869 | −0,1160 |
| 2,2 | 0,8106 | 1,3271 | 5,2 | 0,2754 | −0,1520 |
| 2,3 | 0,7876 | 1,2626 | 5,3 | 0,2642 | −0,1873 |
| 2,4 | 0,7648 | 1,1994 | 5,4 | 0,2536 | −0,2217 |
| 2,5 | 0,7421 | 1,1374 | 5,5 | 0,2433 | −0,2554 |
| 2,6 | 0,7196 | 1,0767 | 5,6 | 0,2333 | −0,2877 |
| 2,7 | 0,6973 | 1,0170 | 5,7 | 0,2237 | −0,3200 |
| 2,8 | 0,6754 | 0,9585 | 5,8 | 0,2145 | −0,3510 |
| 2,9 | 0,6537 | 0,9011 | 5,9 | 0,2056 | −0,3809 |
| | | | 6,0 | 0,1970 | −0,4112 |

$\varphi = 25°$ Cont'd

| $\rho$ | $\lvert\varphi^2 F'\rvert$ | $\alpha$ | $\rho$ | $\lvert\varphi^2 F'\rvert$ | $\alpha$ |
|---|---|---|---|---|---|
| 0 | 1,0000 | 3,1416 | 3,0 | 0,7359 | 0,7602 |
| 0,1 | 1,0392 | 3,0481 | 3,1 | 0,7131 | 0,7086 |
| 0,2 | 1,0716 | 2,9516 | 3,2 | 0,6906 | 0,6420 |
| 0,3 | 1,0972 | 2,8542 | 3,3 | 0,6684 | 0,5843 |
| 0,4 | 1,1165 | 2,7573 | 3,4 | 0,6466 | 0,5277 |
| 0,5 | 1,1302 | 2,6614 | 3,5 | 0,6251 | 0,4719 |
| 0,6 | 1,1389 | 2,5668 | 3,6 | 0,6040 | 0,4171 |
| 0,7 | 1,1431 | 2,4739 | 3,7 | 0,5832 | 0,3633 |
| 0,8 | 1,1434 | 2,3827 | 3,8 | 0,5629 | 0,3104 |
| 0,9 | 1,1401 | 2,2933 | 3,9 | 0,5431 | 0,2584 |
| 1,0 | 1,1338 | 2,2056 | 4,0 | 0,5237 | 0,2072 |
| 1,1 | 1,1248 | 2,1196 | 4,1 | 0,5048 | 0,1570 |
| 1,2 | 1,1134 | 2,0353 | 4,2 | 0,4862 | 0,1076 |
| 1,3 | 1,0999 | 1,9526 | 4,3 | 0,4682 | 0,05914 |
| 1,4 | 1,0846 | 1,8716 | 4,4 | 0,4507 | 0,01146 |
| 1,5 | 1,0678 | 1,7922 | 4,5 | 0,4336 | −0,03540 |
| 1,6 | 1,0496 | 1,7142 | 4,6 | 0,4170 | −0,08143 |
| 1,7 | 1,0303 | 1,6378 | 4,7 | 0,4009 | −0,1264 |
| 1,8 | 1,0100 | 1,5627 | 4,8 | 0,3852 | −0,1708 |
| 1,9 | 0,9889 | 1,4891 | 4,9 | 0,3700 | −0,2141 |
| 2,0 | 0,9671 | 1,4168 | 5,0 | 0,3553 | −0,2568 |
| 2,1 | 0,9448 | 1,3458 | 5,1 | 0,3411 | −0,2985 |
| 2,2 | 0,9220 | 1,2761 | 5,2 | 0,3273 | −0,3395 |
| 2,3 | 0,8990 | 1,2076 | 5,3 | 0,3139 | −0,3796 |
| 2,4 | 0,8757 | 1,1403 | 5,4 | 0,3010 | −0,4188 |
| 2,5 | 0,8523 | 1,0741 | 5,5 | 0,2885 | −0,4573 |
| 2,6 | 0,8289 | 1,0092 | 5,6 | 0,2764 | −0,4950 |
| 2,7 | 0,8054 | 0,9453 | 5,7 | 0,2647 | −0,5319 |
| 2,8 | 0,7821 | 0,8825 | 5,8 | 0,2536 | −0,5680 |
| 2,9 | 0,7589 | 0,8209 | 5,9 | 0,2427 | −0,6029 |
| | | | 6,0 | 0,2325 | −0,6371 |

$\varphi = 30°$

| $\rho$ | $\lvert\varphi^2 F'\rvert$ | $z$ | $\rho$ | $\lvert\varphi^2 F'\rvert$ | $z$ |
|---|---|---|---|---|---|
| 0 | 1,0000 | 3,1416 | 3,0 | 0,8664 | 0,6823 |
| 0,1 | 1,0478 | 3,0615 | 3,1 | 0,8419 | 0,6182 |
| 0,2 | 1,0958 | 2,9671 | 3,2 | 0,8175 | 0,5550 |
| 0,3 | 1,1254 | 2,8807 | 3,3 | 0,7932 | 0,4928 |
| 0,4 | 1,1549 | 2,7638 | 3,4 | 0,7691 | 0,4315 |
| 0,5 | 1,1784 | 2,6874 | 3,5 | 0,7452 | 0,3711 |
| 0,6 | 1,1986 | 2,5717 | 3,6 | 0,7216 | 0,3116 |
| 0,7 | 1,2099 | 2,4772 | 3,7 | 0,6983 | 0,2529 |
| 0,8 | 1,2187 | 2,3842 | 3,8 | 0,6753 | 0,1951 |
| 0,9 | 1,2234 | 2,2925 | 3,9 | 0,6527 | 0,1381 |
| 1,0 | 1,2240 | 2,2030 | 4,0 | 0,6304 | 0,08213 |
| 1,1 | 1,2222 | 2,1137 | 4,1 | 0,6086 | 0,02687 |
| 1,2 | 1,2170 | 2,0265 | 4,2 | 0,5872 | −0,02764 |
| 1,3 | 1,2090 | 1,9409 | 4,3 | 0,5662 | −0,08119 |
| 1,4 | 1,1987 | 1,8567 | 4,4 | 0,5455 | 0,13396 |
| 1,5 | 1,1863 | 1,7740 | 4,5 | 0,5255 | −0,1889 |
| 1,6 | 1,1719 | 1,6926 | 4,6 | 0,5059 | −0,2372 |
| 1,7 | 1,1562 | 1,6128 | 4,7 | 0,4867 | −0,2876 |
| 1,8 | 1,1384 | 1,5340 | 4,8 | 0,4680 | −0,3373 |
| 1,9 | 1,1196 | 1,4586 | 4,9 | 0,4499 | −0,3861 |
| 2,0 | 1,0996 | 1,3896 | 5,0 | 0,4322 | −0,4341 |
| 2,1 | 1,0795 | 1,3257 | 5,1 | 0,4150 | −0,4813 |
| 2,2 | 1,0600 | 1,2330 | 5,2 | 0,3982 | 0,5279 |
| 2,3 | 1,0444 | 1,1896 | 5,3 | 0,3819 | −0,5734 |
| 2,4 | 1,0114 | 1,0982 | 5,4 | 0,3661 | −0,6184 |
| 2,5 | 0,9878 | 1,0179 | 5,5 | 0,3510 | −0,6625 |
| 2,6 | 0,9689 | 0,9487 | 5,6 | 0,3362 | −0,7058 |
| 2,7 | 0,9508 | 0,8816 | 5,7 | 0,3218 | −0,7485 |
| 2,8 | 0,9154 | 0,8135 | 5,8 | 0,3079 | −0,7902 |
| 2,9 | 0,8909 | 0,7474 | 5,9 | 0,2944 | −0,8312 |
| | | | 6,0 | 0,2816 | −0,8715 |

Cont'd

$\varphi = 35°$

| $\rho$ | $\lvert\varphi^2 F'\rvert$ | $z$ | $\rho$ | $\lvert\varphi^2 F'\rvert$ | $z$ |
|---|---|---|---|---|---|
| 0 | 1,0000 | 3,1416 | 3,0 | 1,0315 | 0,6134 |
| 0,1 | 1,0662 | 3,0567 | 3,1 | 1,0063 | 0,5439 |
| 0,2 | 1,1080 | 2,9640 | 3,2 | 0,9803 | 0,4761 |
| 0,3 | 1,1542 | 2,8804 | 3,3 | 0,9541 | 0,4092 |
| 0,4 | 1,1945 | 2,7733 | 3,4 | 0,9279 | 0,3431 |
| 0,5 | 1,2290 | 2,6768 | 3,5 | 0,9017 | 0,2779 |
| 0,6 | 1,2580 | 2,5906 | 3,6 | 0,8756 | 0,2130 |
| 0,7 | 1,2818 | 2,4851 | 3,7 | 0,8495 | 0,1498 |
| 0,8 | 1,3007 | 2,3986 | 3,8 | 0,8236 | 0,08703 |
| 0,9 | 1,3150 | 2,2970 | 3,9 | 0,7980 | 0,02499 |
| 1,0 | 1,3252 | 2,2047 | 4,0 | 0,7726 | −0,03822 |
| 1,1 | 1,3314 | 2,1137 | 4,1 | 0,7475 | −0,09671 |
| 1,2 | 1,3341 | 2,0240 | 4,2 | 0,7227 | −0,1565 |
| 1,3 | 1,3335 | 1,9356 | 4,3 | 0,6982 | −0,2155 |
| 1,4 | 1,3299 | 1,8486 | 4,4 | 0,6742 | −0,2737 |
| 1,5 | 1,3235 | 1,7627 | 4,5 | 0,6506 | −0,3312 |
| 1,6 | 1,3146 | 1,6782 | 4,6 | 0,6273 | −0,3881 |
| 1,7 | 1,3035 | 1,5948 | 4,7 | 0,6045 | −0,4441 |
| 1,8 | 1,2903 | 1,5127 | 4,8 | 0,5822 | −0,4995 |
| 1,9 | 1,2752 | 1,4318 | 4,9 | 0,5603 | −0,5542 |
| 2,0 | 1,2585 | 1,3521 | 5,0 | 0,5389 | −0,6081 |
| 2,1 | 1,2402 | 1,2734 | 5,1 | 0,5180 | −0,6615 |
| 2,2 | 1,2206 | 1,1959 | 5,2 | 0,4976 | −0,7140 |
| 2,3 | 1,1999 | 1,1195 | 5,3 | 0,4777 | −0,7659 |
| 2,4 | 1,1780 | 1,0441 | 5,4 | 0,4583 | −0,8168 |
| 2,5 | 1,1553 | 0,9697 | 5,5 | 0,4394 | −0,8674 |
| 2,6 | 1,1315 | 0,8973 | 5,6 | 0,4212 | −0,9173 |
| 2,7 | 1,1076 | 0,8240 | 5,7 | 0,4033 | −0,9662 |
| 2,8 | 1,0829 | 0,7526 | 5,8 | 0,3859 | −1,0146 |
| 2,9 | 1,0577 | 0,6825 | 5,9 | 0,3691 | −1,0625 |
| | | | 6,0 | 0,3530 | −1,1094 |

$\varphi = 40°$

| ρ | $\lvert\varphi^2 F'\rvert$ | α | ρ | $\lvert\varphi^2 F'\rvert$ | α |
|---|---|---|---|---|---|
| 0 | 1,0000 | 3,1416 | 3,0 | 1,2442 | 0,5524 |
| 0,1 | 1,0042 | 3,0885 | 3,1 | 1,2178 | 0,4792 |
| 0,2 | 1,1250 | 2,9725 | 3,2 | 1,1909 | 0,4068 |
| 0,3 | 1,1831 | 2,8803 | 3,3 | 1,1634 | 0,3352 |
| 0,4 | 1,2352 | 2,7857 | 3,4 | 1,1355 | 0,2644 |
| 0,5 | 1,2806 | 2,6899 | 3,5 | 1,1073 | 0,1943 |
| 0,6 | 1,3230 | 2,5937 | 3,6 | 1,0790 | 0,1250 |
| 0,7 | 1,3588 | 2,4976 | 3,7 | 1,0504 | 0,05634 |
| 0,8 | 1,3896 | 2,4020 | 3,8 | 1,0217 | −0,01157 |
| 0,9 | 1,4155 | 2,3071 | 3,9 | 0,9931 | −0,07879 |
| 1,0 | 1,4365 | 2,2153 | 4,0 | 0,9644 | −0,1453 |
| 1,1 | 1,4536 | 2,1202 | 4,1 | 0,9358 | −0,2112 |
| 1,2 | 1,4663 | 2,0282 | 4,2 | 0,9075 | −0,2763 |
| 1,3 | 1,4752 | 1,9374 | 4,3 | 0,8792 | −0,3409 |
| 1,4 | 1,4806 | 1,8476 | 4,4 | 0,8512 | −0,4048 |
| 1,5 | 1,4825 | 1,7590 | 4,5 | 0,8235 | −0,4680 |
| 1,6 | 1,4813 | 1,6715 | 4,6 | 0,7961 | −0,5306 |
| 1,7 | 1,4772 | 1,5851 | 4,7 | 0,7690 | −0,5927 |
| 1,8 | 1,4704 | 1,4997 | 4,8 | 0,7427 | −0,6540 |
| 1,9 | 1,4611 | 1,4154 | 4,9 | 0,7161 | −0,7149 |
| 2,0 | 1,4495 | 1,3322 | 5,0 | 0,6903 | −0,7751 |
| 2,1 | 1,4358 | 1,2500 | 5,1 | 0,6649 | −0,8346 |
| 2,2 | 1,4202 | 1,1688 | 5,2 | 0,6400 | −0,8937 |
| 2,3 | 1,4028 | 1,0885 | 5,3 | 0,6155 | −0,9521 |
| 2,4 | 1,3838 | 1,0093 | 5,4 | 0,5916 | −1,0101 |
| 2,5 | 1,3633 | 0,9309 | 5,5 | 0,5682 | −1,0673 |
| 2,6 | 1,3416 | 0,8534 | 5,6 | 0,5453 | −1,1241 |
| 2,7 | 1,3187 | 0,7769 | 5,7 | 0,5231 | −1,1802 |
| 2,8 | 1,2947 | 0,7012 | 5,8 | 0,5013 | −1,2360 |
| 2,9 | 1,2698 | 0,6264 | 5,9 | 0,4800 | −1,2908 |
| | | | 6,0 | 0,4594 | −1,3454 |

$\varphi = 45°$ Cont'd

| ρ | $\lvert\varphi^2 F'\rvert$ | α | ρ | $\lvert\varphi^2 F'\rvert$ | α |
|---|---|---|---|---|---|
| 0 | 1,0000 | 3,1416 | 3,0 | 1,5172 | 0,5035 |
| 0,1 | 1,0719 | 3,0660 | 3,1 | 1,4918 | 0,4259 |
| 0,2 | 1,1434 | 2,9825 | 3,2 | 1,4653 | 0,3490 |
| 0,3 | 1,2121 | 2,8936 | 3,3 | 1,4378 | 0,2728 |
| 0,4 | 1,2766 | 2,8012 | 3,4 | 1,4095 | 0,1973 |
| 0,5 | 1,3364 | 2,7067 | 3,5 | 1,3803 | 0,12248 |
| 0,6 | 1,3913 | 2,6111 | 3,6 | 1,3505 | 0,04828 |
| 0,7 | 1,4410 | 2,5151 | 3,7 | 1,3201 | −0,02532 |
| 0,8 | 1,4856 | 2,4190 | 3,8 | 1,2892 | −0,0975 |
| 0,9 | 1,5252 | 2,3232 | 3,9 | 1,2580 | −0,17065 |
| 1,0 | 1,5599 | 2,2280 | 4,0 | 1,2264 | −0,2424 |
| 1,1 | 1,5899 | 2,1334 | 4,1 | 1,1946 | −0,3136 |
| 1,2 | 1,6153 | 2,0396 | 4,2 | 1,1627 | −0,3843 |
| 1,3 | 1,6365 | 1,9466 | 4,3 | 1,1307 | −0,4543 |
| 1,4 | 1,6535 | 1,8546 | 4,4 | 1,0986 | −0,5239 |
| 1,5 | 1,6665 | 1,7635 | 4,5 | 1,0666 | −0,5930 |
| 1,6 | 1,6758 | 1,6733 | 4,6 | 1,0346 | −0,6615 |
| 1,7 | 1,6816 | 1,5841 | 4,7 | 1,0029 | −0,7295 |
| 1,8 | 1,6840 | 1,4957 | 4,8 | 0,9714 | −0,7969 |
| 1,9 | 1,6832 | 1,4083 | 4,9 | 0,9401 | −0,8639 |
| 2,0 | 1,6796 | 1,3218 | 5,0 | 0,9090 | −0,9305 |
| 2,1 | 1,6728 | 1,2360 | 5,1 | 0,8785 | −0,9965 |
| 2,2 | 1,6640 | 1,1516 | 5,2 | 0,8481 | −1,0622 |
| 2,3 | 1,6524 | 1,0677 | 5,3 | 0,8182 | −1,1273 |
| 2,4 | 1,6386 | 0,9847 | 5,4 | 0,7888 | −1,1921 |
| 2,5 | 1,6228 | 0,9026 | 5,5 | 0,7599 | −1,2564 |
| 2,6 | 1,6049 | 0,8212 | 5,6 | 0,7314 | −1,3202 |
| 2,7 | 1,5853 | 0,7406 | 5,7 | 0,7034 | −1,3836 |
| 2,8 | 1,5640 | 0,6608 | 5,8 | 0,6760 | −1,4467 |
| 2,9 | 1,5413 | 0,5818 | 5,9 | 0,6491 | −1,5094 |
| | | | 6,0 | 0,6228 | −1,5699 |

$\varphi = -5°$

| p | $\lvert q^2F' \rvert$ | α | p | $\lvert q^2F \rvert$ | α |
|---|---|---|---|---|---|
| 0 | 1,0000 | 3,1416 | 3,0 | 0,3470 | 1,3306 |
| 0,1 | 0,9872 | 3,0436 | 3,1 | 0,3336 | 1,2942 |
| 0,2 | 0,9686 | 2,9494 | 3,2 | 0,3207 | 1,2588 |
| 0,3 | 0,9462 | 2,8594 | 3,3 | 0,3083 | 1,2245 |
| 0,4 | 0,9213 | 2,7732 | 3,4 | 0,2965 | 1,1911 |
| 0,5 | 0,8949 | 2,6908 | 3,5 | 0,2851 | 1,1586 |
| 0,6 | 0,8675 | 2,6116 | 3,6 | 0,2742 | 1,1269 |
| 0,7 | 0,8397 | 2,5356 | 3,7 | 0,2638 | 1,0961 |
| 0,8 | 0,8117 | 2,4624 | 3,8 | 0,2538 | 1,0662 |
| 0,9 | 0,7839 | 2,3920 | 3,9 | 0,2442 | 1,0371 |
| 1,0 | 0,7563 | 2,3240 | 4,0 | 0,2350 | 1,0087 |
| 1,1 | 0,7292 | 2,2586 | 4,1 | 0,2261 | 0,9812 |
| 1,2 | 0,7027 | 2,1950 | 4,2 | 0,2177 | 0,9544 |
| 1,3 | 0,6768 | 2,1337 | 4,3 | 0,2096 | 0,9286 |
| 1,4 | 0,6515 | 2,0744 | 4,4 | 0,2018 | 0,9032 |
| 1,5 | 0,6270 | 2,0169 | 4,5 | 0,1944 | 0,8785 |
| 1,6 | 0,6032 | 1,9612 | 4,6 | 0,1872 | 0,8546 |
| 1,7 | 0,5802 | 1,9072 | 4,7 | 0,1805 | 0,8316 |
| 1,8 | 0,5580 | 1,8547 | 4,8 | 0,1738 | 0,8090 |
| 1,9 | 0,5365 | 1,8039 | 4,9 | 0,1676 | 0,7866 |
| 2,0 | 0,5157 | 1,7544 | 5,0 | 0,1616 | 0,7656 |
| 2,1 | 0,4958 | 1,7065 | 5,1 | 0,1558 | 0,7453 |
| 2,2 | 0,4765 | 1,6599 | 5,2 | 0,1502 | 0,7245 |
| 2,3 | 0,4580 | 1,6145 | 5,3 | 0,1449 | 0,7054 |
| 2,4 | 0,4402 | 1,5705 | 5,4 | 0,1397 | 0,6865 |
| 2,5 | 0,4230 | 1,5276 | 5,5 | 0,1350 | 0,6691 |
| 2,6 | 0,4066 | 1,4860 | 5,6 | 0,1303 | 0,6510 |
| 2,7 | 0,3908 | 1,4455 | 5,7 | 0,1258 | 0,6336 |
| 2,8 | 0,3756 | 1,4061 | 5,8 | 0,1215 | 0,6171 |
| 2,9 | 0,3610 | 1,3678 | 5,9 | 0,1173 | 0,6014 |
| | | | 6,0 | 0,1134 | 0,5844 |

$\varphi = -10°$ Cont'd

| p | $\lvert q^2F \rvert$ | α | p | $\lvert q^2F \rvert$ | α |
|---|---|---|---|---|---|
| 0 | 1,0000 | 3,1416 | 3,0 | 0,3165 | 1,4346 |
| 0,1 | 0,9791 | 3,0453 | 3,1 | 0,3041 | 1,4014 |
| 0,2 | 0,9634 | 2,9538 | 3,2 | 0,2922 | 1,3693 |
| 0,3 | 0,9250 | 2,8668 | 3,3 | 0,2809 | 1,3380 |
| 0,4 | 0,8851 | 2,7841 | 3,4 | 0,2701 | 1,3075 |
| 0,5 | 0,8446 | 2,7051 | 3,5 | 0,2597 | 1,2779 |
| 0,6 | 0,8038 | 2,6296 | 3,6 | 0,2498 | 1,2492 |
| 0,7 | 0,7632 | 2,5573 | 3,7 | 0,2403 | 1,2212 |
| 0,8 | 0,7231 | 2,4880 | 3,8 | 0,2312 | 1,1941 |
| 0,9 | 0,7435 | 2,4213 | 3,9 | 0,2225 | 1,1677 |
| 1,0 | 0,7147 | 2,3572 | 4,0 | 0,2141 | 1,1421 |
| 1,1 | 0,6867 | 2,2954 | 4,1 | 0,2062 | 1,1171 |
| 1,2 | 0,6596 | 2,2358 | 4,2 | 0,1986 | 1,0931 |
| 1,3 | 0,6334 | 2,1783 | 4,3 | 0,1912 | 1,0694 |
| 1,4 | 0,6081 | 2,1227 | 4,4 | 0,1843 | 1,0466 |
| 1,5 | 0,5837 | 2,0690 | 4,5 | 0,1776 | 1,0245 |
| 1,6 | 0,5602 | 2,0170 | 4,6 | 0,1712 | 1,0030 |
| 1,7 | 0,5376 | 1,9666 | 4,7 | 0,1650 | 0,9821 |
| 1,8 | 0,5160 | 1,9179 | 4,8 | 0,1592 | 0,9617 |
| 1,9 | 0,4952 | 1,8706 | 4,9 | 0,1535 | 0,9421 |
| 2,0 | 0,4752 | 1,8248 | 5,0 | 0,1481 | 0,9228 |
| 2,1 | 0,4561 | 1,7804 | 5,1 | 0,1428 | 0,9040 |
| 2,2 | 0,4378 | 1,7373 | 5,2 | 0,1380 | 0,8864 |
| 2,3 | 0,4202 | 1,6954 | 5,3 | 0,1332 | 0,8691 |
| 2,4 | 0,4034 | 1,6548 | 5,4 | 0,1287 | 0,8522 |
| 2,5 | 0,3872 | 1,6154 | 5,5 | 0,1244 | 0,8356 |
| 2,6 | 0,3718 | 1,5771 | 5,6 | 0,1201 | 0,8200 |
| 2,7 | 0,3571 | 1,5399 | 5,7 | 0,1162 | 0,8039 |
| 2,8 | 0,3429 | 1,5038 | 5,8 | 0,1123 | 0,7893 |
| 2,9 | 0,3294 | 1,4687 | 5,9 | 0,1087 | 0,7758 |
| | | | 6,0 | 0,1051 | 0,7598 |

$\varphi = -15°$

| $\rho$ | $\lvert \varphi F' \rvert$ | $\alpha$ | $\rho$ | $\lvert \varphi F' \rvert$ | $\alpha$ |
|---|---|---|---|---|---|
| 0 | 1 | 3,1416 | 3,0 | 0,2988 | 1,5398 |
| 0,1 | 0,9712 | 3,0478 | 3,1 | 0,2795 | 1,5095 |
| 0,2 | 0,9389 | 2,9594 | 3,2 | 0,2685 | 1,4802 |
| 0,3 | 0,9051 | 2,8759 | 3,3 | 0,2581 | 1,4518 |
| 0,4 | 0,8708 | 2,7969 | 3,4 | 0,2481 | 1,4242 |
| 0,5 | 0,8366 | 2,7217 | 3,5 | 0,2386 | 1,3973 |
| 0,6 | 0,8030 | 2,6501 | 3,6 | 0,2294 | 1,3712 |
| 0,7 | 0,7701 | 2,5818 | 3,7 | 0,2208 | 1,3458 |
| 0,8 | 0,7382 | 2,5163 | 3,8 | 0,2124 | 1,3213 |
| 0,9 | 0,7074 | 2,4536 | 3,9 | 0,2045 | 1,2975 |
| 1,0 | 0,6777 | 2,3933 | 4,0 | 0,1969 | 1,2742 |
| 1,1 | 0,6491 | 2,3354 | 4,1 | 0,1896 | 1,2517 |
| 1,2 | 0,6216 | 2,2796 | 4,2 | 0,1827 | 1,2300 |
| 1,3 | 0,5953 | 2,2259 | 4,3 | 0,1761 | 1,2087 |
| 1,4 | 0,5701 | 2,1741 | 4,4 | 0,1697 | 1,1879 |
| 1,5 | 0,5460 | 2,1241 | 4,5 | 0,1637 | 1,1681 |
| 1,6 | 0,5229 | 2,0758 | 4,6 | 0,1578 | 1,1487 |
| 1,7 | 0,5009 | 2,0291 | 4,7 | 0,1523 | 1,1297 |
| 1,8 | 0,4799 | 1,9839 | 4,8 | 0,1470 | 1,1114 |
| 1,9 | 0,4598 | 1,9402 | 4,9 | 0,1419 | 1,0936 |
| 2,0 | 0,4406 | 1,8978 | 5,0 | 0,1370 | 1,0768 |
| 2,1 | 0,4223 | 1,8569 | 5,1 | 0,1324 | 1,0600 |
| 2,2 | 0,4048 | 1,8172 | 5,2 | 0,1279 | 1,0436 |
| 2,3 | 0,3881 | 1,7787 | 5,3 | 0,1236 | 1,0281 |
| 2,4 | 0,3722 | 1,7413 | 5,4 | 0,1195 | 1,0128 |
| 2,5 | 0,3570 | 1,7051 | 5,5 | 0,1156 | 0,9980 |
| 2,6 | 0,3425 | 1,6701 | 5,6 | 0,1117 | 0,9832 |
| 2,7 | 0,3287 | 1,6360 | 5,7 | 0,1082 | 0,9699 |
| 2,8 | 0,3155 | 1,6029 | 5,8 | 0,1047 | 0,9565 |
| 2,9 | 0,3029 | 1,5707 | 5,9 | 0,1014 | 0,9433 |
| | | | 6,0 | 0,0981 | 0,9302 |

$\varphi = -20°$ Cont'd

| $\rho$ | $\lvert \varphi F' \rvert$ | $\alpha$ | $\rho$ | $\lvert \varphi F' \rvert$ | $\alpha$ |
|---|---|---|---|---|---|
| 0 | 1 | 3,1416 | 3,0 | 0,2895 | 1,6457 |
| 0,1 | 0,9636 | 3,0508 | 3,1 | 0,2598 | 1,6182 |
| 0,2 | 0,9263 | 2,9661 | 3,2 | 0,2486 | 1,5916 |
| 0,3 | 0,8865 | 2,8866 | 3,3 | 0,2389 | 1,5656 |
| 0,4 | 0,8483 | 2,8115 | 3,4 | 0,2297 | 1,5407 |
| 0,5 | 0,8110 | 2,7405 | 3,5 | 0,2209 | 1,5164 |
| 0,6 | 0,7749 | 2,6730 | 3,6 | 0,2125 | 1,4926 |
| 0,7 | 0,7402 | 2,6087 | 3,7 | 0,2045 | 1,4698 |
| 0,8 | 0,7069 | 2,5472 | 3,8 | 0,1968 | 1,4476 |
| 0,9 | 0,6751 | 2,4885 | 3,9 | 0,1895 | 1,4260 |
| 1,0 | 0,6447 | 2,4322 | 4,0 | 0,1825 | 1,4052 |
| 1,1 | 0,6171 | 2,3783 | 4,1 | 0,1759 | 1,3849 |
| 1,2 | 0,5882 | 2,3263 | 4,2 | 0,1695 | 1,3652 |
| 1,3 | 0,5619 | 2,2763 | 4,3 | 0,1634 | 1,3460 |
| 1,4 | 0,5369 | 2,2283 | 4,4 | 0,1576 | 1,3275 |
| 1,5 | 0,5132 | 2,1819 | 4,5 | 0,1521 | 1,3094 |
| 1,6 | 0,4906 | 2,1372 | 4,6 | 0,1468 | 1,2919 |
| 1,7 | 0,4691 | 2,0940 | 4,7 | 0,1417 | 1,2750 |
| 1,8 | 0,4487 | 2,0524 | 4,8 | 0,1368 | 1,2584 |
| 1,9 | 0,4293 | 2,0121 | 4,9 | 0,1321 | 1,2425 |
| 2,0 | 0,4109 | 1,9732 | 5,0 | 0,1277 | 1,2273 |
| 2,1 | 0,3934 | 1,9355 | 5,1 | 0,1235 | 1,2115 |
| 2,2 | 0,3767 | 1,8991 | 5,2 | 0,1193 | 1,1971 |
| 2,3 | 0,3609 | 1,8638 | 5,3 | 0,1155 | 1,1821 |
| 2,4 | 0,3458 | 1,8296 | 5,4 | 0,1117 | 1,1694 |
| 2,5 | 0,3314 | 1,7965 | 5,5 | 0,1082 | 1,1558 |
| 2,6 | 0,3178 | 1,7644 | 5,6 | 0,1046 | 1,1426 |
| 2,7 | 0,3048 | 1,7333 | 5,7 | 0,1014 | 1,1310 |
| 2,8 | 0,2924 | 1,7032 | 5,8 | 0,0983 | 1,1189 |
| 2,9 | 0,2807 | 1,6740 | 5,9 | 0,0952 | 1,1059 |
| | | | 6,0 | 0,0922 | 1,0965 |

$\varphi = -25°$

| p | $\lvert q^2F' \rvert$ | α | p | $\lvert q^2F' \rvert$ | z |
|---|---|---|---|---|---|
| 0 | 1 | 3,1416 | 3,0 | 0,2514 | 1,7522 |
| 0,1 | 0,9565 | 3,0546 | 3,1 | 0,2414 | 1,7273 |
| 0,2 | 0,9125 | 2,9740 | 3,2 | 0,2319 | 1,7031 |
| 0,3 | 0,8693 | 2,8987 | 3,3 | 0,2228 | 1,6798 |
| 0,4 | 0,8276 | 2,8280 | 3,4 | 0,2142 | 1,6571 |
| 0,5 | 0,7876 | 2,7612 | 3,5 | 0,2060 | 1,6351 |
| 0,6 | 0,7495 | 2,6979 | 3,6 | 0,1982 | 1,6138 |
| 0,7 | 0,7133 | 2,6378 | 3,7 | 0,1908 | 1,5932 |
| 0,8 | 0,6789 | 2,5805 | 3,8 | 0,1837 | 1,5732 |
| 0,9 | 0,6463 | 2,5259 | 3,9 | 0,1769 | 1,5537 |
| 1,0 | 0,6155 | 2,4736 | 4,0 | 0,1705 | 1,5348 |
| 1,1 | 0,5863 | 2,4235 | 4,1 | 0,1643 | 1,5164 |
| 1,2 | 0,5588 | 2,3754 | 4,2 | 0,1584 | 1,4987 |
| 1,3 | 0,5327 | 2,3292 | 4,3 | 0,1528 | 1,4816 |
| 1,4 | 0,5080 | 2,2848 | 4,4 | 0,1475 | 1,4648 |
| 1,5 | 0,4846 | 2,2421 | 4,5 | 0,1423 | 1,4484 |
| 1,6 | 0,4626 | 2,2010 | 4,6 | 0,1374 | 1,4330 |
| 1,7 | 0,4417 | 2,1613 | 4,7 | 0,1327 | 1,4176 |
| 1,8 | 0,4219 | 2,1230 | 4,8 | 0,1283 | 1,4028 |
| 1,9 | 0,4032 | 2,0861 | 4,9 | 0,1240 | 1,3886 |
| 2,0 | 0,3854 | 2,0505 | 5,0 | 0,1199 | 1,3747 |
| 2,1 | 0,3686 | 2,0160 | 5,1 | 0,1160 | 1,3605 |
| 2,2 | 0,3527 | 1,9827 | 5,2 | 0,1122 | 1,3478 |
| 2,3 | 0,3376 | 1,9505 | 5,3 | 0,1086 | 1,3352 |
| 2,4 | 0,3233 | 1,9193 | 5,4 | 0,1051 | 1,3226 |
| 2,5 | 0,3097 | 1,8892 | 5,5 | 0,1019 | 1,3103 |
| 2,6 | 0,2968 | 1,8600 | 5,6 | 0,0987 | 1,2988 |
| 2,7 | 0,2845 | 1,8317 | 5,7 | 0,0957 | 1,2877 |
| 2,8 | 0,2729 | 1,8044 | 5,8 | 0,0927 | 1,2768 |
| 2,9 | 0,2619 | 1,7778 | 5,9 | 0,0899 | 1,2655 |
| | | | 6,0 | 0,0872 | 1,2565 |

$\varphi = -30°$ Cont'd

| | $\lvert q^2F' \rvert$ | α | p | $\lvert q^2F' \rvert$ | z |
|---|---|---|---|---|---|
| 0 | 1 | 3,1416 | 3,0 | 0,2360 | 1,8590 |
| 0,1 | 0,9487 | 3,0589 | 3,1 | 0,2266 | 1,8365 |
| 0,2 | 0,9005 | 2,9828 | 3,2 | 0,2177 | 1,8148 |
| 0,3 | 0,8534 | 2,9122 | 3,3 | 0,2092 | 1,7936 |
| 0,4 | 0,8086 | 2,8460 | 3,4 | 0,2012 | 1,7733 |
| 0,5 | 0,7663 | 2,7837 | 3,5 | 0,1935 | 1,7535 |
| 0,6 | 0,7265 | 2,7248 | 3,6 | 0,1862 | 1,7343 |
| 0,7 | 0,6891 | 2,6690 | 3,7 | 0,1792 | 1,7157 |
| 0,8 | 0,6538 | 2,6160 | 3,8 | 0,1726 | 1,6976 |
| 0,9 | 0,6208 | 2,5654 | 3,9 | 0,1663 | 1,6801 |
| 1,0 | 0,5896 | 2,5170 | 4,0 | 0,1603 | 1,6633 |
| 1,1 | 0,5604 | 2,4710 | 4,1 | 0,1546 | 1,6468 |
| 1,2 | 0,5329 | 2,4268 | 4,2 | 0,1491 | 1,6310 |
| 1,3 | 0,5071 | 2,3843 | 4,3 | 0,1439 | 1,6155 |
| 1,4 | 0,4827 | 2,3436 | 4,4 | 0,1389 | 1,6006 |
| 1,5 | 0,4598 | 2,3044 | 4,5 | 0,1341 | 1,5860 |
| 1,6 | 0,4383 | 2,2668 | 4,6 | 0,1296 | 1,5716 |
| 1,7 | 0,4179 | 2,2305 | 4,7 | 0,1252 | 1,5582 |
| 1,8 | 0,3987 | 2,1956 | 4,8 | 0,1211 | 1,5445 |
| 1,9 | 0,3806 | 2,1619 | 4,9 | 0,1171 | 1,5319 |
| 2,0 | 0,3636 | 2,1294 | 5,0 | 0,1133 | 1,5194 |
| 2,1 | 0,3474 | 2,0980 | 5,1 | 0,1096 | 1,5069 |
| 2,2 | 0,3322 | 2,0678 | 5,2 | 0,1061 | 1,4947 |
| 2,3 | 0,3177 | 2,0385 | 5,3 | 0,1028 | 1,4826 |
| 2,4 | 0,3041 | 2,0102 | 5,4 | 0,0995 | 1,4723 |
| 2,5 | 0,2912 | 1,9829 | 5,5 | 0,0964 | 1,4620 |
| 2,6 | 0,2789 | 1,9564 | 5,6 | 0,0936 | 1,4514 |
| 2,7 | 0,2673 | 1,9309 | 5,7 | 0,0907 | 1,4418 |
| 2,8 | 0,2564 | 1,9062 | 5,8 | 0,0881 | 1,4319 |
| 2,9 | 0,2459 | 1,8821 | 5,9 | 0,0853 | 1,4218 |
| | | | 6,0 | 0,0829 | 1,4124 |

$\varphi = -35°$

| $\rho$ | $q^2F'$ | $\alpha$ | $\rho$ | $q^2F'$ | $\alpha$ |
|---|---|---|---|---|---|
| 0 | 1 | 3,1416 | 3,0 | 0,2231 | 1,9669 |
| 0,1 | 0,9434 | 3,0638 | 3,1 | 0,2141 | 1,9458 |
| 0,2 | 0,8895 | 2,9927 | 3,2 | 0,2057 | 1,9262 |
| 0,3 | 0,8388 | 2,9269 | 3,3 | 0,1977 | 1,9074 |
| 0,4 | 0,7914 | 2,8655 | 3,4 | 0,1901 | 1,8891 |
| 0,5 | 0,7471 | 2,8079 | 3,5 | 0,1829 | 1,8714 |
| 0,6 | 0,7059 | 2,7535 | 3,6 | 0,1760 | 1,8541 |
| 0,7 | 0,6674 | 2,7021 | 3,7 | 0,1695 | 1,8375 |
| 0,8 | 0,6316 | 2,6534 | 3,8 | 0,1633 | 1,8214 |
| 0,9 | 0,5981 | 2,6070 | 3,9 | 0,1574 | 1,8057 |
| 1,0 | 0,5668 | 2,5627 | 4,0 | 0,1517 | 1,7905 |
| 1,1 | 0,5376 | 2,5205 | 4,1 | 0,1463 | 1,7758 |
| 1,2 | 0,5103 | 2,4801 | 4,2 | 0,1412 | 1,7615 |
| 1,3 | 0,4847 | 2,4414 | 4,3 | 0,1363 | 1,7478 |
| 1,4 | 0,4608 | 2,4042 | 4,4 | 0,1316 | 1,7345 |
| 1,5 | 0,4383 | 2,3686 | 4,5 | 0,1271 | 1,7212 |
| 1,6 | 0,4172 | 2,3344 | 4,6 | 0,1229 | 1,7086 |
| 1,7 | 0,3974 | 2,3014 | 4,7 | 0,1188 | 1,6964 |
| 1,8 | 0,3788 | 2,2697 | 4,8 | 0,1150 | 1,6846 |
| 1,9 | 0,3613 | 2,2392 | 4,9 | 0,1112 | 1,6730 |
| 2,0 | 0,3448 | 2,2098 | 5,0 | 0,1076 | 1,6619 |
| 2,1 | 0,3292 | 2,1814 | 5,1 | 0,1042 | 1,6510 |
| 2,2 | 0,3146 | 2,1540 | 5,2 | 0,1010 | 1,6401 |
| 2,3 | 0,3008 | 2,1277 | 5,3 | 0,0978 | 1,6301 |
| 2,4 | 0,2877 | 2,1021 | 5,4 | 0,0948 | 1,6205 |
| 2,5 | 0,2754 | 2,0774 | 5,5 | 0,0919 | 1,6104 |
| 2,6 | 0,2636 | 2,0539 | 5,6 | 0,0892 | 1,6015 |
| 2,7 | 0,2527 | 2,0306 | 5,7 | 0,0865 | 1,5918 |
| 2,8 | 0,2423 | 2,0084 | 5,8 | 0,0840 | 1,5820 |
| 2,9 | 0,2324 | 1,9868 | 5,9 | 0,0815 | 1,5745 |
| | | | 6,0 | 0,0793 | 1,5666 |

Cont'd

$\varphi = -40°$

| $\rho$ | $q^2F'$ | $\alpha$ | $\rho$ | $q^2F'$ | $\alpha$ |
|---|---|---|---|---|---|
| 0 | 1 | 3,1416 | 3,0 | 0,2120 | 2,0730 |
| 0,1 | 0,9375 | 3,0691 | 3,1 | 0,2035 | 2,0551 |
| 0,2 | 0,8793 | 3,0034 | 3,2 | 0,1955 | 2,0377 |
| 0,3 | 0,8255 | 2,9427 | 3,3 | 0,1879 | 2,0207 |
| 0,4 | 0,7758 | 2,8863 | 3,4 | 0,1808 | 2,0046 |
| 0,5 | 0,7299 | 2,8335 | 3,5 | 0,1739 | 1,9887 |
| 0,6 | 0,6874 | 2,7838 | 3,6 | 0,1674 | 1,9734 |
| 0,7 | 0,6482 | 2,7369 | 3,7 | 0,1612 | 1,9586 |
| 0,8 | 0,6118 | 2,6925 | 3,8 | 0,1553 | 1,9443 |
| 0,9 | 0,5781 | 2,6503 | 3,9 | 0,1497 | 1,9302 |
| 1,0 | 0,5441 | 2,6106 | 4,0 | 0,1444 | 1,9170 |
| 1,1 | 0,5149 | 2,5718 | 4,1 | 0,1393 | 1,9035 |
| 1,2 | 0,4906 | 2,5351 | 4,2 | 0,1345 | 1,8909 |
| 1,3 | 0,4653 | 2,5004 | 4,3 | 0,1299 | 1,8786 |
| 1,4 | 0,4417 | 2,4666 | 4,4 | 0,1254 | 1,8668 |
| 1,5 | 0,4196 | 2,4344 | 4,5 | 0,1213 | 1,8554 |
| 1,6 | 0,3990 | 2,4035 | 4,6 | 0,1172 | 1,8442 |
| 1,7 | 0,3797 | 2,3738 | 4,7 | 0,1134 | 1,8329 |
| 1,8 | 0,3616 | 2,3452 | 4,8 | 0,1096 | 1,8231 |
| 1,9 | 0,3446 | 2,3178 | 4,9 | 0,1062 | 1,8121 |
| 2,0 | 0,3287 | 2,2914 | 5,0 | 0,1029 | 1,8025 |
| 2,1 | 0,3137 | 2,2659 | 5,1 | 0,0996 | 1,7926 |
| 2,2 | 0,2996 | 2,2413 | 5,2 | 0,0965 | 1,7831 |
| 2,3 | 0,2863 | 2,2176 | 5,3 | 0,0934 | 1,7741 |
| 2,4 | 0,2738 | 2,1948 | 5,4 | 0,0908 | 1,7652 |
| 2,5 | 0,2619 | 2,1727 | 5,5 | 0,0880 | 1,7570 |
| 2,6 | 0,2508 | 2,1514 | 5,6 | 0,0854 | 1,7479 |
| 2,7 | 0,2403 | 2,1308 | 5,7 | 0,0830 | 1,7402 |
| 2,8 | 0,2303 | 2,1109 | 5,8 | 0,0805 | 1,7324 |
| 2,9 | 0,2209 | 2,0917 | 5,9 | 0,0782 | 1,7248 |
| | | | 6,0 | 0,0761 | 1,7174 |

$\varphi = -45°$

| $\rho$ | $\lvert q^2F' \rvert$ | $\alpha$ | $\rho$ | $\lvert q^2F' \rvert$ | $\alpha$ |
|---|---|---|---|---|---|
| 0 | 1 | 3,1416 | 1,5 | 0,4036 | 2,5015 |
| 0,1 | 0,9321 | 3,0750 | 1,6 | 0,3834 | 2,4739 |
| 0,2 | 0,8701 | 3,0149 | 1,7 | 0,3645 | 2,4474 |
| 0,3 | 0,8135 | 2,9596 | 1,8 | 0,3469 | 2,4220 |
| 0,4 | 0,7618 | 2,9084 | 1,9 | 0,3304 | 2,3975 |
| 0,5 | 0,7145 | 2,8608 | 2,0 | 0,3149 | 2,3739 |
| 0,6 | 0,6711 | 2,8156 | 2,1 | 0,3004 | 2,3512 |
| 0,7 | 0,6312 | 2,7732 | 2,2 | 0,2867 | 2,3294 |
| 0,8 | 0,5945 | 2,7332 | 2,3 | 0,2739 | 2,3084 |
| 0,9 | 0,5606 | 2,6952 | 2,4 | 0,2619 | 2,2881 |
| 1,0 | 0,5293 | 2,6590 | 2,5 | 0,2505 | 2,2685 |
| 1,1 | 0,5003 | 2,6246 | 2,6 | 0,2398 | 2,2496 |
| 1,2 | 0,4734 | 2,5917 | 2,7 | 0,2297 | 2,2313 |
| 1,3 | 0,4485 | 2,5603 | 2,8 | 0,2202 | 2,2136 |
| 1,4 | 0,4252 | 2,5303 | 2,9 | 0,2112 | 2,1967 |

| $\rho$ | $\lvert q^2F' \rvert$ | $\alpha$ | $\rho$ | $\lvert q^2F' \rvert$ | $\alpha$ |
|---|---|---|---|---|---|
| 3,0 | 0,2026 | 2,1802 | 4,5 | 0,1163 | 1,9877 |
| 3,1 | 0,1946 | 2,1643 | 4,6 | 0,1125 | 1,9776 |
| 3,2 | 0,1869 | 2,1488 | 4,7 | 0,1088 | 1,9682 |
| 3,3 | 0,1797 | 2,1339 | 4,8 | 0,1053 | 1,9589 |
| 3,4 | 0,1728 | 2,1195 | 4,9 | 0,1020 | 1,9499 |
| 3,5 | 0,1663 | 2,1056 | 5,0 | 0,09879 | 1,9408 |
| 3,6 | 0,1601 | 2,0921 | 5,1 | 0,09576 | 1,9328 |
| 3,7 | 0,1542 | 2,0789 | 5,2 | 0,09280 | 1,9240 |
| 3,8 | 0,1486 | 2,0662 | 5,3 | 0,09003 | 1,9161 |
| 3,9 | 0,1433 | 2,0539 | 5,4 | 0,08734 | 1,9084 |
| 4,0 | 0,1383 | 2,0419 | 5,5 | 0,08481 | 1,9010 |
| 4,1 | 0,1334 | 2,0304 | 5,6 | 0,08227 | 1,8935 |
| 4,2 | 0,1288 | 2,0193 | 5,7 | 0,07988 | 1,8864 |
| 4,3 | 0,1244 | 2,0085 | 5,8 | 0,07760 | 1,8791 |
| 4,4 | 0,1203 | 1,9978 | 5,9 | 0,07542 | 1,8721 |
| | | | 6,0 | 0,07326 | 1,8660 |

Future plans include the publication of tables of Struve functions of orders zero and one for $\rho$ = 0 (0.01) and 0 (0.1) 6, with $\varphi$ = 0 (5°) 90°; and also $G_0(iz)$ and $G_1(iz)$ for $\rho$ = 0 (0.1) 1, $\varphi$ = ±0 (5°) 90° and $\rho$ = 0 (0.1) 6, $\varphi$ = ±45° (5°) 90°.

Bibliography


1. Bursian, V. R. Teoriya elektromagnitnykh poley, primenyayemykh v elektrorazvedke [Theory of the Electromagnetic Fields Used in Electrical Prospecting], part 2, Izd. Leningrad. Gos. Univ., 1936.

2. Bateman. Higher Transcendental Functions, vol. 2, ch.4, 1953.

3. Watson. Theory of Bessel Functions, vol. 1, 1949.

4. Gasanenko, L. B. and G. P. Sholpo. K voprosu o vychislenii polya nizkochastotnogo dipolya v dal'ney zone [Calculation of the low-frequency dipole field in the far zone]. (Fourth paper in this set.)

5. Tables of Bessel Functions $Y_0$ and $Y_1$ for Complex Arguments. NBS, USA, N. Y., 1950.

6. Sheynman, S. M. and G. S. Frantov. Magnitnyy dipol' nad dvukhsloynoy sredoy. Sb. VITR "Novoye v metodike i tekhnike geologorazvedochnykh rabot" [A magnetic dipole above a two-layer medium. Coll. of the All-Union Prospecting Technique Research Institute: "New Methods and Techniques in Geological Prospecting"], No. 1, Leningrad, 1958.

## APPROXIMATE FORMULA FOR A DIPOLE FIELD ABOVE A HORIZONTAL LAMELLAR STRUCTURE WITH A POORLY CONDUCTING BASE

pp. 110-113 L. B. Gasanenko

Simple asymptotic expressions are available for the wave zone of a low-frequency dipole [1,2]; the scale distances $r/d_1$ (relative to the depth of the base) used in frequency sounding are usually less than ten, and for these they give a fairly satisfactory description of the general trend if the base is a nonconductor or has a conductivity much higher than that of the overlying layers. However, if $\sigma_N/\sigma_1 \ll 1$, the wave-zone curves are very different from those found by numerical solution, as Fig. 1 shows by reference to $\tilde{\rho}_\omega$ for $\sigma_2/\sigma_1 = \gamma$ of 1/9 and 1/39. The wave curve deviates from the exact one because the wave expressions are deduced without allowance for the energy propating in the ground; formally speaking, this amounts to neglecting m in expressions containing $n_1 = (m^2 + x_1^2)^{1/2}$. For example, the f(m) of the integral solution

$$e_\varphi^{ur} = r^2 \int_0^\infty J_1(mr)\, 2f(m)\, m^2 dm;$$

$$f(m) = \frac{1}{m + n_1 \tilde{z}_1}; \quad \tilde{z}_1 = \operatorname{cth}\left[n_1 d_1 + \operatorname{Arcth}\frac{n_1}{n_2}\tilde{z}_2\right],$$

is expanded as a power series in m on the assumption that the region of integration that introduces the largest contribution is such that the moduli of the wave numbers for all layers (including the base) are much greater than m. But if $\sigma_N/\sigma_1 \ll 1$ ($1 = 1, 2, \ldots, N-1$), direct calculations for the region having $x_1 r \sim 8$ and $x_N r < 4$ show that the part with $|x_N| < m < |x_1|$ makes the largest contribution.

For this reason, we derive an expression that accounts approximately for the energy propagating in the base; to cal-

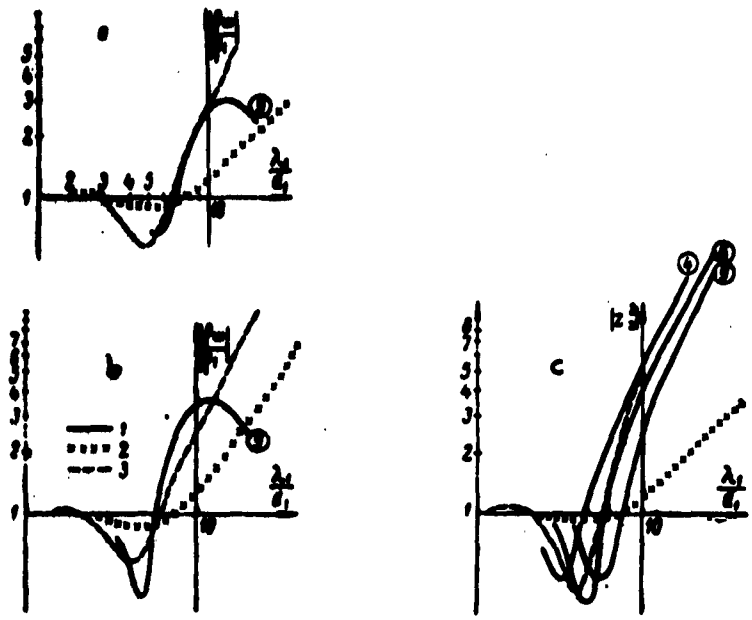

Fig. 1. Field of a vertical magnetic dipole over a stratum having a weakly conducting base: a) relation of the modulus of the apparent resistance (as determined from the tangential component) to wavelength for $\sigma_2/\sigma_1 = 1/9$ and $r/d_1 = 9$; b) the same for $\sigma_2/\sigma_1 = 1/39$ and $r/d_1 = 9$; c) the referred vertical impedance for $\sigma_2/\sigma_1 = 1/9$ and $r/d_1$ of h, 6, and 9; 1) exact curve (from quadratures of integral solutions); 2) wave curve; 3) approximate curve. The encircled numbers are the $r/d_1$.

culate the derivatives we assume that

$$n_l \underset{m\to 0}{\longrightarrow} x_l; \quad n'_l \underset{m\to 0}{\longrightarrow} 0; \quad (1 < l < N);$$

$$n_N \approx m + \frac{1}{2}\frac{x_N^2}{m} \underset{m\to 0}{\longrightarrow} 0; \quad n'_N \underset{m\to 0}{\longrightarrow} 1.$$

Then the apparent resistance is found as

$$\tilde{{}_1\rho}_\infty = x_1^2 f'(0) \approx {}_0z_1^2 + \frac{{}_0z_1^2 - 1}{1 - \frac{\sigma_N}{\sigma_{N-1}}} \prod_{l=2}^{N-1} \frac{1 - {}_0z_l^2}{\frac{\sigma_l}{\sigma_{l-1}} - {}_0z_l^2},$$

in which all ${}_0z_l$ relate to a structure with a nonconducting base. In particular, for a layer above a poorly conducting base,

$$\tilde{{}_1\rho}_\infty \approx \frac{(2-\gamma)\,{}_0z_1^2 - 1}{1-\gamma}; \quad {}_0z_1 = \operatorname{cth} x_1 d_1.$$

Approximate values of the field components are given by

$$e_\varphi \approx \frac{6}{x_1^2 r^2}\,\tilde{{}_1\rho}_\infty; \quad h_r \approx \frac{6}{x_1 r}\,{}_0z_1,$$

and the reduced vertical impedance is

$${}_1z_z \approx \tilde{{}_1\rho}_\infty : {}_0z_1.$$

The wave, approximate, and numerical curves are compared in Fig. 1; if $\gamma = 1/9$ (Fig. 1a), the $|\gamma\tilde{\rho}_\omega|$ given by the approximate formula for $5.5 < \lambda_1/d < 11$ is in good agreement with the quadrature curve for $r/d_1 = 9$. Again, if $\gamma = 1/39$ (Fig. 1b), the approximate curve lies closer to the exact curve than it does to the wave curve. We may say that for $5 < \lambda_1/d_1 < 10$ the approximate curve represents the behavior above a poorly conducting base as well as (or as poorly as) the wave curve represents the behavior above an insulating base.

Figure 1c shows the vertical field impedance for a vertical magnetic dipole above a two-layer structure for which $\sigma_2 = \sigma_1/9$. The approximate curve is close to the $|z_z^2|$ curve for $r/d_1 = 6$. The shape is almost precisely that of the exact curve for $r/d_1 = 9$, but the approximate curve is displaced, the relation between the two being roughly

$$\left|z_z^2\left(\frac{\lambda_1}{d_1}\right)\right| \approx 1.1\left|{}_1z_z^2\left(0.79\,\frac{\lambda_1}{d_1}\right)\right| \quad \left(\frac{r}{d_1} = 9;\ \frac{\sigma_2}{\sigma_1} = \frac{1}{9}\right).$$

The approximate formula is applicable for general purposes at medium wavelengths and at medium values of $r/d_1$.

More accurate expressions could be derived by expanding the formal solutions as power series in $(m - m_o)$, in which $m_o$ is a function of $\lambda$, $r/d_1$, and the structure of the section.

Bibliography


1. Tikhonov, A. N. and D. N. Shakhsuvarov. Elektromagnitoye pole dipolya v dal'ney zone [The electromagnetic field of a dipole in the far zone]. Izv. Akad. Nauk SSSR, ser. geofiz. [News of the Academy of Sciences of the USSR, geophysics series], No. 7 (1959).

2. Van'yan, L. L. K teorii dipol'nykh elektromagnitnykh zondirovaniy [Theory of dipole electromagnetic sounding]. Prikladnaya Geofizika [Applied Geophysics], no. 16. Leningrad, Gostoptekhizdat, 1958.

## DIRECTIONAL ELECTROMAGNETIC SOUNDING

pp. 118-128 G. V. Molochnov

Induction methods are now being extensively used in determining the depths of high-conductivity bodies covered by low-conductivity rocks. The physical principles are the same, no matter what apparatus may be used; a primary electromagnetic field (perhaps from several sources) produces eddy currents in the conducting medium, and these produce their own field, which is called secondary. The structure of the primary field is governed by the shape and size of the source (usually a frame bearing several turns of wire connected to a generator), while that of the secondary field is governed by the source, the frequency, the shape and size of the conductor, the distance from the source, and the electromagnetic parameters of the material. The secondary field is thus the only one of geophysical interest.

It is usual to examine the magnetic component by means of a frame probe; measurements are made of the amplitude and phase for the components along the coordinate axes or of the elements of the polarization ellipse (mainly the inclination of the major axis). Such methods are used at ground level, underground, and in aircraft.

The source coil is set either horizontal or vertical in current methods. The secondary field becomes appreciable only at some distance from the source, so it is usual to make the distance from source to body several times the depth of the body below the surface. This is an essential feature of all electrical methods, and it requires an operator at the detecting end as well as one at the source end with some means of communication between them; but it makes it difficult to measure the phase of the field, although this can provide information on the structure.

The secondary field is always observed together with the primary field, the latter forming a background that increases the error of the result. Attempts have been made to balance out some or all of the primary field, but these have not found

application in practical field work.

In principle, it would be possible to operate induction methods from moving vehicles, but this is made difficult by the need to have source and detector a considerable distance apart. For the same reason, the source and detector must be in different shafts or boreholes when the method is used underground, and even then the region surveyed is only a small part of that between source and detector.

I have developed a method of directional electromagnetic sounding that is free from these disadvantages. The directional sensitivity with respect to the conducting object is available for any frequency and any shape of object. The method is essentially as follows. An alternating current is passed through a coil wound on a frame (the source coil); a second coil (the receiving coil) is rigidly set up within (or near) the source coil, the planes of the two being perpendicular. Then the primary field of the source is not detected by the receiving coil, whereas the secondary field will produce an emf in the receiving coil if the system is suitably placed. The theory is as follows. An inclined magnetic dipole has a moment $M = M_0 \exp(i\omega t)$, in which $M_0$ is amplitude, $\omega = 2\pi f$, f is frequency, and t is time. (The time factor and the subscript zero are henceforth omitted.) The xOy plane is that of the surface of the Earth, the Oz axis being vertical. The dipole lies at the point $(0, 0, h_0)$, the projection on the xOy plane coinciding with the Ox axis. The angle between M and the Ox axis is $\psi$ (Fig. 1).

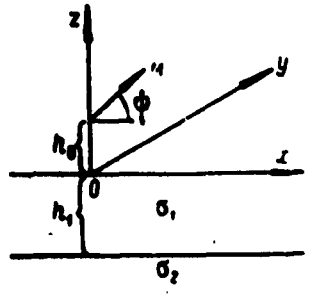


Fig. 1. Inclined magnetic dipole above a two-layer structure.

We take the simple case of two homogeneous and isotropic layers having a horizontal interface; let $\sigma_1$ and $h_1$ be the conductance and thickness of the top layer, the corresponding quantities for the lower layer being $\sigma_2$ and $h_2$ ($= \infty$). The magnetic permeability is taken as unity; the displacement currents in all media are neglected. The conductance of the air, $\sigma_0$, is taken as zero.

The field of an inclined dipole can be considered as made up of the field of a vertical dipole $M_B = M\sin\psi$ and of the field of a horizontal dipole $M_r = M\cos\psi$. Standard solutions for the fields of vertical /1/ and horizontal /2/ dipoles for points on the line $x = 0$, $z = h_0$ give us for the field components of a vertical dipole

$$H_z = -\frac{M_B}{r^3} + M_B \int_0^\infty J_0(nr)\, a n^2 dn, \qquad (1)$$

$$H_y = M_z \int_0^\infty J_1(nr)\, a n^2 dn, \tag{2}$$

$$H_x = 0;$$

and of a horizontal dipole

$$H_x = -\frac{M_x}{r^3} + \frac{M_x}{r} \int_0^\infty J_1(nr)\, a n dn,$$

$$H_y = H_z = 0, \tag{3}$$

in which r is the distance to the point of observation, the $J_{0,1}(nr)$ are Bessel functions of the first kind and of the zero and first orders,

$$a = \frac{n_{01} + n_{12} e^{-2n_1 h_1}}{1 + n_{01} n_{12} e^{-2n_1 h_1}} e^{-2n h_0},$$

$$n_{lk} = \frac{n_l - n_k}{n_l + n_k}, \quad n_l = \sqrt{n^2 + x_l^2}, \quad x_l^2 = i \frac{2\pi^2 \sigma_l f}{c^2}, \tag{4}$$

and $c = 3 \times 10^{10}$ cm/sec. The first terms in (1) and (3) represent the primary field; they become infinite when r = 0. The second terms in (1) and (3), and the $H_y$ of (2), represent secondary fields resulting from conduction. Now $J_1(nr) \to nr/2$ when $r \to 0$, and $J_0(nr) \to 1$, so $H_y \to 0$ in (2), but the second terms in (1) and (3) remain finite. The total fields of (1) and (3) tend to infinity as $r \to 0$, so the conducting medium has relatively little effect at short distances.

An inclined dipole gives at the same points

$$H_x = M \cos\psi \left[ -\frac{1}{r^3} + \frac{1}{r} \int_0^\infty J_1(nr)\, a n dn \right], \tag{5}$$

$$H_y = M \sin\psi \int_0^\infty J_1(nr)\, a n^2 dn, \tag{6}$$

$$H_z = M \sin\psi \left[ -\frac{1}{r^3} + \int_0^\infty J_0(nr)\, a n^2 dn \right]. \tag{7}$$

The field strength normal to the moment and the Oy axis is

(apart from sign)

$$H_{xz} = H_x \sin\psi - H_z \cos\psi = \frac{M}{2} \sin 2\psi \left\{ \int_0^\infty J_0(nr)\, a\, n^2 dn - \right. \tag{8}$$

$$\left. - \frac{1}{r} \int_0^\infty J_1(nr)\, a\, n dn \right\} = M \sin 2\psi\, F(r),$$

in which

$$F(r) = \frac{1}{2} \left\{ \int_0^\infty J_0(nr)\, a\, n^2 dn - \frac{1}{r} \int_0^\infty J_0(nr)\, a\, n dn \right\}. \tag{9}$$

The other component normal to the dipole lies along the Oy axis; it is given by (6). These components of (6) and (8) are determined only by the secondary field; the $H_y$ of (6) is caused by the vertical component of the magnetic field, so it is largest for $\psi = 90°$. I do not consider $H_y$ here, for this is discussed in existing papers. As regards the $H_{xz}$ of (8), the principal feature is that $H_{xz}$ remains finite as $r \to 0$, being

$$H_{xz} = 1/4\, M \sin 2\psi \int_0^\infty a n^2 dn. \tag{10}$$

Another important feature is that $H_{xz}$ varies as sin $2\psi$, so $H_{xz} = 0$ if $\psi$ is 0 or 90° (the secondary field is not detected in these positions). The maximum $H_{xz}$ occurs when $\psi = 45°$, the value being governed by F(r). Figure 2 shows the polar diagram, the two perpendicular lines being the projections of the planes containing the source and receiving coils. The points represent measurements made in air above a sheet of aluminium; here the coils were 10 cm, in diameter (source) and 8 cm (receiver). In what follows, subscript xz is omitted, so $H_{xz} = H$. The integrals in F(r) can be calculated only by numerical integration for any medium generally; but they can be given in approximate form for certain layered media, especially one consisting of an insulator of thickness $h_1$ lying on a base whose conductivity is $\sigma_1 = \sigma$. Let $h_0 + h_1 = h$ here; then

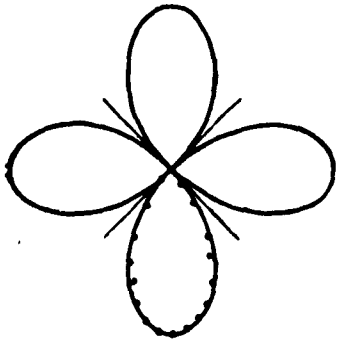

Fig. 2. Polar diagram of the apparatus.

$$\alpha = \frac{n - \sqrt{n^2 + x^2}}{n + \sqrt{n^2 + x^2}} e^{-2nh} = \left(-1 + \frac{2}{x^2} n \sqrt{n^2 + x^2} - 2\frac{n^2}{x^2}\right) e^{-2nh}. \quad (11)$$

As asymptotic series in negative powers of Z is obtained for F(r) if $|Z| = 2h|x| \gg 1$:

$$F(r) = \frac{1}{(2h)^3}\left\{\frac{1 - \frac{1}{2}R^2}{2\left(1 + \frac{1}{4}R^2\right)^{5/2}} - 3\frac{1 - R^2}{\left(1 + \frac{1}{2}R^2\right)^{7/2}} \cdot \frac{1}{Z} + 3\frac{4 - \frac{13}{2}R^2 + \frac{5}{16}R^4}{\left(1 + \frac{1}{4}R^2\right)^{9/2}} \cdot \frac{1}{Z^2} - \ldots\right\}, \quad (12)$$

in which R = r/h. The subsequent terms contain odd powers of Z; only the first terms need be considered if Z is large, the error then not exceeding the absolute value of the first discarded term.

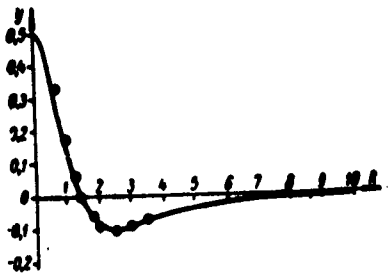

Fig. 3. Relation of $H_{xz}$ to distance for an inclined dipole above an ideally conducting half-space.

Consider the first term within the bracket in (12), which we denote by Y; this corresponds to a perfect conductor. Now Y = ½ for R = 0, and Y at first decreases as R increases, becoming zero when $R = \sqrt{2}$. The maximum negative value of -0.101 occurs when $R = 2\sqrt{3/2}$; thereafter the value tends monotonically to zero (Fig. 3). Measurements (shown by points) have been made above a sheet of aluminium with coils 5 cm in diameter. In this case H is maximal when r = 0, so the receiving coil must be placed at r = 0; then for $\psi = 45°$ we have that

$$H = \frac{M}{2(2h)^3}. \quad (13)$$

For finite conductivity

$$H = \frac{M}{2(2h)^3}\left(1 - \frac{6}{Z} + \frac{24}{Z^2} - \frac{60}{Z^3} + \frac{630}{Z^4} - \ldots\right). \quad (14)$$

The number of terms needed in (14) for a given Z can be

determined if the permissible error in H is specified. The x that appears in Z is best expressed in terms of the wavelength within a layer:

$$x=\frac{1}{c}\sqrt{i}\,2\pi\sqrt{2\sigma f}=\sqrt{i}\,2\pi\sqrt{2}\,\frac{1}{\lambda},$$

in which

$$\lambda=\frac{c}{\sqrt{\sigma f}}. \tag{15}$$

Then (14) can be put as

$$H=\frac{M}{2(2h)^3}\left\{1-(1-i)\frac{3}{4\pi}\frac{\lambda}{h}-i\frac{3}{4\pi^2}\left(\frac{\lambda}{h}\right)^2+(1+i)\frac{15}{64\pi^3}\left(\frac{\lambda}{h}\right)^3=\ldots\right\}\cdot$$
$$=\frac{M}{2(2h)^3}\Phi\left(\frac{\lambda}{h}\right), \tag{16}$$

in which $\Phi$ denotes the expression within braces. Table 1 gives the Re, Im, a (modulus), and $\varphi$ (phase) of $\Phi$ for several $\lambda/h$ and for several termination points. The error in the amplitude is only 0.7% for $\lambda/h = 0.75$, 1.5% for $\lambda/h = 1$, and 5% for $\lambda/h = 1.5$ if the first two terms in (16) are taken, so these terms are sufficient if $\lambda/h$ is small.

The converse problem (determination of h from known M and H) is usually solved by frequency or radial sounding, the resulting curves being compared with theoretical ones. This method is the usual one and is widely used in electrical surveys. The interpretation can be made very much easier if we determine the effective penetration depth [3]. Here we can also use (13) to determine the depth, and from this subtract the effective penetration depth $\Delta h$, which is deduced as follows. Let $\overset{\circ}{H}$ be the field when the conductivity is infinite; then (13) gives

$$h=\frac{1}{2}\sqrt[3]{\frac{M}{2\overset{\circ}{H}}}. \tag{17}$$

(17) will give a depth $D = h + \Delta h$ when the conductivity is finite, and $\Delta h$ is given by

$$\Delta h=\frac{\partial h}{\partial \overset{\circ}{H}}\Delta H, \tag{18}$$

in which $\Delta H$ is the real part of the second term in (16). Then

$$\Delta h=\frac{\lambda}{4\pi}, \tag{19}$$

Table 1

| No. of terms | $\frac{\lambda}{h}$ | Re | Im | $a$ | $\varphi$ |
|---|---|---|---|---|---|
| 1 | | 1 | 0 | 1 | 0 |
| 2 | | 0,8807 | 0,1193 | 0,890 | 7°45′ |
| 3 | 0,5 | 0,8807 | 0,1008 | 0,888 | 6 30 |
| 4 | | 0,8816 | 0,1012 | 0,890 | 6 35 |
| 5 | | 0,8816 | 0,1012 | 0,890 | 6 35 |
| 1 | | 1 | 0 | 1 | 0 |
| 2 | | 0,821 | 0,179 | 0,84 | 12°20′ |
| 3 | 0,75 | 0,821 | 0,1363 | 0,834 | 9 25 |
| 4 | | 0,824 | 0,1395 | 0,846 | 9 35 |
| 5 | | 0,824 | 0,1396 | 0,846 | 9 35 |
| 1 | | 1 | 0 | 1 | 0 |
| 2 | | 0,7613 | 0,2387 | 0,798 | 17°25′ |
| 3 | 1,0 | 0,7613 | 0,1627 | 0,779 | 12 05 |
| 4 | | 0,7689 | 0,1703 | 0,786 | 12 30 |
| 5 | | 0,7687 | 0,1705 | 0,786 | 12 30 |
| 1 | | 1 | 0 | 1 | 0 |
| 2 | | 0,642 | 0,358 | 0,735 | 29°10′ |
| 3 | 1,5 | 0,642 | 0,187 | 0,670 | 16 15 |
| 4 | | 0,6676 | 0,2126 | 0,700 | 17 40 |
| 5 | | 0,6657 | 0,2145 | 0,700 | 17 50 |
| 1 | | 1 | 0 | 1 | 0 |
| 2 | | 0,5226 | 0,4774 | 0,707 | 42°45′ |
| 3 | 2,0 | 0,5226 | 0,1734 | 0,550 | 18 20 |
| 4 | | 0,5831 | 0,2309 | 0,623 | 21 35 |
| 5 | | 0,575 | 0,2389 | 0,623 | 22 35 |

which is the value given previously [3]. Table 2 gives values calculated from (18) by means of Table 1; for simplicity M has been put as 16 and H as 1, so h = 1. The results are clearly satisfactory even for $\lambda/h = 2$.

It has been shown [3] that $\Delta h$ can be determined by means of measurements at two frequencies $f_1$ and $f_2$:

$$\Delta h_1 = \frac{D_2 - D_1}{\sqrt{\frac{f_2}{f_1} - 1}}, \qquad (20)$$

Table 2

| $\frac{\lambda}{h}$ | D from (17) | Δh from (19) | D − Δh | Error, % |
|---|---|---|---|---|
| 0,0 | 1,000 | 0,000 | 1,000 | 0,0 |
| 0,5 | 1,040 | 0,040 | 1,00 | 0,0 |
| 1,75 | 1,058 | 0,058 | 1,000 | 0,2 |
| 1,0 | 1,082 | 0,08 | 1,002 | 0,2 |
| 1,5 | 1,125 | 0,119 | 1,006 | 0,6 |
| 2,0 | (1,17) | 0,159 | (1,011) | (1,1) |

in which $D_1$ and $D_2$ are the depths given by (17) for these frequencies and $h_1$ is the Δh for $f_1$. Then, since Δh is now known, we can determine σ from (19) as

$$\sigma = \frac{c^2}{(4\pi\Delta h)^2 f}. \qquad (21)$$

The effects of finite conductivity in the first layer on the determination of h can be established as for the dipole electromagnetic method [4].

It can be shown that the method is applicable to bodies of finite size; the case of a sphere illustrates this.

An ideally conducting sphere of radius $r_0$ is embedded in a poorly conducting medium; the center lies a distance h below the surface. A dipole inclined at ψ to the horizontal and having a moment M is placed at the epicenter. We assume that the field of the dipole would be homogeneous throughout the volume of the sphere, the contribution from the vertical component being

$$H_{oz} = \frac{2M}{h^3} \sin\psi;$$

and that from the horizontal component being

$$H_{or} = -\frac{M}{h^3} \cos\psi.$$

This is rather a gross simplification, but the general nature of the result is correct. No more exact solution is necessary,

for real bodies are merely more or less isometric.

The secondary field at the epicenter given [5] by a vertical dipole is

$$H_s = -2M \sin\psi \frac{r_0^3}{h^6};$$

and by a horizontal dipole

$$H_r = -\frac{1}{2} M \cos\psi \frac{r_0^3}{h^6}.$$

The field strength in a direction perpendicular to the dipole is

$$H = H_r \sin\psi - H_s \cos\psi = \frac{3}{4} M \sin 2\psi \frac{r_0^3}{h^6}. \qquad (22)$$

The directional feature is retained here also.

The above discussion shows that a directional equipment can be operated at any suitable frequency if the two coils are mutually perpendicular and have a common center (they can be displaced by a distance small relative to the depth of the conducting object, as Fig. 3 shows). The signal from the receiving coil is amplified and fed to a meter or recorder, which is calibrated directly in field strength. The presence of a nearby conductor can be detected by rotating the coils about a horizontal axis in various azimuths until the maximum reading is obtained; the direction is determined rather more precisely from the points of silence, as the polar diagram (Fig. 2) shows. The depth is determined from the maximum reading; the position of the upper surface can be determined if the body is sufficiently large.

The apparatus is compact, which makes the method convenient and economical to use; the receiver and generator can be contained in a single case, so the phase can be measured as well as the amplitude, and this provides more detailed information. The method can be used underground, in aircraft, and in moving land vehicles. Moreover, it can be applied to frequency sounding of layered structures of small depth. In every case the operations are simple and the interpretation is more complete.

## Bibliography


1. Molochnov, G. V. Vertikal'nyy magnitnyy dipol' na poverkhnosti gorizontal'noy sloistoy struktur. Geofizicheskiye metody razvedki [A vertical magnetic dipole on the surface of a horizontal layered structure. Geophysical Prospecting Methods]. Moscow, Gosgeoltekhizdat, 1955.
2. Gasanenko, L. B. and G. V. Molochnov. Elektromagnitnoye pole gorizontal'nogo magnitnogo dipolya nad gorizontal'nosloistoy strukturoy [The electromagnetic field of a horizontal magnetic dipole over a horizontally layered structure]. Uch. Zap. Leningrad. Gos. Univ. [Archives of Leningrad University], No. 249, 1958.
3. Molochnov, G. V. Dipol'nyy elektromagnitnyy metod opredeleniya glubiny zaleganiya sloya konechnoy provodimosti [A dipole electromagnetic method of determining the depth of a layer of finite conductivity]. Vestnik. Leningr. Un-ta [Herald of Leningrad University], No. 10, 1960.
4. Idem. O vliyanii provodimosti pervogo sloya pri opredelenii glubiny zaleganiya provodyashchego osnovaniya dipol'nym elektromagnitnym metodom [Effects of conductivity of the first layer in the determination of the depth of a conducting base by the dipole electromagnetic method]. Uch. Zap. Leningrad. Gos. Univ. [Archives of Leningrad University], No. 286, 1960.
5. Smythe, W. R. Static and Dynamic Electricity. Moscow, Izd. Inost. Lit., 1954.

# COMPARISON OF THE INDUCTION METHOD WITH THE DIPOLE ELECTROMAGNETIC METHOD ON A THIN CONDUCTING PLATE (MODEL)

G. V. Molochnov and G. M. Grebennikov

pp. 129-134

Induction methods are now much used to detect steeply dipping strata. The dipole method [1,2] has given good results for the depths of conducting strata; here the inclination of the magnetic vector is measured for the field of a vertical magnetic dipole. The method has been applied to measure the thickness of floating ice (0.5 to 13 m) on the drifting stations 'North Pole 6' and 'North Pole 9', as well as along the northern sea route in 1958-61 [3]. The error here is less than 3%.

Vertical dipoles have been used in experiments with conducting bodies (plate, cylinder, sphere) in the Geoelectricity Laboratory of the Physics Research Institute, Leningrad University [4]. It has been found that the vertical component of the magnetic field enables one to determine the size and inclination of a plate in horizontal projection (i.e., the shape and position in space).

Here we compare the induction method with the dipole method, the source and receiving sections having identical parameters. The inclination of the total field vector to the horizontal was measured in both cases. The field was produced by a screened frame (a circle of diameter 5.3 cm) fed via a screened cable; the detecting coil had a screened frame 4.7 cm in diameter and worked into a tuned amplifier feeding a MVL-1 vacuum-tube voltmeter. The model was a brass sheet 126 x 33 x 0.1 cm, which was supported on an insulator and was fitted with a means of adjusting the inclination $\gamma$, which was varied from 0° (vertical) to 90° (horizontal) by 15° steps. The top edge of the sheet was always horizontal.

Measurements were made at distances of 20, 30, 40, 50, and 60 cm, with the top edge at depths of 10 and 20 cm. The

Table 1

| r (cm) | Actual h (cm) | Calculated h (cm) | | $\frac{x_1 + x_2}{\alpha_1 + \alpha_2}$ | $\frac{M_1}{M_2}$ |
|---|---|---|---|---|---|
| | | Parabola method | from (1) | | |
| 20 | 10 | 5 | 8,4 | 80 | 7 |
| 30 | | 9 | 9,3 | 59 | 5 |
| 40 | | 11 | 11,5 | 50 | 4 |
| 50 | | 13 | 13,7 | 43 | 3,1 |
| 60 | | 15 | 15,1 | 43 | 3,1 |
| 40 | 20 | — | 19 | — | — |
| 50 | | — | 19,4 | — | — |
| 60 | | — | 20,2 | — | — |

model was moved, the coils being kept fixed. In the dipole method, the sheet was inclined towards the source or towards the detector. Figure 1 shows profile curves for γ of 0, 45, and 90°.

The induction results were worked up to give the angles as usual [5,6]. Table 1 gives the depth of the top edge h as deduced by the parabola method [7] and from [8]

$$h = \frac{x_{m_1 m_2}}{\operatorname{ctg} \alpha_0} \left(\sqrt{1 + \operatorname{ctg}^2 \alpha_0} - 1\right), \qquad (1)$$

in which x is the abscissa corresponding to the extreme angle $\alpha_0$. Table 1 also gives $(x_1 + x_2)/(\alpha_1 + \alpha_2)$, which is used to calculate $H_1/H_2$, which appears in formula (2) of [8]:

$$h = \frac{x_1 + x_2}{\alpha_1 + \alpha_2} \cdot \frac{1}{1 + \frac{H_1}{H_2}}, \qquad (2)$$

in which $x_1$, $\alpha_1$ and $x_2$, $\alpha_2$ are the coordinates of the angle curve to the left and to the right of the origin, $H_1$ and $H_2$ being the strengths of the primary and secondary magnetic fields. We see that the parabola method gives satisfactory results for $r/h \approx 3$-4, while (1) is satisfactory for $r/h \approx$ 2-4.

The position of the electric axis is determined in the usual way in the induction method; in the dipole method, the position of the electric axis of a vertical plate is determined

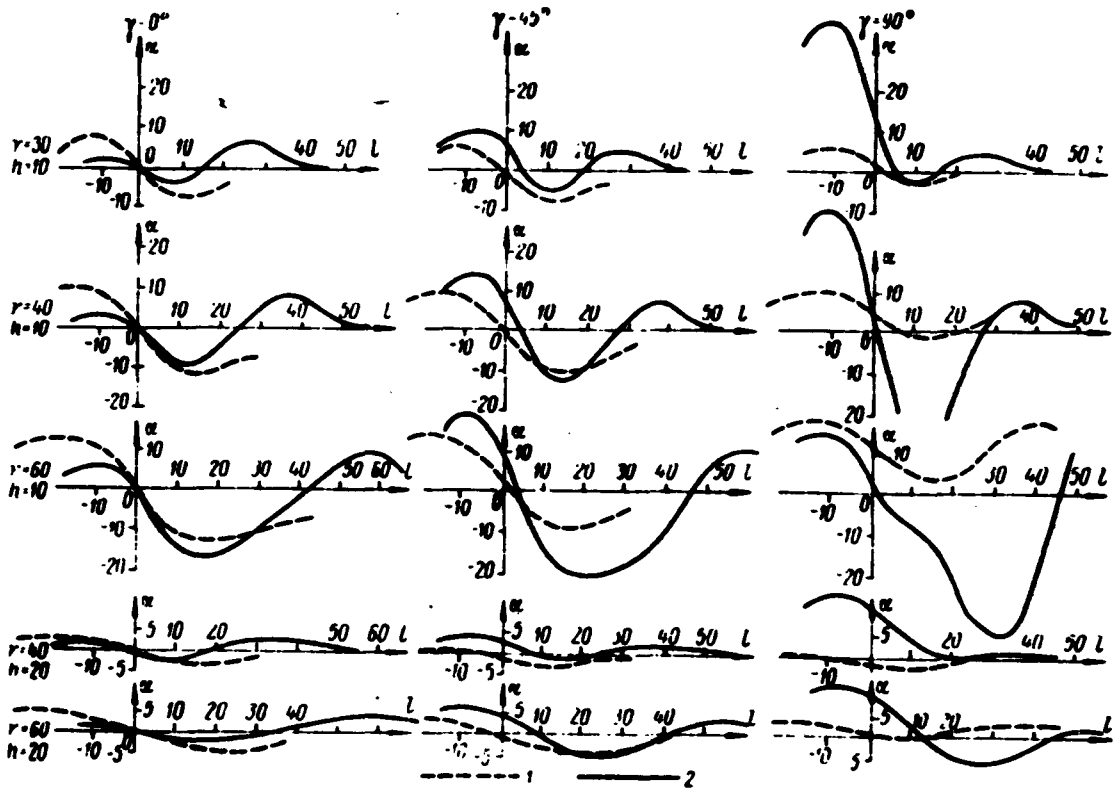


Fig. 1. Profile Curves over the Plate using induction method (1) and dipole electromagnetic method (2).

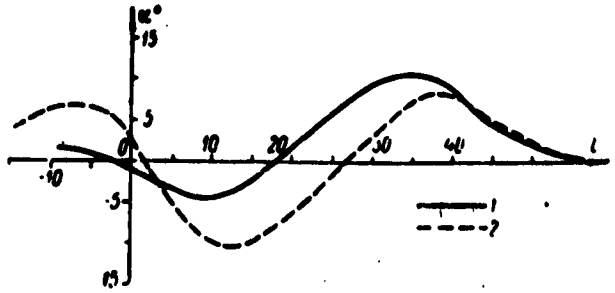


Fig. 2. Profile curves for the dipole method with 1) source-detector setting; 2) detector-source setting.

by the point at which the profile curve meets the axis of abscissas. The profile must be measured twice, as shown by curves 1 and 2 of Fig. 2, if the plate is inclined. The point half-way between the points where these curves meet the axis is then the position of the electric axis.

The depth of the top edge may be deduced from the observation that the distance $l$ between the two points where the curve meets the axis is almost independent of $\gamma$ if the plate is inclined towards the detector, provided that $\gamma < 60°$, as Table 2 shows. Figure 3 shows $l$ as a function of r (the distance)

Table 2

| γ | r | | | | | | |
|---|---|---|---|---|---|---|---|
| | 30 | 40 | 50 | 60 | 40 | 50 | 60 |
| | h = 10 см | | | | h = 20 см | | |
| 8 | 15 | 24 | 33 | 42 | 15 | 27 | 33 |
| 15 | 15 | 25 | 34 | 43,5 | 15,5 | 26 | 35,5 |
| 30 | 15,5 | 25 | 34,5 | 43,5 | 12,5 | 25 | 34 |
| 45 | 14,5 | 24 | 34,5 | 43,5 | 14 | 25 | 33 |
| 60 | 13,5 | 24,5 | 34,5 | 44,5 | — | 22 | 32,5 |
| 75 | 12 | 23,5 | 34 | 42,5 | — | 20 | 31 |
| 90 | 9,5 | 25 | 34,5 | 44 | — | 17,5 | 30 |

for depths of 10 and 20 cm; the relation is a straight line of unit slope which meets the line $l = -5$ at $r = h$. This can be used to determine h.

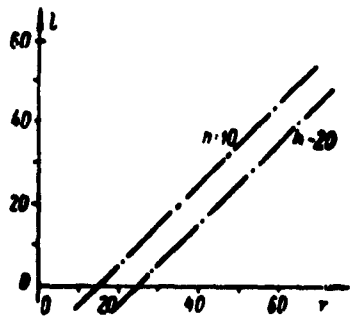


Fig. 3. Relation of i to r.

Table 3 gives the ratio of the maximum angles of inclination of the magnetic field in the two methods; it shows that $\alpha_d/\alpha_i > 1$ if $\gamma > 15°$, the ratio increasing with $\gamma$. This means that the dipole method is best if $\gamma > 15°$.

The position of the electric axis is thus determined reliably in both methods. Induction gives the position of the top edge satisfactorily only for r/h of 3-4, but the dipole method is suitable for any r. Both methods can be used in detailed work, especially since the apparatus is the same.

Table 3

| h | r | γ | | | | | | |
|---|---|---|---|---|---|---|---|---|
| | | 0 | 15 | 30 | 45 | 60 | 75 | 90 |
| 10 | 20 | 1 | 1,5 | 1,63 | 2,25 | 2,56 | 3,56 | 7,9 |
| | 30 | 0,88 | 1,13 | 1,31 | 1,62 | 2,34 | 4,18 | 6,8 |
| | 40 | 0,86 | 0,96 | 1,1 | 1,4 | 2,28 | 3,05 | 4,25 |
| | 50 | 1,12 | 1,33 | 1,36 | 1,48 | 1,77 | 2,11 | 2,8 |
| | 60 | 1,33 | 1,42 | 1,43 | 1,43 | 1,6 | 1,78 | 2,47 |
| 20 | 40 | 0,9 | 1,33 | 1,67 | 1,71 | 2,28 | 3,66 | 5,33 |
| | 50 | 0,87 | 1,0 | 1,25 | 1,5 | 2,12 | 4,0 | 6,8 |
| | 60 | 0,8 | 1,11 | 1,11 | 1,75 | 2,5 | 3,26 | 3,67 |

## Bibliography

1. Molochnov, G. V. Dipol'nyy elektromagnitnyy metod opredeleniya glubiny zaleganiya provodyashchego sloya [The dipole electromagnetic method of determining the depth of a conducting layer]. Vestnik Leningr. un-ta, seriya fiz. i khim. [Herald of Leningrad University, Physics and Chemistry Series], No. 2, 1959.

2. Idem. Dipol'nyy elektromagnitnyy metod opredeleniya glubiny zaleganiya sloya konechnoy provodimosti [The dipole electromagnetic method of determining the depth of a layer of finite conductivity]. Ibid., No. 10, 1960.

3. Molochnov, G. V. and I. V. Cherepanov. Opyt primeneniya elektromagnitnogo metoda dlya opredeleniya tolshchiny morskogo l'da [Use of the electromagnetic method for determining the thickness of sea ice]. Problemy Arktiki i Antarktiki [Problems of the Arctic and Antarctic], No. 3, 1960.

4. Molochnov, G. V. and V. T. Balobayev. Provodyashcheye telo v elektromagnitnom pole vertikal'nogo magnitnogo dipolya [A conducting body in the field of a vertical magnetic dipole]. Uch. Zap. LGU [Archives of Leningrad University], No. 249, 1958.

5. Pylayev, A. M. Opyty s modelyami po metodu induktsii [Experiments with models in the induction method]. Materialy TsNIGRI geofiziki [Materials of the Central Geophysical Prospecting Research Institute], No. 2, 1936.

6. Tarkhov, A. G. Modelirovaniye peremennykh elektromagnitnykh poley v tselyakh geofizicheskoy razvedki [Modeling of alternating electromagnetic fields for the purposes of geophysical prospecting]. Izv. AN SSSR, ser. geofiz. [News of the Academy of Sciences of the USSR, geophysics series], No. 4, 1953.

7. Mikhaylov, I. G. and A. M. Pylayev. Induktsionnyy metod razvedki poleznykh iskopayemykh [The induction method of prospecting for mineral resources]. Moscow, Gosgeoneftteizdat, 1933.

8. Tarkhov, A. G. Geofizicheskaya razvedka metodom induktsii [Geophysical prospecting by the induction method]. Moscow, Gosgeoltekhizdat, 1954.

# REPRESENTATION OF OBSERVATIONAL DATA OF ALTERNATING-CURRENT PROSPECTING AS AN APPARENT SPECIFIC RESISTANCE

A. V. Veshev

pp. 167-186

There are many types of electrical prospecting methods, which use alternating and direct currents; there are also many types of line, methods of examining the fields, and so on. This makes it of value to consider which are the best parameters to use to characterize the field.

The apparent specific electrical resistance (apparent resistance*) is commonly used in d.c. methods, in addition to directly measured quantities (potentials and gradients). This is convenient, for it is independent of the apparatus and method if the medium is homogeneous, though it is in general only a function of the field, being the product of some measured quantity (reduced to unit current) by a coefficient dependent on the geometry of the system (in particular, on the form of the grounds, if these are not point grounds). However, the function is such that it corresponds to the specific resistance if the medium is homogeneous; the coefficient is adjusted accordingly.

The apparent resistance is a function of the component and method if the medium is not homogeneous, but it is still a convenient parameter, for the effect of inhomogeneity may be expressed as a ratio to some parameter common to all systems, which parameter corresponds to the specific resistance of a homogeneous medium. This makes the apparent resistance a convenient parameter for geologic mapping and for structure studies.

Alternating currents are used mainly to detect anomalies in conductance, the results being given directly as the amplitude and phase of the field, as the angles of inclination of the magnetic vector, and so on. Sometimes, as in ratio methods, the results are presented merely as changes in field parameters. This is a rather narrow use of a.c. methods, and it makes it difficult to use the results for structure mapping and resistance measurement; but the methods are actually at least as

---

*This abbreviation will be used in future.

valuable as d.c. ones for these purposes. Before they can be so used, though, there is need for some work on apparatus and on methods of presenting the results. Here I shall deal only with the latter aspect of the matter.

It is best to present the results from a.c. methods as reduced parameters of apparent-resistance type. The parameter to be used is to be chosen on the basis that its dimensions and numerical value must be the same as $\rho$ (the specific resistance) for a homogeneous and isotropic half-space; then an inhomogeneous half-space gives a parameter analogous to the specific resistance. Here we must point out that the apparent resistance will be dependent on the source and on the dimensions of the system if the space is inhomogeneous. It is convenient to denote the d.c. and a.c. values of the apparent resistance by $\bar{\rho}$ and $\bar{\rho}$, by analogy with $\rho$, the frequency being indicated (if necessary) by a subscript to $\bar{\rho}$.

There are great difficulties in calculating $\bar{\rho}$ for artificial electromagnetic fields, for the situation differs from that in d.c. methods, where the potential and the gradient are linearly related to $\rho$ and bear a simple relation to the geometry of the system (the coefficient k has the dimensions of a length and is defined by purely geometrical relationships). The source in an a.c. method is an electric or magnetic dipole, or a very long cable; here the vector potential and the field components have a complicated relation to the reduced distance $\xi = kr$, in which r is the distance from the source and k is the wave-number of the medium. If displacement currents are negligible, and if $k^2$ can be treated as imaginary, we have

$$\xi = 0{,}4\pi r \sqrt{\frac{5f}{\rho}} \approx 2{,}81 r \sqrt{\frac{f}{\rho}}, \qquad (1)$$

in which r is in km, f is in c/s, and $\rho$ is in ohm-m. For field sources of finite size, we have an equivalent quantity $\xi'$:

$$\xi' = \xi l = 0{,}4\pi r l \sqrt{\frac{5f}{\rho}}. \qquad (2)$$

Formula (2) shows that the length $l$ (km) of the source line affects the field pattern; the effects of this length are sometimes described by a parameter P, which for $k^2$ imaginary is given by

$$P = 0{,}4\pi l \sqrt{\frac{5f}{\rho}}, \qquad (3)$$

in which $l$ is in km, $f$ and $\rho$ are in c/s and ohm-m, resp. Now r and f are always known, so $\xi$ and $\xi'$ give us $\bar{\rho}$, provided that there is a unique relation between the measured field

components and $\xi$ or $\xi'$.* The apparent resistance as so found enables one to separate field changes associated with features of the section from changes associated with the apparatus. The apparent resistance will be the specific resistance for a homogeneous half-space no matter what the system and wavelength. Moreover, the asymptotic values will, for a two-layer structure, correspond with the resistances of the two layers. The apparent resistances as found by d.c. and a.c. methods for a given section enable one to compare resolving powers; the problem can also be discussed theoretically to a certain extent, but the a.c. fields must then be represented in terms of parameters corresponding to the apparent resistance**.

The apparent resistance is a function of many parameters, so symbols are needed to indicate the type of apparatus and field. These may be subscripts to $\bar{\rho}$ and $\tilde{\rho}$, such as Э.Г. (horizontal electric dipole), M.B. (vertical magnetic dipole), M.Г. (horizontal magnetic dipole), b.k. (infinite cable), k.k. (finite cable), mz (vertical magnetic component), mr (radial magnetic component), $\varphi$ (azimuthal electric component), and so on. The symbols for the source will be placed in the right upper position, and those for the field in the right lower. For example, $\tilde{\rho}^{b.k}_{mz}$ and $\tilde{\rho}^{M.Г.}_{mz}$ denote respectively the use of the vertical magnetic component from an infinite cable and of the same from a horizontal magnetic dipole. Only the electric field is used in d.c. methods, so there is no need to put a subscript for electric to $\bar{\rho}$. Here we can use symbols such as $\bar{\rho}_n$ (potential system), $\bar{\rho}_r$ (gradient system), $\bar{\rho}_{r.cp}$ (mean gradient system), and so on; the superscript indicates the source type (e.g., $\bar{\rho}^d$, dipole source). These numerous subscripts and superscripts are somewhat inconvenient; in any given case, they may be omitted after the type of source and so on have been stated. This question of notation requires a separate study.

* * *

*The field source is represented as a plane incident wave when natural fields are used, as in magnetotelluric sounding. Here $\tilde{\rho} = 4\pi z/\omega$, in which $z = E/H$ and $\omega$ is frequency. The ratio of any two components will be dependent on $\xi$ for any other form of source, so $\tilde{\rho}$ can then be deduced only from $\xi$.

**Van'yan's $\rho_\omega$ and $\rho_r$ for frequency sounding and for field equilibration with an electric dipole [1,2], and analogous quantities for magnetic dipoles [6], do not satisfy these requirements fully; the $\rho_\omega$ and $\rho_r$ for a homogeneous half-space tend to $\rho$ as limit only for $\xi$ very small (S zone) and very large (wave zone).

It is possible to deduce $\tilde{\rho}$ in any given case only if $\xi$ or $\xi'$ is known; the conditions for this vary with the type of source and can be deduced from the type of variation of the normal field. As an example I consider the use of magnetic dipoles. Here there are many different forms of source and detector [4,5,7-9,11,12], but the main differences relate only to the frequency and to the orientation of the dipoles with respect to the surface and to one another. The real and imaginary parts are recorded for one or more field components, and also the magnitude and inclination of the total field (as in induction methods). The normal fields of magnetic dipoles on the surface of a homogeneous conducting space have been examined [3,4]; the field components are represented as

$$\left.\begin{aligned} H_z^{\text{м.в}} &= -\frac{M}{r^3} h_z^{\text{м.в}}; \quad H_r^{\text{м.в}} = -\frac{M}{r^3} h_r^{\text{м.в}}; \quad H_z^{\text{м.г}} = \frac{M}{r^3} h_z^{\text{м.г}} \\ H_\varphi^{\text{м.г}} &= +\frac{M}{r^3} h_\varphi^{\text{м.г}}; \quad H_r^{\text{м.г}} = +\frac{M}{r^3} h_r^{\text{м.г}}; \quad E_\varphi^{\text{м.в}} = -\frac{i\omega M}{cr^2} e_\varphi^{\text{м.в}} \end{aligned}\right\}, \quad (4)$$

in which $M/r^3$ is the field of a dipole in air (sometimes called the primary field); the upper-case letters represent components of the electromagnetic field, while the lower-case h and e denote changes resulting from the use of a.c. (these arise from conductivity) and are dimensionless quantities called the magnetic and electric numbers (Krayev's notation).

It has been shown [4] that these numbers have the following relations:

$$\begin{aligned} h_r^{\text{м.г}} &= \cos\varphi \left(4 - e_\varphi^{\text{м.в}} - h_z^{\text{м.в}}\right), \\ h_\varphi^{\text{м.г}} &= \sin\varphi \left(e_\varphi^{\text{м.в}} - 2\right), \\ h_z^{\text{м.г}} &= -\cos\varphi h_r^{\text{м.в}}. \end{aligned} \quad (5)$$

In particular, (5) shows that the radial magnetic number of a vertical magnetic dipole is equal to the vertical magnetic number of a horizontal magnetic dipole if $\varphi = 0$. The real and imaginary parts, and also the amplitudes and phases, have been given for the h for $\xi$ up to 20 [3,4]; this range covers all the main practical cases for this type of equipment. The asymptotic expressions and tabulated values [3,4] show that the magnetic numbers are usually multivalued functions of $\xi$; for example $\mathrm{Im}(h_z^{\text{м.в}})$ has a maximum at $\xi = 1.076$ and a minimum at $\xi = 4.808$, while $\mathrm{Re}(h_z^{\text{м.в}})$ has several maxima, the first two turning points being at $\xi$ of 2.382 and 8.4413, and the first zero

at 7.21, the subsequent turning points being separated by intervals of about $\pi$. Again, the Re for $h_r$ and $h_z$ (for $\varphi \neq 90°$) have maxima at $\xi = 4.6$, while the Im have maxima at $\xi = 2.6$, minima at $\xi = 8.0$, and zeros at $\xi = 4.5$.

It is possible to determine $\xi$ from one or other of the magnetic numbers in most cases, provided that the real and imaginary parts are measured separately (with due regard for sign). Such measurements are very tedious to perform and interpret, and the method in this form is applicable only in special circumstances, e.g. over regions known from other evidence to be suitable for detailed examination. It will be shown that a simpler method of determining $\xi$ can be used in nearly all cases.

The relation of $\rho$ to $\xi$ for a homogeneous medium is

$$\rho = 7{,}89\left(\frac{r}{\xi}\right)^2 f, \qquad (6)$$

but real conditions are those of an inhomogeneous half-space, in which case it is better to use the effective value $\bar{\xi}$, which corresponds to a fictitious homogeneous half-space. Then (6) with $\bar{\xi}$ gives us $\bar{\rho}$. The method of determining $\bar{\rho}$ can be greatly simplified if the field work is performed with distances and frequencies such that the entire range in $\bar{\rho}$ corresponds to ranges of monotonic change in the magnetic numbers. The first

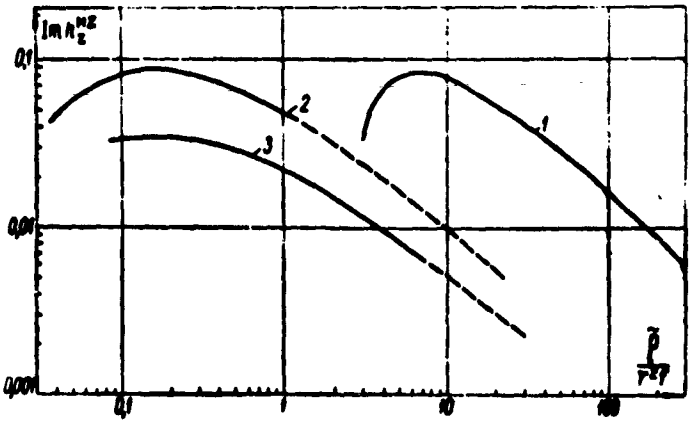


Fig. 1. Relationships for dipoles 1) on the surface; 2) at a height of 50 m; 3) at a height of 100 m.

such range is the best, for this corresponds to low $\xi$ and thus to fairly low frequencies. Figures 1-4 give curves for the first ranges in the magnetic numbers as functions of $\tilde{\rho}/r^2f$; these are convenient for the determination of $\tilde{\rho}$. The relationship is nearly rectilinear over much of the range. Electrical profiling is performed with fixed r and f; the graphs enable one to determine $\tilde{\rho}$ from the magnetic number.

The practical use of these relationships may be established by examining the ranges in $\tilde{\rho}$ they cover. The table below gives the ranges of $\tilde{\rho}$ that correspond to the frequencies used in the AFI and PEMK equipments (75, 125, 375, 1125, 3375, and 7500 c/s), the r being 0.05, 0.1, 0.2, and 0.4 km.

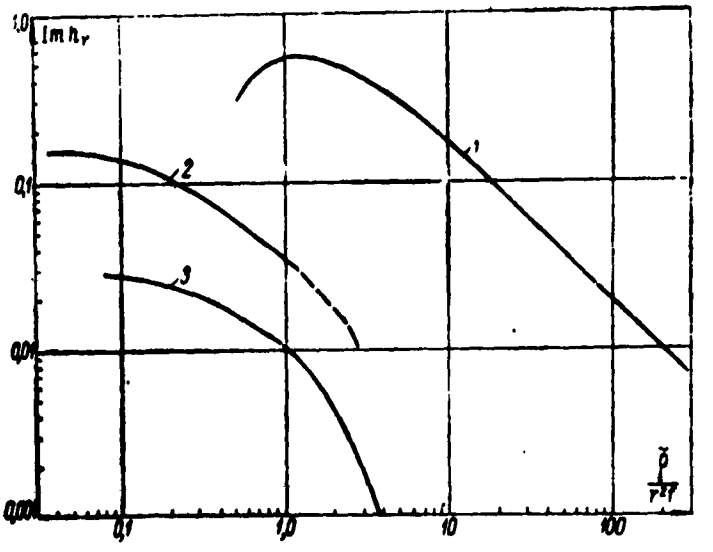


Fig. 2. Relation of $\mathrm{Im}(h_r)$ to $\tilde{\rho}/r^2f$; notation as in Fig. 1.

These ranges are such that the practical $\tilde{\rho}$ very seldom fall outside them. An increase in f displaces the range in $\tilde{\rho}$ towards higher values. The least variation in $\tilde{\rho}$ (about a factor of 100) for given f and r occurs for $\mathrm{Im}(h_2)$; the other components correspond roughly to factors of 1000. On the other hand, the real parts of $h_\theta$ and $h_r$ are large, which would make it very difficult to isolate the imaginary parts of these.

Ranges in $\tilde{\rho}$ for the First Range of Unambiguous Variation in the Magnetic Numbers

| Magnetic number | Distance, km | Range of $\tilde{\rho}$ (Ω-m) for frequency (c/s) of | | | | | |
|---|---|---|---|---|---|---|---|
| | | 75 | 125 | 375 | 1125 | 3375 | 7500 |
| $\mathrm{Im}\, h_z^{M.B}$ | 0,05 | 350—1,5 | 600—2,5 | 1 700—7,0 | 5 500—22,0 | 16 000—65,0 | 35 000—150 |
| | 0,1 | 1 400—6,0 | 2 400—10,0 | 7 400—30,0 | 21 000—90,0 | > 270 | |
| | 0,2 | 5 600—24,0 | 9 600—40,0 | 28 000—120 | > 350 | | |
| | 0,4 | 23 000—95,0 | 37 000—160 | > 460 | | | |
| $\mathrm{Im}\, h_r^{M.B}$ | 0,05 | 150—0,3 | 260—0,5 | 740—1,5 | 2 200—4,6 | 7 000—14,0 | 15 000—30 |
| | 0,1 | 580—1,1 | 960—2,0 | 3 000—5,0 | 9 000—15,0 | 27 000—55,0 | 60 000—120 |
| | 0,2 | 2 300—4,0 | 4 000—8,0 | 12 000—24,0 | 35 000—70 | > 220 | |
| | 0,4 | 9 500—20,0 | 15 000—40 | 50 000—100 | | >300 | |
| $\mathrm{Re}\, h_r^{M.B}$ | 0,05 | 60,0—0,07 | 100—0,12 | 300—0,35 | 900—1,0 | 2 700—3,5 | 6 000—7,5 |
| | 0,1 | 250—0,3 | 400—0,5 | 1 200—1,5 | 3 600—4,5 | 12 000—14 | 25 000—30 |
| | 0,2 | 960—1,2 | 1 600—2,0 | 5 000—6,0 | 16 000—20 | 44 000—60 | 100 000—120 |
| | 0,4 | 4 000—5,0 | 6 500—8,0 | 20 000—25 | 60 000—80 | > 250 | |
| $\mathrm{Im}\, h_\varphi^{M.r}$ | 0,05 | 36,0—0,2 | 55,0—0,43 | 170—1,0 | 500—4,0 | 1 700—12 | 3 700—20 |
| | 0,1 | 150—0,8 | 250—1,5 | 740—4,0 | 2 200—15 | 6 000—35 | 15 000—100 |
| | 0,2 | 550—4,0 | 900—7,0 | 2 700—20 | 8 000—70 | 2 400—180 | 54 000—400 |
| | 0,4 | 2 200—12 | 3 500—25 | 11 000—80 | 32 000—250 | >700 | |
| $\mathrm{Im}\, h_r^{M.r}$ | 0,05 | 36,0—0,1 | 60,0—0,15 | 180—0,5 | 550—1,5 | 1 700—5,0 | 3 500—10 |
| | 0,1 | 150—0,4 | 250—0,6 | 740—2,0 | 2 200—6,0 | 6 800—20 | 15 000—50 |
| | 0,2 | 600—1,5 | 1 000—2,5 | 3 000—8,0 | 9 000—25 | 27 000—70 | 60 000—150 |
| | 0,4 | 2 400—6,0 | 4 000—10 | 12 000—40 | 35 000—100 | > 300 | |

Figures 1-4 also show these functions of $\tilde{\rho}/r^2f$ for dipoles at heights of 50 and 100 m, positions that are used in aerial surveying by induction; these curves have been computed from relationships given by Waite [13,14]. The absolute values of the magnetic numbers decrease as the height increases, while the zone of maxima shifts to smaller $\tilde{\rho}/r^2f$. This means that the usable ranges are extended towards lower $\tilde{\rho}$ in aerial

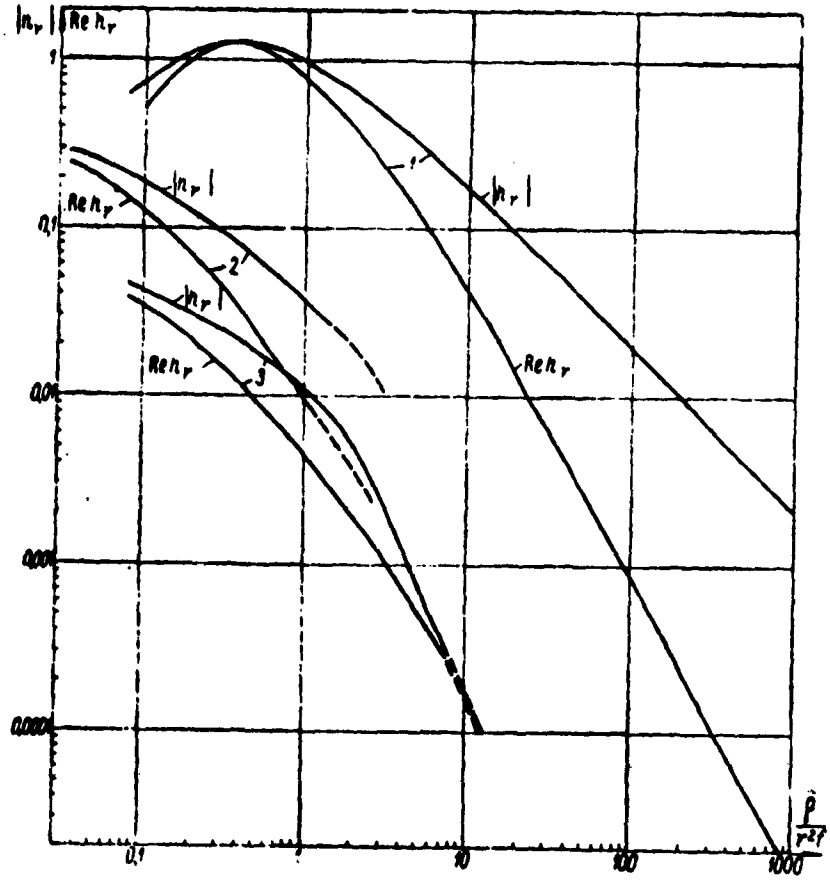


Fig. 3. Relation of $Re(h_r)$ and $|h_r|$ to $\tilde{\rho}/r^2f$; see Fig. 1 for symbols.

surveys. (The subject of aerial surveys generally requires a special study.)

Similar relations between the field components and $\tilde{e}$ may be derived for electromagnetic dipole profiling, in which two mutually perpendicular dipoles are used as sources in conjunction with two identical receiving dipoles (the rotating-field method). In the rotating magnetic field method [9], two identical but mutually perpendicular source coils are used in conjunction with two detecting coils set at right angles to their direction of displacement. The two source coils are fed with currents differing in phase by 90°, which produces a rotating magnetic field in any homogeneous insulating medium. The

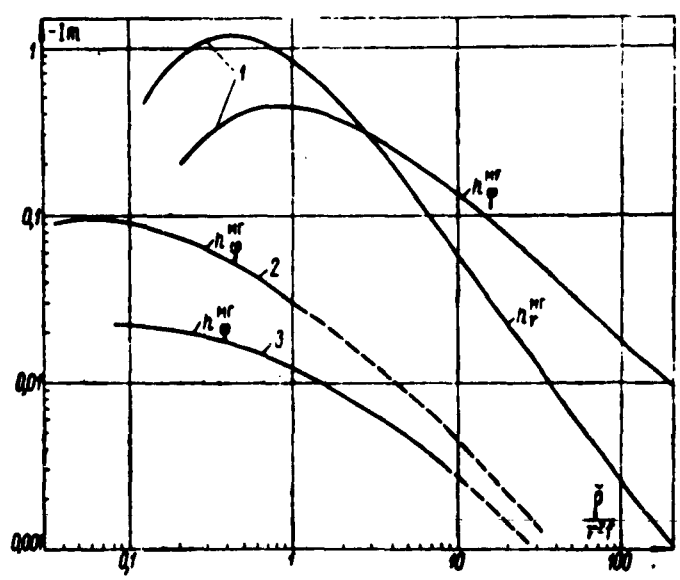


Fig. 4. Relation of $Im(h_r)$ and $Im(h_\varphi)$ to $\tilde{e}/r^2 f$; see Fig. 1 for symbols.

signals received by the detecting coils also differ in phase by 90°. The orientation is such that the field component sensed by the vertical magnetic dipole (a horizontal coil) is $Im(H_z)$, while the one sensed by the horizontal dipole (vertical coil) is $H_\varphi$. The signal in the vertical dipole is displaced in phase by 90°, so the sum of the two signals is

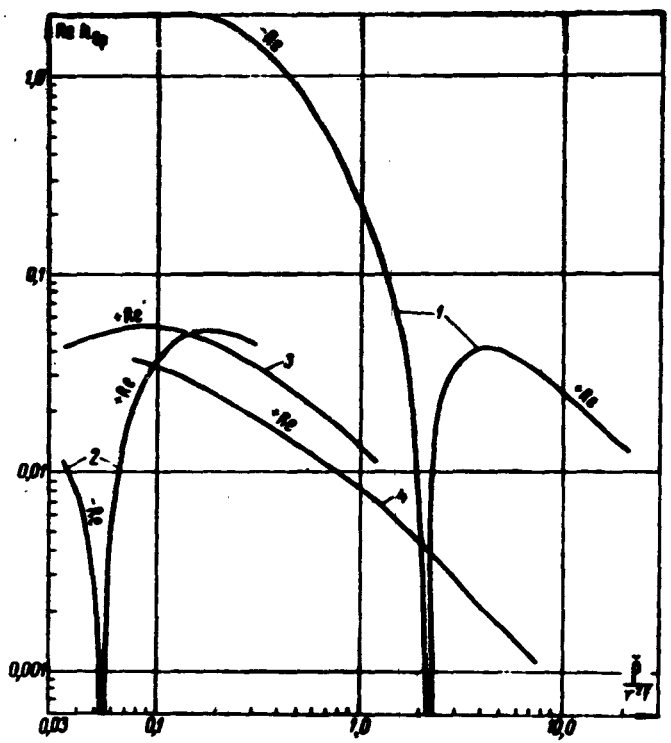


Fig. 5. The rotating-field method; relation of Re to $\tilde{\rho}/r^2 f$ : 1) dipoles at surface of ground; 2) dipoles at height of 25 m; 3) dipoles at height of 50 m; 4) dipoles at height of 100 m.

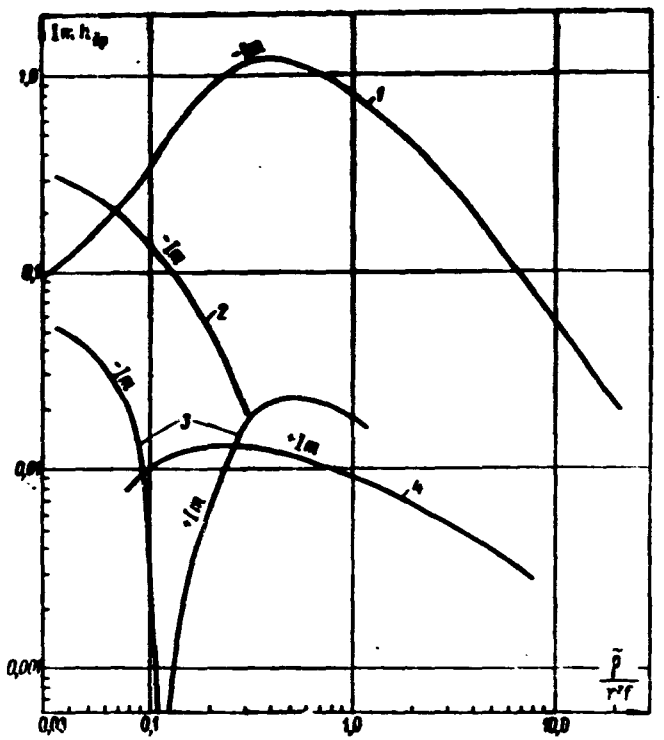


Fig. 6. The rotating-field method; relation of Im to $\tilde{\rho}/r^2 f$. Symbols as in Fig. 5.

$$H_{вр} = H_{\varphi}^{м.г} - H_{z}^{м.в}, \tag{7}$$

in which

$$H_{\varphi}^{м.г} = \frac{M}{r^3} h_{\varphi}^{м.г}; \quad H_{z}^{м.в} = -\frac{M}{r^3} h_{z}^{м.в},$$

and the magnetic number of the rotating field is

$$h_{вр} = h_{\varphi}^{м.г} + h_{z}^{м.в}. \tag{8}$$

These expressions show that the primary fields sensed by the dipoles mutually cancel no matter what r may be. The


Fig. 7. Relation of $|h_r|$ to $\tilde{\rho}/r^2 f$ for dipoles on the surface of the ground.

resultant signal will be zero for a homogeneous insulating space, but a conducting half-space upsets this. The real and imaginary parts of the unbalance signal are dependent on $\tilde{\rho}$, f, and r, as well as on the height (for aerial surveys).

Figures 5 and 6 show these as functions of $\tilde{\varrho}/r^2 f$ for heights of 25, 50, and 100 m on the basis of White's results [13,14] in conjunction with results for the surface [3,4]. Figure 5 shows that the real part has a maximum at $\tilde{\varrho}/r^2 f = 4.3$ for the surface, there being a rapid rise to this point from the zero at $\tilde{\varrho}/r^2 f = 2.25$. The real part is almost constant at about 2.0 for $\tilde{\varrho}/r^2 f = 0.15$ or so. The relationship is of the same form for all heights, but it shifts to smaller $\tilde{\varrho}/r^2 f$ as the height increases; e.g., the maximum lies at 0.17 when the height is 25 m, the zero being at 0.052. The corresponding values for 50 m are 0.09 for the maximum and a value outside the limits of the figure. Both points are outside the limits for a height of 100 m.

The imaginary part is negative at the surface of the ground and has its minimum at $\tilde{\varrho}/r^2 f = 0.42$ (Fig. 6); the minimum lies outside the figure for a height of 25 m. The positive branch appears on the right for a height of 50 m; this has a maximum at $\tilde{\varrho}/r^2 f = 0.55$, the zero being at 0.11 and the minimum outside the figure. Only the positive branch (maximum at 0.24) is seen for 100 m.

These curves show that the imaginary part is of the main interest for ground-level studies, because this shows a single-valued relation to distance for $\tilde{\varrho}/r^2 f > 0.42$; for aerial studies, the real part is more useful, for this gives a single-valued relation for $\tilde{\varrho}/r^2 f > 0.17$ (25 m), $> 0.1$ (50 m), or $> 0.07$ (100 m).

Induction results can also be represented in apparent-resistance form; all that is needed is a certain modification of the field observations, for the existing apparatus enables one to measure the amplitudes of the components as well as the orientation of the magnetic vector. These amplitudes do not vary rapidly over fairly highly differentiated sections, so the method would be of comparatively poor resolving power; this is a result of the distribution of the normal field. The source coil acts as a horizontal magnetic dipole in the induction method, and the field components are examined in the equatorial plane ($\varphi = 90°$). Now (5) shows that the corresponding $h_r$ and $h_z$ are zero no matter what $\tilde{\varrho}$ may be if there are no vertical or inclined inhomogensities; only $h_\varphi$ is finite, and this here coincides with $h_x$. The $\xi$ used in induction commonly range from 2.5 to 7.0, and the modulus of $h_\varphi$ varies little in this range, so the resolution in $\tilde{\varrho}$ is low. A much more useful case is that in which the dipole is oriented for measurements along its axis ($\varphi = 0°$), for here $h_\varphi$ is zero, whereas $h_r$ and $h_z$ are maximal, if the medium is homogeneous. Figure 3 shows the

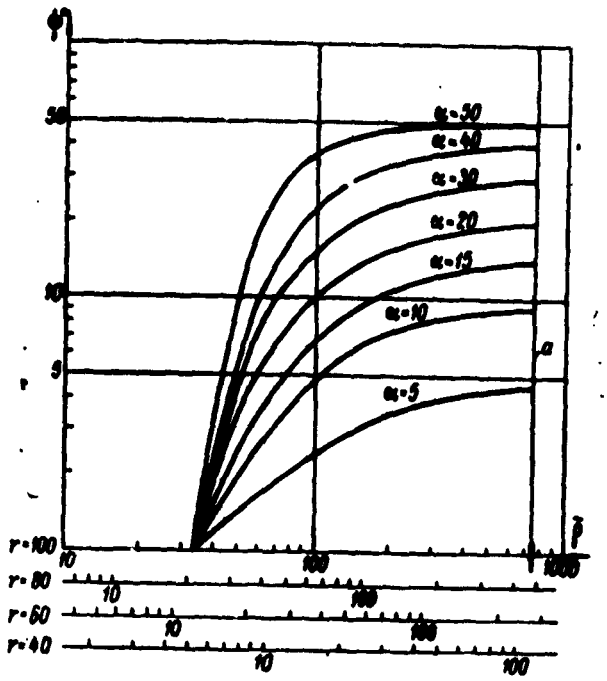


Fig. 8. Curves for determining $\tilde{\rho}_k$ by the inclined coil method.

absolute values of $h_r$ and $h_z$ as functions of $\tilde{\rho}/r^2 f$; here the real and imaginary parts increase together for $2 > \tilde{\rho}/r^2 f \geq 0.2$. The frequencies used in induction (18.75, 37.5, and 75 kc) give $h_r$ such that $\tilde{\rho}$ in excess of 100 ohm-m can be measured, but the determination is not unambiguous for lower $\tilde{\rho}$, for a maximum occurs in $h_r$.

Measurements of $|h_r|$ can be used to calculate $\tilde{\rho}$ directly, for this increases regularly from 1.966 for $\xi = 1.4$ to 4.076 for $\xi = 8.0$; Fig. 7 shows this for $h_r$ as a function of $\tilde{\rho}/r^2 f$. A range of 10-fold variation in $\tilde{\rho}$ is accessible, which for r of 0.1 km corresponds to 40-400 ohm-m at 18.75 kc, 75-750 ohm-m at 37.5 kc, and 150-1500 ohm-m at 75 kc. Further, $\tilde{\rho}$ can be found from angle measurements; I omit details and merely state that existing recommendations require operation at fixed f and variable r; the results are used to determine the r corresponding to $\xi = 1$. Now f is known, so $\tilde{\rho}$ can be found, but the operation is very tedious and is seldom used. In principle,

though, $\xi$ and $\tilde{\sigma}$ can be determined from the inclination for one r only; the use of several r only impairs the interpretation, for $\tilde{\sigma}$ is a function of r if the medium is inhomogeneous. The inclined-coil method is simplified if r is kept constant; the calculations can be simplified or eliminated if $\xi$ is replaced as abscissa by $\tilde{\sigma}/r^2f$, or even by $\tilde{\sigma}$ itself for the fixed r. Figure 8 shows the angle of inclination $\psi$ as a function of $\tilde{\sigma}$ for f = 18.75 kc; the point a corresponds to $\xi$ = 1. Then the $\tilde{\sigma}$ for 18.75 kc is read directly as the abscissa of the point on the curve for the given $\alpha$ whose ordinate is $\psi$. The $\tilde{\sigma}$ so read off must be doubled at 37.5 kc and quadrupled at 75 kc. Of course, $\alpha$, the inclination of the source coil, can be varied during the measurements.

In detailed surveys, in which $\tilde{\sigma}$ must be determined as a function of depth, it is best to use several frequencies. The above curves show that $\tilde{\sigma}$ is found the more precisely the larger the difference between $\alpha$ and $\psi$. The differences are large only for the lower values of $\tilde{\sigma}$, though the above frequencies give reasonable accuracy for r of 50-100 m for $\tilde{\sigma}$ up to 500 or 600 ohm-m.

Wide ranges in $\tilde{\sigma}$ can be covered by existing standard induction equipment only if the frequency range is extended downwards. The precise frequencies required should be derived from field trials.

* * *

The main conclusions to be drawn are as follows.

1. A function of apparent-resistance type should be used in a.c. methods; the value and dimensions of this are the same as those of the specific resistance for a homogeneous medium. This would facilitate the use of electrical methods in structure mapping and would provide a fuller picture of many geological sections. Special subscripts and superscripts are needed to indicate the type of equipment and field used.

2. The apparent resistance is calculable from the observations only if the reduced distance can be determined unambiguously; the conditions that ensure this are dependent on the fields used and on the nature of the section.

3. The value of $\tilde{\sigma}$ can be determined in principle for any distance from the field of a vertical or horizontal magnetic dipole; the methods of observation can be greatly simplified

for short distances. For example, only amplitudes may be needed for some components ($h_r$ and $h_z$, for instance). The maximum usable distance in that case is dependent on the field component employed. The usual distances between dipoles (50 to 200 m) and resistivities (1 to 100 ohm-m or so) require frequencies that should not exceed 7-8 kc. These frequencies can be increased by factors of 1.5 or 2 for aerial use.

4. Induction apparatus employing higher frequencies can also be used to measure $\tilde{\rho}$; rocks of resistance a few hundred ohm-m can be examined by the inclined-coil method, but the technique must be altered. High values of $\tilde{\rho}$ enable one to operate merely with $|h_r|$ or $|h_z|$, or sometimes only with $|h_r|$.

This discussion has been concerned only with theoretical possibilities for the use of apparent resistance. Special studies are needed to evolve detailed methods and techniques.

## Bibliography


1. Van'yan, L. L. Nekotoryye voprosy chastotnykh zondirovaniy gorizontal'nykh naplastovaniy [Some aspects of frequency sounding for horizontal strata]. Prikladnaya Geofizika [Applied Geophysics], No. 23, Gostoptekhizdat, 1959.

2. Idem. Elementy teorii stanovleniya elektromagnitnogo polya [Elements of the theory of build-up of an electromagnetic field]. Ibid., No. 25, 1960.

3. Gasanenko, L. B. Normal'noye pole vertikal'nogo garmonicheskogo nizkochastotnogo mognitnogo dipolya [Normal field of a vertical harmonic low-frequency magnetic dipole]. Uch. Zap. LGU [Archives of Leningrad University], No. 249, issue 10, 1958.

4. Gasanenko, L. B. and G. V. Molochnov. Elektromagnitnoye pole gorizontal'nogo magnitnogo dipolya nad gorizontal'nosloistoy strukturoy [Electromagnetic field of a horizontal dipole over a horizontally layered structure]. Ibid.

5. Mikhaylov, I. G. Elektromagnitnoye pole naklonnoy ramki [The electromagnetic field of an inclined coil]. Mater. TsNIGRI, Geofizika [Archives of the Central Geophysical Prospecting Research Institute, Geophysics], coll. 2, Moscow-Leningrad, 1936.

6. Molochnov, G. V. Chastotnoye elektromagnitnoye zondirovaniye na modeli [Frequency electromagnetic sounding on models]. Uch. Zap. LGU, No. 278, issue 11, 1959.

7. Tarkhov, A. G. Geofizicheskaya razvedka metodom induktsii [Geophysical prospecting by the induction method]. Moscow, Gosgeolizdat, 1954.

8. Tarkhov, A. G., E. M. Ershov, A. I. Katskov, S. R. Maron, and S. F. Fedorov. Instruktivnyye ukazaniya po provedeniyu geofizicheskikh rabot metodom induktsii [Instructions on geophysical work by the induction method]. Moscow, Gosgeolizdat, 1959.

9. Shaub, Yu. B. O primenenii metoda vrashchayushchego magnitnogo polya dlya elektrokartirovaniya [Use of the rotating magnetic field method for electrical mapping]. Izv. AN SSSR [News of the Academy of Sciences of the USSR], No. 10, 1960.

10. Sheynman, S. M. and L. V. Lebedkin. Apparatura dlya mnogochastotnoy elektrorazvedki peremennym tokom. Novoye v metodike i tekhnike geolograzvedochnykh rabot [Apparatus for multifrequency a.c. electrical prospecting. New developments in methods and techniques for geological prospecting work]. Trudy VITR [Transactions of the All-Union Prospecting Technique Institute], coll. 2, Gostoptekhizdat, 1959.

11. Lemberg, A. E. A new electromagnetic device for the surveying of subsurface conductors and its application in Canada. Can. Min. Met. Bull., No. 485, Sept. 1952.

12. Meltner, L. and P. Lasfarques. Le developement actuel de la géophysique et de la géochimie. Application à la recherche des gisements metallifères. Rev. Ind. Min., 40, No. 3, 1958.

13. Wait, I. R. Mutual electromagnetic coupling of loops over a homogeneous ground. Part I. Geophysics, 20, No. 3, 1955.

14. Wait, I. R. Mutual electromagnetic coupling of loops over a homogeneous ground. Part II. Geophysics, 21, No. 2, 1956.

# THE USE OF LOW-FREQUENCY ALTERNATING CURRENT IN ELECTRICAL PROFILING AND SOUNDING

Yu. I. Bulgakov and A. V. Veshev

pp. 187-192

Industrial interference causes serious difficulty in electrical prospecting; the interference is especially strong around ore bodies under exploitation and in mining areas in the Ural, Rudnyy Altai, and so on. It is then usually impossible to use d.c. methods. This interference has many different sources and shows a very complex time course, which we have studied in detail at the Belousovo and Grekhovo deposits in the Rudnyy Altai. The low-frequency interference was recorded with an EAK-3 electronic potentiometer [3]; noise of frequency 5-8 c/s and above was recorded with a small portable oscillograph type MPO-2 fitted with a wide-band amplifier, which provided coverage up to 500 c/s. The detecting line was 20 m long, the largest potentials being 30-40 mv. Figure 1 shows a typical curve, the time marks being of frequency 500 c/s

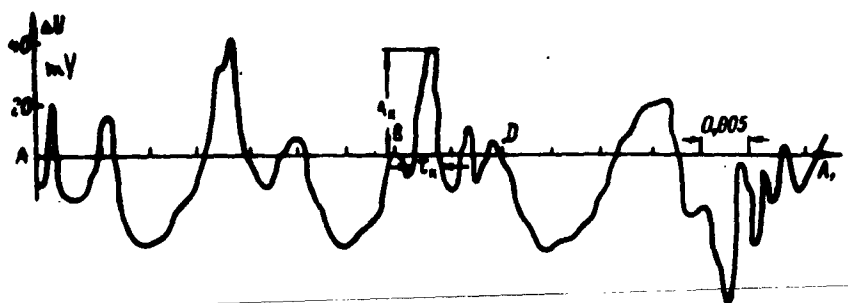


Fig. 1. Industrial interference recorded by the MPO-2. $A_1$ is the zero line, $A_k$ is the peak amplitude, and $\tau_k$ is the width of the peak.

(the abscissa is graduated at intervals of 0.005 sec). The frequency spectrum is very wide.

Figure 2 gives frequency analyses, which were made by a graphical method designed for seismograms [4]. Curve a is a general one, while the others represent the behavior for limiting frequencies of 56, 100, and 375 c/s. The intensity

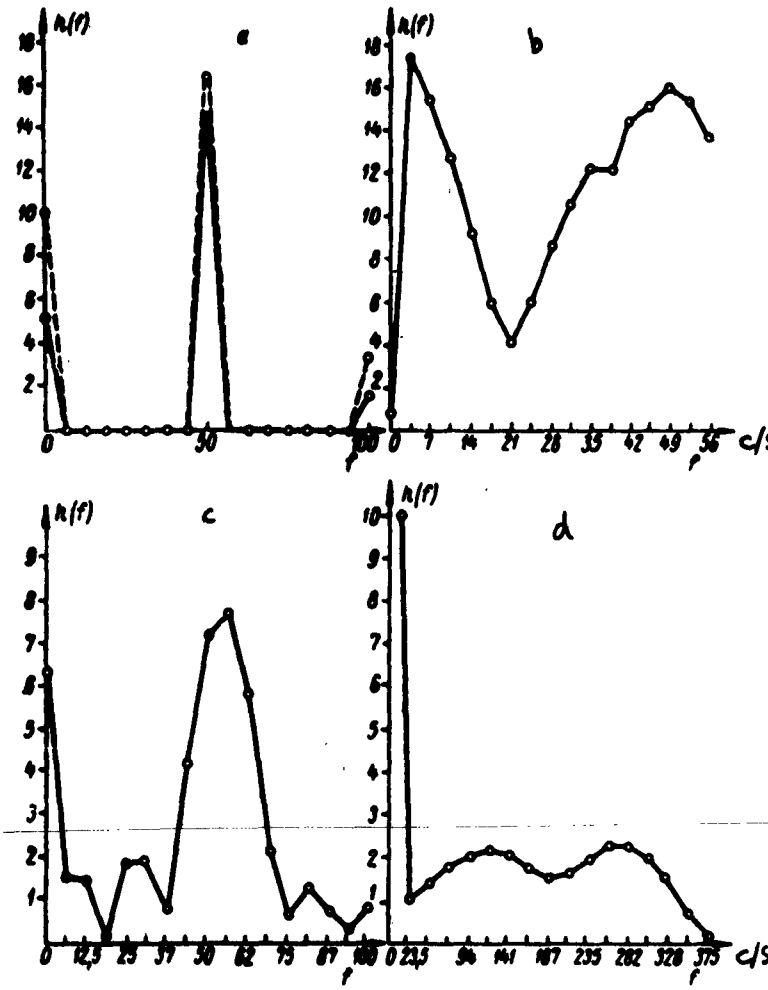


Fig. 2. Frequency analyses of interference; h(f) is the amplitude at frequency f, the unit being $0.01A_k$, in which $A_k$ is the maximum amplitude.

is lowest at 17.23 c/s, with other minima at 37 and 75 c/s. The intensity is highest at 0-5 c/s and at 50, 100, and 150 c/s. The 17-23 c/s region is clearly the best for electrical prospecting, for the frequency is reasonably low,

and one may expect that the results for the short lines usually adequate for ore-bodies will be virtually the same as those for d.c., so the methods for d.c. can be used in interpreting the results.

Theoretical relationships for a homogeneous half-space and for two- and three-layer media are applicable (if the upper layers are of very high resistance) in order to compare the fields and $\rho_k$ for d.c. and a.c. (dipole) methods. Stefanescu [6] has discussed the electromagnet field of a grounded horizontal electric dipole on the surface of a homogeneous half-space; his tables show that the amplitude of the radial component of the electric field is as for d.c. if $\xi \leq 1.0$; the same applies to the azimuthal component to 5% if $\xi \leq 0.7$. Here $\xi = \varkappa r$, in which r is the distance from the center of the dipole (km) and $\varkappa = 0.4\pi(5f/\rho)^{1/2}$, $\rho$ being the resistivity in ohm-m and f the frequency in c/s. The above limits for $\xi$ imply that a dipole 00' operating at 20 c/s over rocks of specific resistances 20 and 200 ohm-m has maximum working ranges of 350 and 1100 m respectively (radial), or 250 and 800 m (azimuthal).

Similar estimates can be made for a horizontally layered medium (also for 20 c/s); Van'yan's three-layer frequency sounding curves [2,3] can be used. An unfavorable section is one having $h_1 = 10$ m, $\rho_1 = 200$ ohm-m, $h_2 = 50$ m, $\rho_2 = 20$ ohm-m, $\rho_3 = \infty$, and $S_{1,2}^{B_1} = 51$. The wavelength for the first layer is $\lambda_1 = 3.162 \times 10^5(\rho/f)^{1/2} = 10^6$ cm = 10 km, and that for the second is $\lambda_2 = 3.162 \times 10^5(\rho/f)^{1/2} = 3.162 \times 10^6$ cm = 3.162 km, so $\lambda_1/h_1 = 1000$ and $\lambda_2/h_2 = 63.2$. The 00' for the determination of $h_1 + h_2$ may be as much as 1000 m [$00'/(h_1 + h_2) = 16.7$]. The above relations enable us to use S curves. The largest differences in the $\rho_k$ will occur for the maximal distances, so we perform our estimate for this case. The S-A curves give us that $\rho_{k,20}$ is $0.98\rho_k$ for the axial dipole system and is $1.05\rho_k$ for the equatorial setting. No curves are available for the case of $\rho_3$ finite, but we give below some examples from field work of 1957 at 20 c/s for $\rho_3$ large but finite.

We used an EP-1 electronic potentiometer and a direct-reading ESK-1 compensator in the d.c. measurements; a vacuum-tube millivoltmeter with a selective amplifier was used in the a.c. measurements. The millivoltmeter has already been described [1]. Results for a profile at Kamysha (AO = OB = 100 m, 00' = 100 m, AB = MN = 10 m, the last being the pitch) gave almost identical $\rho_k$ curves, the largest discrepancies being about 5% and the mean difference 2.6%, which is within the error of the

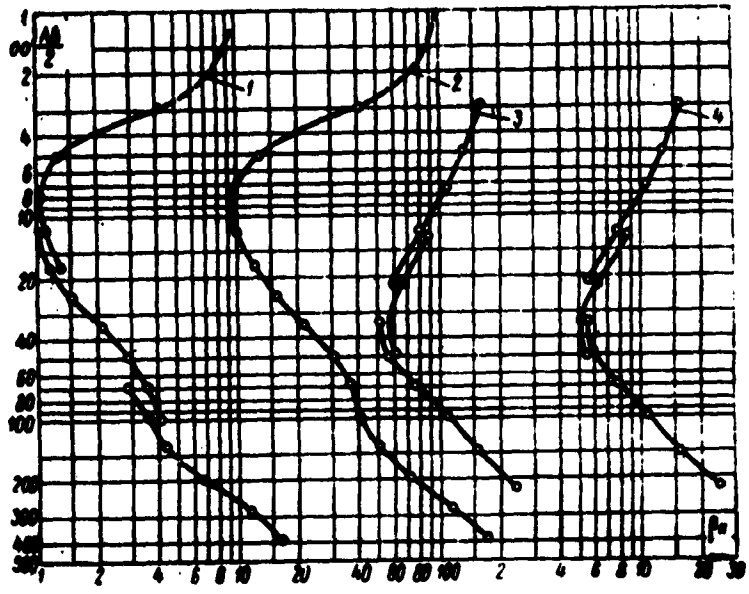

Fig. 3. Curves for $\rho_k$ for symmetrical and dipole methods performed with d.c. and a.c. in the Kamysha area in the Rudnyy Altai: 1) symmetrical electrical method, d.c. (profile 1, PK-29); 2) the same with a.c. (MN = 2 m); 3) $\rho_k$ by d.c. log in borehole 47; 4) the same by an a.c. method.

observations. Figure 3 shows $\rho_k$ curves from symmetrical and dipole methods of vertical electrical sounding; AB = 800 m (maximum) for the first and OO' = 450 m maximum for the second (axial). Here the curves differ by only 1.2%. In addition, curve 2 is for AB = 800 m with MN = 2 m; this short distance was possible on account of the high sensitivity of the vacuum-tube voltmeter (30 μv for full-scale deflection on the M-24 meter), so reliable readings could be made at 10-15 μv, which is one-twentieth of the minimum potential that can be measured with adequate precision in d.c. methods.

There were no parts to be matched up (on account of the

use of differing values of MN), so interpretation of the $\rho_k$ was facilitated. For example, there is a 22% reduction in the number of measurements for the curves of Fig. 3 (14 instead of 18) if only one MN is used.

These results show that the line lengths usual in ore-bearing regions (about 1 km) give $\rho_k$ at 20 c/s virtually the same as those from d.c. methods, so relationships established for d.c. can be used in the interpretations.

Measurements have also been made in other regions of strong interference; in every case good and reproducible results were obtained at 20 c/s.

The advantages of low-frequency a.c. are as follows:

1. The work is more rapid and detailed while retaining the same accuracy.

2. Measurements can be made in the presence of strong industrial interference.

3. The apparatus can be light and portable, for it demands less power in the measuring circuits, so the power sources are lighter.

It would be advantageous in many cases to transfer from d.c. methods to a.c. ones.

## Bibliography


1. Bulgakov, Yu. I. Apparatura dlya izmereniya peremennykh elektricheskikh poley nizkoy chastoty v elektrorazvedke [Apparatus for measuring alternating electric fields of low frequency in electrical prospecting]. Uch. Zap. LGU [Archives of Leningrad University], No. 249, issue 10, 1958.

2. Van'yan, L. L. K teorii dipol'nykh elektricheskikh zondirovaniy [Theory of dipole electric sounding]. Prikladnaya Geofizika [Applied Geophysics], No. 16. Moscow, Gostoptekhizdat, 1957.

3. Idem. Nekotoryye voprosy teorii chastotnykh zondirovaniy gorizontal'nykh naplastovaniy [Some aspects of the theory of frequency sounding for horizontal strata]. Ibid., No. 23, 1959.

4. Gol'tsman, F. M. Grafoanaliticheskiy metod chastotnogo analiza seysmicheskikh voln [Graphical method of frequency analysis for seismic waves]. Vestnik LGU [Herald of Leningrad University], No. 16, physics and chemistry series issue 3, 1956.

5. Karandeyev, K. B. and L. Ya. Mizyuk. Elektronnaya izmeritel'naya apparatura dlya geofizicheskoy razvedki metodami postoyannogo toka [Electronic measuring apparatus for geophysical prospecting by d.c. methods]. Moscow, Gosgeoltekhizdat [State Geological Technique Publishing House], 1958.

6. Stefanescu, S. Das electromagnetische Normalfeld des waagerechten Niederfrequenzdipols. Beitrage zur angewandten Geophysik, 9, No. 3-4, 1942; Gerlands Beitrage zur Geophysik, 61, No. 3, 1950

METHODS OF CALCULATING A POINT-SOURCE FIELD IN THE PRESENCE OF A VERTICAL BED

N. A. Sakharnikov and D. M. Volkov

pp. 193-202

It is necessary to solve for the potential distribution for the field of a point source in the presence of two interfaces (Fig. 1) in order to calculate apparent-resistance curves from electrical profiling above a stratum of low or high resistance.* The potential at any point in the field, $U(r,l)$, can [1] be represented as follows for media I, II, and III respectively:

$$\left.\begin{aligned} u_1(r,\ l) &= \frac{I\rho_1}{2\pi}\int_0^\infty J_0(rx)e^{-lx}\times \\ &\left[1+\frac{k_{12}e^{-2(d-l)x}+k_{22}e^{-2(d+h-l)x}}{1+k_{12}k_{22}e^{-2hx}}\right]dx, \\ u_2(r,\ l) &= \frac{I\rho_1}{2\pi}(1+k_{12})\int_0^\infty J_0(rx)e^{-lx}\frac{1+k_{22}e^{-2(d+h-l)x}}{1+k_{12}k_{22}e^{-2hx}}dx, \\ u_3(r,\ l) &= \frac{I\rho_1}{2\pi}(1+k_{12})(1+k_{22})\int_0^\infty J_0(rx)\frac{e^{-lx}}{1+k_{12}k_{22}e^{-2hx}}dx, \end{aligned}\right\} \quad (1)$$

in which

$$k_{12}=\frac{\rho_2-\rho_1}{\rho_2+\rho_1};\quad k_{22}=\frac{\rho_2-\rho_3}{\rho_2+\rho_3}, \quad (2)$$

*A. V. Veshev posed the problem of the best method of calculation.

Here I is the current from the source electrode; the resistivities $\rho_1$, $\rho_2$, and $\rho_3$ can vary widely, while $k_{12}$ and $k_{23}$ are always less than one. The potential gradient is found by differentiating the expressions in (1) with respect to r or l.

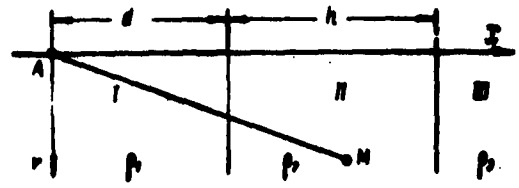


Fig. 1. Coordinate system for calculating the field of a point source in the presence of two interfaces. A, position of source electrode; M, position of detecting electrode; l , distance between electrodes; d, distance from A to nearer interface; r, distance from M to surface of ground; $\rho$, resistivity of corresponding medium.

For the surface, r = 0 and $J_0(rx) = 1$, so the formulas for U(r,l) and E(r,l) are simplified; the apparent resistances for potential and gradient systems respectively are

$$\rho = 2\pi l \frac{U}{I}; \quad \rho = 2\pi l^2 \frac{E}{I}. \tag{3}$$

It is usual to express the apparent resistance by formulas [1] containing infinite series, which for media I to III take the following form for potential systems

$$\begin{aligned} \rho_{k1} &= \rho_1 \left[1 + \frac{k_{12} \cdot l}{2d - l} + \frac{(1 - k_{12}^2) k_{23} \cdot l}{2d + 2h - l} \cdot S_1(a, b_1)\right], \\ \rho_{k2} &= \rho_1 (1 + k_{12}) \left[S_1(a, b_2) + \frac{k_{23} \cdot l}{2d + 2h - l} \cdot S_1(a, b_1)\right], \\ \rho_{k3} &= \rho_1 (1 + k_{12})(1 + k_{23}) \cdot S_1(a, b_3); \end{aligned} \tag{4}$$

and for gradient systems

$$\rho_{k1}=\rho_1\left[1-\frac{k_{12}\cdot l^2}{(2d-l)^2}-\frac{(1-k_{12}^2)k_{22}l^2}{(2d+2h-l)^2}\cdot S_2(a,\ b_1)\right],$$
$$\rho_{k2}=\rho_1(1+k_{12})\left[S_2(a,\ b_2)-\frac{k_{22}\cdot l^2}{(2d+2h-l)^2}\cdot S_2(a,\ b_1)\right],$$
$$\rho_{k3}=\rho_1(1+k_{12})(1+k_{22})\cdot S_2(a,\ b_2),$$

(4')

in which

$$S_l(a,\ b)=\sum_{n=0}^{\infty}\frac{(-a)^n}{(1+bn)^l}\quad(l=1,\quad l=2),$$

(5)

and

$$a=k_{12}\cdot k_{22},\quad b_1=\frac{2h}{2d+2h-l},\quad b_2=\frac{2h}{l}.$$

(6)

Series (5) converges for $|a|<1$, $b\geq 0$ and for $a=1$, $b>0$ for $i=1$ and $i=2$, as well as for $a=-1$, $b>0$ for $i=2$. The ranges of practical interest are as follows:

$$0{,}6<|k_{12}|<0{,}95,\quad 0{,}05\leqslant\frac{h}{l}\leqslant 5,$$
$$0{,}6<|k_{22}|<0{,}95,\quad 0\leqslant\frac{d}{l}\leqslant 10.$$

It is shown below that replacement of the infinite series in (4) by particular sums results in a large volume of computation if the thickness h is small and $k_{12}k_{23}$ is close to +1 or -1. Direct summation for $\rho_k$ involves the calculation of the sum in (5) from the formula

$$S_l(a,\ b)\approx\sum_{n=0}^{N-1}\frac{(-a)^n}{(1+bn)^l}.$$

(7)

Now we estimate the number N of terms in (5) that must be used in direct summation. Let $\Delta$ be the absolute error allowed in the approximate value of $S_l(a,b)$; then a theorem on sign-varying series [2] gives us that the N for $a>0$ must satisfy

$$\frac{a^N}{(1+bN)^l}<\Delta,$$

which, for b small, is equivalent to

$$N > \frac{\log \Delta}{\log a}. \tag{8}$$

If $a < 0$, the terms in (5) are positive, so the remainder after the N terms is

$$R < \frac{|a|^N}{(1+bN)^t(1-|a|)}.$$

To make $R < \Delta$ we must make N such that

$$\frac{|a|^N}{(1+bN)^t} < \Delta \cdot (1-|a|),$$

which for b small is equivalent to

$$N > \frac{\log \Delta}{\log |a|} + \frac{\log (1-|a|)}{\log |a|}. \tag{9}$$

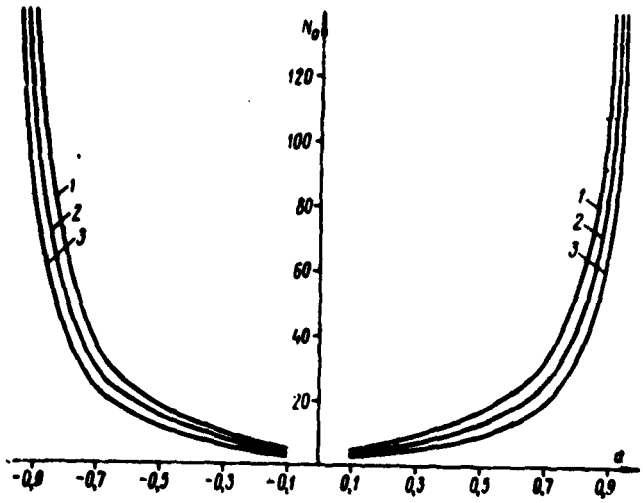


Fig. 2. Graphs of $N_o = f(a)$ for various $\Delta$, for use with (7); $a = k_{12}k_{23}$, $N_o$ is the least N that will satisfy (8) or (9), $\Delta$ is the absolute error allowed in $S_i(a,b)$; values of $\Delta$: 1) 0.00001; 2) 0.0001; 3) 0.001.

Figure 2 shows the relation of a to $N_o$, the least N that satisfies (8) or (9), for various $\delta$. These graphs enable one to determine N for the sum of (5) from (7) of $0 < b < 0.1$; the curves for N as a function of a run somewhat below those of Fig. 2 if $b > 0.1$, but the difference is unimportant, for N varies little for $|a|$ small and decreases as $|a|$ becomes large, but not so much so that (7) becomes useful.

It is practicable to use (7) for $|a|$ small, i.e., for $-0.6 < k_{12}k_{23} < 0.6$; then $N < 20$.

Some ways of simplifying the calculations are illustrated below. Consider, for example, the integral

$$L_i(a, b) = \int_0^\infty \frac{x^{i-1}e^{-x}}{1 + ae^{-bx}}\,dx \quad (i = 1, \cdot\ i = 2), \tag{10}$$

which converges for $|a| < 1$, $b > 0$; $L_i(a,b)$ is such that

$$\int_0^\infty \frac{x^{i-1}\cdot e^{-lx}}{1 + ae^{-bx}}\,dx = \frac{1}{l^i} L_i\left(a, \frac{b}{l}\right), \tag{11}$$

if $l > 0$, as can be seen if we replace x by $x/l$.

We can represent $\rho_k$ in the following integral form, as (1)-(3) imply for $r = 0$, if we use (11) in conjunction with the definition of $L_i(a,b)$. For potential systems

$$\begin{aligned}
\rho_{h1} &= \rho_1\left[1 + \frac{k_{12}l}{2d - l} + \frac{(1 - k_{12}^2)k_{12}\cdot l}{2d + 2h - l}\cdot L_1(a, b_1)\right],\\
\rho_{h2} &= \rho_1(1 + k_{12})\left[L_1(a, b_2) + \frac{k_{23}l}{2d + 2h - l}\cdot L_1(a, b_1)\right],\\
\rho_{h3} &= \rho_1(1 + k_{12})(1 + k_{23})\cdot L_1(a, b_2).
\end{aligned} \tag{12}$$

and for gradient ones

$$\rho_{k1}=\rho_1\left[1-\frac{k_{12}\cdot l^2}{(2d-l)^2}-\frac{(1-k_{12}^2)\,k_{23}l^2}{(2d+2h-l)^2}\cdot L_2(a,\,b_1)\right],$$
$$\rho_{k2}=\rho_1(1+k_{12})\left[L_2(a,\,b_2)-\frac{k_{23}\cdot l^2}{(2d+2h-l)^2}\cdot L_2(a,\,b_1)\right],$$
$$\rho_{k3}=\rho_1(1+k_{12})(1+k_{23})\,L_2(a,\,b_2). \qquad (12')$$

For example, from the first formula in (12),

$$\rho_{k1}=2\pi l\frac{u_1}{I}=\rho_1\cdot l\cdot\int_0^\infty J_0(rx)\,e^{-lx}\left[1+k_{12}e^{-2(d-l)x}+\frac{(1-k_{12}^2)\,k_{23}e^{-2(d+h-l)x}}{1+k_{12}\cdot k_{23}e^{-2hx}}\right]dx.$$

For r = 0

$$\rho_{k1}=\rho_1 l\left[\frac{1}{l}+\frac{k_{12}}{2d-l}+\frac{(1-k_{12}^2)\,k_{23}}{2d+2h-l}\cdot L_1(a,\,b_1)\right].$$

Formulas (4) can be derived from (12) by replacing $L_1(a,b)$ by $S_1(a,b)$; standard transforms [1] enable us to show that these functions are identically equal, for which purpose we replace the integrand in (10) by a convergent series

$$L_1(a,\,b)=\int_0^\infty\left[\sum_{n=0}^\infty(-a)^n\cdot e^{-(l+bn)x}\right]dx.$$

The sequence of integration and summation can be reversed in this case [2], so

$$L_1(a,\,b)=\sum_{n=0}^\infty(-a)^n\cdot\int_0^\infty e^{-(l+bn)x}\,dx=S_1(a,\,b).$$

In the same way we can show that

$$\int_0^\infty\frac{e^{-lx}}{1+ae^{-bx}}\,d\lambda=\sum_{n=0}^\infty\frac{(-a)^n}{l+bn},$$

for all $l > 0$; differentiating k times with respect to $l$ (which is permissible [2]), we have

$$\int_0^\infty \frac{x^k e^{-lx}}{1 + ae^{-bx}}\,dx = k! \sum_{n=0}^{\infty} \frac{(-a)^n}{(l+bn)^{k+1}},$$

which applies for all $l > 0$, $b > 0$, and $|a| < 1$. In particular, if $k = 1$ and $l = 1$, we have from (5) and (10) that

$$L_2(a, b) = S_2(a, b).$$

The integral of (10) can be represented exactly as a finite sum of elementary functions for all a and for rational b if $l = 1$, as may be shown by replacing the variable of integration in (10) by means of the substitution $\exp(-x) = y$:

$$L_1(a, b) = \int_0^1 \frac{dy}{1 + ay^b}, \tag{13}$$

The corresponding indefinite integral can [2] be represented in finite form for any rational b (the substitution is $t^q = y$, in which $b = p/q$), so $L_1(a,b)$ is an elementary function of a for each rational b. In particular

$$L_1(a, 1) = \frac{1}{a}\ln(1+a),$$

$$L_1(a, 2) = \frac{1}{\sqrt{a}}\operatorname{arctg}\sqrt{a}, \quad \text{if} \quad a > 0$$

$$L_1(a, 2) = -\frac{1}{2\sqrt{|a|}}\ln\frac{1-\sqrt{|a|}}{1+\sqrt{|a|}}, \quad \text{if} \quad a < 0.$$

Let $b = 1/n$, in which n is a positive integer; $n > 1$. Then for all a we have exactly that

$$L_1\left(a, \frac{1}{n}\right) = \frac{-n}{(-a)^n}\left[\ln(1+a) + \sum_{k=1}^{n-1}\frac{(-a)^k}{k}\right]. \tag{14}$$

The following transforms of the sum of (5) serve to demonstrate (14):

$$L_1\left(a, \frac{1}{n}\right) = S_1\left(a, \frac{1}{n}\right) = \frac{n}{(-a)^n} \sum_{k=0}^{\infty} \frac{(-a)^{n+k}}{n+k}$$
$$= \frac{n}{(-a)^n}\left[\sum_{k=1}^{\infty} \frac{(-a)^k}{k} - \sum_{k=1}^{n-1} \frac{(-a)^k}{k}\right].$$

From this (14) follows directly if we use the expansion of the logarithm function as a power series.

(14) is suitable for any a and b > 0.05, and also for smaller values of b if |a| is sufficiently small. The series on the right in (14) converges more rapidly than the series in (5), so it is simpler to use (14) for $\rho_k$ than it is to use (7).

The integral in (10), or the equal sum of (5), for a gradient system can be operated on with the transforms

$$S_2\left(a, \frac{1}{n}\right) = \sum_{k=0}^{\infty} \frac{c^k}{\left(1+\frac{k}{n}\right)^2} = \frac{n^2}{c^n} \sum_{k=0}^{\infty} \frac{c^{n+k}}{(n+k)^2}$$

for i = 2, b = 1/n < 1, and a < 0 to give

$$L_2\left(a, \frac{1}{n}\right) = \frac{n^2}{c^n}\left[f(c) - \sum_{k=1}^{n-1} \frac{c^k}{k^2}\right], \tag{15}$$

in which c = -a and

$$f(c) = \sum_{k=1}^{\infty} \frac{c^k}{k^2}. \tag{16}$$

Series (16) converges for all $|c| \leq 1$; f(c) satisfies the functional equation [2]

$$f(c) + f(1-c) + \ln c \cdot \ln(1-c) = \frac{\pi^2}{6} \quad \text{if} \quad 0 < c < 1,$$

which enables one to calculate f(c) for c close to 1 as simply as for c close to zero, for

$$f(c) = \frac{\pi^2}{6} - \ln c \cdot \ln(1-c) - f(1-c).$$

Direct summation of (16) can be used for c close to zero; (16) converges more rapidly than (5), so $\rho_k$ can be calculated from (15) and (16) for a gradient system more simply than from (7). Formula (15) applies also for $c = -a < 0$, i.e., if $k_{12}k_{23} > 0$. For $b = 1$ and any a it can be shown that

$$L_2(a, 1) = -\frac{f(-a)}{a}.$$

Formula (15) can be used for any a and b; the worst value of a as regards the computation is -0.9; but then $a^{25}/25^2 = 0.00016$, so the second term in (15) will contain not more than 25 components no matter what b may be.

The integral of (10) can be calculated approximately to any specified accuracy for all a and b by means of quadrature formulas [3]:

$$L_1(a, b) = \int_0^\infty e^{-x} \cdot \varphi(x)\, dx \doteq \sum_{k=1}^{n} A_k \cdot \varphi(x_k), \tag{18}$$

$$L_2(a, b) = \int_0^\infty x \cdot e^{-x} \cdot \varphi(x)\, dx \doteq \sum_{k=1}^{n} A_k^* \cdot \varphi(x_k^*), \tag{19}$$

in which

$$\varphi(x) = \frac{1}{1 + ae^{-bx}}. \tag{20}$$

The n of (18) and (19) is chosen to suit the accuracy needed in $\rho_k$; $n \geq 5$ is usually sufficient. A table [3] gives the $x_k$ and $A_k$ of (18) for various n; the $x_k$ and $x_k^*$ in (18) and (19) are the roots of polynomials of degree n:

$$L_n^{(\alpha)}(x) = (-1)^n \cdot x^{-\alpha} \cdot e^x \frac{d^n}{dx^n}\left(x^{\alpha+n} e^{-x}\right)$$

for $\alpha = 0$ and $\alpha = 1$ respectively. The $A_k$ and $A_k^*$ are given by

$$A_k = \frac{n!\,\Gamma(\alpha + n + 1)}{x_k \cdot \left[L_n^{(\alpha)'}(x_k)\right]^2},$$

also for $\alpha = 0$ and $\alpha = 1$. Table 1 gives $x_k^*$ and $A_k^*$.

Table 1

Values of $x_k^*$ and $A_k^*$ for Use with Formula (19)

| $n$ | $x^*$ | $A^*$ |
|---|---|---|
| 1 | $x_1 = 2{,}000\,000$ | $A_1 = 1{,}000\,000$ |
| 2 | $x_1 = 1{,}267\,949$<br>$x_2 = 4{,}732\,051$ | $A_1 = 0{,}788\,676$<br>$A_2 = 0{,}211\,324$ |
| 3 | $x_1 = 0{,}935\,822$<br>$x_2 = 3{,}806\,407$<br>$x_3 = 7{,}758\,771$ | $A_1 = 0{,}588\,681$<br>$A_2 = 0{,}391\,216$<br>$A_3 = 0{,}(1)\,201\,024$ |
| 4 | $x_1 = 0{,}743\,291$<br>$x_2 = 2{,}571\,635$<br>$x_3 = 5{,}731\,179$<br>$x_4 = 10{,}953\,894$ | $A_1 = 0{,}446\,869$<br>$A_2 = 0{,}477\,635$<br>$A_3 = 0{,}(1)\,741\,777$<br>$A_4 = 0{,}(2)\,131\,585$ |
| 5 | $x_1 = 0{,}617\,031$<br>$x_2 = 2{,}112\,966$<br>$x_3 = 4{,}610\,533$<br>$x_4 = 8{,}399\,071$<br>$x_5 = 14{,}260\,099$ | $A_1 = 0{,}348\,014$<br>$A_2 = 0{,}502\,280$<br>$A_3 = 0{,}140\,915$<br>$A_4 = 0{,}(2)\,871\,963$<br>$A_5 = 0{,}(4)\,689\,738$ |

Note. The numbers in parentheses indicate the number of noughts between the decimal point and the first significant figure.

The integrals of (10) can be calculated for a close to -1 by means of slightly altered formulas; we put $\varepsilon = 1 + a$ to get

$$\varepsilon \cdot L_1(a, b) = \int_0^\infty e^{-x} \cdot \varphi_0(x)\, dx, \tag{18'}$$

$$\varepsilon \cdot L_2(a, b) = \int_0^\infty x e^{-x} \cdot \varphi_0(x)\, dx. \tag{19'}$$

Formula (18) can be used to find the integral of (18'), and similarly, (19) can be used for (19'); here $\varphi(x)$ is replaced by $\varphi_0(x)$, which is

$$\varphi_0(x) = \frac{\varepsilon}{1 + (\varepsilon - 1)e^{-bx}}$$

and which decreases monotonically from 1 to $\varepsilon$ as x goes from 0 to $\infty$. The values of $\varphi_0(x)$ should be calculated to a high order of accuracy, for the integrals in (18') and (19') are divided by the small quantity $\varepsilon$. For example, $\varphi_0(x)$ must be calculated to a further significant figure for $\varepsilon = 0.1$ (relative to $\varepsilon = 0.9$, that is).

Formulas (18) and (19) do not become more difficult to apply to (10) when h becomes small, although (5) converges less rapidly (for a fixed a) and although the N required in (7) increases. In fact, even when $k_{12}k_{23} = -0.9$ (the worst case), the integral of (10) converges so rapidly that its value differs by less that 0.01% from the definite integral having limits of 0 and 15.

Quadrature formulas can also be used for $r \neq 0$; we merely have to replace x by $x/l$ in (1), which gives

$$U_1(r, l) = \frac{q}{l} \cdot \int_0^\infty e^{-x} \cdot \varphi_1(x)\, dx,$$

$$U_2(r, l) = \frac{q}{l}(1 + k_{12}) \int_0^\infty e^{-x} \cdot \varphi_2(x)\, dx,$$

$$U_3(r, l) = \frac{q}{l}(1 + k_{12})(1 + k_{23}) \int_0^\infty e^{-x} \cdot \varphi_3(x)\, dx, \qquad (20)$$

in which

$$\varphi_1(x) = J_0\left(\frac{rx}{l}\right)\left[1 + \frac{k_{12}e^{-2(d-l)\frac{x}{l}} + k_{23}e^{-2(d+h-l)\frac{x}{l}}}{1 + k_{12}k_{23}e^{-2h\frac{x}{l}}}\right],$$

$$\varphi_2(x) = J_0\left(\frac{rx}{l}\right)\left[1 + k_{23}e^{-2(d+h-l)\frac{x}{l}}\right] : \left(1 + k_{12}k_{23}e^{-2h\frac{x}{l}}\right),$$

$$\varphi_3(x) = I_0\left(\frac{rx}{l}\right) : \left(1 + k_{12}k_{23}e^{-2h\frac{x}{l}}\right), \quad q = \frac{I\varphi_1}{2\pi}.$$

Each $\varphi_i(x)$ (i = 1, 2, 3) decreases monotonically in absolute value, so the integrals of (20) converge rapidly, for exp(-x) is present as well. It is usually sufficient to put n = 5 in (18) in order to calculate the potential.

## Bibliography


1. Zaborovskiy, A. I. Elektrorazvedka (Electrical prospecting). Gostoptekhizdat, 1943.
2. Fikhtengol'ts, G. M. Kurs differentsial'nogo i integral'nogo ischisleniya (Textbook of differential and integral calculus). OGIZ, 1948.
3. Krylov, V. I. Priblizhennoye vychisleniye integralov (Approximate calculation of integrals). Fizmatgiz, 1949.

## INFLUENCE OF THE EARTH-AIR BOUNDARY ON THE ELECTRICAL FIELD OF A POLARIZED SPHERE

pp. 222-225

G. A. Tarasov

Bursian [1] and Petrovskiy [2, 3] have considered the effects of the air-ground boundary on the electric fields of polarized bodies, but they have not made estimates of the magnitude of the effect. The present discussion relates to the field of a vertically polarized and ideally conducting sphere of radius a at a depth $z_0$ from the surface (Fig. 1). The polarization is such that the external field in in an isotropic and unbounded medium may be replaced by the field of two charges $q_0$ equal in magnitude but opposite in sign symmetrically placed with respect to the center of the sphere a distance $2l$ apart, this distance being much less than a, which means that the polarization of the sphere is as nearly uniform as possible. The axis of polarization is directed vertically downwards. The field and the polarization are affected by the presence of the boundary; the potenetial in the space external to the sphere can be represented as the sum of two components. The first, $U_0$, includes the potentials from the two real and two image charges; the value of $U_0$ at the interface is twice that for an unbounded medium. The second includes the potentials $\Delta U_n$ from a system of fictitious charges resulting from successive reflection of the intial ones in the sphere. The potential is put as

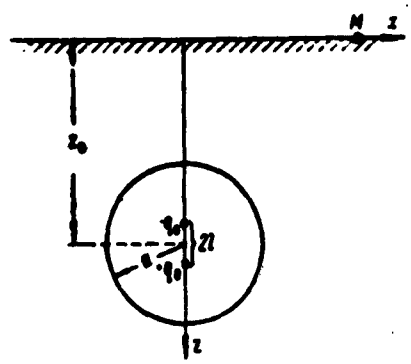


Fig. 1. Scheme for the electric field of a polarized sphere.

$$U_R = U_0 + \sum_{n=1}^{n=\infty} (-1)^n \Delta U_n, \qquad (1)$$

$$U_0 = -2q_0\left\{\frac{1}{[x^2+(z_0-l)^2]^{1/2}} - \frac{1}{[x^2+(z_0+l)^2]^{1/2}}\right\} \quad (2)$$

or, after transformation, as

$$U_0 = -\frac{4q_0\zeta\lambda}{a(\xi^2+\zeta^2)^{3/2}}, \quad (3)$$

in which $\xi = x/a$, $\zeta = z_0/a$, and $\lambda = l/a$. The quantity in $\lambda^2/(\xi^2+\zeta^2)$ is small, so it is neglected. The fields of the real and reflected spheres are accounted for by means of successive reflections of the charges in the spherical surfaces; the correction to $U_0$ from the first reflection may [1] be put as

$$\Delta U_1 = \frac{2q_0a}{2z_0-l}\cdot\frac{1}{\left\{x^2+\left[z_0-\frac{a^2}{2z_0-l}\right]^2\right\}^{1/2}} - \frac{2q_0a}{2z_0+l} \times \frac{1}{\left\{x^2+\left[z_0-\frac{a^2}{2z_0+l}\right]^2\right\}^{1/2}} + \left[-\frac{2q_0a}{2z_0-l}+\frac{2q_0a}{2z_0+l}\right]\cdot\frac{1}{(x^2+z_0^2)^{1/2}} \quad (4)$$

or, after simple but tedious transforms, in which the second-order terms are discarded, as

$$\Delta U_1 = \frac{q_0\lambda}{a\zeta^2(\xi^2+\zeta^2)^{1/2}}\cdot\frac{1}{(\xi^2+\zeta^2-1)}. \quad (5)$$

Then the potential of the sphere as corrected for the first reflection is

$$U_1 = -\frac{4q_0\zeta\lambda}{a(\xi^2+\zeta^2)^{3/2}}\cdot\left[1-\frac{1}{4\zeta^2\left(1-\frac{1}{\xi^2+\zeta^2}\right)}\right]. \quad (6)$$

Then

$$\left|\frac{\Delta U_1}{U_0}\right| = \frac{1}{4\zeta^2\left(1-\frac{1}{\xi^2+\zeta^2}\right)}. \quad (7)$$

Now (7) implies that the quantity on the left is maximal when $\xi = 0$:

$$\left|\frac{\Delta U_1}{U_0}\right|_{\xi=0} = \frac{1}{4\zeta^2\left(1-\frac{1}{\zeta^2}\right)} = \frac{1}{4\zeta(\zeta^2-1)} \quad (8)$$

and minimal when $\xi \to \infty$:

$$\left|\frac{\Delta U_1}{U_0}\right|_{\xi\to\infty} = \frac{1}{4\zeta^2}. \quad (9)$$

That is, the maximum $\Delta U_1/U_0$ occurs at the epicenter, so the fields of the real and reflected spheres are of the greatest interest as regards this point.

Graphical solution of (8) shows that the correction to $U_0$

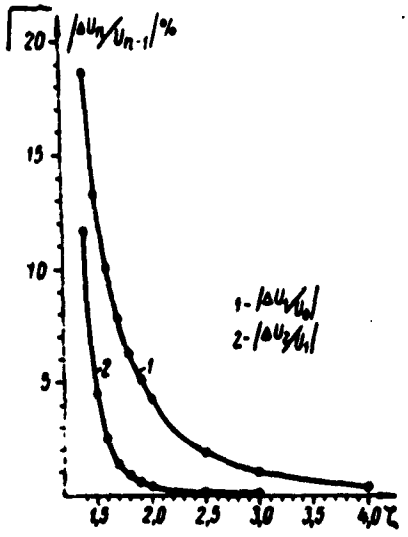


Fig. 2. Correction curves (%) for the extreme value of the potential of a polarized sphere on account of an interface.

for the first reflection is less than 5% if $\zeta \geq 1.9$ and is less than 1% if $\zeta \geq 3$ (Fig. 2).

By analogy with $U_1$, the correction arising from the second reflection, $\Delta U_2$, is given for the turning point as

$$\Delta U_2 = -\frac{2\lambda q_0}{4\zeta^4 a (2\zeta^2 - 1)(2\zeta^2 - 3)}. \quad (10)$$

Then the potential of the sphere as corrected for the second reflection at the turning point is

$$U_2 = -\frac{4q_0\lambda}{a\zeta^3}\left[1 - \frac{1}{4\zeta(\zeta^2 - 1)} + \frac{1}{2\zeta^2(2\zeta^2 - 1)(2\zeta^2 - 3)}\right]. \quad (11)$$

This means that

$$\left|\frac{\Delta U_2}{U_1}\right| = \frac{2(\zeta^2 - 1)}{\zeta(2\zeta^2 - 1)(2\zeta^2 - 3)\left[4\zeta(\zeta^2 - 1) - 1\right]}. \quad (12)$$

Graphical solution of (11) shows that the correction to $U_1$ from the second reflection is less than 5% if $\zeta \geq 1.5$ and is less than 1% if $\zeta \geq 1.8$ (see Fig. 2). Any further calculation is of no value, in view of the smallness of the quantities.

Then we have that the electric field is given within 5% by the zeroth approximation (simple doubling) if the depth of the center of the sphere is more than twice the radius; these values are usable in calculations to 1% if the depth is more than 3 times the radius. A correction should be applied for the first reflection if the depth is less; this correction is adequate for calculations in which up to 5% error is allowed if the depth is more than 1.5 times the radius, or 1.8 times the radius if only 1% error is permissible. Correction should be made for the second reflection for smaller depths.

## Bibliography


1. Bursian, V. R. Teoriya elektromagnitnykh poley, primenyayemykh v elektrorazvedke [Theory of the Electromagnetic Fields Used in Electrical Prospecting], ch. 1, Gostekhizdat, 1933.
2. Petrovskiy, A. A. Yestestvennoye elektricheskoye pole, sozdavayemoye rudnym telom [The natural electrical field produced by an orebody]. Izv. In-ta Prikladnoy Geofiziki [News of the Institute of Applied Geophysics], issue 1, Izd. IPG, 1925.
3. Petrovskiy, A. A. and L. Ya. Nesterov. Elektrorazvedka postoyannnym tokom [D.c. Electrical Prospecting]. Gos. Tekh. Geol. Razved. Izd-vo [State Geol. Prosp. Tech. Publ.], 1932.

LOW-FREQUENCY NCHMU EQUIPMENT FOR PROSPECTING

pp. 241-244 D. R. Barkhatov

The following is a brief description of apparatus designed at the All-Union Institute of Prospecting Geophysics for electrical prospecting at low frequencies; at present it is used mainly for mean-gradient measurements, where it gives very good reproducibility and highly detailed results. It can also be used in profiling and sounding with dipole systems with short distances, and also in some other instances. The apparatus measures potential differences, which can be reduced to apparent specific resistances if necessary. Thecomplete set of equipment consists of a generator combined with a converter and a vacuum-tube millivoltmeter.

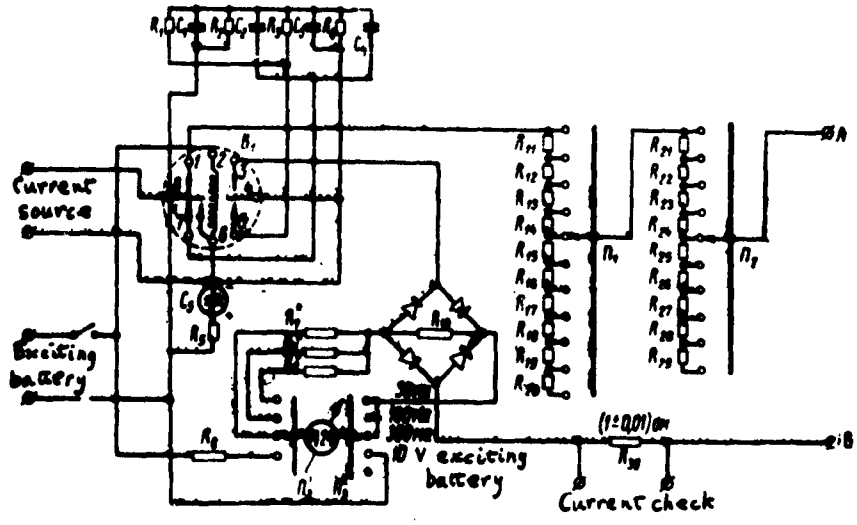


Fig. 1. Circuits of the generator: $R_1$ to $R_4$, 160 ohms; $R_5$, 470 Ω; $R_6$, 100 kΩ; $R_7^*$, ~10 kΩ; $R_8^*$, ~2.5 kΩ; $R_9^*$, ~80 Ω; resistors $R_1$ to $R_9$ are of type MLT-0.5; $R_7$ to $R_9$ are adjusted during calibration; $R_{10}$, 4 Ω (wire); $R_{11}$, 30 Ω (variable wire); $R_{12}$-$R_{20}$, 30 Ω; $R_{21}$-$R_{29}$, 300 Ω; $R_{30}$, 1 ± 0.01 Ω (wire); $C_1$ to $C_4$, 0.05 μF; $C_5$, 5 μF; $B_1$, VS-4.8 vibrator.

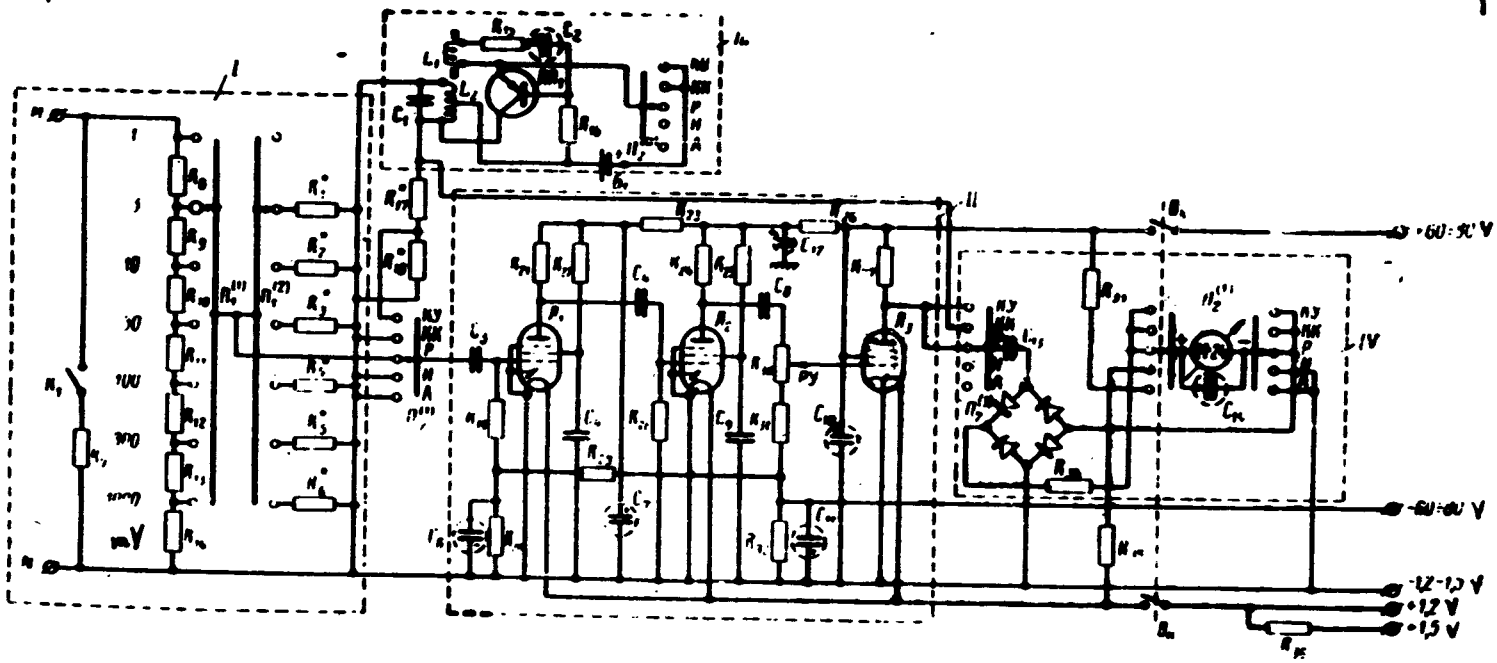

Fig. 2. The vacuum-tube voltmeter: $R_7$, 240 kΩ; $R_8$, 1.3 MΩ; $R_9$, 620 kΩ; $R_{10}$, 180 kΩ; $R_{11}$, 62 kΩ; $R_{12}$, 18 kΩ; $R_{13}$, 6.2 kΩ; $R_{14}$, 2.7 kΩ; $R_{15}$, 4.3 kΩ; $R_{16}$, 20 kΩ; $R_{17}$, 16 kΩ; $R_{18}$, 8 Ω; $R_{19}$, 5.1 MΩ; $R_{20}$, 1.3 kΩ; $R_{21}$, 150 MΩ; $R_{22}$, 510 kΩ; $R_{23}$, 11 kΩ; $R_{24}$, 150 kΩ; $R_{25}$, 510 kΩ; $R_{26}$, 33 kΩ; $R_{27}$, 20 kΩ; $R_{28}$, 1 MΩ; $R_{29}$, 5.1 MΩ; $R_{30}$, 680 kΩ; $R_{31}$, 390 kΩ; $R_{32}$, 2.7 kΩ; $R_{33}$, 1 MΩ; $R_{34}$, 11 kΩ; $R_{35}$, 20 kΩ; $R_{36}$, 4 Ω (wire); $R_1$ to $R_6$, and $R_{37}$, are adjusted during calibration; all resistors (except $R_{37}$, $R_{38}$, and $R_{39}$) are of type MLT-0.5; $C_1$ and $C_{13}$, 1 μF; $C_2$, 3 μF; $C_3$, $C_4$, and $C_8$ are 0.05 μF; $C_5$ and $C_9$ are 2 x 0.5 μF; $C_6$, $C_{11}$, and $C_{14}$ are 20 μF; $C_7$, $C_{10}$, and $C_{12}$ are 10 μF; transistor type P-13; diodes type D2E; $B_1$ is an FBS-0.25 cell; $Л_1$ and $Л_2$ are 1B2P tubes; $Л_3$ is a 2P2P; $L_1$ has 400 turns; $L_2$ has 400 + 400 turns wound on an SB-4 ferrite core.

The main part of the converter is the VS-4.8 vibrator (Fig. 1), which produces an alternating current at 100 ± 10 c/s with a maximum voltage of 300 v and a maximum current of 300 ma (power limit 70 va). The current in the supply circuit is controlled by resistors $R_{11}$ to $R_{19}$, which are inserted in series with the supply AB by the switches $П_1$ and $П_2$. The current is measured by the M-24 meter, which is connected via a bridge rectifier (silicon diodes type D-205). The same instrument serves to check the exciting voltage, which is kept between 4.5 and 6 v. The current in the AB circuit may also be measured with the millivoltmeter, which for this purpose is connected across $R_{20}$ (1 Ω). Spark-quenching RC circuits are fitted in order to stabilize the operation of the synchronous vibrator ($R_1$ to $R_5$ and $C_1$ to $C_5$). The exciting battery consists of four 1.5-TMTs-29.5 cells (3s-L-30) or four 1.48-PMTs-9 cells (2s-L-9), which are housed in the generator case. The sources of current are batteries such as 29-GRMTs-13 (B-30), 69-PRMTs-6 (B-72), 102-AMTs-U-1.0 (BAS-80), and so on, which are connected externally. The converter is contained in a metal case 170 x 200 x 310 mm; the weight without batteries is 2 kg.

The vacuum-tube voltmeter (Fig. 2) consists of the input divider I, the amplifier II, the calibrator III, and the measuring instrument IV. The input divider (range switch) provides ranges of 1, 3, 10, 30, 100, 300, and 1000 mv full scale, the input resistance being constant at 2.4 MΩ. The resistance of the MN circuit is estimated by means of button $K_1$, which throws in a shunt resistor of 240 kΩ ($R_7$). The amplifier is resistance-capacity coupled and is built around subminiature valves; the over-all gain is about 2000. The output is connected to a bridge rectifier, which feeds the M-24 meter; the scale is graduated 0-10 and 5-30, to correspond with the ranges of measurement.

The calibrator serves to check the gain; it is simply an LC oscillator built around the P-13 transistor.

The instrument is fed from a 1.48-PMTs-9 cell (filaments) and a GB-80 battery (plates); the instrument works normally over voltage ranges of 1-1.5 (filaments) and 60-90 (plates). The supply unit is such as to provide 70-80 hours' continuous use.

The millivoltmeter is contained in a metal case 135 x 150 x 280 mm; the weight with the batteries fitted is about 2.5 kg.

The apparatus is simple to make and service; it is also light. It should be usable under a variety of conditions, especially in inaccessible regions. The only disadvantage is that it cannot be used when the level of industrial interference is high.

# CONCERNING THE VERTICAL TORSION BALANCE THEORY

pp. 278-287

B. V. Gran

1. Much attention has been given to the measurement of the vertical gradient of the gravitational acceleration in recent years, for the quantity is useful in geophysics, geodesy, and related fields. The need for a special instrument to measure $U_{zz}$ arose long ago; the problem was considered by Eötvös, while in 1943 Haalck [8] wrote that "the next task of instrumental gravimetry is to produce an instrument for measuring the vertical gradient". In 1920 Berroth [6] proposed a vertical torsion balance for measuring $U_{zz}$*; Sadovskiy [4] has considered the theory of such balances, but no attempt to utilize the method has been described. although the proposal has been discussed more than once [7].

Previous treatments [4,6] deal only with the case in which the center of mass lies on the axis of rotation; the torques produced by the second derivatives of the potential are small. A slight displacement of the center of mass from the axis would produce a torque comparable with that from the second derivatives, so there is some point in considering the case in order to find the permissible limits of such deviation. Here I deduce the equation of equilibrium for a body of arbitrary shape having a horizontal axis of rotation that does not pass through the center of mass. This equation is discussed from the point of view of possible absolute and relative measurements of $U_{zz}$.

2. Consider a solid of arbitrary shape having a horizontal axis and suspended on two elastic fibers. The two coordinate systems to be used are $\zeta\eta\xi$ (mobile, rigidly connected to the body) and xyz (fixed); the origin of both lies at O, the point where the axis of rotation meets a plane passing through the center of mass and normal to that axis. The Oz axis is directed vertically downwards, Ox and Oy lying in a horizontal plane. The $O\eta$ axis is directed along the axis of rotation and so is horizontal; $O\xi$ is normal to $O\eta$, and $O\zeta$ lies normal to the

*I call Berroth's system a vertical torsion balance.

$\xi O\eta$ plane. The torque about $O\eta$ produced by the gravitational forces is

$$M_1 = \int_V (\zeta g_\xi - \xi g_\zeta)\, dm,$$

in which V is the volume of the body, $\xi$ and $\zeta$ are the coordinates of an element of mass dm, and $g_\xi$ and $g_\zeta$ are the components of g in the $\xi\eta\zeta$ coordinate system. This $M_1$ is balanced by an equal torque from the fibers when the system is at equilibrium; if we neglect the sag in the fibers, we have that

$$\tau(\psi - \psi_0) = \int_V (\zeta g_\xi - \xi g_\zeta)\, dm, \tag{1}$$

in which $\tau$ is the torsion constant of the fibers and $\psi_0$ is an angle defining the position of the body when there is no torque in the fiber. Transformation of coordinates gives

$$\begin{aligned} g_\xi &= g_x \cos\alpha_1 + g_y \cos\beta_1 + g_z \cos\gamma_1, \\ g_\zeta &= g_x \cos\alpha_3 + g_y \cos\beta_3 + g_z \cos\gamma_3, \end{aligned} \tag{2}$$

in which $\alpha_i$, $\beta_i$, and $\gamma_i$ are the angles between the axes of the two coordinate systems. The direction cosines are found from the condidtion that the $O\zeta$ axis makes an angle $\theta$ with the Oz axis and that $O\eta$ makes an angle $\varphi$ with Oy. Substitution for the direction cosines in (2) gives that

$$\begin{aligned} g_\xi &= g_x \cos\varphi \cos\theta + g_y \sin\varphi \cos\theta - g_z \sin\theta, \\ g_\zeta &= g_x \cos\varphi \sin\theta + g_y \sin\varphi \sin\theta + g_z \cos\theta. \end{aligned} \tag{3}$$

We expand $g_x$, $g_y$, and $g_z$ as Taylor series on the assumption that the second derivatives are constant within the volume of the body:

$$\begin{aligned} g_x &= (g_x)_0 + U_{xx}\cdot x + U_{xy}\cdot y + U_{xz}\cdot z, \\ g_y &= (g_y)_0 + U_{xy}\cdot x + U_{yy}\cdot y + U_{yz}\cdot z, \\ g_z &= (g_z)_0 + U_{xz}\cdot x + U_{yz}\cdot y + U_{zz}\cdot z. \end{aligned} \tag{4}$$

Here $(g_x)_0 = (g_y)_0 = 0$ and $(g_z)_0 = g_0$. Then the coordinate-transformation formulas give us that

$$\begin{aligned} x &= \xi\cos\varphi\cos\theta - \eta\sin\varphi + \zeta\cos\varphi\sin\theta, \\ y &= \xi\sin\varphi\cos\theta + \eta\cos\varphi + \zeta\sin\varphi\sin\theta, \\ z &= -\xi\sin\theta + \zeta\cos\theta. \end{aligned} \tag{5}$$

We substitute (5) into (4), then (4) into (3), and finally (3) into (1) to get that

$$\tau(\psi - \psi_0) = -g_0 \int_V (\xi\cos\theta + \zeta\sin\theta)\, dm \tag{6}$$

$$+ U_{xx}\int_{\nu}\left\{\left[(\zeta^2-\xi^2)\frac{\sin 2\theta}{2}+\xi\zeta\cos 2\theta\right]\cos^2\varphi\right.$$
$$\left.+(\xi\eta\sin\theta-\eta\zeta\cos\theta)\frac{\sin 2\varphi}{2}\right\}dm+U_{yy}\int_{\nu}\left\{\left[(\zeta^2-\xi^2)\frac{\sin 2\theta}{2}\right.\right.$$
$$\left.\left.+\xi\zeta\cos 2\theta\right]\sin^2\varphi-(\xi\eta\sin\theta-\eta\zeta\cos\theta)\frac{\sin 2\varphi}{2}\right\}dm$$
$$-U_{zz}\int_{\nu}\left[(\zeta^2-\xi^2)\frac{\sin 2\theta}{2}+\xi\zeta\cos 2\theta\right]dm$$
$$+U_{xy}\int_{\nu}\left\{\left[(\zeta^2-\xi^2)\frac{\sin 2\theta}{2}+\xi\zeta\cos 2\theta\right]\sin 2\varphi\right.$$
$$\left.-(\xi\eta\sin\theta-\eta\zeta\cos\theta)\cos 2\varphi\right\}dm+U_{xz}\int_{\nu}\left\{\left[(\zeta^2-\xi^2)\cos 2\theta\right.\right. \quad (6)$$
$$\left.\left.-2\xi\zeta\sin 2\theta\right]\cos\varphi+(\xi\eta\cos\theta+\eta\zeta\sin\theta)\sin\varphi\right\}dm$$
$$+U_{yz}\int_{\nu}\left\{\left[(\zeta^2-\xi^2)\cos 2\theta-2\xi\zeta\sin 2\theta\right]\sin\varphi\right.$$
$$\left.-(\xi\eta\cos\theta+\eta\zeta\sin\theta)\cos\varphi\right\}dm.$$

Let

$$\int_{\nu}(\zeta^2-\xi^2)\,dm=K,\quad \int_{\nu}\xi\eta\,dm=J_1,\quad \int_{\nu}\xi\zeta\,dm=J_2,\quad \int_{\nu}\eta\zeta\,dm=J_3, \quad (7)$$

Now by definition

$$\int_{\nu}\xi\,dm=m\xi_0,\quad \int_{\nu}\zeta\,dm=m\zeta_0, \quad (8)$$

in which m is the mass of the body and $\xi_0$ and $\zeta_0$ are the coordinates of the center of mass. Further, Laplace's equation gives

$$U_{yy}=-U_{xx}-U_{zz}. \quad (9)$$

Then (7)-(9) enable us to transform (6) to give

$$\tau(\psi-\psi_0)=-mg_0(\xi_0\cos\theta+\zeta_0\sin\theta)-$$
$$-\tfrac{1}{2}U_{\Delta}\left[\left(\frac{K}{2}\sin 2\theta+J_2\cos 2\theta\right)\cos 2\varphi+(J_1\sin\theta-J_3\cos\theta)\sin 2\varphi\right]$$
$$+U_{xy}\left[\left(\frac{K}{2}\sin 2\theta+J_2\cos 2\theta\right)\sin 2\varphi-(J_1\sin\theta-J_3\cos\theta)\cos 2\varphi\right] \quad (10)$$
$$+U_{xz}\left[\left(K\cos 2\theta-2J_2\sin 2\theta\right)\cos\varphi+(J_1\cos\theta+J_3\sin\theta)\sin\varphi\right]$$
$$+U_{yz}\left[\left(K\cos 2\theta-2J_2\sin 2\theta\right)\sin\varphi-(J_1\cos\theta+J_3\sin\theta)\cos\varphi\right]$$

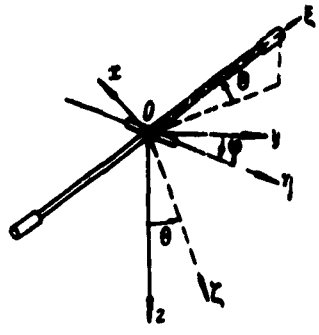


Fig. 1.

$$- \frac{3}{2} U_{zz}\left(\frac{K}{2}\sin 2\theta + J_3 \cos 2\theta\right). \quad (10)$$

$$U_\Delta = U_{yy} - U_{xx}.$$

Then (10) is the equation of equilibrium for a body of arbitrary shape having a horizontal axis of rotation. For a vertical torsion balance (Fig. 1), the symmetry about the $\xi 0\zeta$ and $\eta 0\zeta$ planes makes the central moments $J_1$, $J_2$, and $J_3$ zero, so (10) becomes

$$\tau(\psi - \psi_0) = - mg_0(\xi_0 \cos\theta + \zeta_0 \sin\theta) - \frac{3}{4} U_{zz} K \sin 2\theta$$

$$- \frac{1}{4} U_\Delta K \sin 2\theta \cos 2\varphi + \frac{1}{2} U_{xy} K \sin 2\theta \sin 2\varphi \quad (11)$$

$$+ U_{xz} K \cos 2\theta \cos\varphi + U_{yz} K \cos 2\theta \sin\varphi.$$

The main difference between earlier equations [4, 6] and (11) lies in the first term on the right; this term vanishes if $\xi_0 = \zeta_0 = 0$. Other differences are purely formal, for previously [4, 6] the choice of the mobile coordinate system was not correct, in that the $0\zeta$ axis was directed vertically downwards, so this system was not rigidly linked to the body and, moreover, was not rectangular.

Equation (11) contains the seven unknowns $\psi_0$, $g_0$, $U_\Delta$, $U_{zz}$, $U_{xy}$, $U_{xz}$, and $U_{yz}$, so the balance senses g as well as all the second derivatives. Now $U_{zz}$ contains only the angle $\theta$; let the observations be made in a way such that $\theta$ remains constant at any given point, so only $\varphi$ varies. Then the first two terms on the right in (11) also remain constant, so they determine merely the zero reading $C_0$:

$$C_0 = -\tau\psi_0 + mg_0(\xi_0 \cos\theta + \zeta_0 \sin\theta) + \frac{3}{4} U_{zz} K \sin 2\theta. \quad (12)$$

This cannot give us $U_{zz}$, for (12) contains $\psi_0$ and $g_0$ as unknowns in addition; thus it is impossible to keep $\theta$ constant in absolute determinations of $U_{zz}$, and observations must be made for various values of $\theta$.

Now we consider when the first term in (11) can be neglected; we must have that

$$|mg_0(\xi_0 \cos\theta + \zeta_0 \sin\theta)| < \left|\frac{3}{4} U_{zz} K \sin 2\theta\right|, \quad (13)$$

in which $U_{zz}$ is the minimum value of the vertical gradient that has to be measured. If the balance arm is weightless, we have from (7) that

$$K = -ml^2. \quad (14)$$

in which $l$ is the distance from the axis of rotation to the load. It can be shown that $\theta$ must be $45^0$ if the sensitivity to $U_{zz}$ under these conditions is to be maximal; then (13) can be put as

$$\left| \frac{4g_0(\xi_0 + \zeta_0)}{3\sqrt{2} \cdot U_{zz} \cdot l^2} \right| \leqslant 1. \qquad (15)$$

Let the desired limit be 10 E ($10^{-8}$ cgs units); then (15) gives us that

$$|\xi_0 + \zeta_0| < l^2 \cdot 10^{-11} \text{ см}. \qquad (16)$$

Now a balance arm of total length 50 cm implies that $|\xi_0 + \zeta_0| \leq 0.66 \times 10^{-8}$ cm; (16) also shows that the only way of increasing the permissible deviation from the axis of rotation is to increase $l$, but the effects of temperature and of deflection in the arm increase rapidly with $l$. The system is unworkable for $l = 50$ cm, although in this case $|\xi_0 + \zeta_0|$ should be less than $2.5 \times 10^{-8}$ This shows that the axis of rotation must coincide very precisely with the center of mass for any usable value of $l$; the desired state is not at present attainable. That is, a vertical torsion balance is always a gravimeter as well as gradient meter no matter how carefully it may be adjusted.

3. Consider now a balance with real values of $\xi_0$ and $\zeta_0$. We employ the usual technique to estimate the probable distance to the axis; an analytic balance is a vertical torsion balance if we take the masses of the pans and weights to be concentrated at the points of support. Morozova [2] has shown that the distance from the axis of rotation to the center of mass of the beam must not be less than 100 $\mu$ if the balance is to work stably for loads of 20 to 200 grams; the distance is sometimes reduced to 10 $\mu$, but any further reduction leads to great instability. It would seem possible that especial care under exceptionally good conditions might enable one to make $\xi_0 = \zeta_0 = 1$ $\mu$; then (15) gives us that this deviation of 1 u, with $l$ = 50 cm, gives a torque of $3.4 \times 10^5$ E. N w (11) shows that this torque is reduced by a factor of $\sqrt{2}$ if $\theta$ is reduced from $45^0$ to $0^0$, so the torque would then be only $1.4 \times 10^5$ E. Even so, the balance is subject to a large torque, and this varies with $\theta$; the small quantity can be measured in the presence of the large one only if the latter is constant, the gravimeter being an example of this. That is, the first term in (11) must remain constant at each point if the $U_{zz}$ are to be measured to 5-10 E, so $\theta$ must not alter; but then the absolute value cannot be determined, so a vertical torsion balance cannot be used to measure $U_{zz}$ absolutely. This conclusion is a result of purely practical considerations, not of theory; it is merely that at present there is no sufficiently rigid material for the arm and no adequate mean of bringing the center of mass close enough to the axis of rotation.

4. Consider now the relative measurement of $U_{zz}$ from (11) with $\theta$ constant; (12) reduces the unknowns in (11) to five, and the coefficients to these are functions of $\varphi$ (apart from $C_0$), so readings in five azimuths give us a system of five equations to derive $C_0$. Let the values for two adjacent points be $C_{01}$ and $C_{02}$; then, if $\psi_0$, $g_0$, $\xi_0$, and $\zeta_0$ are constant for these points, we have from (12) that

$$\Delta U_{zz} = \frac{C_{02} - C_{01}}{\frac{3}{4} K \sin 2\theta}, \tag{17}$$

That is, relative measurements of $U_{zz}$ are possible if the above assumptions are obeyed and if $\theta$ varies only slowly with $U_{zz}$ (i.e., remains virtually constant). Now we have to consider the permissible changes in $\psi_0$, $g_0$, $\xi_0$, and $\zeta_0$ as between points. The theory of errors [5] gives us the formula

$$df^2(x, y, \ldots) = \left(\frac{\partial f}{\partial x}\right)^2 \cdot dx^2 + \left(\frac{\partial f}{\partial y}\right)^2 \cdot dy^2 + \ldots, \tag{18}$$

in which $df^2$ is the dispersion of a function whose arguments have dispersions $dx^2$, $dy^2$, ... . Let the of (11) be the function and $\theta$, together with the above four quantities, the arguments; the changes in are small, so we neglect the last five terms on the right. Then (11) and (18) together give us that

$$\tau^2 d\psi^2 = \tau^2 d\psi_0^2 + (m\xi_0 \sqrt{2})^2 dg_0^2 + \left(\frac{mg_0}{\sqrt{2}}\right)^2 d\xi_0^2 + \left(\frac{mg_0}{\sqrt{2}}\right)^2 d\zeta_0^2. \tag{19}$$

On the assumptions that all terms contribute equally, we have

$$\begin{aligned} d\psi_0 &= \frac{d\psi}{2}, \\ dg_0 &= \frac{\tau}{m} \cdot \frac{d\psi}{\xi_0 \sqrt{2}}, \\ d\xi_0 &= d\zeta_0 = \frac{\tau}{m} \cdot \frac{d\psi \sqrt{2}}{g_0}. \end{aligned} \tag{20}$$

Consider $\tau/m$; the equation for the the angular sensitivity of a vertical torsion balnce takes the form*

$$\frac{d\psi}{dU_{zz}} = -\frac{\frac{3}{4} K \sin 2\theta}{\tau + mg_0(\xi_0 \cos\theta - \zeta_0 \sin\theta)} \tag{21}$$

Then (21) becomes in conjunction with (14) for $\theta = 45^0$ and $\xi_0 = \zeta_0$

$$\frac{d\psi}{dU_{zz}} = \frac{3ml^2}{4\tau}. \tag{22}$$

*We can derive (21) from (11) by means of the rule for finding the derivative of an inexplicit function if, in view of the very small changes in $\psi$, we neglect changes in the second derivatives.

Then

$$\frac{\tau}{m} = \frac{3}{4} \cdot \frac{dU_{zz}}{d\psi} \cdot l^3. \qquad (23)$$

We insert (23) into (20) to get

$$\begin{aligned} d\psi_0 &= \frac{d\psi}{2}, \\ dg_0 &= \frac{3}{4} l^3 \cdot \frac{dU_{zz}}{\xi_0 \cdot 2}, \\ d\xi_0 = d\zeta_0 &= \frac{3}{4} \frac{l^3}{2} \frac{dU_{zz}}{g_0}. \end{aligned} \qquad (24)$$

The differentials may be found by putting $d\psi/dU_{zz} = 1''/1$ E; $dU_{zz} = 10$ E, $d\psi = 10''$, $2l = 50$ cm, and $\xi_0 = \zeta_0 = 10^{-4}$ cm, so (24) gives

$$\begin{aligned} d\psi_0 &= 5'', \\ dg_0 &= 16.5 \text{ mgal}, \\ d\xi_0 = d\zeta_0 &= 0.33 \cdot 10^{-8} \text{ cm}. \end{aligned} \qquad (25)$$

(25) shows that the position of the center of mass should not vary more than $0.33 \times 10^{-8}$ cm as between points; this distance is of the order of the dimensions of atoms. Long ago Mendeleyev [1] remarked that the position of the center of gravity of a precision balance relative to the axis of rotation alters with time even if the pans are allowed to swing freely; one of the main causes of this is that temperature fluctuations occur. Also, the ceneter of gravity is appreciably affected if the balance is brought to rest. The examples Mendeleyev gives show that the center of gravity of a precision balance can alter by $10^{-4}$ cm or more, so we may expect that the $\xi_0$ and $\zeta_0$ of a vertical torsion balance will vary by far more than the above limit. Further, (24) shows that the sole means of increasing the permitted range in $\xi_0$ and $\zeta_0$ is to make $l$ large; but $l$ must be increased tenfold in order to increase $\xi_0$ and $\zeta_0$ by factors of 100, which is quite impossible, for the total length of the beam would then be 5 m. Thus the very rigorous demand for stability in the center of mass makes it doubtful whether $U_{zz}$ can be measured even in relative terms.

I do not propose to deal with the equations of motion and sensitivity, for (11) alone gives a sufficiently clear indication of the possibilities of absolute and relative measurement of $U_{zz}$.

## Conclusions

The equation of equilibrium for a vertical torsion balance has been examined; the following deductions have been drawn.

1. The displacement of the center of mass from the axis of rotation cannot be neglected; a displacement of $10^{-4}$ cm causes a torque that is several orders of magnitude larger than that

arising from the second derivatives, and this torque is not even constant during absolute measurements of $U_{zz}$. That is, the instrument actually acts mainly as a gravimeter, and it is impossible to measure gradients of the order of 10 E.

2. Relative measurements on $U_{zz}$ could be made if the tilt of the beam were to remain constant when the balance is moved; but the permissible displacement of the center of mass is then less than 1 Å. Experience with precision balances shows that such stability is at present unattainable, so it is doubtful whether the instrument can make relative measurements of $U_{zz}$.

This means that it would be undesirable to devise some form of vertical torsion balance with the object of measuring $U_{zz}$. The discrepancy between the requirements of theory and the practical possibilities is so great that it would be better to seek other and more promising methods. I consider that measurements with gravimeters at different heights and Jolly's method are suitable for this purpose.

I am indebted to Professor B. A. Andreyev and Dr. V. S. Mironov for valuable discussions.

Bibliography

1. Mendeleyev, D. I. O priyemakh tochnykh ili metrologicheskikh vzveshivaniy [Methods of precision or metrological weighing]. Trudy po metrologii [Papers on Metrology], 1936.
2. Morozova, I. N. Eksperimental'noye issledovaniye prichin nepostoyanstva pokazaniy analiticheskikh vesov [An experimental study of the causes of variation in the readings of analytical balances]. Author's abstract of dissertation, All-Union Metrology research Institute, 1952.
3. Myuller, V. A. Issledovaniye analiticheskikh vesov i mikrovesov sovetskogo proizvodstva [A study of analytical balances and microbalances of Soviet manufacture]. Trudy VNIIM, no. 19 (35), 1939 [Transactions of the All-Union Metrology Research Institute].
4. Sadovskiy, M. A. Velichina $U_{zz}$ i yeye znacheniye v geofizike [$U_{zz}$ and its significance in geophysics]. Trudy IPG, no. 6, 1930.
5. Chebotarev, A. S. Sposob naimen'shikh kvadratov s osnovami teorii veroyatnostey [The least-squares method and the principles of the theory of probability], 1958.
6. Berroth, A. Die vertikalschwingende Drehwaage. Zeits. für Instrum., 40, 1920.
7. Egyed, L. Zur Frage der Schweremessungen in Bohrlochern, Freiberger Forschungshefte, 1960, C, no. 81.
8. Haalck, H. Erwiederung auf die kritische Bermerkung usw. Beitrage zur angewandten Geophysik, 10, 1943.

# PLOTTING WAVE-FRONT CHARTS WITH AN ARBITRARY LAW OF CHANGE IN SEISMIC VELOCITY WITH DEPTH

pp. 292-300

Yu. Ye. Nekrasov

Ray diagrams are used in interpreting seismic observations if the distribution of the seismic velocity in the section is complicated, for the usual mean-velocity method then becomes inapplicable. Methods have been published [1, 3-5] for calculating ray diagrams for given laws of variation of velocity with depth; but the laws must be available in analytic form [3-5], whereas many practical sections have velocity variations too complicated for such methods to be applicable.

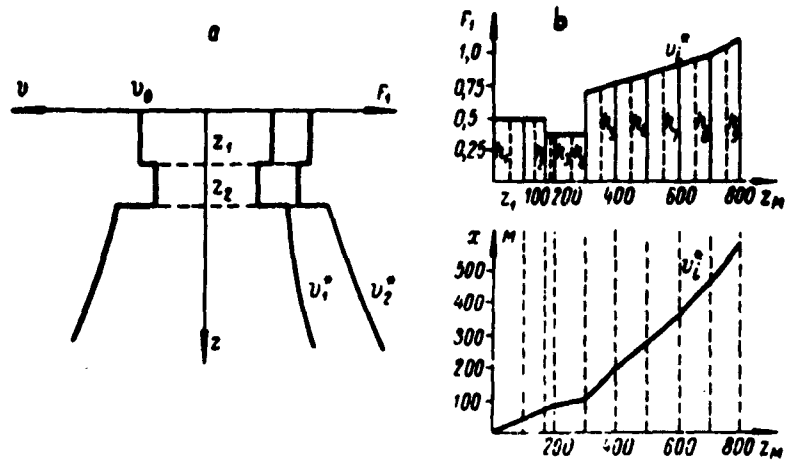


Fig. 1.

Here I give a method that can be used for any graphically specified law of variation; it consists in approximate calculation of the integrals

$$x = \int_0^z \sqrt{\frac{a v(z)}{1 - a^2 v^2(z)}}\, dz, \qquad (1)$$

$$t = \int_0^z \frac{dz}{v(z)\sqrt{1 - a^2 v^2(z)}}. \qquad (2)$$

Here (1) is the equation of a ray, (2) being the time of travel along a ray [2]; x and z are the coordinates of points on the ray, v(z) is the velocity, and $a = 1/v^*$ is the ray parameter. Consider now the construction of rays; here we use the accessory function

$$F_1(v) = \frac{av}{\sqrt{1 - a^2 v^2}}$$

If v(z) is given in graph form, we can construct $F_1(z)$. For the appropriate depths $z_i$ we read off v from the graph of v(z), and from a table** read off the value of $F_1$ corresponding to the given $v^*$; this value is entered on the graph of $F_1(z)$ at the appropriate z (Fig. 1a). A discontinuity in the velocity, as at $z_2$ gives us two values of $F_1(z)$. The points are joined up into a smooth curve; Fig. 1a shows two curves for two values of $v^*$. The next step is to integrate $F_1(z)$, which is best done by the trapezium method as applied to graphs drawn on mm graph paper with depth

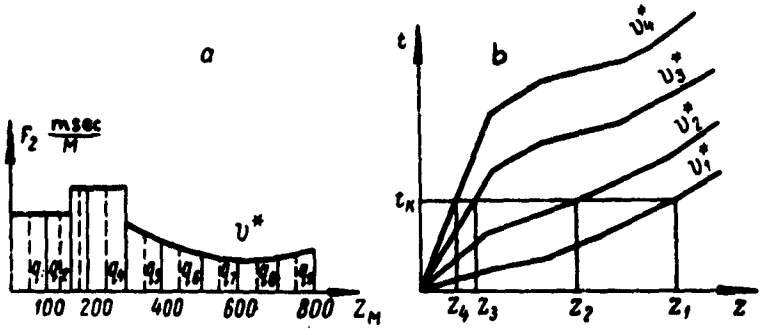


Fig. 2.

scales of 1:1000 and so on. The integration amounts to the determination of the areas

$$S_k = h_k \Delta z_i,$$

in which $z = z_{k+1} - z_k$ (Fig. 1b); if now z is 100 m (for a scale of 1:10 000; 10 m for 1:1000), the area is found simply by multiplying the ordinate $h_k$ by 100 (or 10). Now $S_k$ is numerically equal to the increase in the horizontal path of the ray for the change in depth of $z_{k+1} - z_k$; the sum of the $S_k$ is the horizontal path consequent on penetration to the depth $z_n$, so the problem of constructing the ray is solved.

Consider now the time equation:

$$t = \int_0^z \frac{dz}{v(z)\sqrt{1 - a^2 v^2(z)}}. \qquad (2)$$

*K. A. Nekrasova performed the calculations.

| $v(z)$ | $v^* = 50$ | | $v^* = 30$ | | $v^* = 20$ | | $v^* = 15$ | | $v^* = 12$ | |
|---|---|---|---|---|---|---|---|---|---|---|
| | $F_1$ | $F_2$ | $F_1$ | $F_2$ | $F_1$ | $F_2$ | $F_1$ | $F_2$ | $F_1$ | $F_2$ |
| 1,5 | 0,030 | 0,6675 | 0,050 | 0,6675 | 0,075 | 0,6684 | 0,100 | 0,6702 | 0,126 | 0,6720 |
| 1,6 | 0,032 | 0,6257 | 0,053 | 0,6258 | 0,080 | 0,6270 | 0,106 | 0,6289 | 0,134 | 0,6305 |
| 1,7 | 0,034 | 0,5889 | 0,057 | 0,5893 | 0,085 | 0,5907 | 0,113 | 0,6917 | 0,143 | 0,5942 |
| 1,8 | 0,036 | 0,5562 | 0,060 | 0,5568 | 0,090 | 0,5577 | 0,121 | 0,5596 | 0,152 | 0,5618 |
| 1,9 | 0,038 | 0,5269 | 0,063 | 0,5274 | 0,095 | 0,5288 | 0,128 | 0,5305 | 0,158 | 0,5333 |
| 2,0 | 0,040 | 0,5005 | 0,067 | 0,5010 | 0,100 | 0,5025 | 0,134 | 0,5045 | 0,170 | 0,5071 |
| 2,1 | 0,042 | 0,4766 | 0,070 | 0,4771 | 0,105 | 0,4792 | 0,141 | 0,4810 | 0,178 | 0,4840 |
| 2,2 | 0,044 | 0,4550 | 0,073 | 0,4560 | 0,110 | 0,4572 | 0,149 | 0,4596 | 0,186 | 0,4623 |
| 2,3 | 0,046 | 0,4352 | 0,077 | 0,4361 | 0,116 | 0,4378 | 0,154 | 0,4401 | 0,195 | 0,4433 |
| 2,4 | 0,048 | 0,4170 | 0,080 | 0,4179 | 0,121 | 0,4196 | 0,159 | 0,4218 | 0,204 | 0,4252 |
| 2,5 | 0,050 | 0,4003 | 0,083 | 0,4016 | 0,126 | 0,4032 | 0,170 | 0,4057 | 0,213 | 0,4090 |
| 2,6 | 0,052 | 0,3851 | 0,087 | 0,3861 | 0,131 | 0,3876 | 0,176 | 0,3905 | 0,222 | 0,3940 |
| 2,7 | 0,054 | 0,3706 | 0,090 | 0,3719 | 0,136 | 0,3737 | 0,183 | 0,3764 | 0,231 | 0,3802 |
| 2,8 | 0,056 | 0,3579 | 0,094 | 0,3585 | 0,141 | 0,3607 | 0,189 | 0,3631 | 0,240 | 0,3674 |
| 2,9 | 0,058 | 0,3455 | 0,097 | 0,3465 | 0,146 | 0,3483 | 0,196 | 0,3515 | 0,249 | 0,3556 |
| 3,0 | 0,060 | 0,3340 | 0,100 | 0,3350 | 0,151 | 0,3370 | 0,204 | 0,3401 | 0,258 | 0,3443 |
| 3,1 | 0,062 | 0,3232 | 0,103 | 0,3242 | 0 156 | 0,3265 | 0,210 | 0,3295 | 0,267 | 0,3339 |
| 3,2 | 0,064 | 0,3131 | 0,107 | 0,3144 | 0,161 | 0,3167 | 0,218 | 0,3199 | 0,277 | 0,3241 |
| 3,3 | 0,066 | 0,3037 | 0,110 | 0,3049 | 0,168 | 0,3073 | 0,226 | 0,3108 | 0,286 | 0,3154 |
| 3,4 | 0,068 | 0,2947 | 0,113 | 0,2959 | 0,173 | 0,2986 | 0,233 | 0,3019 | 0,296 | 0,3067 |
| 3,5 | 0,070 | 0,2863 | 0,116 | 0,2877 | 0,178 | 0,2904 | 0,240 | 0,2939 | 0,305 | 0,2989 |
| 3,6 | 0,072 | 0,2786 | 0,121 | 0,2797 | 0,183 | 0,2823 | 0,247 | 0,2860 | 0,315 | 0,2912 |
| 3,7 | 0,074 | 0,2711 | 0,124 | 0,2725 | 0,188 | 0,2750 | 0,254 | 0,2789 | 0,324 | 0,2842 |
| 3,8 | 0,076 | 0,2639 | 0,128 | 0,2653 | 0,193 | 0,2680 | 0,263 | 0,2721 | 0,334 | 0,2773 |
| 3,9 | 0,078 | 0,2572 | 0,131 | 0,2585 | 0,199 | 9,2614 | 0,269 | 0,2655 | 0,344 | 0,2711 |
| 4,0 | 0,080 | 0,2508 | 0,134 | 0,2520 | 0,205 | 0,2551 | 0,276 | 0,2593 | 0,355 | 0,2654 |
| 4,1 | 0,082 | 0,2446 | 0,137 | 0,2461 | 0,209 | 0,2491 | 0,285 | 0,2536 | 0,364 | 0,2595 |
| 4,2 | 0,084 | 0,2388 | 0,141 | 0,2405 | 0,214 | 0,2434 | 0,292 | 0,2480 | 0,374 | 0,2541 |
| 4,3 | 0,086 | 0,2335 | 0,145 | 0,2349 | 0,220 | 0,2382 | 0,298 | 0,2428 | 0,383 | 0,2490 |
| 4,4 | 0,088 | 0,2282 | 0,149 | 0,2298 | 0,226 | 0,2331 | 0,307 | 0,2378 | 0,394 | 0,2444 |
| 4,5 | 0,090 | 0,2231 | 0,152 | 0,2247 | 0,231 | 0,2282 | 0,315 | 0,2329 | 0,404 | 0,2397 |
| 4,6 | 0,092 | 0,2183 | 0,155 | 0,2200 | 0,236 | 0,2234 | 0,322 | 0,2284 | 0,416 | 0,2355 |
| 4,7 | 0,094 | 0,2136 | 0,159 | 0,2153 | 0,242 | 0,2189 | 0,330 | 0,2240 | 0,426 | 0,2313 |
| 4,8 | 0,096 | 0,2094 | 0,162 | 0,2111 | 0,247 | 0,2146 | 0,338 | 0,2200 | 0,437 | 0,2274 |
| 4,9 | 0,098 | 0,2051 | 0,165 | 0,2070 | 0,252 | 0,2104 | 0,346 | 0,2160 | 0,447 | 0,2235 |
| 5,0 | 0,100 | 0,2010 | 0,170 | 0,2028 | 0,258 | 0,2066 | 0,355 | 0,2123 | 0,457 | 0,2200 |
| 5,1 | 0,102 | 0,1968 | 0,173 | 0,1990 | 0,264 | 0,2028 | 0,362 | 0,2086 | 0,470 | 0,2166 |
| 5,2 | 0,104 | 0,1933 | 0,176 | 0,1952 | 0,269 | 0,1991 | 0,370 | 0,2050 | 0,480 | 0,2136 |
| 5,3 | 0,106 | 0,1898 | 0,180 | 0,1916 | 0,275 | 9,1957 | 0,379 | 0,2018 | 0,493 | 0,2104 |
| 5,4 | 0,108 | 0,1859 | 0,183 | 0,1882 | 0,280 | 0,1923 | 0,386 | 0,1985 | 0,504 | 0,2074 |
| 5,5 | 0,110 | 0,1829 | 0,186 | 0,1850 | 0,286 | 0,1892 | 0,396 | 0,1955 | 0,516 | 0,2045 |
| 5,6 | 0,112 | 0,1797 | 0,190 | 0,1819 | 0,292 | 0,1860 | 0,403 | 0,1924 | 0,528 | 0,2020 |
| 5,7 | 0,114 | 0,1765 | 0,193 | 0,1787 | 0,297 | 0,1831 | 0,411 | 0,1896 | 0,540 | 0,1994 |
| 5,8 | 0,116 | 0,1736 | 0,196 | 0,1758 | 0,303 | 0,1802 | 0,419 | 0,1870 | 0,552 | 0,1968 |
| 5,9 | 0,118 | 0,1707 | 0,201 | 0,1730 | 0,308 | 0,1773 | 0,429 | 0,1844 | 0,563 | 0,1946 |
| 6,0 | 0,120 | 0,1678 | 0,204 | 0,1701 | 0,315 | 0,1747 | 0,434 | 0,1820 | 0,578 | 0,1925 |

| $v(z)$ | $v^* = 10,0$ | | $v^* = 9,0$ | | $v^* = 8,0$ | | $v^* = 7,5$ | | $v^* = 7,0$ | |
|---|---|---|---|---|---|---|---|---|---|---|
| | $F_1$ | $F_2$ | $F_1$ | $F_2$ | $F_1$ | $F_2$ | $F_1$ | $F_2$ | $F_1$ | $F_2$ |
| 1,5 | 0,152 | 0,6739 | 0,170 | 0,6780 | 0,190 | 0,6779 | 0,204 | 0,6803 | 0,219 | 0,6821 |
| 1,6 | 0,162 | 0,6333 | 0,181 | 0,6353 | 0,206 | 0,6301 | 0,219 | 0,6398 | 0,234 | 0,6414 |
| 1,7 | 0,173 | 0,5974 | 0,192 | 0,5992 | 0,217 | 0,6021 | 0,233 | 0,6039 | 0,250 | 0,6069 |

| $v(z)$ | $v^*$ 10,0 | | $v^*$ 9,0 | | $v^* = 8{,}0$ | | $v^*$ 7,5 | | $v^* = 7{,}0$ | |
|---|---|---|---|---|---|---|---|---|---|---|
| | $F_1$ | $F_2$ | $F_1$ | $F_2$ | $F_1$ | $F_2$ | $F_1$ | $F_2$ | $F_1$ | $F_2$ |
| 1,8 | 0,188 | 0,5647 | 0,204 | 0,5669 | 0,232 | 0,5705 | 0,247 | 0,5721 | 0,266 | 0,5750 |
| 1,9 | 0,196 | 0,5389 | 0,217 | 0,5388 | 0,245 | 0,5420 | 0,262 | 0,5444 | 0,282 | 0,5471 |
| 2,0 | 0,204 | 0,5102 | 0,228 | 0,5128 | 0,258 | 0,5165 | 0,278 | 0,5192 | 0,298 | 0,5219 |
| 2,1 | 0,215 | 0,4869 | 0,240 | 0,4876 | 0,271 | 0,4936 | 0,291 | 0,4960 | 0,315 | 0,4993 |
| 2,2 | 0,226 | 0,4462 | 0,253 | 0,4690 | 0,286 | 0,4730 | 0,304 | 0,4751 | 0,331 | 0,4789 |
| 2,3 | 0,236 | 0,4468 | 0,265 | 0,4496 | 0,300 | 0,4539 | 0,321 | 0,4566 | 0,348 | 0,4606 |
| 2,4 | 0,247 | 0,4292 | 0,277 | 0,4322 | 0,315 | 0,4367 | 0,338 | 0,4400 | 0,365 | 0,4437 |
| 2,5 | 0,258 | 0,4132 | 0,290 | 0,4167 | 0,328 | 0,4211 | 0,350 | 0,4252 | 0,382 | 0,4283 |
| 2,6 | 0,269 | 0,3981 | 0,302 | 0,4019 | 0,344 | 0,4085 | 0,370 | 0,4100 | 0,400 | 0,4144 |
| 2,7 | 0,280 | 0,3846 | 0,315 | 0,3882 | 0,359 | 0,3936 | 0,387 | 0,3975 | 0,418 | 0,4013 |
| 2,8 | 0,292 | 0,3720 | 0,328 | 0,3759 | 0,374 | 0,3811 | 0,402 | 0,3859 | 0,437 | 0,3899 |
| 2,9 | 0,303 | 0,3604 | 0,340 | 0,3642 | 0,390 | 0,3700 | 0,420 | 0,3740 | 0,455 | 0,3789 |
| 3,0 | 0,315 | 0,3494 | 0,355 | 0,3539 | 0,404 | 0,3596 | 0,437 | 0,3639 | 0,474 | 0,3691 |
| 3,1 | 0,326 | 0,3392 | 0,367 | 0,3435 | 0,418 | 0,3496 | 0,455 | 0,3545 | 0,494 | 0,3600 |
| 3,2 | 0,338 | 0,3300 | 0,381 | 0,3346 | 0,437 | 0,3419 | 0,472 | 0,3457 | 0,516 | 0,3515 |
| 3,3 | 0,349 | 0,3210 | 0,395 | 0,3258 | 0,454 | 0,3327 | 0,492 | 0,3378 | 0,536 | 0,3440 |
| 3,4 | 0,362 | 0,3129 | 0,409 | 0,3177 | 0,471 | 0,3250 | 0,509 | 0,3301 | 0,557 | 0,3365 |
| 3,5 | 0,374 | 0,3049 | 0,424 | 0,3102 | 0,487 | 0,3179 | 0,528 | 0,3232 | 0,579 | 0,3303 |
| 3,6 | 0,386 | 0,2977 | 0,437 | 0,3032 | 0,504 | 0,3110 | 0,548 | 0,3166 | 0,601 | 0,3242 |
| 3,7 | 0,398 | 0,2906 | 0,452 | 0,2967 | 0,522 | 0,3051 | 0,566 | 0,3110 | 0,624 | 0,3187 |
| 3,8 | 0,411 | 0,2845 | 0,467 | 0,2913 | 0,540 | 0,2999 | 0,590 | 0,3056 | 0,648 | 0,3137 |
| 3,9 | 0,424 | 0,2784 | 0,480 | 0,2846 | 0,559 | 0,2937 | 0,610 | 0,3002 | 0,672 | 0,3089 |
| 4,0 | 0,437 | 0,2726 | 0,496 | 0,2790 | 0,576 | 0,2887 | 0,631 | 0,2955 | 0,679 | 0,3049 |
| 4,1 | 0,451 | 0,2677 | 0,513 | 0,2740 | 0,596 | 0,2842 | 0,654 | 0,2914 | 0,723 | 0,3011 |
| 4,2 | 0,463 | 0,2625 | 0,528 | 0,2698 | 0,617 | 0,2796 | 0,676 | 0,2875 | 0,751 | 0,2976 |
| 4,3 | 0,477 | 0,2575 | 0,542 | 0,2646 | 0,638 | 0,2759 | 0,699 | 0,2836 | 0,778 | 0,2949 |
| 4,4 | 0,490 | 0,2531 | 0,561 | 0,2606 | 0,659 | 0,2722 | 0,724 | 0,2796 | 0,809 | 0,2921 |
| 4,5 | 0,504 | 0,2489 | 0,578 | 0,2566 | 0,681 | 0,2690 | 0,751 | 0,2778 | 0,837 | 0,2914 |
| 4,6 | 0,516 | 0,2448 | 0,597 | 0,2531 | 0,703 | 0,2656 | 0,778 | 0,2736 | 0,872 | 0,2884 |
| 4,7 | 0,532 | 0,2410 | 0,613 | 0,2496 | 0,726 | 0,2630 | 0,806 | 0,2732 | 0,908 | 0,2875 |
| 4,8 | 0,548 | 0,2376 | 0,630 | 0,2462 | 0,751 | 0,2606 | 0,834 | 0,2713 | 0,947 | 0,2869 |
| 4,9 | 0,562 | 0,2340 | 0,649 | 0,2433 | 0,776 | 0,2583 | 0,866 | 0,2700 | 0,981 | 0,2858 |
| 5,0 | 0,578 | 0,2310 | 0,670 | 0,2407 | 0,800 | 0,2561 | 0,896 | 0,2695 | 1,019 | 0,2857 |
| 5,1 | 0,593 | 0,2280 | 0,688 | 0,2386 | 0,829 | 0,2547 | 0,928 | 0,2675 | 1,065 | 0,2867 |
| 5,2 | 0,609 | 0,2252 | 0,708 | 0,2367 | 0,856 | 0,2530 | 0,964 | 0,2671 | 1,111 | 0,2875 |
| 5,3 | 0,626 | 0,2228 | 0,731 | 0,2338 | 0,889 | 0,2523 | 0,997 | 0,2665 | 1,169 | 0,2899 |
| 5,4 | 0,642 | 0,2202 | 0,751 | 0,2315 | 0,915 | 0,2509 | 1,036 | 0,2668 | 1,220 | 0,2921 |
| 5,5 | 0,656 | 0,2177 | 0,774 | 0,2302 | 0,950 | 0,2508 | 1,080 | 0,2678 | 1,268 | 0,2938 |
| 5,6 | 0,675 | 0,2154 | 0,797 | 0,2286 | 0,981 | 0,2501 | 1,125 | 0,2690 | 1,334 | 0,2962 |
| 5,7 | 0,694 | 0,2137 | 0,820 | 0,2270 | 1,013 | 0,2499 | 1,178 | 0,2712 | 1,407 | 0,3001 |
| 5,8 | 0,712 | 0,2118 | 0,844 | 0,2257 | 1,050 | 0,2500 | 1,222 | 0,2724 | 1,484 | 0,3035 |
| 5,9 | 0,731 | 0,2100 | 0,870 | 0,2248 | 1,091 | 0,2506 | 1,276 | 0,2747 | 1,575 | 0,3163 |
| 6,0 | 0,751 | 0,2083 | 0,895 | 0,2237 | 1,134 | 0,2521 | 1,336 | 0,2782 | 1,673 | 0,3250 |

| $v(z)$ | $v^* = 6{,}5$ | | $v^* = 6{,}0$ | | $v^* = 5{,}5$ | | $v^* = 5{,}0$ | | $v^* = 4{,}8$ | |
|---|---|---|---|---|---|---|---|---|---|---|
| | $F_1$ | $F_2$ | $F_1$ | $F_2$ | $F_1$ | $F_2$ | $F_1$ | $F_2$ | $F_1$ | $F_2$ |
| 1,5 | 0,237 | 0,6849 | 0,258 | 0,6887 | 0,284 | 0,6930 | 0,315 | 0,6968 | 0,328 | 0,7018 |
| 1,6 | 0,254 | 0,6452 | 0,277 | 0,6485 | 0,304 | 0,6532 | 0,338 | 0,6644 | 0,354 | 0,6631 |
| 1,7 | 0,271 | 0,6096 | 0,296 | 0,6135 | 0,325 | 0,6184 | 0,362 | 0,6258 | 0,379 | 0,6289 |
| 1,8 | 0,289 | 0,5780 | 0,315 | 0,5824 | 0,346 | 0,5879 | 0,386 | 0,5952 | 0,404 | 0,5992 |

| $v(z)$ | $v^* = 6{,}5$ | | $v^* = 6{,}0$ | | $v^* = 5{,}5$ | | $v^* = 5{,}0$ | | $v^* = 4{,}8$ | |
|---|---|---|---|---|---|---|---|---|---|---|
| | $F_1$ | $F_2$ | $F_1$ | $F_2$ | $F_1$ | $F_2$ | $F_1$ | $F_2$ | $F_1$ | $F_2$ |
| 1,9 | 0,306 | 0,5607 | 0,335 | 0,5553 | 0,368 | 0,5612 | 0,411 | 0,5721 | 0,431 | 0,5734 |
| 2,0 | 0,324 | 0,5258 | 0,355 | 0,5308 | 0,391 | 0,5371 | 0,437 | 0,5466 | 0,457 | 0,5501 |
| 2,1 | 0,342 | 0,5033 | 0,374 | 0,5081 | 0,414 | 0,5155 | 0,462 | 0,5247 | 0,485 | 0,5319 |
| 2,2 | 0,362 | 0,4836 | 0,395 | 0,4888 | 0,437 | 0,4963 | 0,490 | 0,5061 | 0,516 | 0,5115 |
| 2,3 | 0,379 | 0,4651 | 0,416 | 0,4710 | 0,460 | 0,4789 | 0,518 | 0,4897 | 0,546 | 0,4955 |
| 2,4 | 0,396 | 0,4484 | 0,437 | 0,4550 | 0,484 | 0,4630 | 0,548 | 0,4762 | 0,578 | 0,4812 |
| 2,5 | 0,417 | 0,4333 | 0,459 | 0,4401 | 0,509 | 0,4488 | 0,578 | 0,4615 | 0,610 | 0,4680 |
| 2,6 | 0,437 | 0,4196 | 0,482 | 0,4270 | 0,537 | 0,4355 | 0,609 | 0,4504 | 0,645 | 0,4602 |
| 2,7 | 0,459 | 0,4075 | 0,504 | 0,4148 | 0,565 | 0,4252 | 0,641 | 0,4396 | 0,670 | 0,4458 |
| 2,8 | 0,479 | 0,3959 | 0,528 | 0,4040 | 0,591 | 0,4148 | 0,676 | 0,4310 | 0,717 | 0,4390 |
| 2,9 | 0,498 | 0,3852 | 0,553 | 0,3940 | 0,621 | 0,4062 | 0,712 | 0,4234 | 0,759 | 0,4310 |
| 3,0 | 0,521 | 0,3758 | 0,578 | 0,3849 | 0,649 | 0,3973 | 0,751 | 0,4167 | 0,800 | 0,4270 |
| 3,1 | 0,521 | 0,3758 | 0,578 | 0,3849 | 0,683 | 0,3905 | 0,791 | 0,4115 | 0,846 | 0,4223 |
| 3,2 | 0,567 | 0,3592 | 0,631 | 0,3695 | 0,715 | 0,3843 | 0,834 | 0,4068 | 0,895 | 0,4198 |
| 3,3 | 0,590 | 0,3520 | 0,661 | 0,3634 | 0,751 | 0,3788 | 0,879 | 0,4032 | 0,948 | 0,4196 |
| 3,4 | 0,616 | 0,3457 | 0,689 | 0,3589 | 0,786 | 0,3742 | 0,926 | 0,4016 | 1,001 | 0,4167 |
| 3,5 | 0,642 | 0,3397 | 0,720 | 0,3530 | 0,827 | 0,3705 | 0,981 | 0,4003 | 1,066 | 0,4175 |
| 3,6 | 0,665 | 0,3334 | 0,751 | 0,3472 | 0,867 | 0,3674 | 1,038 | 0,4000 | 1,134 | 0,4202 |
| 3,7 | 0,694 | 0,3292 | 0,784 | 0,3434 | 0,909 | 0,3652 | 1,100 | 0,4016 | 1,212 | 0,4252 |
| 3,8 | 0,723 | 0,3249 | 0,820 | 0,3406 | 0,958 | 0,3644 | 1,169 | 0,4049 | 1,279 | 0,4314 |
| 3,9 | 0,754 | 0,3213 | 0,856 | 0,3374 | 1,006 | 0,3638 | 1,247 | 0,4097 | 1,392 | 0,4398 |
| 4,0 | 0,781 | 0,3173 | 0,898 | 0,3360 | 1,063 | 0,3650 | 1,335 | 0,4167 | 1,507 | 0,4521 |
| 4,1 | 0,814 | 0,3143 | 0,935 | 0,3341 | 1,118 | 0,3656 | 1,434 | 0,4270 | 1,642 | 0,4689 |
| 4,2 | 0,846 | 0,3116 | 0,981 | 0,3334 | 1,185 | 0,3691 | 1,551 | 0,4390 | 1,809 | 0,4928 |
| 4,3 | 0,884 | 0,3105 | 1,026 | 0,3332 | 1,260 | 0,3738 | 1,688 | 0,4558 | 2,019 | 0,5250 |
| 4,4 | 0,922 | 0,3092 | 1,080 | 0,3347 | 1,335 | 0,3794 | 1,853 | 0,4875 | 2,283 | 0,5669 |
| 4,5 | 0,962 | 0,3063 | 1,134 | 0,3362 | 1,428 | 0,3872 | 2,066 | 0,5099 | 2,658 | 0,6313 |
| 4,6 | 1,003 | 0,3079 | 1,195 | 0,3386 | 1,520 | 0,3975 | 2,353 | 0,5556 | 3,341 | 0,7605 |
| 4,7 | 1,046 | 0,3079 | 1,263 | 0,3426 | 1,643 | 0,4092 | 2,756 | 0,6230 | 4,790 | 1,0438 |
| 4,8 | 1,098 | 0,3096 | 1,344 | 0,3489 | 1,792 | 0,4277 | 3,428 | 0,7463 | | |
| 4,9 | 1,152 | 0,3115 | 1,419 | 0,3544 | 1,974 | 0,4515 | 4,964 | 1,0363 | | |
| 5,0 | 1,207 | 0,3136 | 1,507 | 0,3617 | 2,176 | 0,4785 | | | | |
| 5,1 | 1,268 | 0,3166 | 1,614 | 0,3720 | 2,491 | 0,5272 | | | | |
| 5,2 | 1,338 | 0,3210 | 1,739 | 0,3861 | 2,893 | 0,5882 | | | | |
| 5,3 | 1,413 | 0,3265 | 1,894 | 0,4040 | 3,630 | 0,7092 | | | | |
| 5,4 | 1,497 | 0,3337 | 2,086 | 0,4248 | 5,350 | 1,0060 | | | | |
| 5,5 | 1,603 | 0,3436 | 2,302 | 0,4787 | | | | | | |
| 5,6 | 1,700 | 0,3522 | 2,611 | 0,4988 | | | | | | |
| 5,7 | 1,827 | 0,3665 | 3,060 | 0,5624 | | | | | | |
| 5,8 | 1,994 | 0,3831 | 3,671 | 0,6897 | | | | | | |
| 5,9 | 2,170 | 0,4066 | 5,533 | 0,9264 | | | | | | |
| 6,0 | 2,400 | 0,4320 | | | | | | | | |

| $v(z)$ | $v^* = 4{,}6$ | | $v^* = 4{,}4$ | | $v^* = 4{,}2$ | | $v^* = 4{,}0$ | | $v^* = 3{,}8$ | |
|---|---|---|---|---|---|---|---|---|---|---|
| | $F_1$ | $F_2$ | $F_1$ | $F_2$ | $F_1$ | $F_2$ | $F_1$ | $F_2$ | $F_1$ | $F_2$ |
| 1,5 | 0,345 | 0,7057 | 0,363 | 0,7092 | 0,382 | 0,7138 | 0,404 | 0,7094 | 0,420 | 0,7257 |
| 1,6 | 0,371 | 0,6667 | 0,391 | 0,6707 | 0,412 | 0,6768 | 0,437 | 0,6821 | 0,462 | 0,6862 |
| 1,7 | 0,398 | 0,6329 | 0,418 | 0,6369 | 0,443 | 0,6435 | 0,470 | 0,6502 | 0,498 | 0,6568 |
| 1,8 | 0,426 | 0,6039 | 0,448 | 0,6086 | 0,474 | 0,6154 | 0,504 | 0,6282 | 0,534 | 0,6313 |
| 1,9 | 0,454 | 0,5807 | 0,479 | 0,5838 | 0,508 | 0,6116 | 0,540 | 0,5981 | 0,578 | 0,6079 |

| $v(z)$ | $v^* = 4{,}6$ | | $v^* = 4{,}4$ | | $v^* = 4{,}2$ | | $v^* = 4{,}0$ | | $v^* = 3{,}8$ | |
|---|---|---|---|---|---|---|---|---|---|---|
| | $F_1$ | $F_2$ | $F_1$ | $F_2$ | $F_1$ | $F_2$ | $F_1$ | $F_2$ | $F_1$ | $F_2$ |
| 2,0 | 0,483 | 0,5856 | 0,509 | 0,5609 | 0,541 | 0,5688 | 0,578 | 0,5777 | 0,620 | 0,5882 |
| 2,1 | 0,513 | 0,5353 | 0,542 | 0,5420 | 0,578 | 0,5498 | 0,617 | 0,5596 | 0,665 | 0,5718 |
| 2,2 | 0,544 | 0,5173 | 0,578 | 0,5249 | 0,616 | 0,5342 | 0,658 | 0,5444 | 0,710 | 0,5571 |
| 2,3 | 0,578 | 0,5018 | 0,612 | 0,5097 | 0,654 | 0,5195 | 0,703 | 0,5316 | 0,760 | 0,5462 |
| 2,4 | 0,612 | 0,4883 | 0,652 | 0,4975 | 0,697 | 0,5081 | 0,751 | 0,5208 | 0,815 | 0,5362 |
| 2,5 | 0,648 | 0,4766 | 0,690 | 0,4859 | 0,740 | 0,4975 | 0,800 | 0,5223 | 0,872 | 0,5305 |
| 2,6 | 0,684 | 0,4664 | 0,731 | 0,4766 | 0,789 | 0,4900 | 0,856 | 0,5061 | 0,937 | 0,5269 |
| 2,7 | 0,723 | 0,4570 | 0,778 | 0,4695 | 0,839 | 0,4836 | 0,915 | 0,5018 | 1,009 | 0,5260 |
| 2,8 | 0,766 | 0,4501 | 0,824 | 0,4625 | 0,898 | 0,4801 | 0,981 | 0,5003 | 1,093 | 0,5291 |
| 2,9 | 0,812 | 0,4443 | 0,877 | 0,4587 | 0,956 | 0,4769 | 1,052 | 0,5205 | 1,185 | 0,5348 |
| 3,0 | 0,860 | 0,4400 | 0,933 | 0,4560 | 1,019 | 0,4762 | 1,134 | 0,5043 | 1,289 | 0,5438 |
| 3,1 | 0,913 | 0,4371 | 0,991 | 0,4541 | 1,098 | 0,4394 | 1,227 | 0,5106 | 1,407 | 0,5571 |
| 3,2 | 0,970 | 0,4348 | 1,059 | 0,4550 | 1,176 | 0,4822 | 1,335 | 0,5217 | 1,561 | 0,5797 |
| 3,3 | 1,032 | 0,4354 | 1,134 | 0,4587 | 1,270 | 0,4904 | 1,459 | 0,5382 | 1,747 | 0,6098 |
| 3,4 | 1,098 | 0,4369 | 1,220 | 0,4638 | 1,378 | 0,5010 | 1,614 | 0,5580 | 1,999 | 0,6623 |
| 3,5 | 1,171 | 0,4403 | 1,310 | 0,4715 | 1,497 | 0,5139 | 1,806 | 0,5903 | 2,367 | 0,7342 |
| 3,6 | 0,255 | 0,4460 | 1,422 | 0,4673 | 1,662 | 0,5382 | 2,066 | 0,6369 | 3,040 | 0,8905 |
| 3,7 | 0,352 | 0,4541 | 1,550 | 0,4983 | 1,862 | 0,5714 | 2,434 | 0,7112 | 4,294 | 1,1905 |
| 3,8 | 1,466 | 0,4669 | 1,715 | 0,5222 | 2,131 | 0,5838 | 3,050 | 0,8432 | | |
| 3,9 | 1,603 | 0,4850 | 1,912 | 0,5540 | 2,512 | 0,6930 | 4,394 | 1,1547 | | |
| 4,0 | 1,756 | 0,5051 | 2,182 | 0,5999 | 3,113 | 0,8170 | | | | |
| 4,1 | 1,960 | 0,5371 | 2,565 | 0,6725 | 4,584 | 1,1455 | | | | |
| 4,2 | 2,240 | 0,5831 | 3,179 | 0,7937 | | | | | | |
| 4,3 | 2,617 | 0,6515 | 4,584 | 1,0929 | | | | | | |
| 4,4 | 3,258 | 0,7752 | | | | | | | | |
| 4,5 | 4,696 | 1,0684 | | | | | | | | |

| $v(z)$ | $v^* = 3{,}6$ | | $v^* = 3{,}4$ | | $v^* = 3{,}2$ | | $v^* = 3{,}0$ | | $v^* = 2{,}9$ | |
|---|---|---|---|---|---|---|---|---|---|---|
| | $F_1$ | $F_2$ | $F_1$ | $F_2$ | $F_1$ | $F_2$ | $F_1$ | $F_2$ | $F_1$ | $F_2$ |
| 1,5 | 0,459 | 0,7331 | 0,493 | 0,7429 | 0,531 | 0,7553 | 0,578 | 0,7696 | 0,604 | 0,7788 |
| 1,6 | 0,497 | 0,6974 | 0,533 | 0,7087 | 0,579 | 0,7225 | 0,630 | 0,7386 | 0,664 | 0,7508 |
| 1,7 | 0,536 | 0,6676 | 0,578 | 0,6794 | 0 627 | 0,6944 | 0,688 | 0,7136 | 0,724 | 0,7262 |
| 1,8 | 0,578 | 0,6414 | 0,626 | 0,6553 | 0,681 | 0,6725 | 0,751 | 0,6944 | 0,794 | 0,7097 |
| 1,9 | 0,620 | 0,6192 | 0,675 | 0,6349 | 0,737 | 0,6536 | 0,820 | 0,6807 | 0,868 | 0,6964 |
| 2,0 | 0,671 | 0,6024 | 0,729 | 0,6188 | 0,802 | 0,6410 | 0,895 | 0,6711 | 0,958 | 0,6925 |
| 2,1 | 0,717 | 0,5858 | 0,784 | 0,6050 | 0,870 | 0,6317 | 0,981 | 0,6671 | 1,046 | 0,6862 |
| 2,2 | 0,774 | 0,5747 | 0,849 | 0,5967 | 0,943 | 0,6242 | 1,078 | 0,6685 | 1,169 | 0,6993 |
| 2,3 | 0,833 | 0,5663 | 0,920 | 0,5907 | 1,028 | 0,6238 | 1,195 | 0,6771 | 1,302 | 0,7138 |
| 2,4 | 0,895 | 0,5593 | 0,999 | 0,5893 | 1,134 | 0,6305 | 1,335 | 0,6964 | 1,478 | 0,7441 |
| 2,5 | 0,964 | 0,5556 | 1,085 | 0,5900 | 1,265 | 0,6419 | 1,504 | 0,7220 | 1,700 | 0,7886 |
| 2,6 | 1,044 | 0,5559 | 1,192 | 0,6028 | 1,395 | 0,6609 | 1,739 | 0,7722 | 2,004 | 0,8621 |
| 2,7 | 1,134 | 0,5602 | 1,310 | 0,6101 | 1,575 | 0,6911 | 2,066 | 0,8496 | 2,572 | 1,0030 |
| 2,8 | 1,242 | 0,5695 | 1,456 | 0,6349 | 1,818 | 0,8717 | 2,592 | 0,9921 | 3,732 | 1,3793 |
| 2,9 | 1,346 | 0,5834 | 1,643 | 0,6831 | 2,153 | 0,8190 | 3,793 | 1,3514 | | |
| 3,0 | 1,501 | 0,6017 | 1,871 | 0,6881 | 2,683 | 0,9851 | | | | |
| 3,1 | 3,658 | 0,6250 | 2,240 | 0,7906 | 3,871 | 1,2903 | | | | |
| 3,2 | 1,960 | 0,6854 | 2,838 | 0,9416 | | | | | | |
| 3,3 | 2,283 | 0,7559 | 3,986 | 1,2469 | | | | | | |
| 3,4 | 2,865 | 0,8913 | | | | | | | | |
| 3,5 | 4,218 | 1,2376 | | | | | | | | |

| $v(z)$ | $v^* = 2{,}8$ | | $v^* = 2{,}7$ | | $v^* = 2{,}6$ | | $v^* = 2{,}5$ | | $v^* = 2{,}4$ | |
|---|---|---|---|---|---|---|---|---|---|---|
| | $F_1$ | $F_2$ | $F_1$ | $F_2$ | $F_1$ | $F_2$ | $F_1$ | $F_2$ | $F_1$ | $F_2$ |
| 1,5 | 0,635 | 0,7899 | 0,670 | 0,8026 | 0,706 | 0,8157 | 0,751 | 0,8333 | 0,805 | 0,8562 |
| 1,6 | 0,697 | 0,7622 | 0,737 | 0,7764 | 0,784 | 0,7843 | 0,832 | 0,8130 | 0,895 | 0,8389 |
| 1,7 | 0,763 | 0,7396 | 0,812 | 0,7582 | 0,865 | 0,7782 | 0,928 | 0,8026 | 1,003 | 0,8333 |
| 1,8 | 0,837 | 0,7241 | 0,888 | 0,7429 | 0,962 | 0,7704 | 1,038 | 0,8006 | 1,134 | 0,8403 |
| 1,9 | 0,922 | 0,7163 | 0,991 | 0,7413 | 1,067 | 0,7692 | 1,169 | 0,8097 | 1,297 | 0,8628 |
| 2,0 | 1,019 | 0,7123 | 1,104 | 0,7452 | 1,212 | 0,7862 | 1,335 | 0,8347 | 1,507 | 0,9042 |
| 2,1 | 1,136 | 0,7205 | 1,237 | 0,7570 | 1,366 | 0,8058 | 1,547 | 0,8772 | 1,806 | 0,9843 |
| 2,2 | 1,276 | 0,7369 | 1,407 | 0,7849 | 1,596 | 0,8562 | 1,853 | 0,9569 | 2,283 | 1,1338 |
| 2,3 | 1,444 | 0,7639 | 1,628 | 0,8313 | 1,903 | 0,9346 | 2,347 | 1,1468 | 3,428 | 1,5528 |
| 2,4 | 1,646 | 0,8091 | 1,955 | 0,9158 | 2,420 | 1,0905 | 3,428 | 1,4881 | | |
| 2,5 | 1,984 | 0,8889 | 2,434 | 1,0526 | 3,480 | 1,4493 | | | | |
| 2,6 | 2,527 | 1,0428 | 3,630 | 1,4451 | | | | | | |
| 2,7 | 3,630 | 1,3928 | | | | | | | | |

| $v(z)$ | $v^* = 2{,}3$ | | $v^* = 2{,}2$ | | $v^* = 2{,}1$ | | $v^* = 2{,}0$ | |
|---|---|---|---|---|---|---|---|---|
| | $F_1$ | $F_2$ | $F_1$ | $F_2$ | $F_1$ | $F_2$ | $F_1$ | $F_2$ |
| 1,5 | 0,863 | 0,8803 | 0,935 | 0,9132 | 1,017 | 0,9506 | 1,134 | 1,0081 |
| 1,6 | 0,972 | 0,8718 | 1,059 | 0,9099 | 1,176 | 0,9643 | 1,335 | 1,0438 |
| 1,7 | 1,100 | 0,8741 | 1,222 | 0,9294 | 1,392 | 1,0091 | 1,614 | 1,1161 |
| 1,8 | 1,258 | 0,8929 | 1,422 | 0,9652 | 1,662 | 1,0784 | 2,066 | 1,2739 |
| 1,9 | 1,472 | 0,9363 | 1,723 | 1,0482 | 2,125 | 1,2361 | 3,050 | 1,6863 |
| 2,0 | 1,764 | 1,1377 | 2,193 | 1,2048 | 3,113 | 1,6340 | | |
| 2,1 | 2,240 | 1,1669 | 3,224 | 1,6077 | | | | |
| 2,2 | 3,293 | 1,5674 | | | | | | |

The table gives values of

$$F_2(v) = \frac{1}{v\sqrt{1 - a^2v^2}}$$

as a function of v; the t(z) curve is needed in order to construct isochronous curves, and this is found by integrating $F_2(z)$ as for $F_1(z)$ by means of tabulated values of $F_2$. Figure 2a shows this function in terms of z. The problem is then merely one of graphical integration, which in this case it is convenient to perform with scales of 1:10 000 (or 1:1000) for depth and 1 msec/m per 10 cm for $F_2$. Here it is also convenient to take an interval in z of 100 m (or 10 m); then the area $Q = q_n z$ is readily found by multiplying $q_n$ by 100 (or 10), while the sum of the $Q_k$ is t(z) for the path of parameter $v^*$ down to a depth of $z_n$. All graphs should be drawn on one piece of paper (Fig. 2b) in order to costruct the isochronous curves; on this we draw a horizontal line with $t_k$ = constant to meet the t(z) curves for each ray with the parameter $v^*$ at points $z_i$, which correspond to this time $t_k$ of travel along the rays. The rays already constructed for the depths $z_i$ are marked with points corresponding to this $t_k$; these points are joined up into a smooth isochronous curve.

The table gives $F_1(v)$ and $F_2(v)$ for thirteen values of $v^*$; now (1) and (2) contain $v(z)/v^*$, so the table of $F_1$ can be used to construct curves of $F_1(z)$ for rays with parameters $nv(z)/v^*$, but the v(z) in the table must then be reduced by factors of n. Again, the table of $F_2(v)$ can be used to find values of $F_2$ for velocities $v_i$ not listed.

We can put $F_2(v)$ in the form

$$F_2(v) = \frac{v^*}{v\sqrt{v^{*2} - v^2}} = n\frac{nv^*}{nv\sqrt{n^2v^{*2} - n^2v^2}}.$$

so for the $v_i$ we find the $F_2(v)/n$ on the $nv^*$ curves opposite $v(z) = nv$. Thus the table of $v_i$ is suitable for constructing the rays and curves for sections having any velocities. The calculations are no more troublesome than those in the method based on representing v(z) in the form of a piecewise-linear curve [4, 5].

## Bibliography


1. Berzon, I. S. Ob opredelenii trayektoriy seysmicheskikh luchey i poley vremen v sredakh s peremennymi skorostami [The determination of the trajectories of seismic rays and of the transit time for media with variable velocities]. Izv. Akad. Nauk SSSR, ser. geofiz. [News of the Academy of Sciences of the USSR, geophysics series], no. 1, 1948.
2. Gamburtsev, G. A. Osnovy seysmorazvedki [Principles of Seismic Prospecting]. Gostoptekhizdat, 1958.
3. Puzyrev, N. N. O putyakh utocheniya metodov interpretatsii dannykh seysmorazvedki [Means of improving methods of interpretation in seismic prospecting]. Sborn. Prikladnaya Geofizika [Applied Geophysics Symposium], no. 12, 1955.

4. Idem. Metodika interpretatsii dannykh seysmorazvedki metodom otrazhennykh voln [Methods of interpreting the Results of Seismic Surveys by the Reflected-Wave Method]. Gostoptekhizdat, 1959.
5. Idem. Postroyeniye luchevykh diagramm pri proizvol'nom zakone izmeneniya skorosti s glubinoy [Construction of ray diagrams for an arbitrary law of variation of velocity with depth]. Sborn. Prikladnaya Geofizika [Applied Geophysics Symposium], no. 2, 1945.

END

2187
CSO: 2507-N